Cleaved tau derived from human tauopathy brain induces disease-associated deficits in a novel mouse model

Bondulich, Marie Katrin

Awarding institution:
King's College London

Cleaved tau derived from human tauopathy brain induces disease-associated deficits in a novel mouse model

Marie Katrin Bondulich

Thesis submitted in fulfilment of the degree of Doctor of Philosophy

Department of Basic and Clinical Neuroscience

Institute of Psychiatry, Psychology & Neuroscience

King's College London

September 2016

Declaration

I hereby declare that all of the work presented in this thesis is my own except for the haemagglutinin immunostaining which was conducted in the laboratory of Professor Jean-Pierre Brion (Brussels) and the RT-PCR which was performed by Tong Guo (King's College London).

Publication arising from this thesis:

Bondulich MK, Guo T, Meehan C, Manion J, Rodriguez Martin T, Mitchell JC, Hortobagyi T, Yankova N, Stygelbout V, Brion J-P, Noble W, Hanger DP (2016) Tauopathy induced by low level expression of a human brain-derived tau fragment in mice is rescued by phenylbutyrate. Brain 139:2290–2306.

Hanger, D.P. Lau, D.H.W. Philips, E.C. **Bondulich, M.K.** Guo, T. Woodward, B.W. Pooler, A.M. Noble, W. (2014). Intracellular and extracellular roles of tau in neurodegenerative disease. Journal of Alzheimer's Disease, 40:S37-S45

Atherton, J. Kurbatskaya, K. **Bondulich, M.** Croft, C.L. Garwood, C.J. Chhabra, R. Wray, S. Jeromine, A. Hanger, D.P. Noble, W. (2014) Calpain cleavage and inactivation of the sodium calcium exchanger-3 occur downstream of Aβ in Alzheimer's disease. Ageing Cell, 13:49-59.

Marie Bondulich,
September 2016

Acknowledgements

There are many people I would like to thank for their continuous support and help in the production of this thesis. First of all, I would very much like to thank my main supervisor Professor Diane Hanger for not only giving me this excellent opportunity, but also for her continuous guidance, scientific contribution, trust, and expertise throughout my PhD studentship. It was Diane's constant encouragement that lead me to thrive to be the best independent researcher I could be. I would also like to thank my second supervisor Dr. Wendy Noble, for always providing me with any needed guidance especially in lab meetings. Of course, I couldn't have done this without my fellow lab members and Team Tau. I am thankful for the moral support, the lunches and the pub outings. I was very honoured to have great input from excellent BSc and MSc students and I thank them for their contributions and for making my first time as a supervisor such an enjoyable experience. I want to massively thank my CrossFit girls especially Laura, Teya, Netsai, Emma and Katy. You girls are amazing and always lift my spirits. Our many workouts and evening Woodoven's got me through many stressful times. I am very grateful for my amazing supportive family, both mine and Max's. Your constant support towards my goals means a lot and I hope I make you proud. Finally, I would like to thank my other half Max. I don't think I could have done any of this without your constant support, your statistical and referencing knowledge and your endless encouragement. Thank you for putting up with me through the challenging 3 years of my thesis and for helping me be the best I possibly can.

Abstract

Human neurodegenerative tauopathies exhibit pathological tau aggregates in the brain along with diverse clinical features including cognitive and motor dysfunction. Post-translational modifications of tau, including tau phosphorylation and truncation, are characteristic features of human tauopathy. We previously identified a highly phosphorylated and truncated form of tau associated with the development of disease in humans. We have generated a new mouse model of tauopathy in which this human brain-derived, tau fragment (Tau35) is expressed under the control of the human tau promoter. Notably, unlike most existing mouse models of tauopathy, the Tau35 transgene encoding truncated wild-type tau, is expressed at less than 10% of the amount of endogenous mouse tau.

Behavioural and phenotypic assessments showed that Tau35 mice exhibit a disease-associated phenotype of reduced survival, clasping, kyphosis and defective motor function. Cognitive testing in the Morris water maze also revealed a deficit in spatial learning and hippocampal dependent memory. Neuropathological examination using a range of antibodies to tau, including phosphorylated and conformational epitopes, showed a progressive accumulation of aggregated and phosphorylated tau inclusions, comprising both endogenous and transgenically expressed tau. Alterations in several disease-associated proteins were also detected in Tau35 mice, including kinase activity, and proteins involved in autophagic-lysosomal and synaptic function, suggesting a toxic gain of function of this tau fragment. Importantly, we found that a pharmacological agent reverses the molecular and behavioural neurodegenerative phenotype apparent in Tau35 mice. Backcrossing the original mixed background Tau35 mice onto a pure C57BL/6 background revealed that the previously observed behavioural deficits were preserved in this mouse model. A novel cell based CHO-Tau35 phosphorylation assay was successfully established in which to test potential therapeutic compounds.

These results show for the first time that minimal expression of a wild-type human disease-associated tau fragment in Tau35 mice causes a profound and progressive tauopathy, which can be rescued by pharmacological

intervention. Tau35 mice therefore represent a highly disease-relevant animal model in which to investigate molecular mechanisms underlying tau-associated neurodegeneration and to develop novel and innovative therapies for human tauopathies.

Contents

List of Figures

List of Tables

Abbreviations

AD	Alzheimer's disease
AEP	Asparaginyl endopeptidase
Akt	Protein kinase B
ANOVA	Analysis of variance
ApoE	Apolipoprotein E
APP	Amyloid precursor protein
Atg	Autophagy related genes
Aβ	Amyloid-β
AV	Autophagic vacuole
BACE	β-site amyloid precursor protein cleaving enzyme
bp	Base-pair
BSA	Bovine serum albumin
CaMKII	Ca2+ /calmodulin-dependent protein kinase II
CBD	Corticobasal degeneration
Cdk5	Cyclin-dependent kinase 5
CHO	Chinese hamster ovary

CHOP	CCAAT-enhancer-binding protein homologous protein
CK1	Casein kinase 1
CNS	Central nervous system
CNP	2',3'-Cyclic-nucleotide 3'-phosphodiesterase
CREB	cAMP response element binding protein
CSF	Cerebrospinal fluid
DAPK	Death-associated protein kinase
DMSO	Dimethyl sulfoxide
DTT	Dithiothreitol
Dyrk1A	Dual-specificity protein kinase 1
EHT	Eicosanoyl-5-hydroxy-tryptamide
ER	Endoplasmic reticulum
ERK	Extracellular signal-regulated kinase
ES	Embryonic stem cell
ESLB	Extra strong lysis buffer
FAD	Familial Alzheimer's disease
FTD	Frontotemporal dementia

FTLD	Frontotemporal Lobar Degeneration
GFAP	Glial fibrillary acidic protein
GSK3	Glycogen synthase kinase-3
GWAS	Genome-wide association study
HA	Haemagglutinin
HDAC	Histone deacetylase
HMGCR	3-Hydroxy-3-methylglutaryl-CoA reductase
HTRA1	Human high temperature requirement serine protease A1
Hsp	Heat shock protein
ICC	Immunocytochemistry
IHC	Immunohytochemistry
Ig	Immunoglobulin
I2PP2A	PP2A inhibitor
JNK	c-Jun N-terminal kinase
KI	Kyphotic index
KO	Knockout

LAMP	Lysosomal-associated membrane protein
LC3	Microtubule-associated protein 1-light chain 3
LTP	Long-term potentiation
LRRK2	Leucine-rich repeat kinase 2
MAPT	Microtubule associated protein tau
MARK	Microtubule affinity-regulating kinase
MBD	Microtubule binding domain
MT	Microtubule
MVB	Multivesicular bodies
NAD	Nicotinamide adenine dinucleotide
NFT	Neurofibrillary tangle
NGS	Normal goat serum
NHS	Normal horse serum
NMDA	N-methyl-D-aspartate
NSE	Neuron specific enolase
OA	Okadaic acid
O-GlcNAc	O-linked β-N-acetylglucosamine acetylation

PB	Pick body
PBA	Sodium 4-phenylbutyrate
PBS	Phosphate-buffered saline
PD	Parkinson's disease
PDGF	Platelet-derived growth factor
PDPK	Proline directed protein kinase
PE	Phosphatidylethanolamine
PFA	Paraformaldehyde
PHF	Paired helical filament
PiD	Pick disease
PKA	Protein kinase A
PKB	Protein kinase B
PNS	Peripheral nervous system
PP1	Protein phosphatase 1
PP2A	Protein phosphatase 2A
PP2C	Protein phosphatase 2C
PRD	Proline-rich domain

PS	Presenilin
PSD95	Post-synaptic density protein 95
pSer	Phosphorylated on serine residue
pThr	Phosphorylated on threonine residue
PSK	Prostate-derived sterile 20-like kinase
PSP	Progressive supranuclear palsy
p62/SQSTM1	sequestosome 1 sequestosome 1
RT	Reverse transcription
SAPK	Stress-activated protein kinase
Ser	Serine
SERT	Serotonin transporter
SF	Straight filament
SNARE	Soluble N-ethylmaleimide-sensitive factor attachment protein receptor
TBS	Tris-buffered saline
TDP43	TAR DNA-binding protein-43
TFEB	Transcription factor EB

Thr	Threonine
Tyr	Tyrosine
UPR	Unfolded protein response
VAMP1	Vesicle-associated membrane protein 1
WB	Western blot
WT	Wild-type
WHO	World Health Organization
β -ME	β-Mercaptoethanol

CHAPTER 1

1.1 Tau Protein

Tau, a neuron specific microtubule-associated protein, is encoded by the *MAPT* gene on chromosome 17 in humans and is found primarily in axons of the central nervous system (CNS). The primary identified role of tau was to promote the polymerisation of tubulin into microtubules (MTs), which are important for axonal transport (Witman et al., 1976; Ávila et al., 2002). However, tau is now well known as a multifunctional protein involved in adult neurogenesis, modulation of a number of signalling pathways, possible cholinergic signalling role of secreted tau, synaptic roles through interaction with Src-family kinases such as fyn, DNA damage protection and roles in nuclear organisation (Sjöberg et al., 2006; Reynolds et al., 2008; Gómez-Ramos et al., 2009; Ittner et al., 2011; Sultan et al., 2011; Spillantini and Goedert, 2013).

In neurons, tau is essential for a variety of functions including morphogenesis, axonal outgrowth, axonal vesicle and protein transport, neuronal plasticity and is implicated in the development and progression of tauopathy neurodegenerative diseases (Trinczek et al., 1999; Buée et al., 2000; Sultan et al., 2011; Iqbal et al., 2015). At a mechanical level, tau stimulates MT stabilisation and suppresses MT dynamics (Tint et al., 1998). Tau is most abundantly expressed in CNS neurons but can also be found in the somatodendritic compartment of neurons, oligodendrocytes, and in non-neuronal tissues, and in its pathological form in peripheral tissue, as well as to a lesser extent in heart, lung muscle, pancreas, fibroblast, kidneys and testes (Trojanowski et al., 1989; Ingelson et al., 1996; Vanier et al., 1998; Gu et al., 2002; Maurage et al., 2004; Rouzier et al., 2005; Souter and Lee, 2009). Sequence analysis has distinguished four main structural components in tau; an N-terminal domain, a proline-rich domain, a MT and a C-terminal domain (Figure 1.1). The MT binding repeats in tau are each separated by short stretches of 13-14 amino acids. The entire repeat/inter-repeat region is

positively charged, facilitating electrostatic interactions between tau and the negatively charged MT surface. The C-terminal tail of tau contains both basic and acidic sub regions and indirectly regulates tau binding to MTs (Brandt and Lee, 1993).

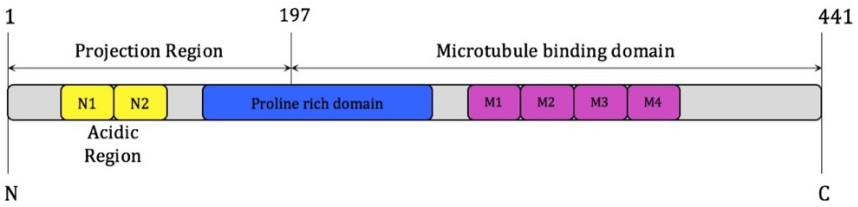

Figure 1.1: Schematic representation of human CNS full-length tau protein. Representation of the largest tau isoform (441 amino acids long). The proline rich domain is highlighted in blue. There are either three or four microtubule-binding repeat regions (M1-M4) (pink) depending on alternative splicing of exon 10 encoding M2. The number of acidic repeats in yellow (N1, N2) at the N-terminal of the protein alters depending on the isoform (Williams, 2006).

1.1.1 Alternative splicing of tau

The *MAPT* gene of over 100 kb consists of 16 exons and is located on human chromosome 17q21 (Figure 1.2). Alternative splicing of exons occurs in 70% of vertebrate genes, and splicing variants are regulated both temporarily and spatially, to produce functionally diverse proteins with differing affinities (Lander et al., 2001). Alternative splicing of tau results in multiple variants and it is a major contributor to proteomic complexity (Andreadis, 2005). Exons 1, 4, 5, 7, 9, 11, 12, and 13 are constitutive tau exons. Exons 14 is present in mRNA, but has not been detected in tau protein (Goedert et al., 1989a, 1989b; Andreadis et al., 1992; Sawa et al., 1994). Alternative splicing of exons 2, 3 and 10 (E2, E3, E10) generates six distinct tau isoforms ranging from 352 – 441 amino acids and are tightly regulated developmentally (Figure 1.2) (Hong et al., 1998). Functionally 4R tau is known to bind and assemble MTs with greater affinity than 3R tau (Goedert and Jakes, 1990; Butner, 1991; Gustke et al., 1994).

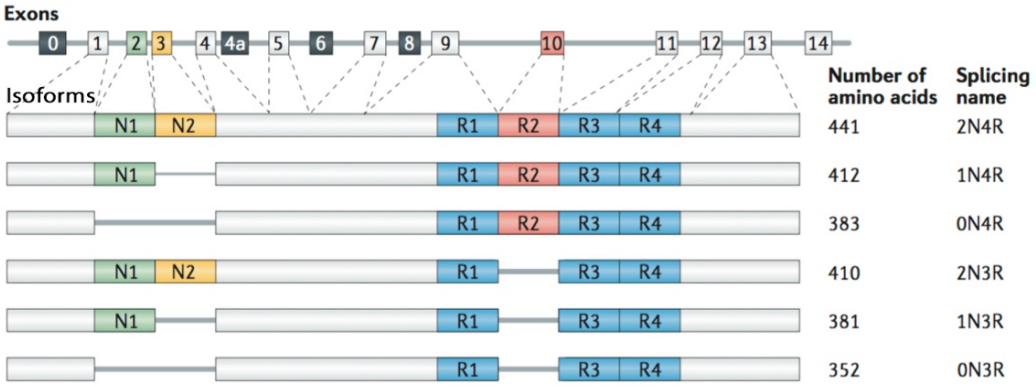

Figure 1.2: The human MAPT gene encompassing the 16 exons and six isoforms of tau and their domain structures expressed in the human adult CNS. Human tau gene contains 16 exons. Human tau isoforms are formed from alternative splicing of exons, 2, 3 and 10. Exon 2 and 3 together, or exon 2 alone, can be included or excluded in the N-terminal projection domain (exon 2: green and exon 3: yellow). Exon 10 alternative splicing in the C-terminal region results in the production of either three or four tubulin-binding repeats, 3R and 4R, respectively (3R: blue, 4R: red) (Wang and Mandelkow, 2015).

Tau isoforms differ from each other by the presence of either three or four repeats in the carboxy-terminal (C-terminal) half, and the presence or absence of one or 2 inserts of 29 or 58 amino acids in the amino terminal (N-terminal) region of tau (Figure 1.2) (Goedert et al., 1989a, 1989b; Himmler et al., 1989; Lee et al., 1989). Three tau isoforms contain exon 10 (E10+, 4R tau) and three tau isoforms lack exon 10 (E10+, 3R tau) (D'Souza et al., 1999). The largest of the tau isoforms in the human CNS comprises 441 amino acids (Figure 1.1, Figure 1.2) (Lee et al., 1989). Normal adult human brain expresses approximately equal levels of 3R and 4R tau and regulation of alternative splicing is particularly important because mutations causing changes in the 3R:4R ratio result in neurodegenerative disease (Figure 1.2). Although most tau isoforms are primarily expressed in the CNS in the peripheral nervous system (PNS), tau can be found as a high molecular weight tau isoform

expressing exon 4A, yielding a ~100kDa protein (Nunez, 1988; Couchie et al., 1992; Goedert et al., 1992b).

1.2 Tauopathies

Highly phosphorylated aggregates of tau deposited in the CNS may be a key driver of the group of neurodegenerative diseases collectively known as tauopathies. These disorders include Alzheimer's disease (AD), corticobasal degeneration (CBD), progressive supranuclear palsy (PSP) and certain frontotemporal dementias (FTD) (Hernández and Avila, 2007). The tauopathies differ by affected brain regions and cell types, as well as by the biochemical features of aggregated tau in each disorder (Table 1) (Wang and Mandelkow, 2015). Abnormalities in the ratio of tau isoforms are associated with a variety of different tauopathies (Table 1). Whereas AD and control brains each exhibit approximately equal amounts of 4R and 3R tau isoforms in the brain; PSP and CBD exhibit predominantly 4R tau, PiD predominantly 3R tau, and in frontotemporal dementia and parkinsonism linked to chromosome 17 with a mutation in the tau gene (FTLD-tau) the isoform predominance depends on which tau mutation is present (Table 1) (Hong et al., 1998; Arai et al., 2003; de Silva et al., 2006). The neuropathological hallmark of tauopathies is the aggregation of insoluble, fibrous protein into brain lesions. In tauopathy brain, tau is highly phosphorylated and is polymerised into paired helical filaments (PHF) and/or straight filaments (SF) forming neurofibrillary aggregates (Table 1) (Iqbal et al., 2010). The characteristic tau aggregates present in different tauopathies differ in both phosphorylation status and in the accumulation of specific tau isoforms, enabling a biochemical classification of the tauopathies (Sergeant et al., 2005).

Table 1*:* Summarising the different tau pathologies characteristic of the major tauopathies and showing the typical filament types present in these diseases. PHF: paired helical filaments. SF: straight filaments, AD: Alzheimer disease, FTD: frontotemporal dementia, PSP: progressive supranuclear palsy, CBD: corticobasal degeneration, PiD: Pick's disease, NFT: neurofibrillary tangles (adapted from Williams et al 2006)

Disease	**Ratio (3R:4R)**	**Tau pathology**	**Filament type**	**Clinical features**
AD	3R and 4R	NFTs	PHF (and SF)	Cognitive impairment, cortical dementia, amnestic, rare movement problems
PSP	4R	PSP tangles	SF	Frontal dysexecutive, cognitive impairment, asymmetric onset of motor dysfunction, axial rigidity, tremor, late falls
PiD	3R	Pick bodies	SF	Frontal dysexecutive, progressive non-fluent aphasia, semantic dementia, rare movement problems
CBD	4R	Neuronal tau inclusions	SF	Parietal, frontal dysexecutive, asymmetric parkinsonism, alien limb
FTD	4R	Tangles, neuronal and glial tau inclusions	PHF and/or SF	Frontal behaviour cognitive impairment, symmetric rigidity and bradykinesis, opthalmoplegia

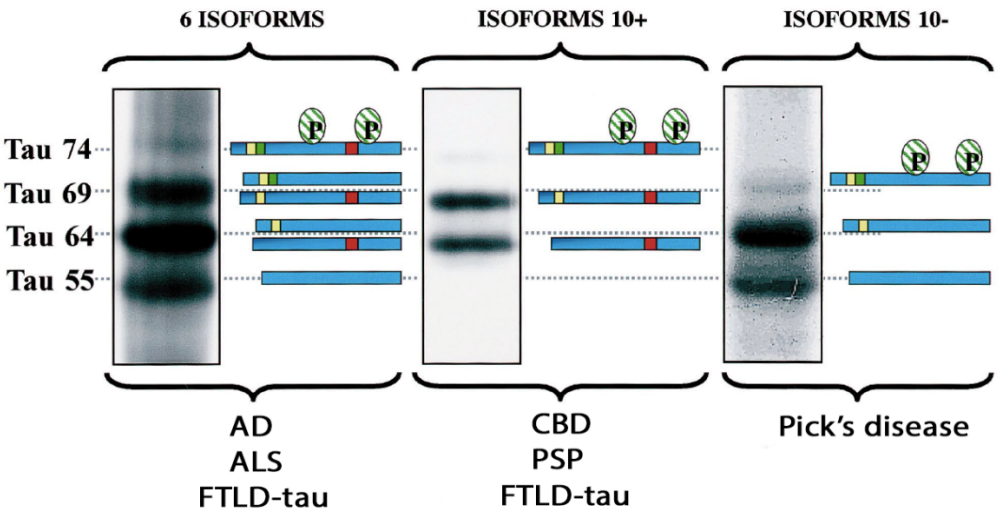

Figure 1.3: Stylised western blots showing the predominant tau isoforms present in different tauopathies. AD contains both 4R and 3R tau isoforms, tau pathology in PSP and CBD contains mainly 4R tau, while in PiD mainly 3R tau is present. In FTLD-tau the pattern is more varied with some cases containing both 3R and 4R tau, and others characterised by predominantly 4R or 3R tau. (adapted from Buée et al., 2000).

1.2.1 Alzheimer's disease

Age is the biggest risk factor for AD, which is by far the most prevalent of the tauopathies in people over the age of 65 (60% of dementia cases), affecting approximately 6% of the population and 50% of people over the age of 90, with 800,000 people in the UK alone affected by the disease (Wimo et al., 2013, WHO 2013). Current predictions are that AD will affect 1 in 85 people globally by 2050, making it a global epidemic (Brookmeyer et al., 2007; Norton et al., 2014). This rise will largely be due to improved healthcare and increases in an ageing populations, which will have a huge economic impact (Wimo et al., 2013).

In AD brain, neural tissue and peripheral nerves contain tau which is abnormally phosphorylated. Tau is the major protein component of neurofibrillary tangles (NFTs), one of the pathological hallmark lesions of the

disease (Tortosa et al., 2011). NFTs are primarily composed of aggregated β-sheet-rich PHF structures (Iqbal et al., 1975; Yagishita et al., 1981; Wood et al., 1986; Goedert et al., 1989a). NFTs are primarily localised to the cell soma of degenerating neurons and glia but they also occur in cell processes as neuropil threads (Braak and Braak, 1986; Gómez-Isla et al., 1997). Once neuronal death occurs, NFTs remain in the extracellular spaces and become associated with microglia and invading astrocytic processes (Ikeda et al., 1992). Nevertheless, it remains unclear whether NFTs are cytotoxic. Interestingly, Braak and colleagues (Braak and Braak, 1991) found that NFT spreading follows a consistent pattern throughout the brain in AD which allows the disease to be neuropathologically categorised into six primary stages as well as correlating brain pathology to disease severity and clinical phenotypes. As seen in Figure 1.4 at first NFTs appear in the transentorhinal/peripheral cortex (Braak stage I), followed by the CA1 region of the hippocampus (Braak stage II). Following from that NFTs appear and accumulate in the limbic structures such as the subiculum of the hippocampus (Braak Stage III), then amygdala, thalamus and claustrum (Braak Stage IV). Finally, NFTs spread to the isocortical areas, with associative areas affected first (Braak Stage V), followed by the primary sensory, motor and visual areas (Braak Stage VI) (Figure 1.4) (Hyman et al., 1984; Arnold et al., 1991; Braak and Braak, 1991). This hierarchical pattern of NFTs and degeneration amongst the brain regions is very consistent and regularly used as a diagnostic tool (NIA-Reagan Working Group, 1997).

AD brain is also characterised by the deposition of amyloid β (Aβ) in extracellular spaces and blood vessels as amyloid plaques, which, along with tau deposition, are used to diagnose disease neuropathologically at post-mortem (Wong et al., 1985). Unlike tau, Aβ plaque deposition does not correlate with cognitive decline, nevertheless biochemical and genetic evidence has identified that Aβ is a critical early trigger leading to tauopathy and neuronal dysfunction (Hardy and Selkoe, 2002) with the spread of amyloid pathology being more obvious in cortical and subcortical regions (Figure 1.4). Aβ plaques are generated by the extracellular deposition of proteolytic fragments derived from the amyloid precursor protein (APP).

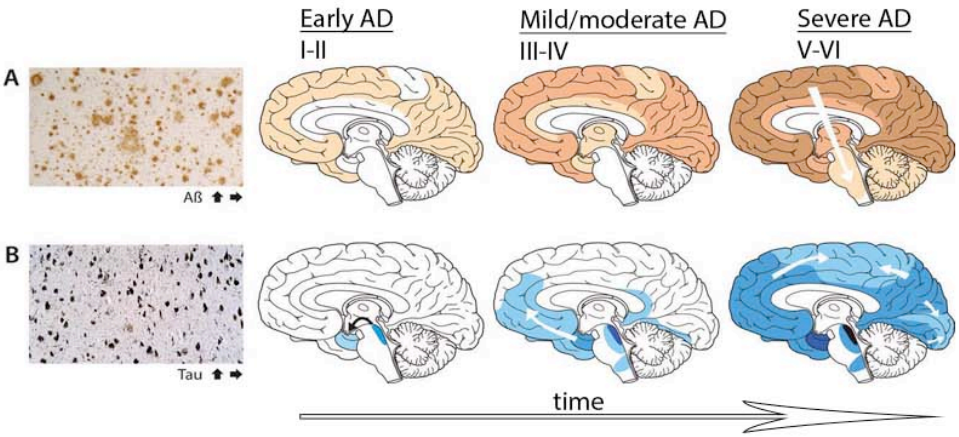

Figure 1.4: Accumulation of β-amyloid and tau in AD brain shows characteristic patterns of spreading. (a) Cross section of β-amyloid (Aβ) plaques labelling which first appear in the neocortex, cortex and finally subcortical regions. **(b)** Cross section of paired helical filaments (PHF) and neuropathological staging of severity. NFT load in early AD (Braak stages I-II) occurs first in the locus coeruleus and trans entorhinal area (CA1, subiculum and entorhinal cortex). followed by spreading to neighbouring limbic system regions such as the amygdala and hippocampus in later stages of mild/moderate AD (Braak stages III and IV) and finally to connected neocortical brain regions and rest of the brain in late stage severe AD (Braak stages V-VI) as indicated by black and white arrows in the bottom 3 brains (adapted from Jucker and Walker, 2011).

APP is cleaved sequentially by beta-site APP cleavage enzyme-1 (BACE1) and γ-secretase, the latter yielding $A\beta_{40}$ or $A\beta_{42}$. $A\beta_{42}$ is more readily aggregated, believed to be more toxic, and is the predominant form of Aβ deposited in plaques (Wilquet and De Strooper, 2004). Throughout the progression of AD, Aβ is continuously deposited in the extracellular matrix, and with increasing involvement of neurites, over time this results in the formation of dense core neuritic plaques that are also tau-positive. Unlike diffuse plaques, mature amyloid plaques stain with Congo red and Thioflavin S and have high β-sheet content, indicating the presence of misfolded fibrillar Aβ (Irvine and El-Agnaf, 2008). Extensive research has implicated Aβ in the pathogenesis of AD by analysis of its distinctive histopathology. For example, there is an association between Aβ plaques and neuronal cell death in the areas primarily affected in AD, such as the hippocampus and frontotemporal cortices (Masters et al., 1985; Rogers and Morrison, 1985). The vast majority of AD cases are sporadic, with no known genetic cause, however a proportion of AD cases (approximately 2.2%), are familial, and these result from inherited mutations in either APP, presenilin-1, or presenilin-2 (Wilquet and De Strooper, 2004), the latter two being required for full proteolytic activity of γ-secretase (Zhang et al., 2006). Furthermore, it is unclear whether the Aβ plaques themselves underlie this deficit. Clinicopathological studies have shown only weak correlation between plaque density and severity of cognitive impairment, and suggest that plaque pathogenesis is mediated by NFTs in late stage AD (Serrano-Pozo et al., 2011).

1.2.2 Progressive supranuclear palsy

Progressive supranuclear palsy (PSP) is a relatively rare tauopathy with a prevalence of approximately 6/100,000 (Nath et al., 2001). However, this is likely to be an underestimate as PSP is significantly under diagnosed in the clinic due to substantial variation in presentation leading to late-stage identification of cases and because it is often clinically misdiagnosed as Parkinson's disease (PD) (Schrag et al., 1999). PSP has some clinical similarities with AD, such as behavioural and cognitive impairment. However, the presenting symptoms are normally associated with motor impairments, such as ataxia, loss of balance, supranuclear vertical gaze paralysis, postural instability, and nuchal and troncular dystonia (Steele et al., 1964, 2014; Morris et al., 1999; Henderson et al., 2000), partially explaining its frequent misdiagnosis as PD.

The varied tau aggregation distribution may explain some of the symptomatic differences with AD (Zampieri and Di Fabio, 2006). In PSP, the gross structural appearance of tau-containing globose tangles are most commonly found in the basal ganglia, brainstem (particularly the midbrain focusing on supranuclear eye movements) frontal lobes and the cerebellum (a region associated with movement). Tangles are also found in the spinal cord as far down as the lumbar region in PSP, which may account for other problems such as incontinence. The gross structural appearance of tau inclusions in PSP are comprised of straight filaments compared to the other tauopathies see Table 1 (Warren and Burn, 2007).

PSP is the second most common case of degenerative Parkinsonism as first recognised by Steel and et al., (1964). Neuropathologically tangles in PSP patients are primarily localised to subcortical regions, found in both neurons and glia. Takanashi et al., (2002) found that people with PSP had a 4R:3R tau isoform ratio that varied from 1.28 to 4.04 in the globus pallidus, whereas in the frontal cortex the tau isoform ratio varied from 0.37 to 1.42 (the ratio in normal adult brain being approximately 1) (Takanashi et al., 2002). The results from that study suggest that differing tau isoform ratios might be due to variable degrees of degeneration in the different brain regions in PSP

(Takanashi et al., 2002). The predominance of highly phosphorylated aggregates of 4R tau isoforms in PSP, indicates a possible role in the progression of degeneration (Quadros et al., 2007). Unlike the characteristic triplet pattern of phosphorylated tau bands observed in AD brain on western blots, PSP exhibits a characteristic doublet of pathological tau proteins (Figure 1.3), indicating biochemical differences in tau between these two disorders (Flament et al., 1991).

1.2.3 Corticobasal degeneration

Corticobasal degeneration (CBD) is another example of a rare tauopathy with a prevalence of around 7 in 100,000 people (Mahapatra et al., 2004). CBD clinical features comprise a mixture of motor and cognitive symptoms, including dementia. Neuropathologically, CBD features tau inclusions that are both intraneuronal and extraneuronal, formed into both PHFs and SFs (Table 1) (Mahapatra et al., 2004). Like PSP, CBD is a 4R tauopathy, occurring as a result of damage to the basal ganglia and loss of myelination in the substantia nigra (Scaravilli et al., 2005). CBD can be distinguished neuropathologically from PSP by its asymmetric atrophy of frontal and parietal regions and gliosis (Scaravilli et al., 2005; Wadia and Lang, 2007). Due to the largely undiagnosed nature and low prevalence of CBD, very little is understood regarding the pathogenesis of the disease (Williams and Lees, 2009; Mathew et al., 2012).

1.2.4 Frontotemporal lobar degeneration-tau

Frontotemporal lobar degeneration-tau (FTLD-tau) is the term used for a group of non-AD degenerative dementias with focal cortical neuronal loss gliosis and tau inclusions (McKhann, 2001). FTLD-tau is a group of familial neurodegenerative tauopathies characterised by language and memory impairment, motor deficits and behavioural abnormalities, which may reflect the differential degeneration of specific brain regions (Foster et al., 1997). Autosomal inheritance of FTLD-tau suggest that *MAPT* mutations plays a critical role in these disorders, and linkage analysis has located several mis-

sense mutations in different exons of the *MAPT* gene (Hutton et al., 1998; Poorkaj et al., 1998; Spillantini et al., 1998; D'Souza et al., 1999). Subsequentially, several other missense and deletion/silent disease causing mutations in *MAPT* were found in FTLD-tau (Ghetti et al., 2015). The presence of tau as the main component of NFTs prompted the hypothesis that tau changes are causally related to neurodegeneration. This was confirmed in documented cases of FTLD-tau caused by a *MAPT* mutation (P30IL), where tau dysfunction led to neuronal death (Hutton et al., 1998; Poorkaj et al., 1998). Silent mutations have been identified to alter the 3R:4R tau ratio making tau more favourable for hyperphosphorylation (Alonso et al., 2004). Furthermore, 4R tau binds MTs more readily than 3R tau and altered tau ratios lead to distinct tauopathies (Lu and Kosik, 2001). The various missense and silent mutations in the tau gene which are associated with FTLD-tau are shown in Figure 1.5 and Table 2 (Dickson et al., 2011; Iqbal et al., 2015).

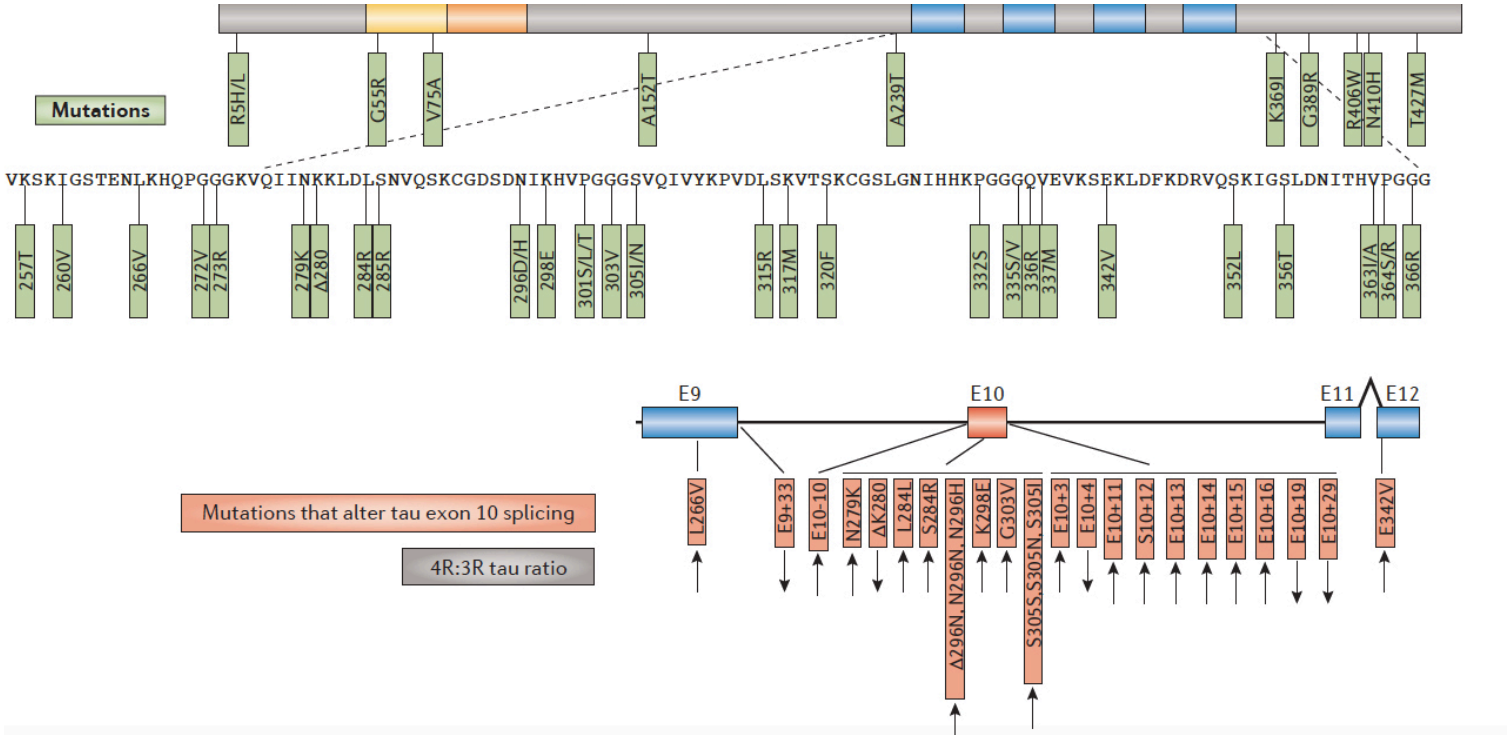

Figure 1.5: Tau mutations in FTLD-tau. Schematic image of full length human tau showing various missense mutations (green) and silent mutations (red) found in FTLD-tau. Several mutations that can affect alternative splicing of *MAPT* pre-mRNA, giving rise to isoform imbalance of the 3R:4R tau ratio (Iqbal et al., 2015).

Table 2: Classification of most common subtypes of FTLD-tau compared to Alzheimer's Disease. FTLD-tau = frontotemporal lobar dementia-tau, with *MAPT* mutation (Dickson et al., 2011).

Disorder	**Anatomy (major areas affected in typical cases)**	**Major clinical feature**
4R TAUOPATHIES		
Corticobasal degeneration	Cortex and basal ganglia	Focal cortical syndrome and parkinsonism
Progressive supranuclear palsy	Basal ganglia, brainstem and cerebellum	Atypical parkinsonism
FTLD-tau	Cortex, basal ganglia and brainstem	Focal cortical syndrome and parkinsonism
3R TAUOPATHIES		
Pick's disease	Cortex and limbic lobe	Dementia and focal cortical syndromes
FTLD-tau	Cortex, basal ganglia and brainstem	Dementia and focal cortical syndromes
3R + 4R TAUOPATHIES		
Alzheimer disease	Cortex and limbic lobe	Dementia
FTLD-tau	Cortex and limbic lobe	Dementia and psychosis

1.2.5 Pick's Disease

Pick's disease (PiD) is a rare form of neurodegeneration characterised by a distinct progressive frontotemporal dementia that accounts for approximately 2% of dementias (Takeda et al., 2012). People with PiD have clinical signs of frontal disinhibition, apathy, memory deficits, and apraxia, as well as mood disturbances and language impairments (Constantinidis et al., 2008). Neuropathologically, there is progressive cortical atrophy mainly of the anterior and frontal temporal lobes, white matter degeneration, achromatic neurons and intraneuronal lesions known as Pick bodies (PBs) in the hippocampus, selective brainstem nuclei and cerebral cortex (Yoshimura, 1989; Hauw et al., 1994; Feany and Dickson, 1996; Constantinidis et al., 2008; Takeda et al., 2012). Studies have also shown glial inclusions and NFTs in PBs (Hof et al., 1994; Probst et al., 1996; Good, 2003; Dickson, 2006). PiD brains have been described as randomly oriented straight fibrils with PBs showing the presence of loosely arranged SFs (Takauchi et al., 1984; Kato and Nakamura, 1990; Murayama et al., 1990). People with PiD exhibit a reduced 4R:3R tau ratio in the frontal gyrus, superior temporal gyrus and cerebellum. In sporadic PiD, the main pathological tau isoform is 3R (Flament et al., 1991; Delacourte et al., 1996), although immunohistochemically examination also identified the 4R tau isoform in PiD (Ishizawa et al., 2000).

1.3 Phosphorylation of tau

Tau protein has a high propensity to become phosphorylated, the longest human CNS tau isoform contains 80 serine and threonine residues, as well as 5 tyrosine residues, (Goedert et al., 1989a). Human 2N4R tau can be phosphorylated on at least 45 different sites, including serine, threonine and tyrosine residues (Hanger et al., 2007, 2009; Gendron and Petrucelli, 2009). Tau extracted from control adult human brain at post-mortem, contains 2-3 phosphates per mole of tau (Köpke et al., 1993). In AD tau phosphorylation is increased 3-4 fold, to 8 phosphates per mole (Köpke et al., 1993; Mawal-Dewan

et al., 1994). In control brain, the extent of tau phosphorylation is high in fetal brain and decreases with age, in tauopathies however, the degree of tau phosphorylation increases with disease progression (Mawal-Dewan et al., 1994; Rösner et al., 1995; Buée et al., 2000). Highly phosphorylated tau may represent a dysfunctional form of tau as it neither binds/promoted MT stability, in fact, it inhibits/disrupts assembly of MTs (Khatoon et al., 2002; Alonso et al., 2006). Furthermore, several studies have implicated pathological tau species, including synthetic tau fibrils to sequester and drive soluble tau into NFTs and tangle like inclusions in both cell cultures and animal models (Alonso et al., 1996; Clavaguera et al., 2009; Frost et al., 2009; Nonaka et al., 2010; Guo and Lee, 2013; Iba et al., 2013). However, the exact mechanisms leading to neurodegeneration in the tauopathies are not yet known.

One proposed mechanism for the neurodegeneration observed in AD and other tauopathies is the removal of tau from MTs caused by increased tau phosphorylation. The removal of tau from the MTs destabilises them, leading to disruption of protein and organelle transport throughout the axon (Roy et al., 2005). The likelihood of further tau processing increases as the amount of free cytosolic tau increases due to the dissociation of tau from MTs. Another proposed neurodegenerative mechanism is that increased tau phosphorylation may result from a reduction in protein phosphatase activity, such as protein phosphatase 1 (PP1), PP2A and/or PP2C (Ballatore et al., 2007; Spillantini and Goedert, 2013; Driver et al., 2014). Notably, PP1 and PP2A activity are diminished by 20-30% in AD brain (Spillantini and Goedert, 2013; Iqbal et al., 2015) suggesting a potential role for phosphatases in AD (Gong et al., 1993; Liu et al., 2005; Rahman et al., 2005).

Although the link between tau phosphorylation and the propensity of tau to aggregate is unclear (Lippens et al., 2007), preventing tau phosphorylation with kinase inhibitors at AD-relevant epitopes diminishes tau aggregation and is neuroprotective in transgenic mutant mice (Hong et al., 1997; Pérez et al., 2003; Noble et al., 2005). The spectrum of tau phosphorylation identified with antibodies specific for phosphorylated tau and by mass spectrometry is partially summarised in Figure 1.6 and to a fuller extent in: (http://bit.ly/1SpzgoL).

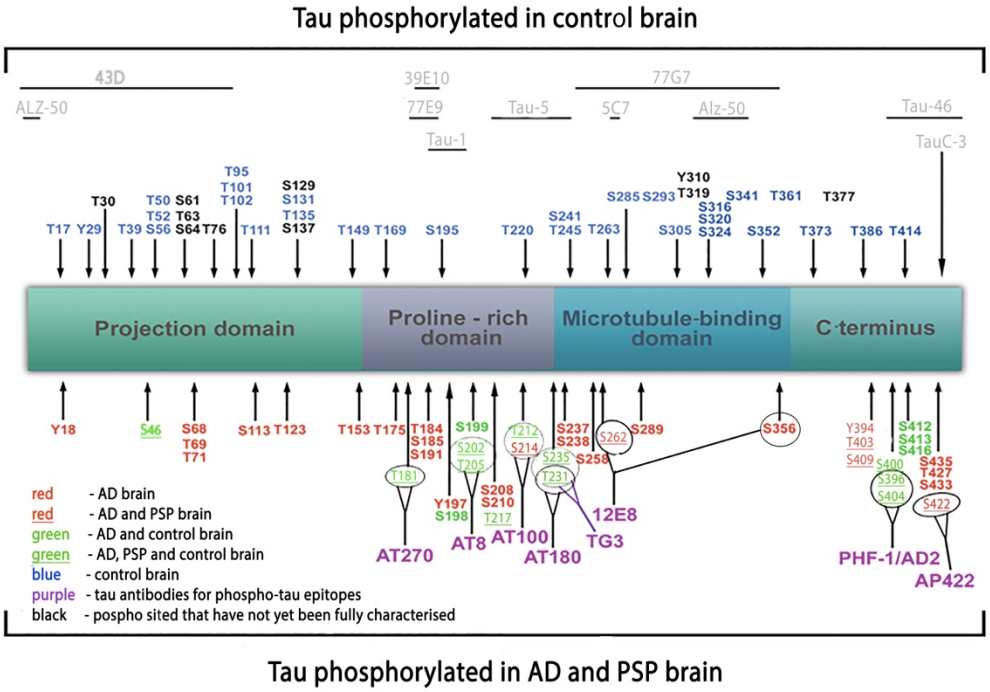

Figure 1.6: Phosphorylation sites and epitopes on tau protein in control AD and PSP brain. Amino acids phosphorylated in control (blue) AD (red) control and AD (green) PSP and AD (red) and PSP, AD and control (green) and not yet fully characterised sites (black). Monoclonal tau antibodies specific for phosphorylated tau epitopes (purple) and non-phosphorylated and phosphorylation independent tau epitopes (grey). Alz-50 (aa 2–10, aa 312–342), 43D (aa 1–100), 77E9 (aa 185–195), 39E10 (aa 189–195), Tau-5 (aa 210–230), 5C7 (aa 267–278), Tau-1 (aa 195, 198, 199 and 202), 77G7 (aa 270–375), Tau-46 (aa 404–441), TauC-3 (tau cleaved at aa 421) (adapted from Šimić et al., 2016).

1.3 Tau kinases

The overall state of tau protein phosphorylation is a function of the balance between the activities of tau protein kinases and phosphatases. Phosphorylation of tau can affect the ability of tau to bind to and stabilise MTs and tau is therefore a substrate for several different protein kinases (Singh et al., 1994; Johnson and Stoothoff, 2004; Avila, 2006; Hanger et al., 2009). A large number of protein kinases have been implicated in the abnormal phosphorylation of tau, including glycogen synthase kinase 3α/β (GSK3α/β), cyclin-dependent kinase 5 (Cdk5), protein kinase A (PKA), calcium/calmodulin-dependent protein kinase-II (CaMKII), mitogen-activated protein (MAP) kinase, extracellular signal-regulated kinase (ERK 1/2), p38 MAPK, c-Jun N-terminal kinase (JNK), prostate-derived sterile 20-like kinases (PSKs) and other stress-activated protein kinases further sumarised here: (http://bit.ly/1SpzgoL) (Baumann et al., 1993; Pei et al., 2003; Ballatore et al., 2007; Martin et al., 2013; Tavares et al., 2013). Therefore, targeting tau kinases to reduce tau phosphorylation may be of therapeutic benefit (Hanger et al., 2009). The C-terminal region of tau comprises the KXGS motifs (Figure 1.7) which can be phosphorylated by kinases such as the MT affinity-regulating kinase (MARK), CaMKII, PKA and PSK (Johnson and Stoothoff, 2004; Hanger et al., 2007; Tavares et al., 2013). Phosphorylation of KXGS motifs can reduce interaction between tau and MTs (Biernat et al., 1993; Biernat and Mandelkow, 1999) and may constitute an early event in the pathogenesis of tauopathy (Nishimura et al., 2004).

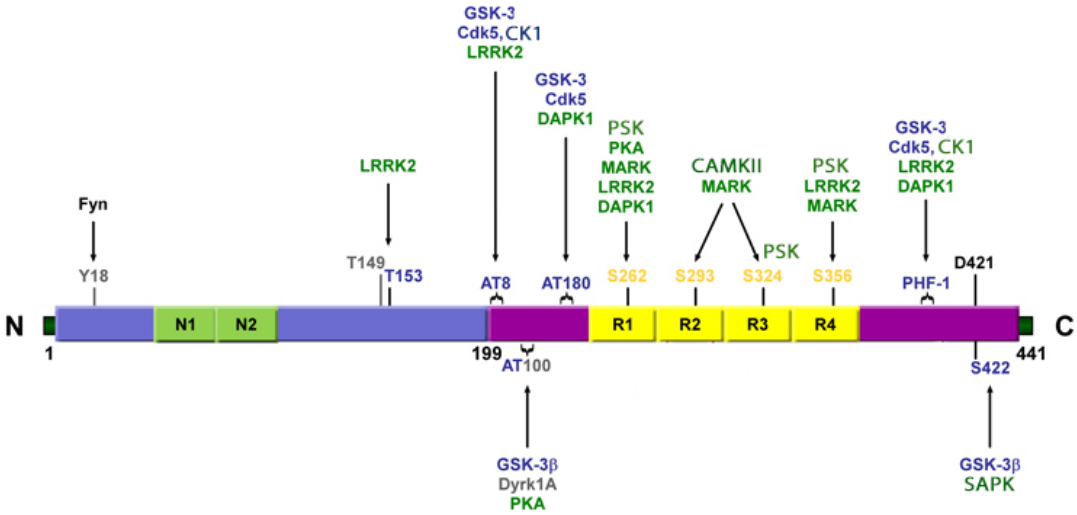

Figure 1.7: Protein kinases phosphorylating tau. The diagram illustrates the sites identified on tau as being phosphorylated by several candidate tau kinases. KXGS motifs (yellow text), and other sites (represented in grey) can be phosphorylated by proline-directed kinases (represented in blue) and non-proline directed Ser/Thr kinases (represented in green). Antibody epitopes AT8, AT100, AT180, and PHF-1 comprise dual and triple serine/threonine residues (indicated by brackets). GSK3: Glycogen synthase kinase 3β/α, Cdk5: Cyclin-dependent kinase5; CK1: casein kinase 1, MARK: MT affinity-regulating kinase; LRRK2: leucine-rich repeat kinase2; DAPK: Death-associated protein kinase; Dyrk1A: dual-specificity protein kinase 1, SAPK: stress-activated protein kinase, PSK: Prostate-derived Sterile 20-like kinases (adapted from Tenreiro et al., 2014).

1.4.1 Proline-directed protein kinases and non-proline directed protein kinases

Several phosphorylation sites on tau are immediately followed by a proline residue, suggesting that these are phosphorylated by proline-directed protein kinases (PDPKs). Examples of candidate tau PDPKs include GSK3α/β, Cdk5 and ERK1/2, all of which have been shown to phosphorylate tau at similar sites in AD (Wang et al., 1998; Anderton et al., 2001; Liu et al., 2002; Hanger et al., 2009). GSK3α/β and Cdk5 are expressed abundantly in control brain (Woodgett, 1990) and have previously been linked to all stages of pathology in tauopathies particularly AD (Hanger et al., 1992; Tsai et al., 1993; Lew et al., 1994; Pei et al., 1999). Non-PDPKs also phosphorylate tau at numerous sites. For instance, PKA phosphorylates tau at Ser214, Ser217, Ser396/404 and at Ser416 (Litersky et al., 1996; Wang et al., 1998; Anderton et al., 2001; Robertson et al., 2004; Hanger et al., 2007), whereas PKA and MARK phosphorylate tau at Ser262 (Scott et al., 1993; Drewes et al., 1997). CaMKII phosphorylates tau at Ser262/356 and Ser416 (Steiner et al., 1990; Singh et al., 1996; Sironi et al., 1998). Interestingly, the phosphorylation of tau by non-PDPKs substantially increases GSK3 and Cdk5 phosphorylation, suggesting the possibility of tau priming by non-PDPKs (Singh et al., 1995a, 1995b; Wang et al., 1998; Cho, 2003).

1.4.1.1 Glycogen synthase kinase 3

Glycogen synthase kinase 3 (GSK3) has been proposed as one of the most significant tau kinases and it exists as two structurally similar isoforms, GSK3α and GSK3β. GSK3 exhibits unconventional characteristics whereby it is a constitutively active PDPK, with its substrate optimally requiring pre-phosphorylation by another kinase. The GSK3 enzyme is inhibited by phosphorylation in response to stimulation of the insulin and Wnt signalling

pathways. GSK3 is involved in several cellular mechanisms including gene transcription, glycogen metabolism, apoptosis and MT stability (Welsh and Proud, 1993; Troussard et al., 1999; Anderton et al., 2001; Brion et al., 2001; Turenne and Price, 2001). Although both GSK3α and GSK3β phosphorylate tau most research has been based around GSK3β. GSK3β has previously been linked to long term potentiation (LTP) impairment, Aβ production, inflammation and neuritic damage (Hooper et al., 2008; DaRocha-Souto et al., 2012). Overexpressing GSK3β in mice transgenic for human tau, results in tau hyperphosphorylation at sites similar to those seen in tau in AD brain, as well as reducing the axonopathy compared with mice expressing only human tau (Spittaels et al., 2000). Interestingly, in the GSK3/tau double transgenic mice, motor impairment is less severe than in mice overexpressing human tau alone. Furthermore, inhibition of GSK3 by lithium attenuated phosphorylation in double transgenic and mutant human tau overexpression models (Hong et al., 1997; Pérez et al., 2003; Ballatore et al., 2007). Non-specific kinase inhibition by the small molecule non-specific kinase inhibitor, K252a, reduced tau aggregate formation and ameliorated motor symptoms in P301L tau transgenic mice (Le Corre et al., 2006). Unfortunately, GSK3β inhibitors tested in phase II clinical trials, including lithium, trideglusib and valproic acid have so far been unsuccessful (Iqbal et al., 2015). This could be due to the fact that GSK3β is a multifunctional kinase with many diverse roles in the CNS (e.g., apoptosis and neuroinflammation). These results imply the need for more specific targets to selective inhibit functions of GSK3β-mediated tau phosphorylation or inhibition of other kinases modifying tau at different epitopes (e.g. MARK2 and LRRK2) (Tenreiro et al., 2014; Iqbal et al., 2015).

1.4.1.2 Cyclin-dependent kinase 5

Cdk5 is another major candidate tau kinase, which may be key to the underlying tau pathology seen in tauopathies. Cdk5 is responsible for phosphorylating tau at epitopes which are known to be usually over

hyperephosphorylated in AD (Paudel et al., 1993; Ohshima et al., 1995; Castro-Alvarez et al., 2014). Overexpression of Cdk5 in mutant tau mice leads to tau aggregation and cortical NFTs (Noble et al., 2003), as well as significant memory decline and neurodegeneration (Cruz et al., 2003). In order for Cdk5 to be activated, calcium influx through N-methyl-D-aspartate receptor (NMDA) receptors activates calpain which cleaves Cdk5 activators p35 to p25 and p10 (Patrick et al., 1999). The p35/Cdk5 subsequentially phosphorylates p35 and becomes degraded through the proteasome (Patrick et al., 1998). P25 becomes a stable complex with Cdk5, where it may increase tau phosphorylation due it increased activation in neurodegenerative tauopathies (Cruz et al., 2003). Interestingly, when overexpressing p25 in transgenic mice, tau becomes hyperphosphorylated (Cruz et al., 2003; Noble et al., 2003). Cdk5 may also indirectly lead to tau phosphorylation via GSK3β. Cdk5 can induce phosphorylation and activation of protein kinase B (PKB/Akt) (a serine/threonine kinase that is involved in cell survival pathways thereby increasing tau phosphorylation of tau in tauopathies (Li et al., 2003). The phosphorylation of Ser235 and SerSer400 therefore leading to an even greater increase in tau phosphorylation by GSK3β (Figure 1.8) (Li et al., 2006).

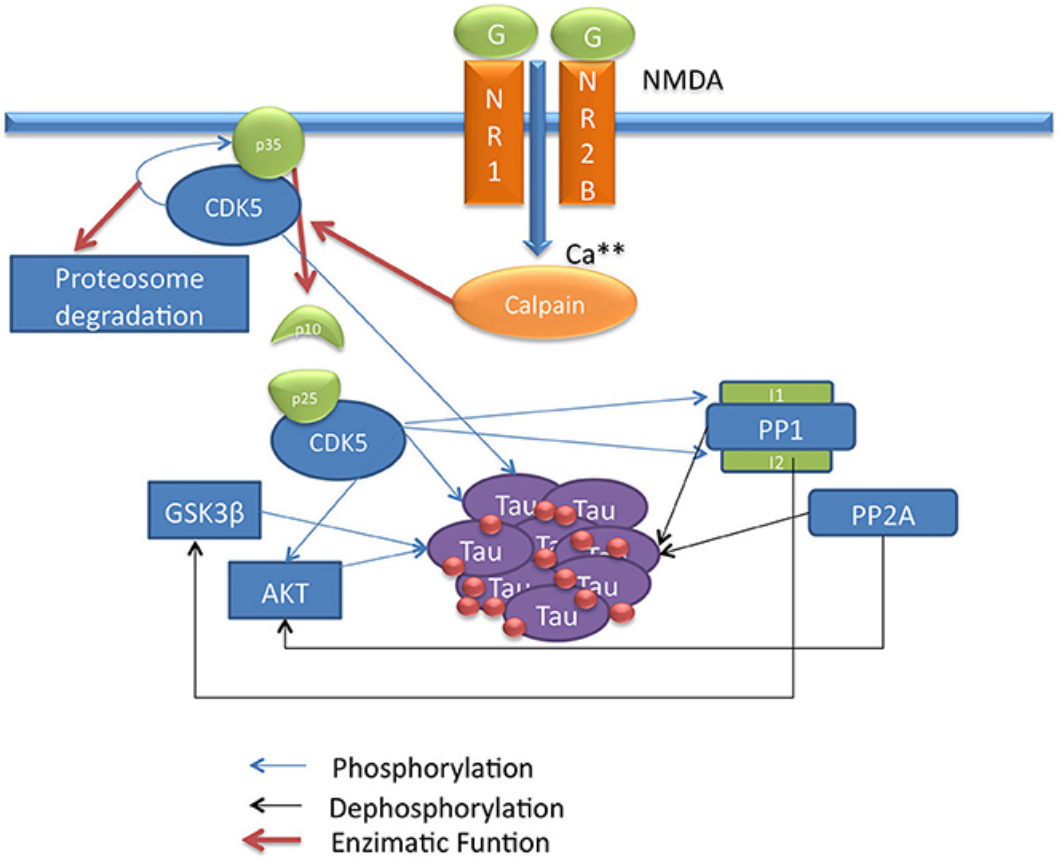

Figure 1.8: Schematic diagram of Cdk5 signalling pathway in tau phosphorylation. Diagram shows direct and indirect ability of Cdk5 to phosphorylate tau.CDK5: cyclin kinase 5 PP1: protein phosphatase 1, PP2A: protein phosphatase 2A, NMDA NR1/2b: N-methyl-D-aspartate receptors NR1/2b, GSK3: glycogen synthase kinase 3, AKT: protein kinase B (Castro-Alvarez et al., 2014).

1.5 Tau truncation and tau fragments in tauopathies

Tau is tightly regulated and exhibits several different and complex post-translational modifications including phosphorylation, isomerisation, ubiquitination, *O*-linked β-*N*-acetylglucosamine acetylation (O-GlcNAc), oxidation nitration glycosylation, acetylation and proteolytic cleavage (Wischik et al., 1988b; Goedert et al., 1992a; Novak et al., 1993; Alonso et al., 2001; Gorath et al., 2001; Liu et al., 2004a; Guillozet-Bongaarts et al., 2005; Mondragón-Rodríguez et al., 2008, 2014; Min et al., 2010; Kolarova et al., 2012). Although tau aggregates are a seminal diagnostic neuropathological feature of tauopathies, the generation of tau fragment can be a toxic event regardless of tau aggregation status. Truncation is a post-translational modification of tau that occurs in AD and other tauopathies, either at the N- or C–terminus, or at both termini (Novak et al., 1993; Zilka et al., 2006; García-Sierra et al., 2008; Wang et al., 2010; Derisbourg et al., 2015). Truncation of tau increases during disease progression in tauopathies and this can influence neurofibrillary pathology as well as phosphorylation and accumulation of misfolded insoluble forms of tau (Kovacech and Novak, 2010; Wang et al., 2010). Although monomeric tau is likely to be a proteosomal substrate, there is increasing evidence that tau is a substrate for a wide range of proteases.

1.5.1 Proteases responsible for tau truncation

Several proteases have been shown to act on tau, including thrombin (Olesen, 1994; Wang et al., 1996b; Khlistunova et al., 2006), aminopeptidases (Karsten et al., 2006; Sengupta et al., 2006), human high temperature requirement serine protease A1 (HTRA1) (Tennstaedt et al., 2012), calpains (Canu et al., 1998; Xie and Johnson, 1998), and caspases (Chung et al., 2001; Fasulo et al., 2002; Horowitz, 2004). Proteolysis can lead to the generation of potentially toxic tau fragments which may play a role in disease pathogenesis (Figure 1.9). Tau fragments may be trafficked into cellular compartments and cause cell

death, neuronal loss and/or tau aggregation in a variety of tauopathies (Wischik et al., 1988b; Arai et al., 2004; Zilka et al., 2006; Igaz et al., 2008).

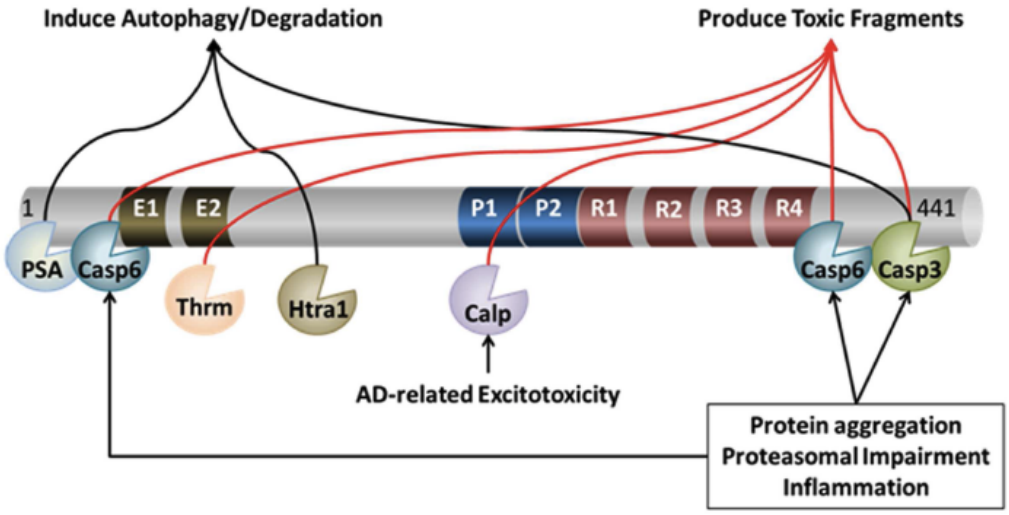

Figure 1.9: Schematic representation of proteolytic cleavage of tau. Tau is subject to cleavage at different proteolytic sites by a number of different proteases. Cleavage can lead to either exacerbation of or protection from neuronal loss. For instance, cleavage by calpains (Calp; purple) or caspases (Casp; dark green) and thrombin (Thrm; beige) can lead to the production of toxic tau species that can exacerbate pathology. However, cleavage of tau by puromycin-sensitive aminopeptidase (PSA), Human high temperature requirement serine protease A1 (Htra1) and often also caspase 3 can generate fragments for degradation potentially protecting neurons from tauopathy related neuronal death (Chesser et al., 2013).

1.5.2 Tau fragmentation and implications for tauopathies

Several previous studies have identified the importance of tau fragments present in human tauopathy brains, with some tau fragments also appearing in cultured cells in response to Aβ (Gamblin et al., 2003; Arai et al., 2004; Guillozet-Bongaarts et al., 2005; Khlistunova et al., 2007; Delobel et al., 2008; García-Sierra et al., 2008; Amadoro et al., 2010; Hanger and Wray, 2010; Ferreira and Bigio, 2011).

Much *in vitro* research has centred on the pro-apoptotic caspases, since tau contains three consensus sequences for caspase cleavage, namely residues Asp22-Asp25, Asp345-Asp348 and Asp418-Asp421 cleaved by caspase-3. Of these residues, Asp421 appears to be the preferred cleavage site in tau, and mutation of this residue results in resistance to toxicity in neuroblastoma cells exposed to apoptosis-inducing agents (Chung et al., 2001; Fasulo et al., 2002; Gamblin et al., 2003; Rametti et al., 2004; Rissman et al., 2004; Guillozet-Bongaarts et al., 2006). The expression of an N-terminal tau fragment truncated at Asp421 (Δtau) in BL21(DE3) cells, increased the extent of cell death in comparison to full-length tau, suggesting a possible toxic gain of function when tau is cleaved at this site (Chung et al., 2001). A variety of different tau constructs have been used in attempts to generate tau aggregates in transfected cells and mammalian models. However, these studies have required either mutant forms of truncated tau, or additional treatment of cells with agents that promote tau aggregation (Table 3) (Zilka et al., 2006; Amadoro et al., 2010; Filipcik et al., 2012). These combined results suggest a need for expression of more pathophysiologically relevant forms of human truncated tau to understand the mechanisms underlying the role of tau in the pathogenesis of the tauopathies.

Table 3:Characteristics of tau fragments investigated in cell and animal models. Summary of several existing tau fragments, their presence in tauopathy human brain, aggregation status and accordant models. N/A: not available.

Tau fragment (sequence)	Presence in tauopathy brain	Intact C-terminus	Aggregates in transfected cells	Phosphorylation increases aggregation	Transgenic in vivo model?	Reference
Δtau (1-421)	Yes	No	Only when co-transfected with GSK3	Yes	No	(Chung et al., 2001; Cho and Johnson, 2004)
Tau_{RD} and Tau_{RD} ΔK280 (244-372)	No	No	2-9% of stably expressing transfected cells	Phosphorylation precedes aggregation	Yes	(Mocanu et al., 2008)
TauRD ΔK280 with I277P and I308P (244-372)	No	No	No	No	Yes	(Khlistunova et al., 2006)
NH2 fragment	Yes	No	No	N/A	No	(Amadoro et al., 2010)
3R tau fragment (residues 151-391)	No	Yes	N/A	N/A	Yes	(Filipcik et al., 2012)
4R tau fragment (residues 151-391)	Yes	Yes	N/A	N/A	Yes	(Zilka et al., 2006)
Tau35	Yes	Yes	Yes	Yes	Yes	(Wray et al., 2008; Bondulich et al., 2016)

Several previous studies of human post-mortem tissue have identified the importance of tau fragments present in human tauopathy brains in which there is an overproduction of 4R tau isoforms (PSP, CBD and the majority of FTDP-17T cases) (Arai et al., 2004; Wray et al., 2008). Antibodies specific for Δtau label tangles in the CA1 (cornus ammonis 1) region of the hippocampus of AD brain (Gamblin et al., 2003). However, labeling of inclusions in other tauopathies is much less intense, predicting differences in the proportion of neural and glial pathology in these related disorders (Guillozet-Bongaarts et al., 2007). One study, using a novel monoclonal antibody DC39N1, specific for the first N terminal insert N1 (residues 45-73) (Figure 1.1), demonstrated that the N-terminus of tau, particularly the N1 insert encoded by exon 2, is present in a sub-population of tau in NFTs (Amadoro et al., 2004; Soltys et al., 2005). Notably, these N-termini, when released during truncation events, could have a deleterious effect on neurons (Amadoro et al., 2004, 2014). Various other forms of cleaved tau have been shown to initiate tau aggregation which suggests that this process is an integral part of disease pathogenesis in the tauopathies (Wischik et al., 1988b; Chung et al., 2001; Arai et al., 2004; Zilka et al., 2006; Zhang et al., 2009, 2014; Melis et al., 2015). Amador and colleagues (2010) identified a 17 kDa, N-terminal tau fragment that is produced in response to Aβ oligomer exposure in cultured mature SH-SY5Y human neuroblastoma cells and in rat hippocampal neurons. This tau fragment is responsible for mitochondrial NH2-derived tau peptide degeneration of synapses (Amadoro et al., 2010). Furthermore, in *Drosophila*, expression of a C terminal truncated tau showed greater stability, degrade faster and seemed less toxic than full length tau or N-terminal truncated tau due to the unstable nature of C-terminal truncated fragments (Geng et al., 2015). However, the hypothesis of which fragments are more toxic remains largely unclear and therefore further investigation is required to fully establish the relationship between truncated tau species and tauopathies.

1.5.3 Tau35 fragment in human tauopathy

A novel C-terminal tau fragment (termed Tau35) has been identified in post-mortem human brain in both PSP and CBD and FTLD-tau (4R tauopathies and 4R mutation cases) (Wray et al., 2008). Tau35 was absent from AD (equal 4R:3R tauopathy), PiD (3R tauopathy), and control human brain. Tau35 co-enriches and partially co-purifies with full-length insoluble tau in these same brain fractions (Wray et al., 2008). Using antibody epitope scanning, it was found that Tau35 is N-terminally truncated and corresponds to a 4R tau isoform (Figure 1.10) (Wray et al., 2008). Mass spectrometric analysis revealed that Tau35 lacks the N-terminus and that the C-terminus of Tau35 precisely matches that of full-length tau (Wray et al., 2008). Therefore, compared to full length tau, Tau35 corresponds to an insoluble fragment of tau that spans residues in the C-terminal half of 4R tau with an intact C-terminus (Figure 1.10). Phosphorylation analysis indicated that more than 75% of the phosphorylation sites identified previously in insoluble tau from AD brains resides in the sequence corresponding to Tau35 (Hanger et al., 2002, 2007; Wray et al., 2008). The characterisation of a novel murine model expressing the Tau35 fragment is described in more detail later in this thesis (Table 3).

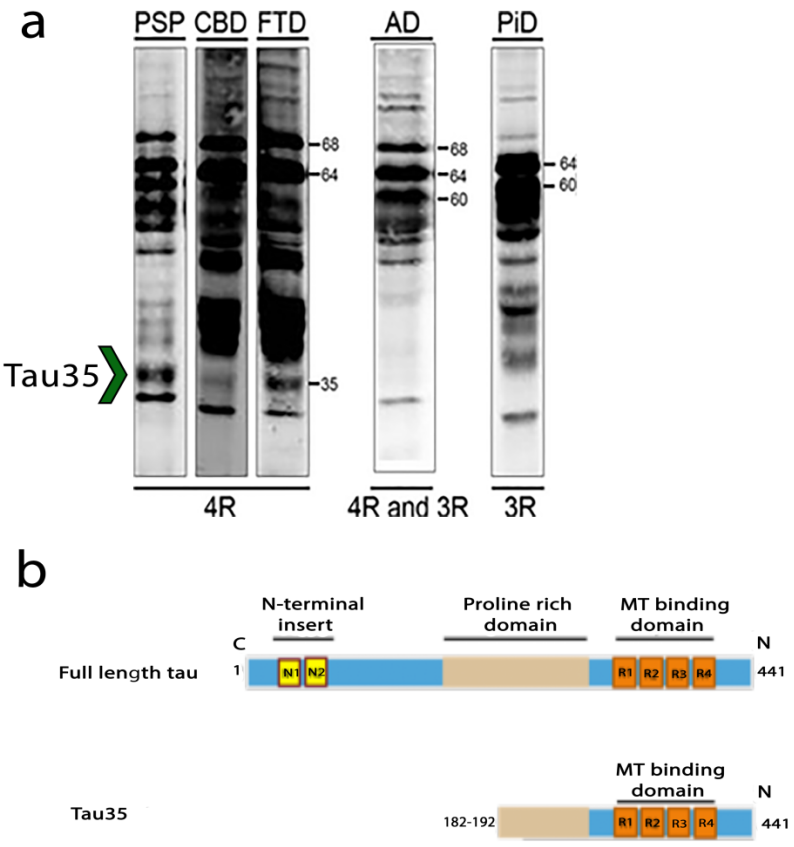

Figure 1.10: Tau35 fragment linked to tauopathies with 4R isoform imbalance. (a) Western blots probed with an antibody which recognises the C-terminus of tau (TP70) identified a 35 kDa (green arrowhead) truncated tau species only in the insoluble brain fractions of 4R tau isoform-related disorders (progressive supranuclear palsy, PSP; corticobasal degeneration, CBD; frontotemporal dementia, FTD), but not in Alzheimer's disease (AD), 3R tau isoform-predominant Pick's disease (PiD), or control brain. Intact tau in the insoluble fractions is indicated at 60-68 kDa **(b)** Structure of full-length tau and Tau35 including four microtubule-binding domains (orange), truncation at N-terminus within proline-rich domain (beige) and an intact C-terminus (Hanger & Wray, 2010; Wray et al., 2008).

1.6 Tau degradation

The ubiquitin–proteasome system (UPS) and the autophagy-lysosomal system are the two major pathways responsible for the degradation of intracellular proteins. Previous research has focused primarily on the proteasome because this was considered to be the primary pathway for tau degradation (David et al., 2002; Yen, 2011; Rodríguez-Martín et al., 2013). Nevertheless, autophagy and lysosomal degradation of tau is becoming of increasing interest (Feuillette et al., 2005; Lee et al., 2013). However, the exact contribution of each of these pathways to tau clearance is still not fully understood and is of great interest for understanding the mechanisms underlying human tauopathies. For the purpose of this thesis, the main focus will be on autophagy and lysosomal degradation.

1.6.1 Autophagic degradation of tau

Autophagy is the catabolic process involving lysosomal degradation of cytoplasmic material. Whereas the proteasomes are mostly responsible for short lived proteins, autophagy degrades a number of long lived proteins, as well as damaged organelles, such as mitochondria and peroxisomes (Johansen and Lamark, 2011), and pathogenic bacteria (Ivanov and Roy, 2009; von Muhlinen et al., 2012). There are three major forms of autophagy: microautophagy, macroautophagy and chaperone mediated-autophagy. The most common of these sub-types is macroautophagy, which is discussed here and referred to as autophagy. Autophagic degradation involves the formation of a double membraned autophagophore, which expands to allow engulfing of cytoplasmic substrates, including tau, for degradation. Once formed into an enclosed vesicle (autophagosome), this is trafficked to the lysosome, where it fuses to form the autophagic vacuole (AV). Lysosomal cathepsins then degrade the inner membrane of the AV, as well as its contents (Figure 1.11) (Chesser et al., 2013). It has also been observed that increased accumulation of AVs is apparent in AD brains and mouse models of tauopathy, indicating abnormal

autophagy in neurons (Lin et al., 2003; Yu et al., 2004; Nixon et al., 2005). The autophagosome is labelled by the MT associated protein 1A/1B light chain 3 (LC3) (He and Klionsky, 2009). Cytosolic LC3 (LC3-I) is conjugated to phosphatidylethanolamine (PE) to localise the resultant LC3-II (a LC3-PE conjugate) on the autophagosome before it fuses with the lysosome (Kabeya, 2000). As intra-autophagosomal LC3-II is degraded by lysosomes, it is frequently used as a marker for autophagosome formation, and its degradation is to monitor autophagic flux (Tanida et al., 2005).

Other important components of the lysosomal-autophagy process include, sequestosome 1 (p62/SQSTM1) which acts as a receptor, facilitating the removal of damaged proteins and organelles by lysosomes (Bjørkøy et al., 2006; Ichimura et al., 2008). P62 has previously been shown to exist in NFTs, indicating that p62 may correlate with the appearance of tauopathy (Reynolds et al., 2007; Alonso et al., 2008). Indeed, CBD and PSP brains show abnormal accumulation of p62, as well as LC3 and colocalisation with hyperphosphorylated tau (Piras et al., 2016). However, LC3-II can often be difficult to interpret as it is itself degraded by autophagy and accumulation of AVs in AD brain may reflect defective lysosomal clearance, rather than induced autophagy. Therefore, it is difficult to determine whether this increase in AVs reflects excessive autophagosome formation and/or impaired autophagosome degradation at different stages of tau pathology (Lee et al., 2013).

The lysosomal enzyme cathepsin D (an aspartyl protease), degrades tau in cultured hippocampal cells (Bednarski and Lynch, 2002). Treating hippocampal cells with chloroquine impairs cathepsin D function, and this has been linked to increased full-length tau and accumulation phosphorylated tau (Bednarski and Lynch, 2002; Bendiske and Bahr, 2003). Incubating rat tau with cathepsin D *in vitro* resulted in an increase in cleaved tau fragments of sizes 23-29 kDa in hippocampal cultures (Bednarski and Lynch, 2002). Interestingly, cysteine protease inhibition prevented generation of these tau fragments by cathepsin D, suggesting a possible role for cathepsin D in degrading tau outside the lysosome, although this is likely to occur at a very reduced rate since a previous study showed limited proteolytic activity of cathepsin D above pH 6.0 (Johnson et al., 1991).

It has previously been shown that both LC3-I and LC3-II interact with MT-associated proteins, such as MAP1A/B, and this facilitates their association with MTs (Mann and Hammarback, 1994; Wang et al., 2006). MT-associated proteins regulate the dynamics of tubulin dimers constantly polymerising and depolymerising, facilitating the trafficking of organelles along MT tracks (Desai and Mitchison, 1997; Downing, 2000; Nogales, 2001; Heald and Nogales, 2002). MTs are constantly modified after assembly to enhance their function. One such modification is acetylation, which results in an increased flux of vesicles along acetylated MTs (Bulinski, 2007; Dompierre et al., 2007). Recently Xie and colleagues showed that acetylated MTs are required for fusion of autophagosomes with lysosomes to form autolysosomes (Xie et al., 2010), providing an important link between acetylation and autophagic degradation of substrate proteins. It is becoming evident that the autophagy-lysosomal pathway plays a key role in the clearance of phosphorylated tau in the tauopathies. Furthermore, this suggests that elevated autophagy may be beneficial for neurons affected by tauopathy by preventing accumulation of tau aggregates.

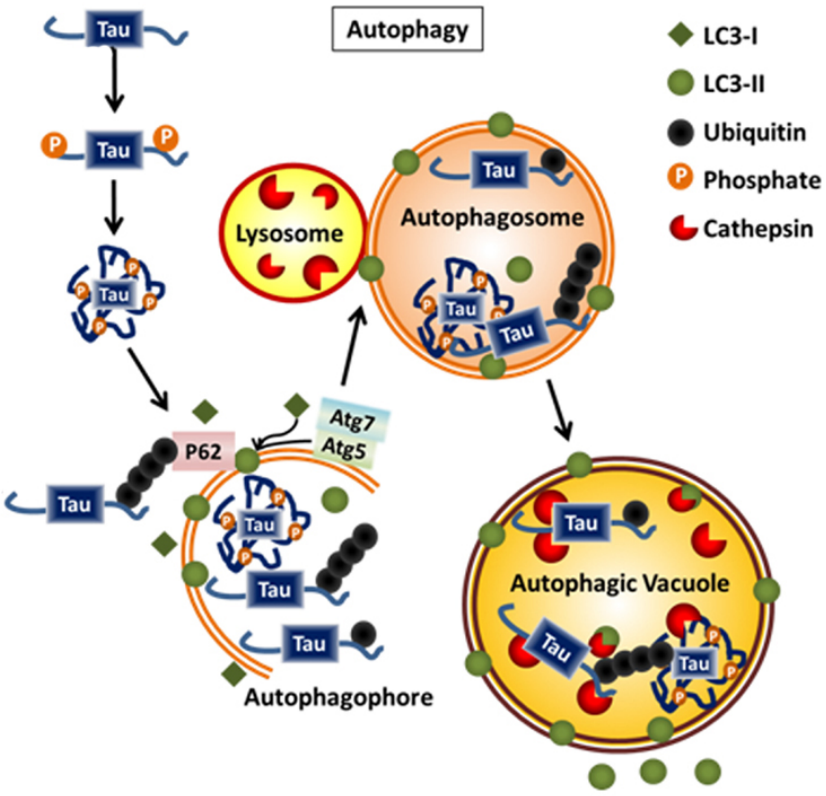

Figure 1.11: Schematic representation of tau degraded via autophagy. The nature of post-translational modification or aggregation determines by which system tau is degraded. If tau is truncated or hyperphosphorylated, it can bind to ubiquitinated membrane proteins (such as p62), bind to cytosolic LC3 which gets conjugated to LC3-II, become internalised into autophagophores, which then merge with lysosomes to form the autophagic vacuole where tau and LC3-II are degraded by cathepsins. Once the contents are fully degraded the lysosome is regenerated via acidification through vascular ATPase's (adapted from Chesser et al., 2013).

1.7 Tau propagation

Tau propagation is now a well characterised phenomenon through which tau pathology may systematically spreads through defined brain regions (Frost et al., 2009). The original concept developed from human prion disease and animal models of transmissible diseases, such as Creutzfeldt-Jakob disease in humans and scrapie in sheep, whereby brain extracts from infected hosts introduced into unaffected individuals was able to transmit the disease (Prusiner, 1982). In AD, tau exhibits a consistent pattern of spreading throughout the brain (Figure 1.4, Braak staging I-VI) (Braak and Braak, 1991). Different tauopathies exhibit a somewhat different pathological cell-type, or regional propagation pattern and this difference may potentially be due to differing metabolic rates due to oxidative stress (Gerst et al., 1999; Aoyama et al., 2006; Yan et al., 2013), differing neuronal vulnerability such as loss of myelination (Braak et al., 1996), or even differing vulnerability to toxins (Nave and Werner, 2014).

In vivo a number of factors can influence tau propagation, including the source of the seed protein, the type of tau isoform, the precise tau species and the passage of time (Figure 1.12) (Gerson and Kayed, 2013; Ahmed et al., 2014; Gerson et al., 2014; Medina and Avila, 2014). Injection of brain homogenates from six different tauopathies (AD, PiD, PSP, CBD, tangle only dementia and argyrophilic grain disease) into the ALZ17 mouse line (expressing the longest human brain tau isoform of 441 amino acids), resulted in tau-positive inclusions 6 months post-injection, which progressively spread over time (Clavaguera et al., 2013). With the exception of PiD, the tau inclusions resembled those seen in the specific human disease from which they were derived, indicating the disease-related spreading and seeding of human inclusions in the mice (Figure 1.13) (Clavaguera et al., 2013). Control injections of homogenates from the brains of people exhibiting amyloidosis post-mortem failed to show tau or amyloid pathology in these mice. Interestingly following injection of PiD brain homogenate, mice developed only very mild pathology, which did not resemble PD pathology. This was possibly due to the fact that

that PiD is a 3R tauopathy and as ALZ17 mice are 4R human tau overexpressing mice, it may be that 3R tau cannot seed aggregation of 4R tau. Tau aggregation can also be induced by recombinant tau fibrils in cells and tau PS19 transgenic mice, which express human 1N4R tau with the P301S mutation, driven by the murine prion protein promoter (Guo and Lee, 2013; Iba et al., 2013).

Emerging evidence suggests that tau spreads through neuronal connectivity. When inoculating tau aggregates from human tauopathy brains or from transgenic mice, this triggered a time-dependent seeding and spreading of tau pathology to synaptically connected regions in P301S tau-expressing transgenic mice as well as in wild-type mice (Clavaguera et al., 2009; Holmes and Diamond, 2014). However, the exact type of tau species and precise mechanism underlying tau transmission remain to be elucidated with some summarised in Figure 1.12.

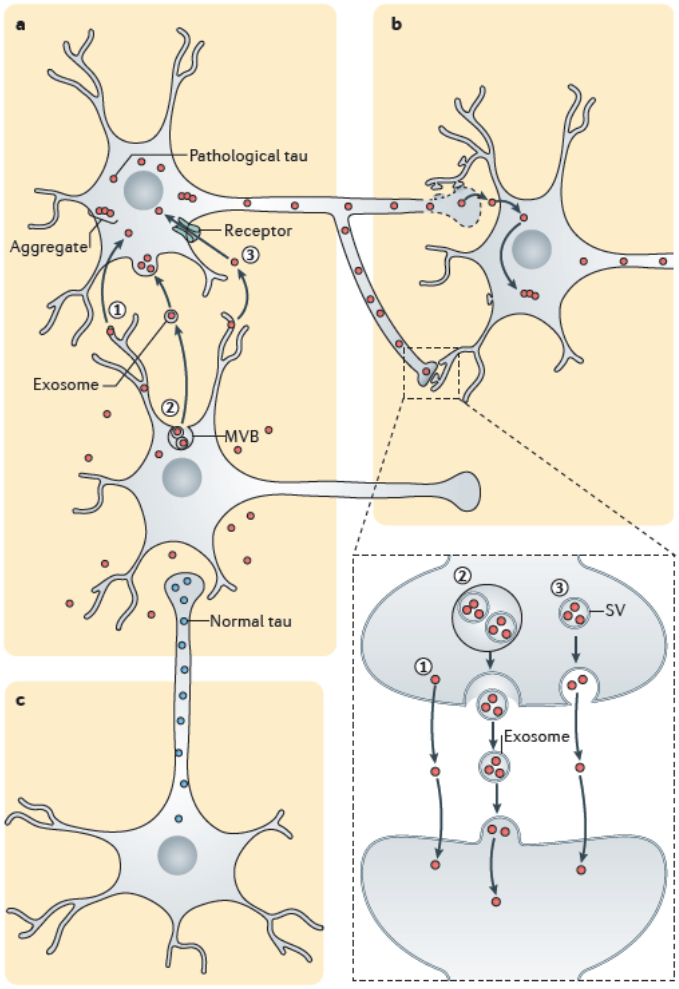

Figure 1.12: Schematic diagram of potential mechanisms of neuronal tau propagation. (a) Tau transmission occurs through a proximity-dependent transynaptic manner whereby donor neurons release tau and seed through exocytosis (1 and 3), or vesicle such as exosomes derived from multivesicular bodies (MVB) (2) which can deliver their contents into recipient adjacent neurons. Tau can also be internalised by endocytosis (1), or through receptors (3). **(b)** Degenerating neurons can lead to leakage of the presynaptic membrane, allowing presynaptic tau seeds to diffuse across the synaptic cleft (top synapse). Tau may be released from the presynaptic terminal via exocytosis (1) or via exosomes (2), or synaptic vesicles (3). Once released, tau seeds can be taken up by postsynaptic neurons and further initiate tau aggregation. **(c)** Upstream of the circuit tau pathology can occur later on (Wang and Mandelkow, 2015).

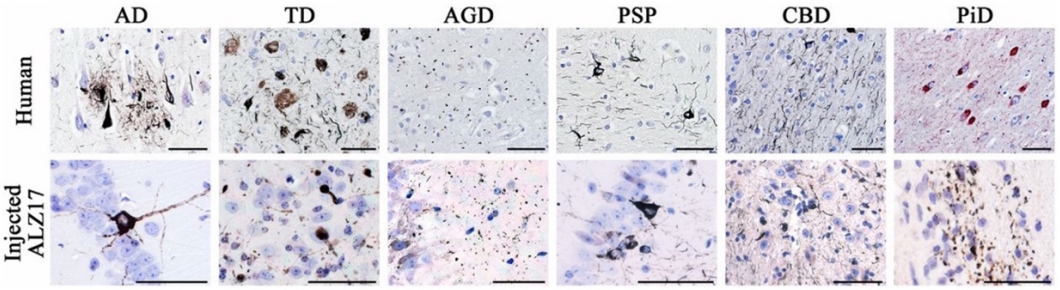

Figure 1.13: Human tauopathy and ALZ17 injected mice showing Gallyas silver-positive tau inclusions in the hippocampus. Pathological tau hallmark lesions observed in human tissue used for brain extract preparation. Upper row: Gallyas stained tissue visualising human tau pathology in different tauopathies using AT100. Lower row: tau lesions in the ALZ17 mice injected with human brain extracts from different tauopathies. Scale bars = 50 μm. Sections were counterstained with haematoxylin (Clavaguera et al., 2013).

1.8 Synaptic dysfunction and tau

As well as being primarily an axonal protein, several studies have established that tau is also present at the synapse (Harris et al., 2012; Tai et al., 2012; Pooler et al., 2014; Spires-Jones and Hyman, 2014). As previously mentioned, tau correlates with cognitive impairment, which also closely matches with synaptic density, with AD brains exhibiting extensive synaptic loss throughout disease progression (Masliah et al., 1989; DeKosky and Scheff, 1990; Serrano-Pozo et al., 2011). Synaptic dysfunction is believed to be an early event in tauopathies (de Calignon et al., 2012) with changes in the synaptic proteome often associated with the dysfunction of synapses in neurodegenerative diseases (Marttinen et al., 2015). There are a number of key proteins associated specifically with the synapse including synaptophysin, synaptotagmin, post-synaptic density protein 95 (PSD95), synapsin-1 and synaptobrevin (Figure 1.14).

Synaptophysin is one of the most commonly used markers of synapses since it is involved in vesicular endocytosis and vesicular recycling (Kwon and Chapman, 2011). Previous research from AD post-mortem brain found that NFT bearing neurons had reduced synaptophysin expression compared to neurons lacking NFT (Callahan and Coleman, 1995; Callahan et al., 1999). The number of spine-associated synapses and the amount of synaptophysin labelling is also reduced in the hippocampus of mice expressing pro-aggregant tau species (comprising the MT binding domains with a deletion of lysine 280 [ΔK280]). However, a similar loss and synaptophysin labelling was also observed in mice expressing anti-aggregated tau construct (ΔK280 deletion with two point mutations at I277P and I308P), suggesting that tau aggregation may not be essential for synaptic loss (Eckermann et al., 2007; Van der Jeugd et al., 2012).

A more recently examined synaptic marker is synapsin1, which is responsible for holding vesicles close to the active zone (Bloom et al., 2003). Previous research identified synapsin1 as a tau-interacting protein (Kang et al., 2013). Tau was found to interact with several synaptic proteins involved in pre-synaptic signalling transduction such as synapsin1, synaptotagmin and synaptophysin (Liu et al., 2016). Interestingly, interaction network analysis by mass spectrometry revealed tau interacting proteins including actin. Both tau and synapsin1 have previously been shown to interact with actin. Whereas, synapsin1 is an actin-bundling protein regulating clustering of synaptic vesicles (Bloom et al., 2003), tau can interact with actin and mediate neuronal degeneration by altering the organisation of the actin cytoskeleton (Fulga et al., 2007). Therefore, as both tau and synapsin1 co-immunoprecipitated, both with each other and with actin, Liu and colleagues proposed that these interact with actin in wild type (WT) C57BL/6 mice therefore, suggesting that tau can potentially interact with synapsin1 via actin, altering actin dynamics, and possibly presynaptic vesicle transport, which could result in synaptic failure in neurodegeneration (Liu et al., 2016).

Synaptobrevin or vesicle-associated membrane protein 1 (VAMP1) is a protein involved in the vesicular SNARE (soluble N-ethylmaleimide-sensitive factor attachment protein receptor) mechanism that is associated with

synaptic vesicle fusion to the plasma membrane during synaptic transmission (Schoch et al., 2001). Synaptotagmin1 is a synaptic calcium sensor involved in calcium-dependent neurotransmitter release (Vrljic et al., 2010). Both synaptobrevin and synaptotagmin1 have previously been found to be reduced in AD post mortem brain (Reddy et al., 2005). PSD95 is a scaffolding protein required for post-synaptic NMDA receptors and is critical for regulating synaptic plasticity (Kornau et al., 1995; El-Husseini et al., 2000). Endogenous tau in the dendrites and postsynapses has been found to bind to PSD95/NMDA receptor complexes in both mice and rats (Ittner et al., 2010; Mondragon-Rodriguez et al., 2012) and is postulated to do so by interaction with the tyrosine kinase fyn (Lee et al., 1998; Bhaskar et al., 2005; Ittner et al., 2010; Usardi et al., 2011; Lau et al., 2016).

Synapsin1, PSD95, synaptophysin and synaptotagmin have also been identified by mass spectrometry as tau interacting proteins (Liu et al., 2016), implicating them and their interaction with tau in disease pathogenesis. A summary of the location of synaptic proteins is shown in Figure 1.14. Investigating the role of tau at the synapse is essential and potentially interesting for developing new therapeutic strategies for protecting synapses in dementia.

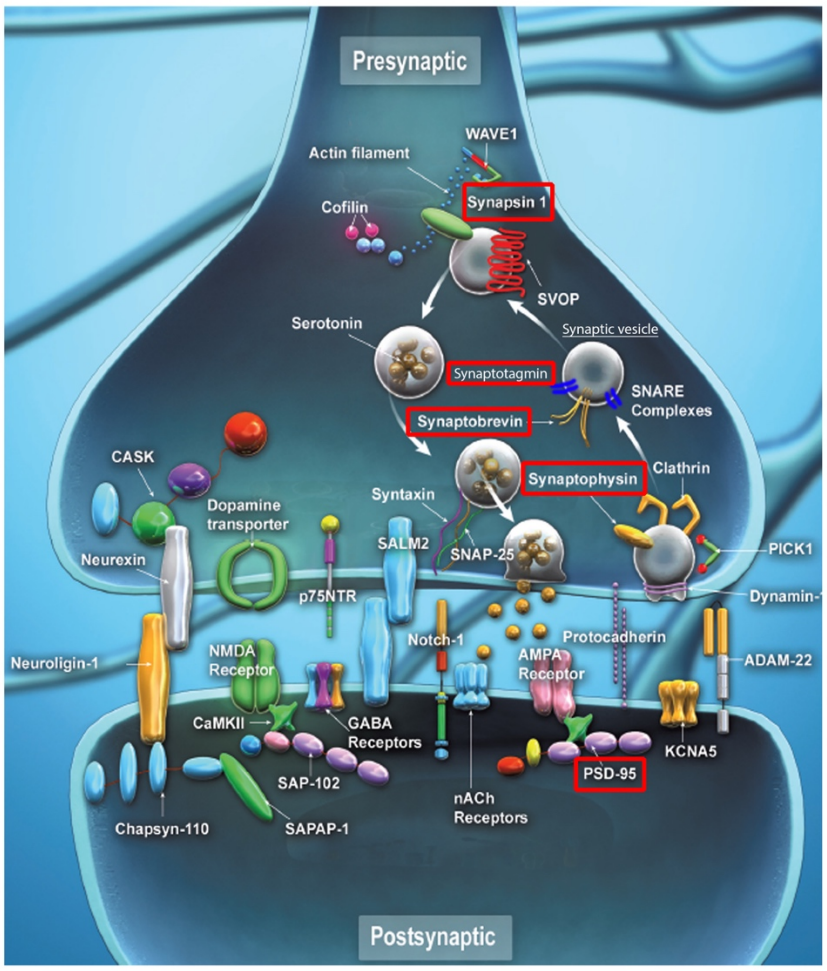

Figure 1.14: Summary diagram showing the distinct location of several key pre- and post- synaptic proteins. Pre-synaptic vesicle proteins synaptophysin, synaptobrevin and synaptotagmin are located on the synaptic vesicle membrane. The post-synaptic density marker 95 (PSD95) is located on the post synaptic membrane (image adapted from http://www.biolegend.com/category_synaptic_function).

1.9 Mouse models of tauopathies

Advances in genetic and transgenic approaches have had a major impact on the understanding of tauopathies. Several neurodegenerative changes can be reproduced and observed in transgenic mouse models with many of these accurately replicating aspects of pathological and behavioural changes, similar to those seen in human tauopathies and related disorders. Tau knockout (KO) mice show that tau depletion is not detrimental although some minor defects do exist compared to WT animals. Mice lacking tau reproduce and survive relatively normally, most likely because at least some of the functions of tau can be compensated for by other proteins (Harada et al., 1994; Takei et al., 2000; Dawson et al., 2007; Gómez de Barreda et al., 2010). The defects in TauKO are observed as mice age, such as an altered sleep-wake cycle and parkinsonism-like symptoms (Cantero et al., 2010; Lei et al., 2012). These symptoms however, may depend on the genetic background of the particular tau KO mouse. Most existing mouse models are not good representations of AD because they are disadvantaged by expression of abnormally high levels of mutant or wild-type proteins (2- to 15- fold, usually amyloid, presenilin-1, and/or tau), often at anatomical sites that are not relevant to disease (for example, reviewed in (Ishihara et al., 1999; Spittaels et al., 1999; Probst et al., 2000; Noble et al., 2010; Filipcik et al., 2012)). These mouse models may exhibit substantial artefacts *in vivo* because increases in tau expression are detrimental to neuronal function (Ebneth et al., 1998). Some models express lower levels of tau at more physiological levels such as the N279K (Dawson et al., 2007) and A152T tau (Maeda et al., 2016), or the P301L tau knock in mice (Rodríguez-Martín et al., 2016). Nevertheless, these are all tau mutants and mutations account for only a minority of human tauopathies. Recent literature has focused on modelling diseases such as AD and FTLD-tau (Denk and Wade-Martins, 2009), whilst other tauopathies remain largely unexplored, and mouse models that accurately resemble human tauopathies are yet to be established. A summary of the key transgenic mouse models in current use are provided in Table 4. Notable amongst current models of tauopathy is the use of

different promoters including the Thy 1.2 promoter, which drives neuron-specific expression of transgene expression in the CNS (Aigner et al., 1995; Caroni, 1997; Feng et al., 2000) and is therefore unrelated to the normal pattern of tau expression, which could potentially lead to abnormal tau distribution (Denk and Wade-Martins, 2009; Zilka et al., 2009; Noble et al., 2010). In addition, transgenic models of tauopathy in rodents are complicated by the fact that endogenous tau in adult mice is expressed only as the 4R tau isoform (Lee et al., 1988).

Table 4: Summarising the phenotype of transgenic rodent models expressing tau, tau truncation and tau seeding models: Summary of the majority of existing mouse models of tau expressing or seeding mouse models. Unless stated otherwise all transgenes are human. Transgene expression levels when reported are represented as fold-change to endogenous mouse tau. All models are murine unless otherwise stated. CaMKII: calmodulin-dependent protein kinase-II; CMV: cytomegalovirus; CNP: 2',3'-cyclic nucleotide 3' phosphodiesterase; GFAP: glial fibrillary associated protein; HMGCR: 3-hydroxy-3-methylglutaryl coenzyme A reductase; LTP: long-term potentiation; NF: neurofilament; NFT: neurofibrillary tangle; NR2B: NMDA receptor 2B; NSE: neuron specific enolase; PDGF-β: platelet-derived growth factor-β; PrP: prion protein. ND: no data (adapted from Noble et al., 2010)

Common name	Transgene	Promoter	Regional expression	Molecular phenotype	Axonal Degeneration	Accelerated neuronal loss	Cognitive or Motor deficit	Reference
Single wild-type human tau isoforms								
Line 7	0N3R	Mouse PrP	Cortex, hippocampus amygdala, brainstem, spinal cord	5-fold tau over-expression. Phosphorylation of neuronal and astrocytic tau. Altered tau conformation and compartmentalisation. Congophilic neurofibrillary tau inclusions with straight filaments	Degeneration of axons and reduced axonal transport	ND	Motor weakness	(Ishihara et al., 1999, 2001)

Line 23	0N3R	HMGCR	Cortex, hippocampus, striatum, thalamus, brainstem	Transgenic tau accounts for 14% of all tau protein in brain. Phosphorylated tau in cell body, dendrites and axons. No NFTs	ND	ND	ND	(Brion et al., 1999)
GFAP-tau	1N4R	Human GFAP	Cortex, thalamus, brainstem, spinal cord	2-fold tau over-expression in cortex. Tufted astrocytes, age-dependent accumulation of filamentous tau in cortex, brain stem and spinal cord	ND	Focal neuron Degeneration in areas with high levels of filamentous tau	Reduced motor function.	(Forman, 2005; Dabir, 2006)
WT 16	1N4R	Mouse PrP	Cortex, hippocampus, amygdala, brainstem, spinal cord	5-fold tau over-expression. Perikaryal and dendritic tau localisation. No progressive somatodendritic accumulation of phosphorylated tau	No	No	No	(Yoshiyama et al., 2007)
Line 14	2N3R	Mouse α-tubulin (Tα-1)	Cortex, hippocampus, amygdala, brainstem and spinal cord	5.5-fold tau over-expression. No neuronal tau aggregates, age-dependent accumulation of hyperphosphorylated tau and tau filaments in oligodendrocytes and astrocytes	ND	Cell loss, mainly of glial cells, in aged Mice	Motor weakness and muscle twitching/ spasms	(Higuchi et al., 2002)

Htau40-1	2N4R	Mouse Thy1	Cortex, brainstem and spinal Cord	4-fold tau over-expression. Somatodendritic localisation of phosphorylated tau. No NFTs, astrogliosis	Axonal dilations with NF accumulations	Wallerian Degeneration of peripheral Nerves	Sensorimotor dysfunction	(Spittaels et al., 1999)
Alz 7	2N4R	Human Thy1	Cortex, hippocampus, striatum, thalamus, midbrain	5-fold tau over-expression. Cell body, axon and dendritic localisation of hyperphosphorylated tau. No NFTs	ND	ND	ND	(Götz et al., 1995)
Tau-4R2N	2N4R	Mouse Thy1	Cortex, amygdala, hippocampus, thalamus, brainstem, spinal cord	4-fold tau over-expression. Somatodendritic phosphorylated tau. No tau aggregation.	Dilated axons in brain and spinal cord. Axonal dystrophy	ND	Early severe motor disturbances	(Terwel et al., 2005)
Alz 17	2N4R	Mouse Thy1	Cortex, hippocampus, amygdala, brainstem, spinal cord	1.5-fold tau over-expression. Tau present in somatodendritic regions and dendrites	Enlarged axons with spheroids containing NF and tau	Signs of Wallerian degeneration	Muscle weakness	(Probst et al., 2000)
WTau-Tg	2N4R	CaMKII	Cortex, hippocampus, striatum, thalamus	3 to 5-fold tau over-expression. Phosphorylation of soluble tau. No NFTs. Increased activity of parahippocampal regions	ND	No obvious neurodegeneration, but synapse loss is apparent	Impaired place learning and memory. No motor deficit.	(Kimura et al., 2007)

Tau KOKI	2N4R knock-in	Mouse Thy1	Forebrain, spinal cord	Mildly increased tau phosphorylation in forebrain and spinal cord, no abnormal tau conformations, insoluble tau or NFTs.	No	ND	Severe motor impairments	(Terwel et al., 2005)
T-WT	Human tau minigene	Human MAPT	Cortex, hippocampus, thalamus, midbrain, brainstem, spinal cord, basal ganglia	3 to 5-fold tau over-expression. Approximately equal 4R:3R tau ratio. No accumulation of tau in cell bodies. No NFTs or tufted astrocytes	ND	ND	ND	(Dawson et al., 2007)
hTau-A152T (CaMKII-tTA/TRE-hTau-A152T) hTau-WT (similar expression levels to hTau-A152T)	1N4R isoform of hTau-A152T	Second-generation minimal promoter that harbors tetracycline response elements (pTRE-Tight) transgene expression requires co-expression of the	Cortex, hippocampus	Tau levels in both lines were 4- to 5-fold higher in the cortex and 3- to 4-fold higher in the hippocampus. Cortical and hippocampal tau fragment levels were lower in hTau-A152T than hTau-WT mice Full-length hTau protein to hTau mRNA was higher in hTau-A152T. Increased neuronal dysfunction in hTau-A152T mice. Hyperphosphorylated and	ND	At 20–23 months, hTau-A152T, but not hTau-WT, mice had neuronal loss in dentate gyrus and CA3 but not in CA1	Decreased body weight in both lines. nest building impairments in middle-aged hTau-A152T mice and deficits in spatial learning and memory in old hTau-	(Maeda et al., 2016)

		tetracycline transactivator protein (tTA) In this “tet-off” system, binding of tTA to TRE, and consequently transgene expression, can be prevented by feeding mice chow containing doxycycline (DOX). tTA expression is directed to excitatory forebrain neurons by the calcium/calmodulin-dependent		conformational tau in both lines. No tau inclusions.			A152T mice. Higher spontaneous epileptic spike activity at baseline in hTau-A152T mice.	

		protein kinase II a promoter (CaMKII-tTA)						
Genomic mouse and human tau								
mTau	Entire mouse tau Gene	Mouse MAPT	Endogenous expression pattern	Approximately 1.8-fold tau over- expression. Tau hyperphosphorylation and accumulation of insoluble tau from 15 to 18 months. Reactive gliosis and vacuolization	ND	Trend towards neuronal loss in aged mice (>22 months)	ND	(Adams et al., 2009)
8c	Entire human tau Gene	Human MAPT	Endogenous expression pattern	3 to 4-fold tau over-expression Somatodendritic and synaptic accumulation of tau. Increased 3R:4R tau ratio. Phosphorylation and abnormal tau conformations in neurons and axons	No	No	No motor abnormalities	(Duff et al., 2000)

Htau	Entire human tau gene (mouse tau KO background)	Human MAPT	Endogenous expression pattern	Age-dependent somatodendritic accumulation of hyperphosphorylated, insoluble tau. Argyrophilic NFTs. Paired helical tau filaments. Cell-cycle re-entry of degenerating neurons	ND	Ventricular enlargement and reduced cortical diameter with ageing. Selective loss of cortical and hippocampal neurons, not related to NFTs.	Spatial learning deficits, perturbed long-term potentiation	(Andorfer et al., 2003; Andorfer, 2005; Polydoro et al., 2009)
FTDP-17T mutant human tau								
n/a	G272V (2N4R)	Mouse PrP/ CaMKII (tet off)	Brainstem, spinal cord	Inclusions of phosphorylated insoluble tau in neurons and oligodendrocytes. Straight and twisted tau filaments	ND	ND	ND	(Götz et al., 2001)
SJLB9 and UBJAP18	N279K (0N4R)	Mouse PrP	Hippocampus	1.5 to 1.6-fold tau over-expression. Increased tau phosphorylation in hippocampus. Dendritic tau accumulation. No NFTs	ND	ND	Impaired spatial and active avoidance learning. No locomotor deficits	(Taniguchi et al., 2005)

T-279	N279K (human tau minigene)	Human MAPT	Cortex, hippocampus, thalamus, midbrain, brainstem, spinal cord, basal ganglia	Mutant tau expression is 10-fold lower than endogenous tau. Significant over-expression of 4R tau. Accumulation of phosphorylated tau in neurons. Argyrophilic NFTs. Tufted astrocytes containing tau filaments.	Axonal spheroids with accumulated neurofilaments.	Degeneration of neuronal processes from 18 weeks. Dopaminergic neuron loss. Increased caspase-3 activity.	Acute progressive motor disturbances in 25% of mice before 52 weeks of age. Learning and memory impairments from 23 weeks of age.	(Dawson et al., 2007)
C-279	N279K (human tau minigene)	CMV	Frontal cortex, hippocampus	9-fold tau over-expression. Significant over-expression of 4R tau. No accumulation of tau in soma. No NFTs or tufted astrocytes.	ND	ND	ND	(Dawson et al., 2007)

Htau40ΔK280	ΔK280 (2N4R) expressed postnatally	CMV/CaMKII (tet-off)	Cortex, hippocampus	1 to 3-fold tau over-expression. Increased accumulation of insoluble human tau from 4 months of age. Somatodendritic tau accumulation. Abnormal tau conformations. Increased tau phosphorylation with age. Tau pathology reversed upon suppression of transgene	ND	40% loss of spine synapses at 13 months	ND	(Eckerman et al., 2007)
Htau40ΔK280/PP	ΔK280/I277P/I308P (2N4R) expressed postnatally	CMV (tet-off)	Cortex, hippocampus	1 to 3-fold tau over-expression. No accumulation of insoluble human tau. Somatodendritic tau accumulation. Some tau phosphorylation with ageing. Tau pathology reversed upon suppression of transgene	ND	20% loss of spine synapses at 13 months	ND	(Eckerman et al., 2007)

RDtau ΔK280	ΔK280 (residues 244-372 of 2N4R tau)	CMV/CaM KII (tet-off)	Cortex, hippocampus	0.7-fold transgenic tau expression compared to endogenous tau. Insoluble phosphorylated tau from 3 months (decreased at 12 months) and NFTs containing mutant and endogenous tau from 3 months after gene expression. Abnormal conformation of mouse tau. Cortical astrogliosis.	ND	Progressive Hippocampal neuronal loss from 5 months after gene expression. 27% decrease in spine synapses 9.5 months after gene expression.	ND	(Mocanu et al., 2008)
Rdtau ΔK280/PP	ΔK280/I277P/I308P (residues 244-372 of 2N4R tau)	CMV/CaM KII (tet-off)	Cortex, hippocampus	0.7-fold transgenic tau expression compared to endogenous tau. No insoluble tau or NFTs. Low levels of tau phosphorylation at sites including those phosphorylated by MARK kinase.	ND	No increase in neuronal loss compared to wild-type.	ND	(Mocanu et al., 2008)
JNPL3	P301L (0N4R)	Mouse PrP	Cortex, brainstem, spinal cord	2-fold tau over-expression. Accumulation of hyperphosphorylated (64kDa) insoluble tau with age. NFTs and Pick body-like inclusions from 4.5 months. Fibrillary gliosis in spinal cord.	Axonal degeneration, vacuolar myelinopathy. Granular axonal spheroids containing	48% loss of motor neurons in spinal cord in aged mice. Decreased density of synaptic boutons in	Progressive motor disturbances from 4.5 months. Impaired cognitive	(Hutton et al., 2000; Lin et al., 2003; Arendash et al., 2004; Zehr et al., 2004;

				Hyperphosphorylated mutant tau is cross-linked by transglutaminase. Fragmentation of Golgi apparatus. Phenotype in females is accelerated and more aggressive.	neurofilaments	contact with NFT-bearing neurons. Oligodendrocyte apoptosis	performance	Halverson, 2005; Liazoghli et al., 2005; Katsuse et al., 2006)
pR5	P301L (2N4R)	Mouse Thy1.2	Cortex, hippocampus, brainstem, spinal cord	Age-dependent accumulation of hyperphosphorylated, aggregated and insoluble tau in somatodendritic regions. NFTs with straight and twisted filaments from 6 months of age. Astrogliosis. Mitochondrial dysfunction	ND	Neuronal apoptosis	Impaired spatial reference memory from 6 months of age.	(Gotz et al., 2001; David et al., 2005; Pennanen et al., 2006)

Tau-4R-P301L	P301L (2N4R)	Mouse Thy1	Cortex, brainstem, spinal cord	4-fold tau over-expression. Reduced tau phosphorylation in young P301L mice compared to wild-type. Abnormal tau conformations and hyperphosphorylated and aggregated tau accumulate in aged mice. NFTs from 6 months.	No axonal dilations or degeneration	ND	Only minor late motor problems. Improved long-term potentiation and memory in young mice. Cognitive impairments in aged mice.	(Terwel et al., 2005; Boekhoorn, 2006)
PLT-34	P301L (1N4R)	Mouse CNP	Basal ganglia, spinal cord	Accumulation of hyperphosphorylated, insoluble, filamentous tau in oligodendrocytes with age. Impaired vesicular transport in oligodendrocytes.	Progressive loss of myelin in spinal cord from 9 months of age, axonal degeneration from 6 months.	Age-dependent loss of oligodendrocytes, significant at 12 months of age.	Progressive motor impairments, limb twitching.	(Hutton et al., 2000)

TgTauP301L	P301L (2N4R)	Hamster PrP	Cortex, hippocampus, amygdala, brainstem, spinal cord	Age-related accumulation of hyperphosphorylated, conformationally altered, ubiquitinated and insoluble tau. NFTs and glial tangles with wavy filaments. Severe reactive astrocytosis and activation of microglia.	ND	Brain atrophy by 18 months, particularly in temporal lobe and hippocampus.	No gross motor deficits. No spatial memory impairment, but reduced working memory.	(Murakami et al., 2006; Sasaki et al., 2008)
GFAP/TauP301L	P301L (1N4R)	GFAP	Brainstem, spinal cord	1.25 to 2-fold tau over-expression. Hyperphosphorylated, ubiquitinated and filamentous tau pathology develops in astrocytes with ageing. Reactive astrocytosis. Argyrophilic astrocyte tangles from 12 months	Reduced glutamate transport activity	ND	Reduced motor function from 4 months of age.	(Dabir, 2006)

rTg4510	P301L (0N4R)	CaMKII (tet off)	Forebrain, hippocampus	13-fold tau over-expression. Tau hyperphosphorylation, conformational changes and NFTs in cortex from 4 months, in hippocampus from 5.5 months. Straight tau filaments. Accumulation with aggregated tau multimers with age that correlate with extent of memory decline. DNA fragmentation, caspase-3 activation and caspase-3 mediated tau cleavage in hippocampus and frontal cortex, that is not directly associated with neuronal death. Slowed tau turnover in aged mice. Phenotype in females is accelerated and more aggressive.	Signs of axonal degeneration.	77% loss of CA1 Hippocampal neurons and gross forebrain atrophy by 10 months. Neuronal death not related to NFT formation.	Reduced retention of spatial reference memory from 2.5 months. No apparent motor abnormalities.	(Ramsden, 2005; Santacruz et al., 2005; Berger et al., 2007; Ramalho et al., 2008; Spires-Jones et al., 2008; Rocher et al., 2010)

Line 2541	P301S (0N4R)	Mouse Thy1.2	Cortex, hippocampus, brainstem, spinal cord	2-fold tau over-expression. Hyperphosphorylated insoluble tau in neurons from 5-6 months of age. NFTs and Pick-body like inclusions from 6 months of age. 'Half-twisted' ribbon-like tau filaments. Activation of MAP kinases. Microglial activation and induction of inflammatory mediators. Caspase-3 cleaved tau present in soluble and filamentous tau preparations.	ND	Non-apoptotic death of motor neurons from 6 months (up to 49% loss in anterior horn of spinal cord).	Muscle weakness, tremor, severe paraparesis	(Allen et al., 2002; Bellucci et al., 2004; Delobel et al., 2008)

PS5 and PS19	P301S (1N4R)	Mouse PrP	Cortex, hippocampus	3 to 5-fold tau over-expression. Age-dependent increase in highly phosphorylated insoluble tau from 3 months of age. Reduced binding of mutant tau to microtubules. NFTs in neocortex, hippocampus and amygdala at 5 months, with randomly oriented filaments. Microglial activation and astrogliosis. Impaired synaptic plasticity.	Axonal spheroids containing neurofilaments and tau.	20% and 45% reduction in cerebral brain and hippocampus volumes, respectively at 12 months of age.	Hindlimb clasping and limb retraction from 3 months of age. Hindlimb paralysis by 7 months.	(Yoshiyama et al., 2007)
Tg214	V337M (2N4R)	PDGF-β	Cortex, hippocampus	Mutant tau expression is 10-fold lower than endogenous tau. Hyperphosphorylated, insoluble tau and NFT formation between 4 and 11 months of age. Straight tau filaments.	ND	Degenerating neurons in areas of high tau expression, including the hippocampus. Decreased number of functional neurons with age.	Reduced spontaneous locomotion. Impaired cognition, but not spatial recognition.	(Tanemura et al., 2001, 2002)

K3	K369I (2N4R)	Mouse Thy1.2	Cortex, hippocampus, basal Ganglia	2.9-fold tau over-expression. Age-dependent accumulation of hyperphosphorylated intraneuronal insoluble tau aggregates and NFTs. Disturbed kinesin motor complex formation. Interaction of phosphorylated tau with c-Jun N-terminal kinase interacting protein-1.	Amyotrophy and spinal cord degeneration. Axonal swellings and spheroids from 2-5 months. Impaired Axonal transport from 6 weeks.	Significant loss of Dopaminergic neurons between 12 and 24 months.	Impaired working memory from 4 months of age. Muscle tremors from 4 weeks. Progressively worsening gait and postural stability.	(Ittner et al., 2008, 2009)
Tg748, Tg502, Tg492 and Tg483	R406W (2N4R)	CaMKII	Hippocampus	Mutant tau accounts for 7-18% of total tau. Somatodendritic accumulation of phosphorylated, insoluble and ubiquitinated tau with age. A subset of neurons in aged mice contain NFTs. Mainly straight tau filaments.	ND	Degenerating neurons in aged mice	No locomotor dysfunction Impaired contextual and cued fear conditioning. Increased immobility in forced swim test.	(Tatebayashi et al., 2002)

RW lines 34 and 65	R406W (2N4R)	Mouse PrP	Brainstem and spinal cord	8 to 10-fold tau over-expression. Development if insoluble tau inclusions and reduced microtubule-binding of tau with age in brain and spinal cord. Somatodendritic hyperphosphorylated tau. NFTs and fibrillary glial tau inclusions in aged mice. Straight tau filaments.	Retardation of slow axonal transport.	ND	Progressive motor weakness. Postural dystonia.	(Zhang et al., 2004)
TgTauR406W	R406W (2N4R)	Hamster PrP	Cortex, hippocampus, amygdala, brainstem, spinal Cord	0.8-fold mutant tau expression compared to endogenous tau. Accumulation of phosphorylated and ubiquitinated tau in brain and spinal cord neurons from 10 months of age. NFTs in hippocampus and amygdala of 14 month old mice. Straight tau filaments. Cortical astrogliosis and microgliosis	ND	Loss of neurons in amygdala of aged mice	Decreased locomotor ability and acquired memory loss from 10 months onwards.	(Ikeda et al., 2005)

Ala152Thr -Tau	A152T, hTau40^{AT} (2N4R)	Murine Thy1.2	pan-neuronal expression in the brain and spinal cord	1-2-fold mutant tau. Tau conformation and Tau-hyperphosphorylation combined with Tau missorting into the somatodendritic compartment of neurons starting at 2/3 months. Tau aggregation including co-aggregates of endogenous mouse tau and exogenous human tau, accompanied by loss of synapses (especially presynaptic failure) and neurons. From 10 months onwards mice show prominent neuroinflammatory response (increased activation of microglia and astrocytes). Strong induction of autophagy.	ND	Neuronal death from 16 months.	Spatial reference memory from ~16 months of age	(Sydow et al., 2016)

Co-expression of mutant tau								
THY-Tau22	G272V, P301S (1N4R)	Mouse Thy1.2	Cortex, hippocampus, dentate gyrus, amygdala, low levels in spinal cord	2 to 5-fold tau over-expression. Age dependent tau hyperphosphorylation and abnormal tau conformations starting from 3 months. Progressive redistribution of tau to cell bodies. NFTs visible at 6 months, and ghost tangles at 12 months. Mainly straight tau filaments. Increased neurogenesis and re-activation of the cell cycle during tau hyperphosphorylation and aggregation. Accumulation of astrocytes and microglia around neurons with phosphorylated tau.	ND	34% loss of pyramidal neurons from 12 months of age. Decreased synaptic transmission.	No motor deficits. Impaired spatial learning from 2-3 months, and decreased spatial memory from 10 months.	(Schindowski et al., 2006, 2008; Belarbi et al., 2009)

Tg30Tau	G272V, P301S (1N4R)	Mouse Thy1.2	Cortex, hippocampus, brainstem, spinal cord, sciatic Nerve	4 to 6-fold tau over-expression. Somatodendritic localisation of phosphorylated tau in 18 day-old mice, hyperphosphorylated tau species from 3 months. Caspase-cleaved tau only in year-old mice. NFTs from 3 months of age. Mainly straight filaments. Increased numbers of astrocytes and microglia. Accumulation of phosphorylated GSK3, JNK and ERK1 in tau inclusions.	Axonopathy, myelin destruction. Axonal swellings and spheroids with accumulation of degraded mitochondria and neurofilaments .	Decreased brain weight and hippocampal volume at 12 months of age	Severe motor deficit, hindlimb paresis from 8 months. Postural dytonia in aged mice.	(Leroy et al., 2007)
DM-htau	K257T, P301S (0N4R)	Rat MAPT	Cortex, hippocampus, brainstem, spinal cord	Mutant tau accounts for 5-10% of total tau. Age-dependent increases in hyperphosphorylated insoluble tau. NFTs and reactive astrogliosis from 6 months of age. Twisted tau filaments.	ND	Degenerating neurons.	No motor deficit. Hippocampal plasticity deficit. Inability to induce short- term potentiation. Spatial	(Rosenman et al., 2008)

							memory deficit.	
VLW	G272V, P301L, R406W (2N4R)	Mouse Thy1	Cortex, hippocampus, striatum, spinal cord	1 to 2.5-fold tau over-expression. Age-dependent tau hyperphosphorylation and accumulation of insoluble tau in NFTs. Conformational changes and tau truncation following increased tau phosphorylation. Straight and twisted tau filaments. Lysosomal abnormalities.	ND	No	Episodic memory deficits	(Lim et al., 2001; Ribé et al., 2005; Mondragón-Rodríguez et al., 2008; Navarro et al., 2008)
Transgenic rat model of tauopathy								
SHR318, SHR72, SHR	Human truncated tau (4R 151-391)	Human Thy1	Cortex, hippocampus, brainstem, spinal cord	2.5-fold tau over-expression. Age-related accumulation of somatodendritic phosphorylated, insoluble tau. Argyrophilic NFTs in brain and spinal cord	ND	No	Altered spatial navigation. Hindlimb clasping and muscle weakness.	(Zilka et al., 2006; Hrnkova et al., 2007; Koson et al., 2008)
n/a	Human truncated tau (3R tau151-391)	Human Thy1	Cortex, hippocampus, brainstem.	Progressive neurofibrillary degeneration in the isocortex. NFT's appeared as early as 9 months of age and increased in an age-	ND	No	Reduced lifespan.	(Filipcik et al., 2012)

				dependent manner. Hyperphosphorylated and conformational tau. Sarkosyl insoluble tau at 10 months of age suggesting that the insoluble tau aggregates in the brain are composed of both truncated and endogenous rat wild-type tau.				
Triple transgenic models of AD								
3 x Tg-AD	Tau P301L (0N4R), PS1 M146V knock-in, $APP_{KM670/671NL}$	Mouse Thy1.2	Cortex, hippocampus hypothalamus, thalamus, brainstem	6 to 8-fold transgene over-expression. Progressive increase in Aβ production, plaque deposition, tau phosphorylation and NFT production with age. Amyloid deposition precedes NFT formation. Caspase-cleaved tau is apparent in adult mice. Microglial activation and release of pro-inflammatory mediators in young mice.	ND	Synaptic dysfunction from 6 months of age.	Deficits in LTP correlate with increased plaque burden. Reduced long-term retention from 4 months.	(Oddo, 2003; Oddo et al., 2003; Rissman et al., 2004; Billings et al., 2005; Janelsins et al., 2005)

n/a	Tau P301L (2N4R), PS2 N141I, $APP_{KM670/671NL}$	Mouse Thy1.2 (tau), Mouse Thy1 (APP),	Cortex, hippocampus, amygdala,	Increased Aβ production with age. Phosphorylation of tau at Thr231 and Ser422 from 4 months, phosphorylation at Ser422 associated with increased Aβ production. NFTs and plaques visible from 8 months.	ND	No loss of Hippocampal neurons at 16 months of age.	Impaired spatial learning from 4 months of age.	(Grueninger et al., 2010)
Tau truncation model								
Tau35	Truncated N-terminal tau (4R, 182-441)	Human tau promoter	Throughout entire brain and spinal cord	10% of endogenous mouse tau. Hyperphosphorylation of tau from 2 months if age. Pre-tangle like structures from 8 months of age. Impaired synaptic integrity. Impaired autophagy lysosomal degradation. Increased GSK3β activity. Reduced acetylated tubulin activity.	ND	No significant loss of hippocampal neurons.	Reduced survival. Kyphosis. Clasping. Imparired motor phenotype from 1 months of age and cognitive function from 8 months of age.	(Bondulich et al., 2016)

E391-3608 E391-3610	4R1N human C-terminal truncated tau at glutamic acid 391 (E391)	Thy1.2 neuron-specific promoter	Truncated tau is distributed in a somatodendritic pattern in the hippocampus, amygdala and cortex	Total tau levels were ~1.9-fold greater than normal endogenous mouse tau in E391-3608 mice and ~2.6-fold greater in E391-3610 mic. There were similar levels of total tau among transgenic and non-transgenic animals in soluble tau fraction indicated that expression of the human transgene was relatively low compared to that of endogenous mouse tau. Pretangle tau, including accumulation of tau in insoluble fraction, somatodendritic redistribution, formation of pathologic conformations, and dual phosphorylation of tau at sites associated with AD pathology. E391-3610 mice exhibited higher accumulation of truncated tau species than E391-3608 mice Atypical neu-	ND	ND	ND	(McMillan et al., 2011)

				rites. Tau pathologic conformation (as detected by Alz50, MC1, and Tau2) in the EC and amygdala in E391-3608 but not E391-3610 mice				

1.9.1 Mouse models exhibiting tau truncation

Several studies have identified tau fragments in mouse brains over-expressing mutant forms of tau, suggesting a pivotal role of tau cleavage in neurodegenerative diseases (Delobel et al., 2008; Zhang et al., 2009; Maeda et al., 2016). Maeda and colleagues recently developed a model expressing hTau (expressing all six isoforms of human tau, but do not express mouse tau)-A152T (a risk factor for FTD and AD) (Maeda et al., 2016). Mice showed increased tau fragmentation and developed age dependent neuronal loss and cognitive impairment implicating tau fragments in these processes (Maeda et al., 2016). McMillan and colleagues generated two mouse lines with either high or low expression of human 4R tau with a C-terminal truncation at Glu391 (lines E391-3610 and E391-3608, respectively) (McMillan et al., 2011). Despite low transgene expression in the E391-3608 line, these mice exhibited pre-tangle pathology, including accumulation of insoluble tau, as well as dual phosphorylation of tau (Ser 202 and Thr 205), similar to that seen in AD brain. However, this model lacked any tangle pathology and cannot therefore be considered a complete model in which to study the generation of tau aggregation.

Several rodent studies have identified the importance of mutant tau in the development of tau pathology (Denk and Wade-Martins, 2009; Zilka et al., 2009). However, many of these models failed to identify the development of tau pathology, particularly when trying to examen the pathological differences between FTLD-tau and AD (Denk and Wade-Martins, 2009; Zilka et al., 2009). Nevertheless, although these animal models failed to produce extensive tau pathology, it has been demonstrated that neurofibrillary degeneration can be generated solely from tau fragments (Zilka et al., 2006; Filipcik et al., 2012). The first rat models expressing human truncated tau were generated by Filipcik and Novak (2012), who identified neurofibrillary degeneration. Transgenic rats expressing truncated human wild-type 4R tau (comprising tau residues 151-391), develop extensive tau pathology in the brainstem and spinal cord only (Table 4) (Filipcik et al., 2012). In contrast, transgenic rats expressing truncated human wild-type 3R tau (comprising tau residues 151-

391) develop pathology in the isocortex (Zilka et al., 2006; Koson et al., 2008; Filipcik et al., 2012). This indicates that distinct tau fragments associated with 3R and 4R tau isoforms can selectively influence NFT formation, thus making cleaved tau fragments valuable targets for therapeutic intervention.

1.10 Aims and objectives of this thesis

The aim of this project is to investigate the molecular and behavioural phenotypes in a new transgenic mouse model of tauopathy that expresses the human tauopathy-related tau fragment, Tau35, that was first identified in diseased human postmortem brain. The hypothesis under investigation states that N-terminal tau truncation drives tau aggregation and tangle formation, leading to biochemical and behavioural changes in the transgenic mice that mirror those present in human tauopathies.

The specific objectives of this project were:

1. To determine the behavioural phenotype of Tau35 mice and to monitor how this progresses as the mice age.
2. To determine whether increased tau phosphorylation occurs in Tau35 mice and how this progresses as the mice age.
3. To investigate the temporal development and progression of tau aggregation and pathological tau lesions in Tau35 mice.
4. To determine whether the changes observed in Tau35 mice can be rescued or prevented upon treatment with potential therapeutic agents, such as phenylbutyrate.
5. To investigate whether altering the strain background of Tau35 mice influences the biochemical and behavioural abnormalities observed in these animals.
6. To establish a cell-based assay to investigate the effects of potential therapeutic compounds on phosphorylation of the Tau35 tau fragment.

CHAPTER 2

Material and Methods

2.0 Materials

All reagents were from Sigma Aldrich Company Limited unless otherwise stated. All plasticware used for tissue culture was purchased from Fisher Scientific Ltd., UK. Ultrapure water was used to prepare all solutions (Elgar® Maxima water purification system).

2.1 Animals and tissue

All transgenic mice used in this study were male Tau35 (hemizygous), expressing tau35 cDNA with a hemagglutinin tag (HA) under the control of the human tau promoter with targeted insertion into the *Hprt* locus (genOway "Quick Knock-in™" technology). Mice were bred on a 75% ;25% C57 Black 5(C57BL/6); 129/Ola mice (129Ola) background and reared in-house. Transgenic animals were identified by genotyping using Real time PCR (RT-PCR), as described below. Control mice were wild type (WT) male littermates. All mice were weaned at 3 weeks of age. All animals had unlimited access to water and rodent chow (RM1 for all mice except breeders, which received RM3, Special Diet Services, Essex, UK). Mice were singly or group housed with a 12-hour light-dark cycle with constant room temperature. Genotype-blinded behavioural assessments were conducted on transgenic and WT mice during the light phase.

2.2 General biochemistry reagents

PCR reagents

REDExtract-N-Amp for tissue PCR extraction kit:	Extraction solution tissue preparation solution neutralising solution B REDExtract-N-Amp PCR reaction mix

Table 5. Primers and sequence used for PCR genotyping

Primer	Primer sequence 5' to 3' (number of bases)
Forward Tau35	CGTATGTGATGGACATGGAGATGGAGG (27)
Reverse Tau35	GCCTCCCTCTTATTAAGGACGCTGAGG (27)
Forward HPRT	TGTCCTTAGAAAACACATATCCAGGGTTTAGG (32)
Reverse HPRT	CTGGCTTAAAGACAACATCTGCAGAAAAA (30)

Buffers and tissue lysis solution

50x TAE buffer (1 litre)	242 g Tris base 57.1 ml Glacial acetic acid 100 ml 0.5 M EDTA pH 8.0
Ethidium bromide	10mg/ml
Agarose	1.2g in 120ml of 1xTAE
Tris-buffered saline (TBS), pH 7.6	50mM Trizma base 150 mM NaCl In ultra-pure H_2O
Phosphate-buffered saline (PBS), pH 7.4	137mM NaCl 2.7mM KCl

	10mM Na_2HPO_4 2mM KH_2PO_4 In ultra pure H_2O
PBS-Tween (PBS-T)	PBS containing 0.05% (v/v) Tween 20
Extra strong lysis buffer (ESLB), pH 7.5	10 mM Tris-HCl 75 mM NaCl 0.5 % (w/v) sodium dodecyl sulfate (SDS) 20 mM sodium deoxycholate 1 % (v/v) Triton X-100 2 mM Na_3VO_4 1.25 mM NaF 10 mM Ethylenediaminetetraacetic acid (EDTA) Complete mini protease inhibitor cocktail tablet, 1 tablet in 10 ml (Roche Diagnostics Ltd., UK)
TBS homogenisation buffer	50 mM TBS, pH 7.4 1 mM NaF 1 mM Na_3VO_4 1 mM PMSF

	Mini protease inhibitor cocktail tablet, 1 tablet in 10 ml (Roche Diagnostics Ltd., UK) in ultrapure H_20
2 x protein loading buffer (National Diagnostics Ltd., UK)	0.5 M Tris-HCl, pH 6.8 4.4 % (w/v) sodium dodecyl sulfate (SDS) 20 % (v/v) glycerol 2 % (v/v) 2-mercaptoethanol (β-ME) 0.01 % (w/v) bromophenol blue
1 % N-Lauroylsarcosine sodium salt (sarkosyl) solution	1 % Sarkosyl in TBS from 20 % (w/v) sarkosyl stock solution

2.2.1 SDS-polyacrylamide gel electrophoresis (SDS-PAGE) reagents

Sodium dodecyl sulphate	30% (w/v) Acrylamide
Polyacrylamide gel electrophoresis	0.5% (w/v) Bis-acrylamide from Stock Acrylamide (National Diagnostics)

10% Resolving gel, pH 8.3	10% (w/v) Acrylamide (National Diagnostics) 25% (v/v) Resolving gel buffer (National Diagnostics) 0.01% Ammonium persulphate (APS) 0.1% (v/v) N,N,N',N'tetramethylethylen diamine (TEMED)
4% Stacking gel, pH 6.8	4% (w/v) Acrylamide (National Diagnostics) 25% Stacking gel buffer (National Diagnostics) 0.075% (w/v) APS 0.15% (v/v) TEMED
Running buffer, pH 8.3	192mM Glycine 25mM Tris base 0.1% (w/v) SDS
Molecular weight markers	IRDye (680/800) Protein Marker (Li-Cor)

Transfer buffer, pH 8.3	25mM Tris 200mM Glycine 20% (v/v) Methanol
Laemlli sample buffer (2x)	25mM Tris-HCl 4% (w/v) SDS 20% (v/v) Glycerol 0.01% (w/v) Bromophenol blue 100mM dithiothreitol (DTT)
Blocking solution and antibody diluent	5% (w/v) Dried skimmed milk in TBS

2.2.2 Immunohistochemistry reagents

TBS-antifreeze	30% (v/v) Ethylene glycol 15% (w/v) Sucrose 0.05% (w/v) Sodium azide in TBS
Paraformaldehyde (PFA)	4% (w/v) PFA in PBS
Cryoprotectant	30% (w/v) Sucrose in PBS

OCT	Cryo-embedding media (Fisher Scientific)
Peroxidase blocking solution	0.6% (v/v) H_2O_2 in methanol
Blocking solutions	2% (v/v) Normal horse serum (NHS), (Vector Laboratories) in TBS or 2% (v/v) Normal goat serum (NGS), (Vector Laboratories) in TBS
Antibody diluent	1% (v/v) NHS in TBS or 1% (v/v) NGS in TBS
Secondary antibodies	Biotinylated horse anti-mouse IgG (Vector Laboratories) in 1% (v/v) NHS in TBS Biotinylated goat anti-rabbit IgG (Vector Laboratories) in 1% (v/v) NGS in TBS

Avidin-Biotin complex (ABC)	4 drops of avidin, 4 drops biotin in 10ml TBS (Vectastain Elite ABC kit, Vector Laboratories)
3,3'—Diaminobenzidine (DAB)	4 drops Buffer stock, 8 drops DAB reagent, 4 drops H_2O_2 added to 10ml H_2O from DAB peroxidase substrate kit (Vector Laboratories)
Acid rinse solution	2% (v/v) Glacial acetic acid in H_2O
Bluing solution	1.5% (v/v) of 30% (v/v) NH_4OH in 70% (v/v) ethanol
Thioflavin S staining solution	0.1% (v/v) Thioflavin S in H_2O
Eosin staining solution	0.5% Eosin Y solution in 1% (w/v) acetic acid (Merck Millipore)
Gill's Haematoxylin solution	

2.2.3 In Cell Western (ICW) reagents

4 % paraformaldehyde (PFA)	4 % Paraformaldehyde (PFA) 4% (w/v) PFA in TBS, or diluted in PBS from 16 % liquid PFA stock solution (Alfa Aesar, Johnson Matthey Co., MA, USA)
Permeabilisation solution	Permeabilisation solution 5 % (w/v) bovine serum albumin (BSA) in TBS 0.1 % (v/v) Triton X-100
ICC blocking solution	5 % (w/v) BSA in TBS 0.05 % (v/v) Triton X- 100

2.2.4 Antibodies

Table 6: Primary antibodies used on western blots (WB) and immunohistochemistry (IHC). Information on epitope and antigen, species, working dilution, manufacturer and blocking solution are given N/A: not applicable.

Antibody	Epitope and specificity	Species (monoclonal/ polyclonal)	WB	IHC	Source	Blocking reagent
Acetylated tubulin	Acetylated α-Tubulin [6-11B-1]	Mouse monoclonal	1/1,000	N/A	Abcam,(Piperno and Fuller, 1985)	5 % (w/v) milk blocking solution
DAKO	Tau, phosphorylation-independent	Rabbit IgG /polyclonal	1/10,000	N/A	Dako Ltd., UK	5 % (w/v) milk blocking solution
GSK3	Glycogen synthase kinase 3α and β (GSK3α/β) Clone: 1H8	Mouse IgG monoclonal	1/1,000	N/A	Enzo Life Science Ltd; Exeter, UK	5 % (w/v) milk blocking solution
pGSK3	GSK3α/β phosphorylated at Ser21 (α) and Ser9 (β)	Rabbit IgG polyclonal	1/500	N/A	Cell Signalling Inc., MA, USA	5 % (w/v) milk blocking solution
NSE (BBS/NC/VI-H14)	Neuron specific enolase, human specific	Mouse IgG monoclonal	1/2,000	N/A	Dako, Ltd., UK	5 % (w/v) milk blocking solution
p62	Human p62 (14 amino acids near C-terminus)	Mouse IgG monoclonal	1/1,000	1/500	Abcam, Ab91526	5 % (w/v) milk blocking solution /NHS

PHF1	Tau phosphorylated at Ser396/404	Mouse IgG monoclonal	1/2,000	1/00	Kind gift from Professor Peter Davies (Albert Einstein College of Medicine, New York)	5 % milk blocking solution/ NHS
PSD95	endogenous levels of total PSD95 protein.	Rabbit IgG polyclonal	1/1,000	N/A	Cell Signalling technology (Danvers, US)	5 % milk blocking solution
Synapsin1	Bovine brain synapsin1	Mouse IgG monoclonal	1/1,000	N/A	Merck Millipore (Darmstadt, Germany)	5 % milk blocking solution
Synaptophysin	Human Synaptophysin	Mouse IgG monoclonal	1/2,000	N/A	Enzo (Lausen, Switzerland)	5 % milk blocking solution
Synaptobrevin	Synaptobrevin [VAMP], SP11	Mouse IgG monoclonal	1/1,000	N/A	Merck Millipore (Darmstadt, Germany)	5 % milk blocking solution
Synaptotagmin	Rat Synaptotagmin aa. 72-223	Mouse IgG monoclonal	1/1,000	N/A	BD Transduction (Franklin Lakes, US)	5 % milk blocking solution
HA.11 clone 16B12	HA tag on Tau35 protein	Mouse IgG monoclonal	1/1,000	N/A	Covance	5 % milk blocking solution
β-actin	N-terminal end of the β-isoform of actin	Rabbit IgG polyclonal	1/5,000	N/A	Abcam plc, UK	5 % milk blocking solution
β-actin (AC-74)	N-terminal end of the β-isoform of actin	Mouse IgG	1:5,000	N/A	Sigma-Aldrich Company Ltd., UK	5 % milk blocking solution
Anti-LC3	Human, rat and mouse LC3A/B-I and LC3A/B-II	Rabbit IgG polyclonal	1/1,000	N/A	Sigma-Aldrich, L7543	5 % milk blocking solution
Cathepsin D	C-terminus of cathepsin D of human origin	Goat IgG polyclonal	1/2,000	N/A	Santa Cruz Biotech, SC6486	5 % milk blocking solution
Hemagglutinin (HA)	HA tag (YPYDVPDYA)	Mouse IgG monoclonal	1/1,000	N/A	Covance, HA.11	5 % milk blocking solution

TOC1	Tau oligomers	Mouse IgG monoclonal	N/A	1/00	L.I. Binder	NHS
AT8	Tau pSer202/pThr205	Mouse IgG monoclonal	N/A	1500	Thermo Scientific	NHS
TP007	Tau N-terminus (amino acids 1-16)	Rabbit IgG polyclonal	N/A	1/500		NGS
Glial fibrillary acidic protein (GFAP)	Mammalian GFAP	Rabbit IgG polyclonal	1/1,000	1/500	DAKO	5 % milk blocking solution /NHS
MC1	Detects conformational epitopes of abnormally phosphorylated tau	Mouse IgG monoclonal	N/A	1/500	Kind gift from Professor Peter Davies (Albert Einstein College of Medicine, New York)	NHS

Table 7: Secondary antibodies used for WB and IHC

Secondary antibody	**WB**	**IHC**	**Host**	**Company**
Anti-mouse IgG AlexaFluor680	1/10000	N/A	Goat	Invitrogen/Molecular Probes
Anti-rabbit IgG IRDye800	1/10000	N/A	Goat	Rockland Laboratories
Anti-mouse IgG, horseradish peroxidase linked with whole antibody	1/1000	N/A	Sheep	GE Healthcare Life Sciences
Anti-rabbit IgG, horseradish peroxidase linked with whole antibody	N/A	1/1000	Donkey	GE Healthcare Life Sciences
Biotinylated anti-mouse IgG (H+L)	N/A	1/1000	Mouse	Vector Laboratories
Biotinylated anti-rabbit IgG (H+L)	1/1000	N/A	Rabbit	Vector Laboratories

2.3 Methods

2.3.1 Generation of Tau35 mice

Tau35 mice were generated by targeted knock-in of the Tau35 cDNA construct fused at the C-terminus to a HA tag (Fig. 1B). The construct was expressed under the control of the human tau promoter and targeted to the *Hprt* locus using "Quick Knock-in™" targeting (genOway, Lyon, France). The vector was transfected into E14Tg2a embryonic stem cells derived from 129/Ola mice. Clones were selected and validated on Southern blots. Confirmed clones were subsequently injected into C57BL6/J blastocysts. Heterozygous females were generated by mating the F1 generation of the male chimeras with C57BL/6 females. Heterozygous females were then crossed with wild-type C57BL/6J males or with a transmitting chimera allowing the generation of hemizygous males and heterozygous females that were interbred to generate homozygous females, and these mice were imported from genOway. Genotype-blinded behavioral assessments were conducted on male hemizygous transgenic and WT mice during the light phase. All animal experiments were carried out in accordance with the Animal (Scientific Procedures) Act 1986 (UK), under relevant Home Office project and personal licences, and conformed to international guidelines on the ethical use of animals.

2.3.2 Preparation of mouse brain homogenates

Mice were sacrificed by cervical dislocation and brains were dissected into four regions (frontal region; hippocampus and associated cortex; amygdala; brain stem and cerebellum). Tissue was frozen immediately in liquid nitrogen and stored at -80 until use. Tissue was disrupted in 1ml ice-cold extra strong lysis buffer (ESLB) per brain region using a Dounce homogeniser.

2.3.3 Protein assay

Protein concentration of brain homogenates was determined using a biconchoninic acid (BCA, Thermo Scientific) protein assay according to the manufacturer's instruction.

2.3.4 SDS-PAGE and western blotting

Samples were heated at 100˚C for 5 min, and centrifuged for 5 min at 16,000g(av). 5-20µg protein was loaded onto 10% (w/v) polyacrylamide gels and electrophoresed at 150V for 80 min or until blue dye ran off the bottom of the gel. Separated proteins were transferred to 0.2 um nitrocellulose membranes (Whatman) using a wet transfer system (Bio-Rad). Nitrocellulose membranes, sponges, and filter papers (Whatman) were soaked in transfer buffer prior to assembly in the blotting cassette and electro-blotted at 100V for 60 min. To reduce non-specific binding, membranes were incubated in blocking buffer for 1 hour at ambient temperature, prior to incubation in primary antibody (Table 6), overnight at 4˚C. After washing 3 times in PBS, membranes were incubated in the appropriate fluorophore-conjugated secondary antibody (Table 7) for 1 hour at ambient temperature. Antigens were visualised and quantified using an Odyssey® infrared imaging system (Li-Cor Biosciences, Cambridge, UK). All figures of blots throughout this thesis show 2 selected lanes per genotype/dose from the same blot.

2.3.5 PCR genotyping

Mouse ear notches were incubated in REDExtract-N-Amp (0.25 ml per sample) at ambient temperature for 10 min, followed by the addition of neutralising solution B. Samples were cycled using primers (Table 5) and REDExtract-N-Amp PCR reaction mix. The following cycling conditions were used:
One denaturing cycle at 94°C for 2 min
35 cycles of 94°C for 30 s, 55 ºC for 30 s, and 68°C for 5 min.

PCR products were electrophoresed on 1.2% (w/v) agarose gels and visualised using ethidium bromide.

2.3.6 Immunohistochemistry

Tau35 hemizygous mice and WT littermate mice, aged between 2 and 18 months, were used in this study. Mice were sacrificed by intraperitoneal injection of terminal anaesthetic (pentorbarbital at 50mg/kg), followed by transcardial perfusion with PBS followed by 4% (w/v) PFA in PBS. The brains and muscle tissue were excised, dissected and post-fixed in 4% (w/v) PFA before incubating in PBS for 24 hours at ambient temperature. Tissue samples were cryoprotected in 30% (w/v) sucrose in PBS for 24 hours at ambient temperature and transferred into PBS. Brain tissue was frozen for 30 seconds in isopentane, pre-cooled to -90°C in dry ice, and stored at -80°C. Muscle samples were embedded in OCT mounting medium and frozen in chilled isopentane and stored at -80°C.

2.3.7 In-cell western assays

Cells plated at a density of 100,000 cells per well on 96-well plates were used for in-cell western assays. Cells were washed with TBS pre-warmed to 37 °C and fixed in 4 % (v/v) PFA in TBS for 15 minutes at 37 °C. All traces of PFA were removed by three washes with TBS, and cell membranes were permeabilised by the addition of permeabilisation solution for 2 minutes at room temperature. After a brief wash with PBS, non-specific binding was blocked by incubation in ICC blocking solution for 1 hour at ambient temperature. Following blocking, primary antibody, diluted in ICC blocking solution, was added and left to incubate overnight at 4 °C. The primary antibody was then removed, followed by three washes in TBS and incubation with the appropriate species of fluorophore-coupled secondary antibodies, diluted in BSA blocking solution, for 1 hour at ambient temperature. The secondary antibody was then removed and the cells washed 3 times with PBS. The Odyssey® infrared scanning system (Li-Cor Biosciences Ltd., UK) was used

to detect infra-red fluorescence emissions at 700 nm and 800 nm. Data were exported to Excel (Microsoft Corp., USA), where calculations were performed to standardise the immunoreactivies of proteins of interest against either total tau or β-actin). Statistical analysis was performed using Graphpad Prism (Ver 5.01, Graphpad Software Inc., CA, USA).

2.3.8 Tissue sectioning

Brain and quadriceps and latissimus muscle samples were sectioned using a cryostat (Leica CM1860, Leica Microsystems). Samples were mounted onto a specimen disc using OCT mounting medium and sectioned as follows: Brain tissue for analysis by DAB immunohistochemistry was cut into 30µm coronal sections and stored free floating in TBS-antifreeze at -20°C.

2.3.9 DAB staining of mouse brain tissue

Free floating sections of mouse brain (2-16 months of age) were removed from antifreeze and transferred to Netwell inserts (Sigma) Sections were washed in TBS and treated with peroxidase blocking solution to quench the sections before being blocked blocking solution before incubating in primary antibody (Table 6) for 24 hours at 4°C. After washing in TBS, sections were incubated in the appropriate biotinylated secondary antibody (Table 7). The staining was developed using the ABC system, followed by further washes in TBS before incubation in DAB. Sections from Tau35 and control mouse brain were incubated in DAB for identical periods of time while the colour developed. Sections were washed in H_2O, then TBS, prior to mounting onto Superfrost microscope slides and air drying overnight at ambient temperature. Dried sections were washed in running tap water, counterstained using Gill's Haemotoxylin solution, for 2 min then rinsed in running tap water, differentiated in 2% (v/v) glacial acetic acid and rinsed again in tap water. Sections were blued using blueing solution and dehydrated in increasing concentrations of ethanol (70%, 95% and 100% (v/v)), before clearing in

xylene (Fisher Scientific Ltd). Sections were mounted in DPX mounting medium (Sigma), coverslipped and allowed to set. Images of hippocampal (primarily cortical area 1 and 3 (CA1/3)) and cortical regions of mouse brains were captured from DAB-stained tissue using an EVOS XL Core Imaging system (Thermo Fisher Scientific).

2.3.10 Muscle staining with haematoxylin and eosin and muscle analysis

Muscle sections from mice aged 8 and 16 months were brought to ambient temperature and outlined using a Pap pen (Sigma-Aldrich). Sections were washed in TBS and blocked in blocking solution. Sections were incubated in primary antibody (Table 6) for 24 hours at 4°C. Muscle sections were stained using DAB. Sections from Tau35 and control mouse muscle tissue were incubated in DAB for identical periods of time while the colour developed. Sections were washed in water, then TBS, prior to staining with haematoxylin for 2 min. Following counterstaining with Gill's haematoxylin, differentiation and bluing, the muscle sections were incubated in eosin for 10 minutes. Excess eosin was removed by repeated washes in water and sections were dehydrated in increasing concentrations of ethanol (70%, 90% and 100% (v/v)) before being cleared in xylene and mounting in DPX (Sigma). Muscle sections were imaged using an EVOS XL Imaging system. The number of individual muscle fibres harbouring internal nuclei was expressed as a percentage of the total muscle fibres. The minimal Ferret's diameter of 20–40 fibres from three animals of each genotype was calculated using ImageJ to determine the distribution of muscle fibre sizes. For analysis 3 slides were used per mouse and 10 different images from every muscle section were counted and measured.

2.3.11 Extraction of aggregated tau from Tau35 mouse brain

For sarkosyl extraction, frozen mouse hippocampal sections were homogenised in fresh homogenisation buffer using a Tissue Master-125 Omni International mechanical homogeniser (Omni Tissue Master 125) with a final concentration of 100 mg/ml. Samples were centrifuged in a bench top centrifuge at maximum speed 13,000g(av) for 20 min at 4 °C. The supernatant (low speed supernatant, LSS) was collected and an aliquot was frozen at -20 °C for total brain western blots, and pellets were stored at -20 °C. Sodium lauroyl sarcosinate (sarkosyl; Sigma-Aldrich) was added to the remaining supernatant, resulting in a final sarkosyl concentration of 1% (w/v). Samples were incubated at ambient temperature for 30 min with shaking before centrifuging at 100,000 g(av) for 1h at ambient temperature. The high speed supernatant (HSS, sarkosyl-soluble fraction) was collected and stored at -20°C. The remaining pellet (sarkosyl-insoluble fraction) was washed with 1% sarkosyl by centrifuging at 100,000 g(av) for 10 min, then resuspended in 2x Laemmli buffer with 5% β-merceptoethanol and stored at -20 °C. For western blots the LSS and HSS fractions were mixed 1:1 with 2x Laemmli buffer with 5% β-mercaptoethanol.

2.3.12 Animals, behavioural analysis and drug treatment

2.3.12.1 Animals

All mice used in this study were male animals, either expressing Tau35 or of the equivalent background (wild-type, WT) strain. Mice were bred and reared in-house and were weaned at 3 weeks of age. Transgenic animals were identified by PCR. Control mice were WT male littermates. All animals had unlimited access to rodent chow (RM1 for all mice except breeders which received RM3 from Special Diet Services, Essex, U.K.) and water. Mice were singly or group housed with a 12hour light-dark cycle with constant

temperature. Genotype-blinded behavioural assessments were conducted on transgenic and WT mice during the light phase.

2.3.12.2 Mouse survival time

All mice were sacrificed when reaching end stage using cageside observations of their body posture, eye appearance and activity level. Kaplan-Meier survival curves were for constructed for Tau35 and WT mice to analyse cumulative and median survival times using GraphPad Prism (n=10 for each genotype).

2.3.12.3 Limb clasping reflex

Mice were suspended by their tail for 20 seconds and assessed for hind and forelimb clasping. Mice were scored on a binary scale, as either clasping or not clasping, and the percentage of mice clasping within each age group (1-18 months) was calculated.

2.3.12.4 Assessment of kyphosis

To assess kyphosis mice were carefully dissected and tissue dissolved in 1% (w/v) KOH, 20% (v/v) glycerol, following careful dissection of the spine. The kyphosis index (KI) was then determined by the following formula, adapted from Laws & Hoey 2004. Distance between the last cervical vertebra, corresponding the dip in the neck area or posterior edge of L6, and the caudal margin of the sixth lumbar vertebra (=length), divided by the length of a perpendicular line to the most dorsal edge of the vertebra at the point where the greatest curvature occurred (=height) (Figure 3.9a). Data were analysed using one-way ANOVA.

2.3.12.5 Rotarod performance

Rotarod analysis was performed on a UgoBasile7650 accelerating Rotarod (Linton Instruments, Diss, UK), modified to accelerate from 4 to 40 rpm over a period of 500s. All mice received an initial training session of 2 minutes at 2 revolutions per minute (rpm) to allow the animals to acclimatise. Mice were tested once a month for 4 consequitive days and the average of 3 readings of their latency to fall from the Rotarod was recorded. Data were analysed using one-way ANOVA (Hockly et al. 2003).

2.3.12.6 Grip strength

Test mice were assessed for forelimb and All limb grip strength using the Linton Instrumentation Grip Strength Meter. Animals were lowered by their tail towards a metal grid and allowed to grasp the grid with either their forelimbs only or all four limbs. Mice were then pulled steadily away from the apparatus with constant force. Average of 3 readings per mouse were taken and analysed. Data were analysed using ANOVA.

2.3.12.7 Olfactory habituation

Mice were placed in a clean standard housing cage with bedding, and allowed to acclimatise for 24 hours. Before testing, bedding was removed and odours were presented as follows: 3 x water (neutral), 3 x bananas (non-social), and 3 x age-matched male mouse urine (social). Banana essence (Natural Products Co-Op) was diluted 1/100 in water and urine was diluted 1/250 in water. The time each mouse spent sniffing each odour was quantified for each trial (adapted from Young & Goldstein 2012).

2.3.12.8 Locomotor activity

At eight months of age, the locomotor activity of animals was assessed in a 60 cm diameter circular open field environment. Mice were placed in the outer part of the arena facing the outer wall and allowed to explore the open field freely for 30 min. The open field was divided into three circular zones (outer, middle, and inner) and the number of entries made by each mouse and the time spent in each zone was quantified. Trials were videoed and analysed using EthovisionXT 7.1 (Noldus, The Netherlands). Data were analysed using ANOVA.

2.3.12.9 Morris water maze

A pool of 1.2 m diameter was filled with opacifier (Acusol OP301, DOW chemical company) and water and maintained at ambient temperature (21°C). The maze was surrounded by spatial cues on the wall. The pool was divided into quadrants on the tracking device (target, opposite, left and right). Visible platform training was performed on day one followed by fixed non-visible platform training for the next four consecutive days, with four trials per day. Average swim speed, path length, and time taken to reach the platform were tracked using EthovisonXT 7.1. One hour after the final trial on day 5, a one minute probe trial was conducted in which the platform was removed, and the percentage time spent in each quadrant was recorded. Spatial learning for each day was analysed using one-way ANOVA.

2.3.12.10 Treatment of mice with phenyl butyrate

Phenylbutyrate (PBA) was prepared by titrating equimolecular amounts of 4-phenylbutyric acid (Sigma-Aldrich) with sodium hydroxide to pH 7.4 and filter sterilised. Groups of eight Tau35 and wildtype mice (7.5 and 8.5 months) were treated with PBA (400 mg/kg, intraperitoneally daily) or vehicle (sterile water) for 6 weeks (Ricobaraza et al., 2009) (n = 8 per treatment group).

2.3.4 Statistical analysis

All statistical analysis was performed using SPSS software except for the survival Kaplan Meier curve for which graph pad prism was used. To check data was normally distributed, the Levine test for homogeneity of variance and Kolmogorov-Smirnov test were used to test for normality. One-way ANOVA was used to compare between groups, as indicated above for all data except for Kaplan Meier survival curve which used the Log-rank (Mantel-Cox) test. For ICW analysis, effect size was measured using Cohens D with ranking 0.2: small, 0.5: medium and 0.8: large effect size.

CHAPTER 3

Expression of a human-tauopathy-derived N-terminally truncated tau fragment in mice causes behavioural, biochemical and pathological deficits

3.1 Introduction

Tauopathies have distinct clinical presentations which are characterised by progressive cognitive and/or motor dysfunction. Neuropathologically, tauopathies exhibit highly phosphorylated aggregates of the microtubule-associated protein tau in brain and peripheral nerve. Whereas Alzheimer's disease (AD) shows primarily a cognitive dysfunction other tauopathies, such as progressive supranuclear palsy (PSP), corticobasal degeneration (CBD), Pick's disease (PiD), and FTLD-tau present mainly with motor deficits and later stage cognitive decline (Neary et al., 1988; Lee et al., 2001; Goedert and Spillantini, 2011) Previous mouse models of tauopathy have focused almost entirely on modelling of diseases such as AD (e.g. 3xTg and specific tau mutations causal for FTLD-tau (FTD associated with *MAPT* mutations)) (Oddo et al., 2003). Although tau mutations account for a small percentage (~2%) of tauopathies, the majority of these disorders are sporadic and of unknown cause, and for these novel animal models are urgently required. Existing rodent models of human tauopathy invariably involve significant overexpression of mutant or wild-type (WT) tau under the control of a variety of different promoters (Denk and Wade-Martins, 2009; Zilka et al., 2009; Noble et al., 2010). These lines may exhibit substantial over-expression artefacts since increased tau is detrimental to neuronal function (Ebneth et al., 1998). Therefore, new models expressing low levels of physiologically relevant tau are essential to fully elucidate the mechanism of tau *in vivo*.

Tau truncation is a pathological modification altering the subcellular localisation and leading to the accumulation of toxic truncated fragments causing cellular dysfunction, cell death, neuronal loss and/or increased tau phosphorylation and aggregation in a variety of tauopathies (Wischik et al., 1988a; Novák, 1994; Amadoro et al., 2004; Arai et al., 2004; Igaz et al., 2008; Quintanilla et al., 2009). Numerous mammalian models exist that replicate the normal and pathological functions of tau but very few are available to model tau truncation and disease manifestation. The first tau truncation rat model expressing human truncated tau was generated by Felicia and Novak (Filipcik et al., 2012), who identified extensive neurofibrillary degeneration generated by the expression of a tau fragment. These findings demonstrate the important association of truncated fragments of 3R and 4R isoforms of human WT tau with distinct tangle formation. Nevertheless, both these rat models did not show extensive neuronal loss implicating truncated tau in tangle formation.

Our lab previously identified a highly phosphorylated C-terminal tau fragment in the brains of people affected by 4R tauopathies (Wray et al., 2008) the most common tau isoform imbalance observed in the tauopathies (Goedert and Spillantini, 2011). To evaluate the pathological role of this truncated tau species, a new transgenic mouse line (Tau35 mice) expressing this disease-associated tau fragment under the control of the human tau promoter was generated (Bondulich et al., 2016). In contrast to the majority of mouse overexpression models in the current literature, transgene expression in Tau35 mice is <10% of the total amount of tau (data provided by Tong Guo, King's College London) and therefore non-physiological functions of over-expressed tau are avoided. In addition, Tau35 mice also provide a model for tauopathies such as PSP and CBD, for which no mammalian models expressing WT tau currently exist. Nevertheless, the commonalities in tau-associated neurodegeneration between the different tauopathies suggest that Tau35 mice provide a human disease-relevant model with which to further our understanding of the molecular mechanisms underlying related disorders, such as AD.

In this chapter, the biochemical, neuropathological and behavioural characterisation of the new Tau35 mice line is described. Evidence is provided

that low level expression of an N-terminally truncated human derived tau fragment in Tau35 mice leads to the development and progression of a human tauopathy-like disease phenotype (Bondulich et al., 2016). The abnormalities in Tau35 mice include altered tau processing and neuropathology, deficits in cognitive and motor function, muscle degeneration and impaired proteostasis

3.2 Results

In order for a mouse model to be an effective translational parallel to human disease, it is essential to evaluate its pathophysiological profile and how well this parallels disease progression seen in humans. This chapter aims to characterise aspects of the (1) behavioural, (2) biochemical and (3) pathological changes observed in the Tau35 transgenic mice compared to WT littermates and to determine how this parallels the clinical manifestations of human tauopathies. These experiments used male mice only to avoid the complications of the oestrous cycle during different stages and ages of mouse behaviour. Additionally, as the transgene was X-linked, males were used to prevent potential X-linked inactivation in female mice which can affect expression levels. Successful baseline evaluation allows further investigation into Tau35 mice, leading to a potential new model of human tauopathy.

3.2.1 Generation and transgene expression of Tau35 mice

3.2.1.1 Generation of Tau35 mice

The Tau35 truncated fragment of tau was first identified by this laboratory in diseases in which 4R tau accumulates in the brain (Wray et al., 2008). Antibody epitope scanning was used to confirm that Tau35 is an N-terminally truncated, C-terminal intact fragment that contains 4R microtubule-binding repeats, and which exists both in PSP and CBD but is absent from AD and control brains

(Wray et al., 2008). Mass spectrometry analysis revealed that the C-terminus of Tau35 precisely matches that of full-length tau. In full length tau the amino terminal domain of tau contains two inserts (N1, N2), followed by a central proline-rich domain and MT binding domain, which comprises four repeats (R1-R4). Tau35 retains the majority of the proline-rich domain, four MT binding repeats and an intact C-terminus (Figure 3.1b). To evaluate the pathological role of this species of truncated tau, a new transgenic mouse line (Tau35 mice) expressing this disease-associated tau fragment was generated via targeted insertion of human Tau35 construct under the control of the human tau promoter at the hypoxanthine phosphoribosyltransferase (*Hprt*) locus (Bronson et al., 1996). This strategy ensures single copy gene integration thereby eliminating the requirement to generate and characterise multiple founder lines and reduces the potential for any possible complications due to over expression of the transgene, which has previously been a major factor in several other transgenic lines (Götz et al., 2007). Use of the human tau promoter regulates expression of tau to regions in which tau is normally expressed. In order to distinguish transgenic Tau35 from endogenous mouse tau, a haemagglutinin (HA) tag was fused to the C-terminal of the Tau35 sequence (Figure 3.1a). Mice were genotyped for accurate analysis prior to any behavioural, biochemical or pathological testing. Genotyping of the animals resulted in either a double band (upper band: 535bp; lower band: 677bp), indicating heterozygous females, a single lower band (677bp), indicating WT male or female mice and an upper single band, indicating hemizygous male or homozygous female mice (Figure 3.1c).

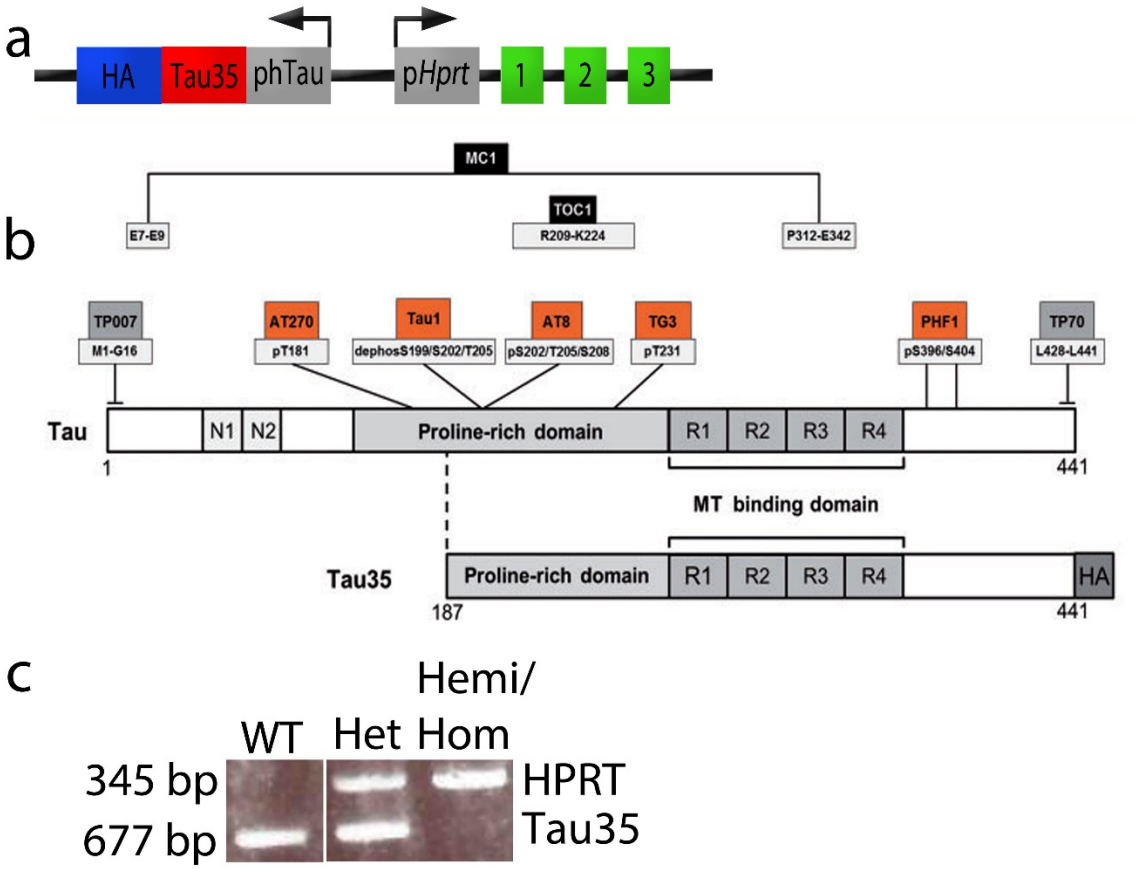

Figure 3.1: Tau35 construct and genotyping outcome. (a) Construct used to generate Tau35 mice with the human tau promoter (phTau), upstream of the Tau35 sequence with the hemagglutinin tag (HA). The hypoxanthine phosphoribosyltransferase promoter (p*Hprt*) and exons 1, 2, 3, enabled targeted integration of the Tau35-HA transgene. **(b)** schematic representation of the expressed Tau35-HA protein in comparison to full-length human tau (441 amino acids). The epitopes of the phospho-dependent (orange boxes), conformation-dependent (black boxes) and region-specific (grey boxes) tau antibodies used in this study are indicated above full length tau. **(c)** Agarose gel showing Tau35 and WT genotyping, lower *Hprt* band only represents WT, lower 677 bp and upper 345 bp bands represents Het females, upper band only represents homozygous female or hemizygous male mice.

3.2.1.2 Transgene expression in Tau35 mice

In order to confirm expression of the Tau35-HA transgene in the mice, RT-PCR was used to discriminate transgenically encoded mRNA yielding an HA band in Tau35 but not WT mice confirming expression of HA-Tau35 in these animals (work by Tong Guo) (Bondulich et al., 2016). Tau35-HA transgene expression was determined relative to endogenous mouse tau by PCR (work by Tong Guo) (Bondulich et al., 2016). The total amount of tau mRNA was similar in WT and Tau35 mice, showing that Tau35 does not disturb expression of endogenous tau. The amount of mouse tau mRNA in Tau35 mice comprised 93% ± 2% of total tau expression. Hence, Tau35 transgene expression is estimated to comprise <10% of total tau mRNA, similar to a previous report using the same promoter in tau mutant mice (Dawson et al., 2007).

Translation of the transgenic tau fragment was verified in Tau35 mice by immunohistochemical labelling and on western blots using an HA antibody (Figure 3.2). The distribution of HA labelling closely matches endogenous mouse tau expression in the Allen Developing Mouse Brain Atlas (©2014 Allen Institute for Brain Science. Available from: http://mouse.brain-map.org/ (Lein et al., 2007), including expression in the hippocampus, the cortex, basal nuclei, pontine grey, superior and inferior colliculus, and cerebellum. HA immunoreactivity was intense in cell bodies and dendrites of neurons, but was very weak or absent from axons in white matter tracts. The glial cells were not HA-positive. No HA labelling was apparent in WT mouse brain.

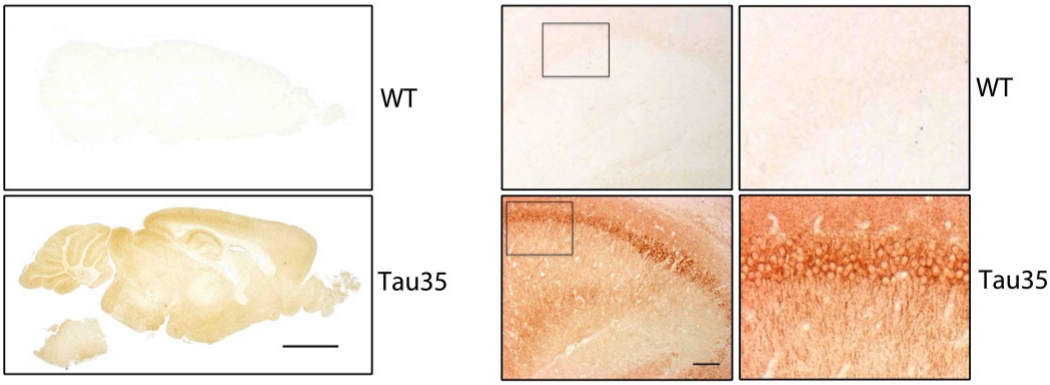

Figure 3.2: Transgene level expression in Tau35. Sagittal sections show widespread HA labelling in Tau35 mouse brain (scale bar=2 mm). Higher magnifications of the hippocampal CA1 region show strongly HA-positive pyramidal neurons in Tau35 mice (scale bar=200 μm).

To determine the levels of Tau35 protein expression in the Tau35 transgenic mice compared to their WT littermates, different mouse brain regions and spinal cord were analysed for Tau35 expression levels on western blots probed with an antibody against HA (Figure 3.3). An HA-positive species corresponding to Tau35 was detected at ~35kDa in all brain regions tested (frontal cortex, hippocampus and associated cortex, amygdala, brain stem and cerebellum) and also in the spinal cord of transgenic mice, but not in WT animals. Blots were probed with antibody to β-actin as a loading control. Analysis of transgenic Tau35-HA expression, relative to β-actin, indicated no significant differences in expression between these brain regions but higher levels in both hippocampus and amygdala (Figure 3.3).

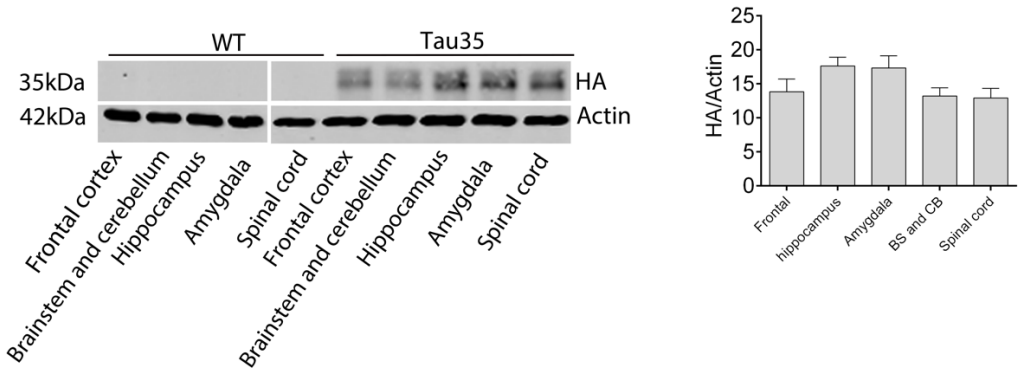

Figure 3.3: Protein level expression in Tau35 brain and spinal cord. Western blots of different brain regions and spinal cord show HA protein expression only in Tau35 mice. Quantification shows similar transgene expression in all brain regions and spinal cord of HA relative to β-actin. Results are shown as mean ± SEM (n=3 mice for each genotype).

3.2.2 Behavioural characterisation of Tau35 mice

For behavioural analyses, groups of n=8-40 male Tau35 and WT mice were tested serially between the ages of 1 and 18 months of age, as described in section 2.3.12 Animals, behavioural analysis and drug treatment.

3.2.2.1 Survival is reduced in Tau35 mice

The life spans of WT and Tau35 mice were determined and used to construct a Kaplan-Meier survival curve (Figure 3.4). Tau35 mice had a median survival of 717 days compared to 788 days in WT mice (Log-rank (Mantel-Cox) test, $P<0.05$)), showing that low-level expression of Tau35 significantly decreases life-span.

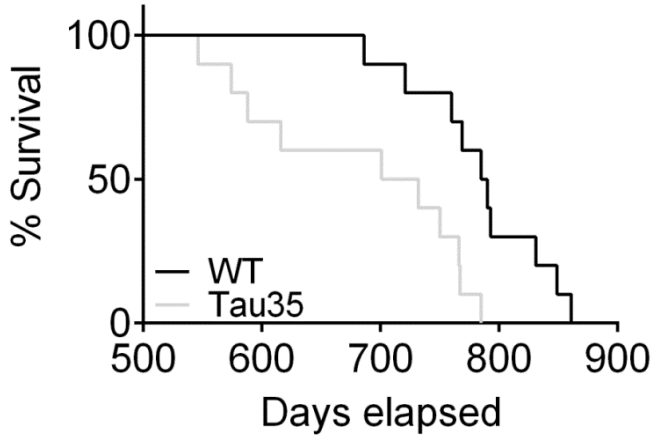

Figure 3.4: Survival of Tau35. Kaplan-Meier survival plots of Tau35 mice and WT littermates. Tau35 have a median lifespan of 717 days, compared to 788 days for WT mice, n=10 for each genotype.

3.2.2.2 Tau35 exhibit no changes in weight with aging

Despite their reduced survival, there was no statistically significant difference in the mean weight of Tau35 and WT mice between the ages of 2 and 18 months (Figure 3.5, P>0.05). This indicates that Tau35 protein expression did not influence weight in these mice.

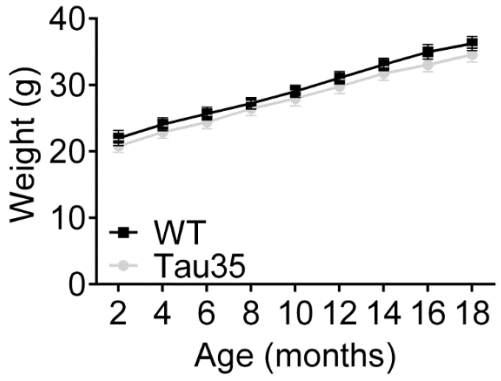

Figure 3.5: Tau35 and WT mice body weight. Graph showing the body weights of age-matched Tau35 and WT mice between 2 and 18 months of age. Values represent mean and ± SEM, n=8 per genotype.

3.2.2.3 Tau35 mice exhibit an early limb clasping phenotype

Aberrant clasping of forelimbs and/or hindlimbs is a marker of disease progression in a number of neurodegenerative mouse models and has been seen most typically in mouse models of Huntington's disease, but has also been observed in other mouse models of neurodegenerative disease, particularly in AD models (Lin, 2001; Filali et al., 2012). The Tau35 mice showed a biphasic and marked clasping phenotype (Figure 3.6a). At two to three months of age, when clasping was first observed, approximately 2% of Tau35 mice exhibit a clasping phenotype, with an incidence of 5% at 4 months of age (Figure 3.6a). The incidence of limb clasping in Tau35 mice increased markedly to 26% at five months of age. There was a steady increase in the incidence of clasping from 6 to 11 months and another marked increase at 12 months, by which time when 82% of Tau35 mice exhibited a clasping phenotype. By 16 months, 100% of the Tau35 mice exhibited clasping (Figure 3.6b). Limb clasping was not observed in any WT mice of the same ages. These results demonstrate a progressive age-related loss of the normal limb extension reflex in Tau35 mice.

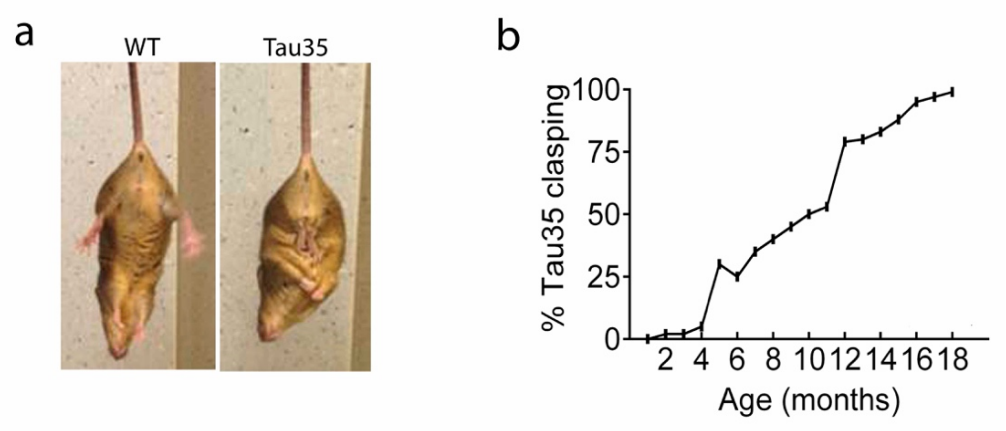

Figure 3.6: Expression of Tau35 induces progressive limb clasping. (a) Tau35-expressing mice clasp their hind limbs and forelimbs from an early age when suspended by the tail (left, WT, wild-type; right, Tau35) both at 8 months of age. **(b)** The proportion of Tau35 mice exhibiting clasping was determined at intervals between 1 and 18 months of age. Limb clasping is apparent in Tau35 mice from 2 months of age with all Tau35 animals affected by 18 months (n=40). Clasping was not observed in wild-type (WT) mice at any age examined.

3.2.2.4 Tau35 mice exhibit early onset motor learning deficits

A variety of human tauopathies show an early and extensive motor dysfunction prior to the appearance of any cognitive impairment, and particularly in PSP, CBD and FTLD-tau. Therefore, motor learning coordination skills were determined by measuring Rotarod performance of Tau35 mice. Motor coordination was assessed on an accelerating Rotarod from 1-16 months of age. Compared to WT mice, Tau35 mice showed a significant decrease in their latency to fall from the Rotarod, from the first day tested at 1 month of age and consecutively at all ages tested (Figure 3.7a, $P<0.05$), Tau35 mice showed a progressive deterioration with age, indicating an impairment in their motor coordination ability. To further assess skilled behavioural learning, the data were analysed for single day performance over the four day testing period at the ages of one, two, four and six months. Tau35 showed impaired motor

learning performance at all ages with and an overall inability to learn to remain on the Rotarod compared to WT mice which showed learning behaviour at 1 and 2 months of age (Figure 3.7b-e). Testing for motor co-ordination and learning ability showed that Tau35 mice have a reduced motor learning ability, which decreased with age, indicating a progressive age-related defect in motor co-ordination (Figure 3.7).

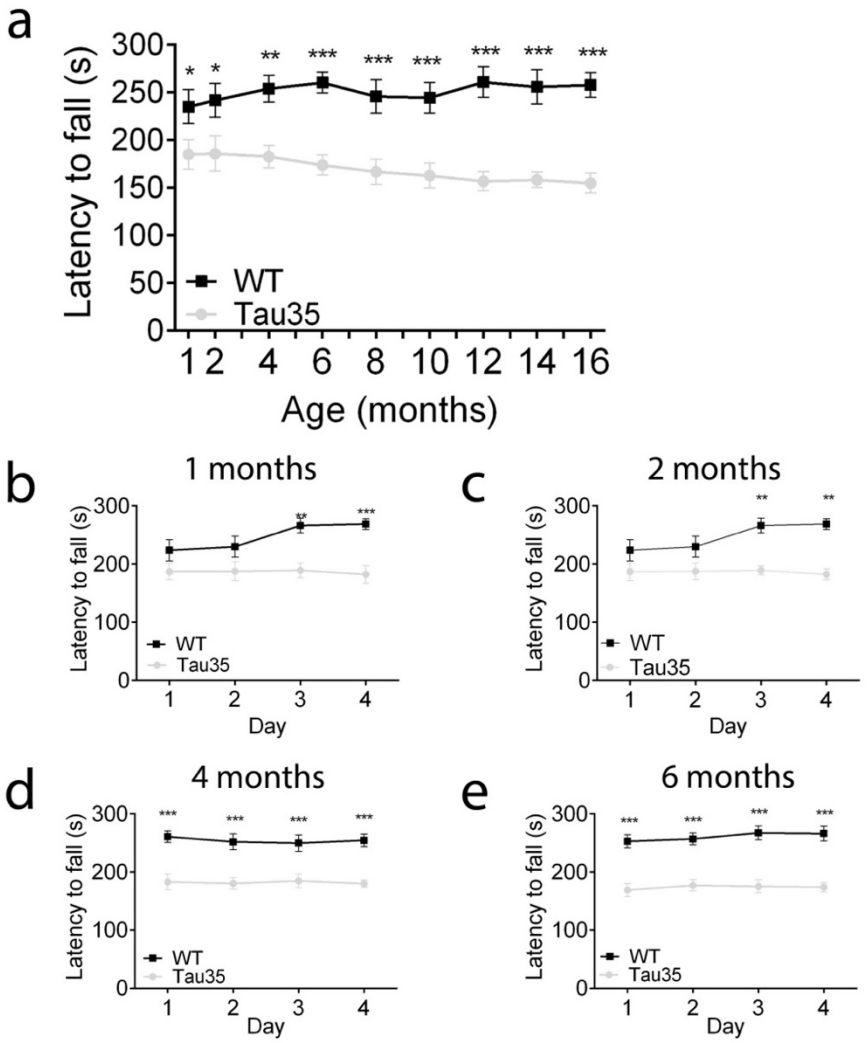

Figure 3.7: Motor learning performance of Tau35 and WT mice (a) Mean latency to fall from an accelerating Rotarod for Tau35 and WT mice between 1 and 16 months of age. Tau35 mice show a significant impairment compared to WT mice at all ages tested. **(b-e)** Individual days of Rotarod performance between 1 and 6 months of age. Values shown are mean ± SEM, n=8 for each genotype. **P<0.01, ***P<0.001, ANOVA.

3.2.2.5 Tau35 mice exhibit neuromuscular deficits

Motor deficits are often attributed to reduced neuromuscular strength, therefore the grip strength was tested of either the forelimbs only or all limbs in Tau35 mice aged 4-16 months. Whereas WT mice exhibited a steady increase in grip strength across this age range, it was apparent that Tau35 mice showed a significant reduction in grip strength from the age of 6 months, which decreased further up to 16 months of age (Figure 3.8, $P<0.001$). Tau35 mice showed no significant difference in forelimb grip strength compared to WT mice at all ages tested (Figure 3.8). These results show a progressive deterioration in muscle tone of Tau35 mice from an early age and the rate of decline accelerates slightly between 8 and 12 months of age. Interestingly, the results of the grip strength test parallel the increase in clasping seen in Tau35 mice at 5 months (Figure 3.6).

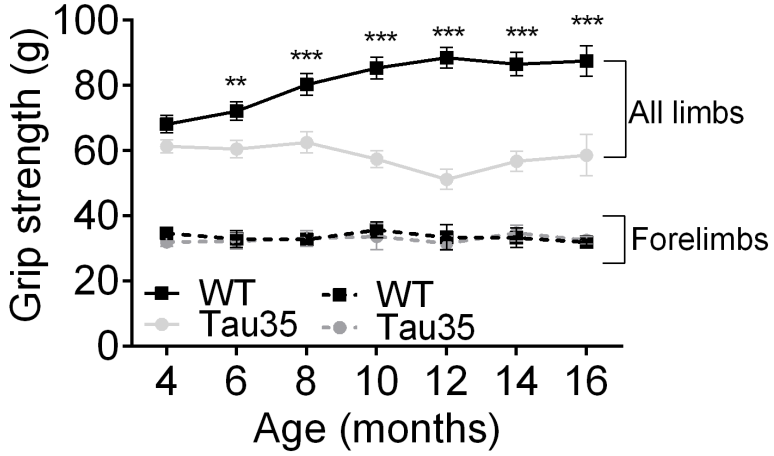

Figure 3.8: Grip strength of Tau35 and WT mice. Grip strength of Tau35 and WT mice at 4-16 months of age. WT mice show an age-related increase in grip strength, whereas Tau35 mice show a progressive decline from 6 months of age. Values shown are mean ± SEM, n=8 for each genotype, **P<0.01, ***P<0.001, ANOVA.

3.2.2.6 Tau35 mice exhibit curvature of the spine (kyphosis)

Kyphosis is a curvature of the spine that is observed primarily in mouse models of muscular dystrophy, and prion disorders, and is not a common symptom of human tauopathies but rather of neuromuscular diseases (Laws, 2004). Nevertheless, kyphosis has previously also been reported in parkin null mice, and in mice over-expressing human mutant tau and Niemann–Pick type C mice (Pacheco et al., 2008; Rodríguez-Navarro et al., 2008). The kyphotic index (KI) was determined as described by (Laws, 2004) to quantify the degree of kyphosis in Tau35 and WT animals aged 4-14 months (Figure 3.9a). However, instead of measuring KI from radiographs (which were not readily available) the spines of mice were manually determined (see section 2.3.12.4 Assessment of kyphosis Figure 3.9a, b). WT mice had a KI of 4.4-4.6 at all ages examined, similar to previously reports (Laws, 2004; Vianello et al., 2014). Tau35 mice aged 4 months also exhibited a KI of 4.5, similar to their WT counterparts. However, the KI of Tau35 mice decreased to 3.8 at 6 months of age and continued to steadily decline to 2.9 by 14 months of age (Figure 3.9c). This reduction in the KI of Tau35 mice demonstrates a progressive worsening of spine curvature in these animals with increasing age. These data paralleled those of the grip strength and limb clasping neuromuscular deficits seen in Tau35 mice.

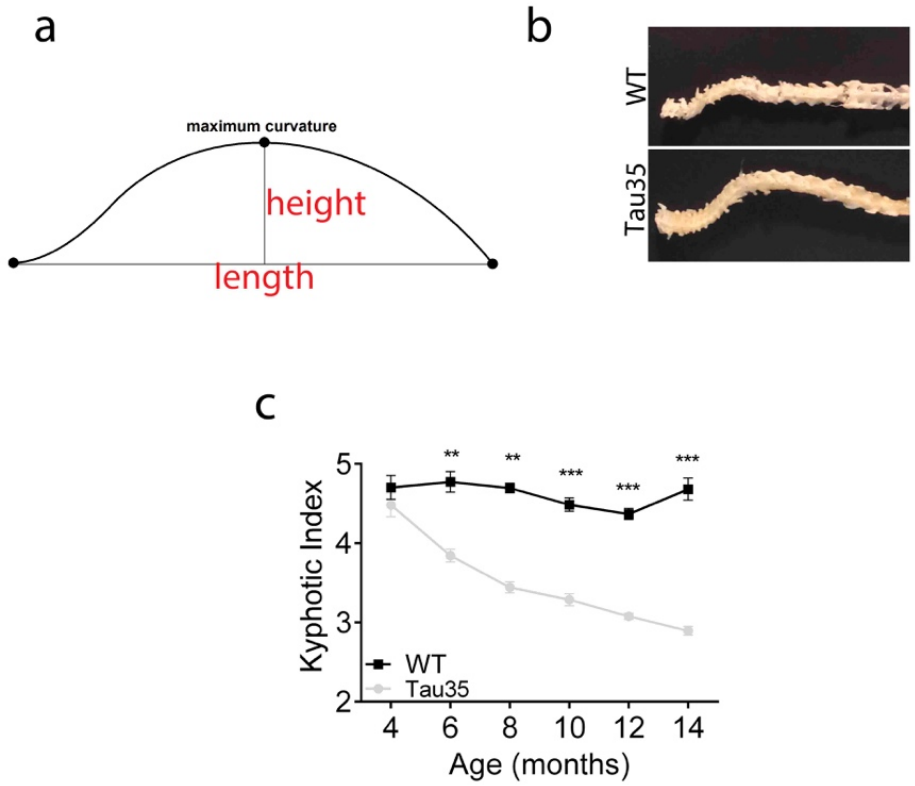

Figure 3.9: Kyphosis phenotype of Tau35. (a) Kyphosis index (KI)=length of spine/height at point of maximum curvature. **(b)** Skeletal structure shows spine curvature in Tau35 mice that is not apparent in WT mice at 14 months of age. **(c)** There is a marked reduction in the kyphosis index in Tau35 mice from 6 months of age, indicating progressive spinal curvature. The degree of kyphosis was determined at 4-14 months of age. Values shown are mean ± SEM, n=8 mice per genotype, **P < 0.01, ***P < 0.001, ANOVA.

3.2.2.7 Locomotor activity is not reduced in Tau35 at 8 months of age.

In order to test for any patterns of anxiety or abnormal behaviour, locomotor activity was tested in Tau35 mice at 8 months of age using the open field test. Tau35 mice showed no significant differences in either time spent in each zone (Figure 3.10a) or the total distance travelled (Figure 3.10b). No abnormal rearing or other behaviours were observed upon visual analysis of the behavioural patterns in Tau35 mice.

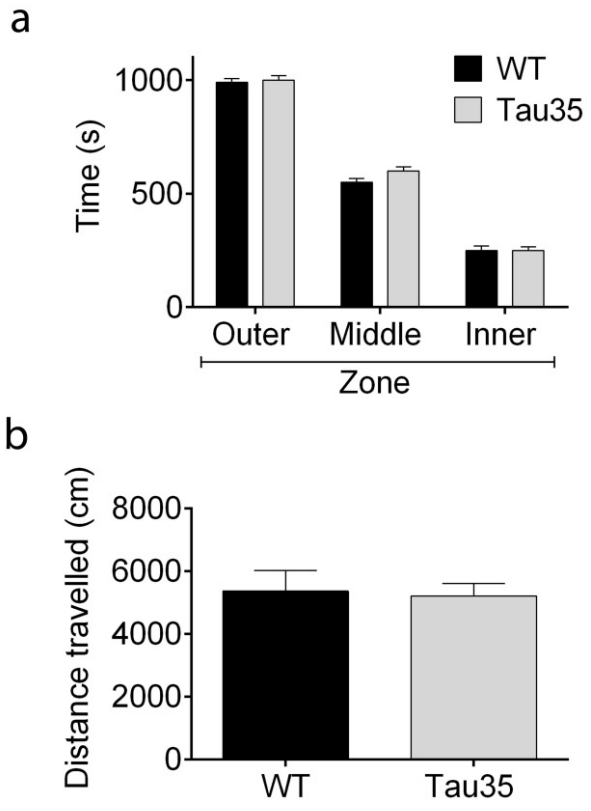

Figure 3.10: Locomotor activity was monitored in the open field test. (a) Results are expressed as the time spent in the outer, middle or inner zone of the open field during an observation period of 30 min. **(b)** Total distance travelled in the 30min spent in the open field. Tau35 and WT mice at 8 months of age, indicating that there are no significant differences in anxiety between the two genotypes. Values shown are mean ± SEM, n=8 for each genotype.

3.2.2.8 Spatial learning and memory is impaired in Tau35 mice

The Morris water maze is a well-established memory test for long-term spatial hippocampal-dependent learning encompassing the acquisition and spatial localisation of relevant visual cues that are then processed, consolidated, retained and sub-sequentially retrieved in order to navigate and find a hidden platform to escape the water (Morris, 1984). At 2, 4 and 6 months of age, Tau35 mice showed no significant differences during the visible platform and four consecutive non-visible platform learning days in their ability to find the platform (spatial learning), compared to WT controls (Figure 3.11a-c). However, by 8 months of age, Tau35 mice exhibited longer escape latencies over the four days of testing compared to WT controls and this was significantly impaired by day 4 (Figure 3.11d). The ability of Tau35 mice to learn the location of the platform was further decreased at the age of 10 months, at which point Tau35 mice showed a significantly reduced ability to find the hidden platform on days 3 and 4 (Figure 3.11e). By 12 months of age, the impaired ability of Tau35 mice to learn the location of the platform was even further reduced (Figure 3.11f). These results indicate an age-dependent spatial learning impairment in Tau35 mice.

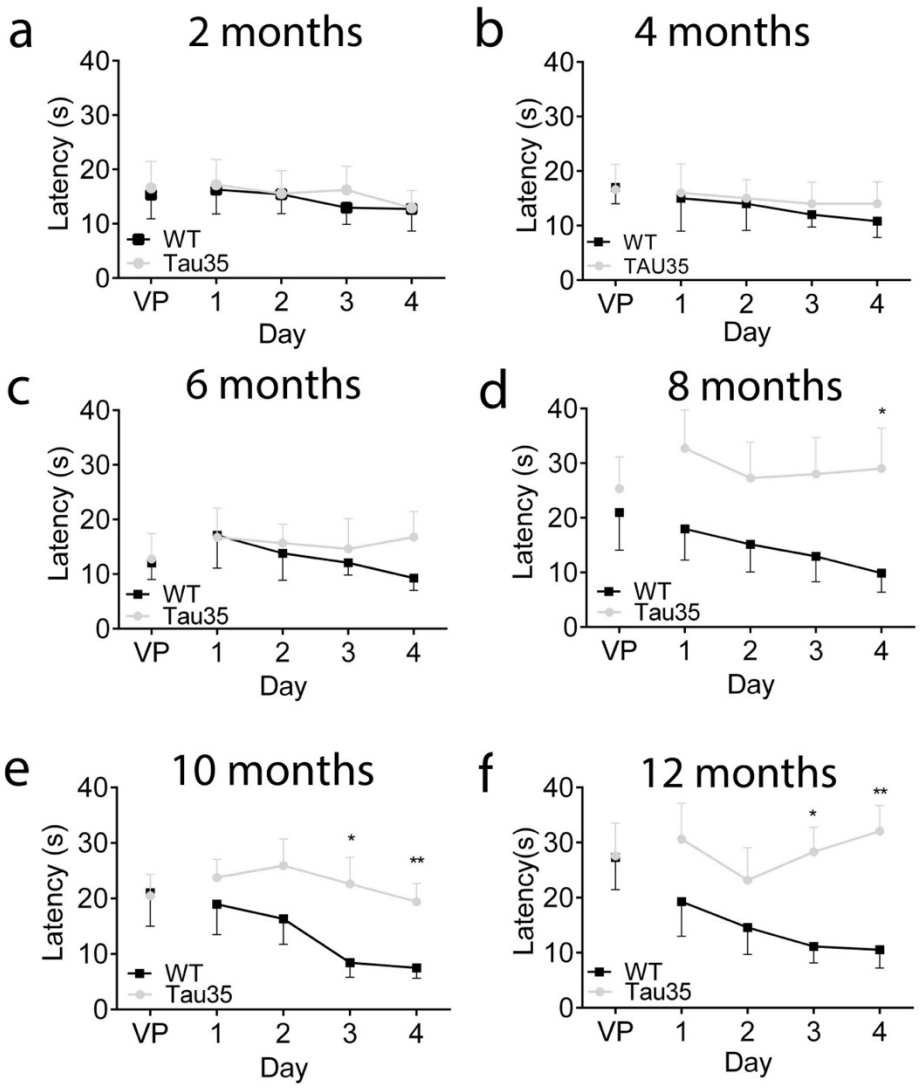

Figure 3.11: Latency testing in the Morris water maze. (a-f) Graphs showing the time taken for Tau35 and WT mice, at 2-12 months of age, during visible platform training (VP) on day one and latency to reach the hidden platform in the Morris water maze on days 1-4. Values represent mean and ± SEM, n=8 per genotype, *P<0.05, **$P < 0.01$, ANOVA.

3.2.2.9 Hippocampal dependent memory is impaired in Tau35 mice

To asses hippocampal-dependent memory, a probe trial was conducted with the WT and Tau35 mice 24 hours after hidden platform training. This showed that hippocampal-dependent memory was impaired from 8 months of age in Tau35 mice, which paralleled their defective ability to locate the hidden platform (Figure 3.12a, P<0.001). Hippocampal-dependent memory progressively deteriorated further with age at 10 and 12 months (Figure 3.11a, P<0.001, P<0.001, respectively). To assess time % occupancy in target quadrant, data from the 8 months old cohort were analysed. As expected, Tau35 mice spent less % of the time in the target quadrant during the probe trial when the platform was removed, further demonstrating their impaired hippocampal-dependent memory (Figure 3.11b; P<0.001).

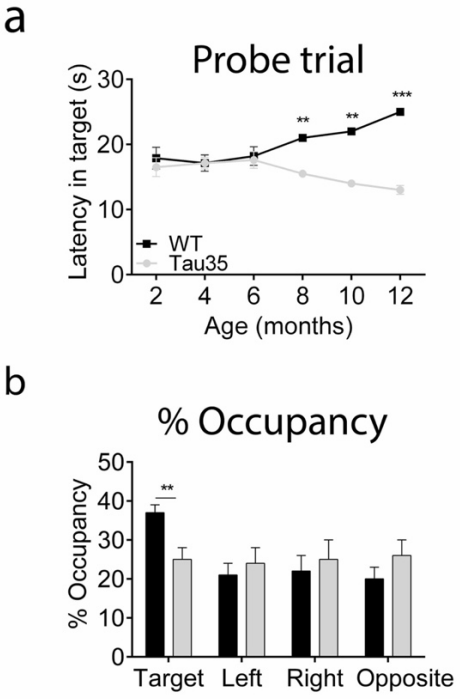

Figure 3.12: Hippocampal dependent memory in Tau35 (a) During the probe trial (60s), Tau35 mice show reduced latency on target compared to WT mice. **(b)** The percentage occupancy of the target quadrant is significantly reduced for Tau35 mice compared to WT mice aged 8 months. Values shown are mean ± SEM, n=8 mice for each genotype, **P<0.01, ***P<0.001, ANOVA.

3.2.2.10 The distance swum in the Morris water maze, but not swim speed, is increased in Tau35 mice

To validate whether the hippocampal-dependent memory deficit in Tau35 mice was related to a reduced ability to swim, the total swim distance to the hidden platform and the swim speed of mice was determined. Tau35 mice showed a longer travelling distance to the target platform compared to WT mice, which correlated with the increased time spent searching for the platform in these animals, indicating a reduced ability to locate the platform (Figure 3.13a; $P<0.05$). Neuromuscular impairment could potentially compromise the swimming ability of Tau35 mice. However, Tau35 did not show any significant reduction in swim speed (Figure 3.13b). These results indicate that, although Tau35 mice have apparent motor and neuromuscular deficits (Rotarod and grip strength, respectively), their swim speed was not compromised (Figure 3.13b). Thus, the progressive reduction in the ability of Tau35 mice to find the hidden platform in the Morris water maze is due to cognitive impairment, rather than to defective motor function, or increased anxiety in these animals.

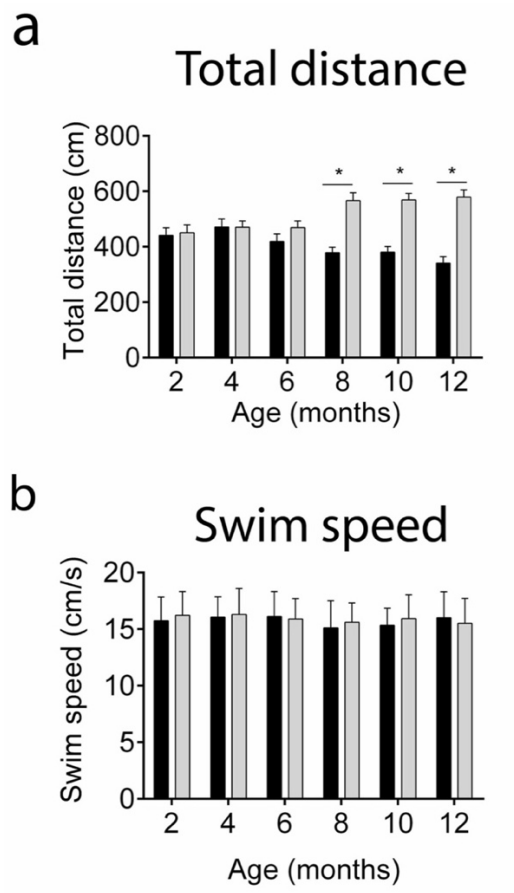

Figure 3.13: Total distance and swim speed in Tau35 (a) Total swim speed at 2, 7 and 8 months of age. **(b)** Total distance travelled to escape platform at 8 months of age. Values shown are mean ± SEM, n=8 mice for each genotype, *P<0.05, ANOVA.

3.2.2.11 Olfactory habituation is not impaired in Tau35 mice

The time mice spend investigating novel odours is used as an indicator of olfactory perception and function, as well as non-associative memory (Freedman et al., 2013). When olfactory habituation was assessed at 8 months of age in Tau35 and WT mice, no significant difference was observed in habituation/dishabituation of novel olfactory cues (Figure 3.14). Tau35 and WT mice each spent longer sniffing social odours compared to non-social and control odours and the heights of the curves confirms that the mice have the

sensory ability to discriminate between different odours and to habituate, as well as being able to discriminate social (urine) from non-social (banana) odours (Figure 3.14) (Silverman et al., 2010). This indicates that Tau35 mice experienced no differences in non-associative short-term memory olfaction or olfactory function or anxiety aged 8 months. This is an important finding because it shows that Tau35 mice exhibit normal olfactory learning and potentially they do not have impaired short-term memory, although further test would have to be conducted to confirm this finding.

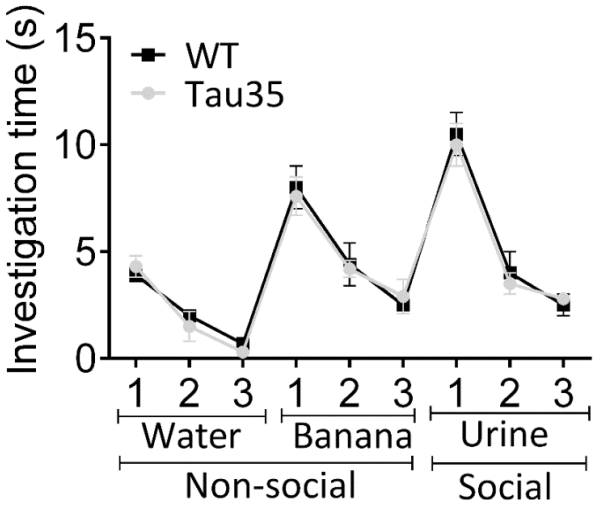

Figure 3.14: Olfactory habituation/dishabituation is not impaired in Tau35 mice. Graph showing the presentation of water, non-social (banana) and social odours (urine) to Tau35 and WT mice. Decreased investigation time indicates habituation to novel odours. Values represent mean and ± SEM, n=8 per genotype.

3.2.3 Biochemical analysis of Tau35 mice

To gain more insight into the behavioural changes seen in Tau35 mice, biochemical analyses were performed. Brain homogenates from Tau35 and WT littermates aged 14 months were prepared from hippocampus and associated cortex, as described in section 2.3.2 Preparation of mouse brain homogenates. Samples were assessed on western blots using antibodies directed against key proteins of interest.

3.2.3.1 Tau is phosphorylated at several different epitopes in Tau35 mice whereas the total amount of tau is unchanged

A major feature of human tauopathies is increased tau phosphorylation at a myriad of phosphorylation sites (Hanger et al., 2009). When examining western blot analysis of hippocampal homogenates from Tau35 and WT mice at 14 months of age, it was apparent that the total amount of total tau was similar in Tau35 and WT mice (Figure 3.15a, right). Interestingly this was in-line with the equivalent amounts of tau mRNA expression observed in these animals, indicating physiologically relevant amounts of tau expression in these mice, even in the presence of the transgene. When probed with an antibody for the PHF1 epitope pSer396/Ser404, western blots showed a 2.7-fold increase in PHF1 immunoreactivity, relative to total tau (Figure 3.15, $P<0.05$) in the hippocampus and associated cortex (Figure 3.15a). This increase in PHF1 in Tau35 mice was accompanied by the appearance of a slower migrating tau species in both PHF1 and total tau blots (Figure 3.15, red arrowheads). Significant changes in tau phosphorylation were also found at epitopes corresponding to: TG3 (Figure 3.16a, pT231, 5.72- fold increase), AT270 (Figure 3.16b, pT181, 3.6- fold increase), and Tau.1 (Figure 3.16c, dephosphorylated S199/S202/T205, 1.3- fold decrease). These results indicate that expression of Tau35 induces phosphorylation of a number of tauopathy related tau epitopes. The fact that this phosphorylation occurs both inside (PHF1, TG3, and Tau.1) and outside (AT270) the transgenically

expressed tau sequence shows that expression of this tau fragment influences tau phosphorylation of endogenous mouse tau.

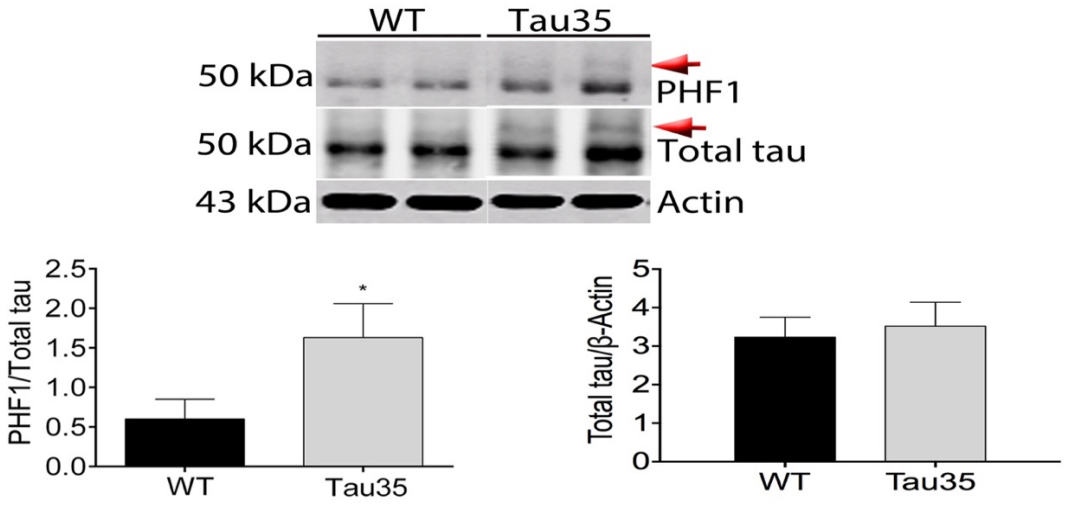

Figure 3.15: PHF1 antibody immunoreactivity in Tau35 and WT mice hippocampus at 14 months of age. Western blots show PHF1 (pS396/Se04), total tau, and β-actin reveal a significant increase in tau phosphorylation in Tau35 mice, compared to wild-type (WT) mice, whereas the total amount of tau relative to β-actin is equivalent in both genotypes. Higher molecular weight tau bands are visible seen in Tau35 (red arrows). Values represent mean and ± SEM, n=6, $P<0.01$, $^{*}P<0.05$, ANOVA.

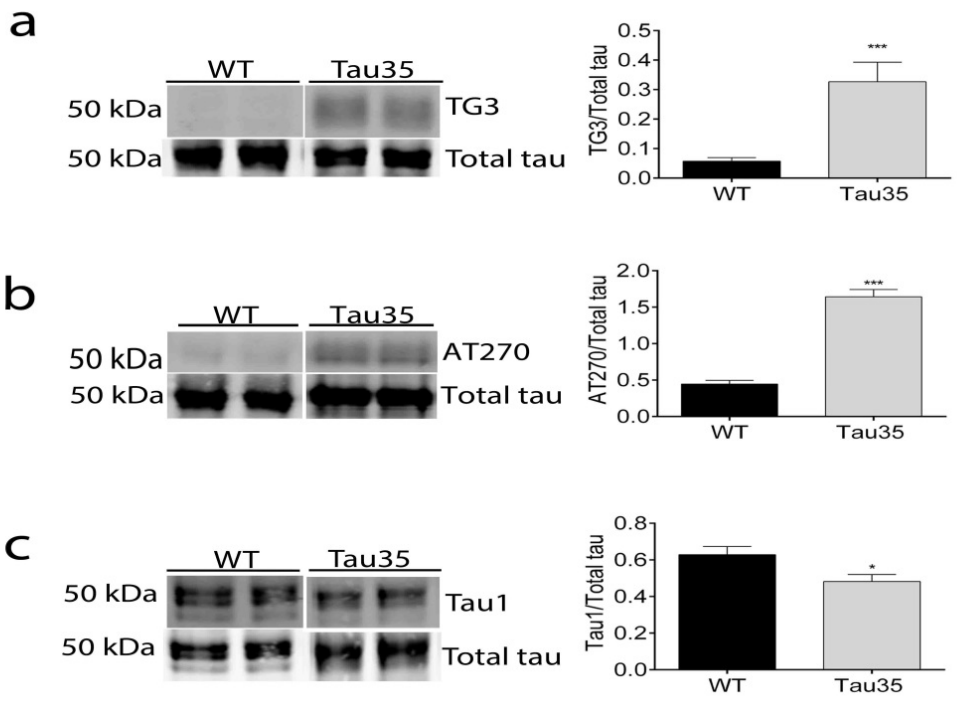

Figure 3.16: Phosphorylation dependent antibody labelling in Tau35 and WT mice. (a) TG3 (pT231) relative to total tau reveals an increase level in Tau35 compared to WT mice **(b)** AT270 (pT181) relative to total tau shows an increase in Tau35 compared to WT mice. **(c)** Tau.1 (S199/S202/T205) dephosphorylated tau relative to total tau shows a decrease in Tau35 compared to WT mice. Values shown are mean ± SEM, n=6 for each genotype, *P<0.05, ***P<0.001, ANOVA.

3.2.3.2 The amount of sarkosyl-insoluble and sarkosyl-soluble tau is equivalent in Tau35 and WT mice

The amount of sarkosyl-insoluble tau has previously been identified in a variety of transgenic mouse models, indicating an increase in highly aggregated tau species. Sarkosyl-soluble and insoluble fractions were prepared from Tau35 and WT mouse hippocampus at 14 months of age. Tau35 mice showed no significant differences in the amounts of tau present in sarkosyl-insoluble and soluble fractions, compared to WT mice (Figure 3.17). These results

indicate that sarkosyl-insoluble, highly aggregated tau species do not accumulate appreciably in Tau35 mice aged 14 months.

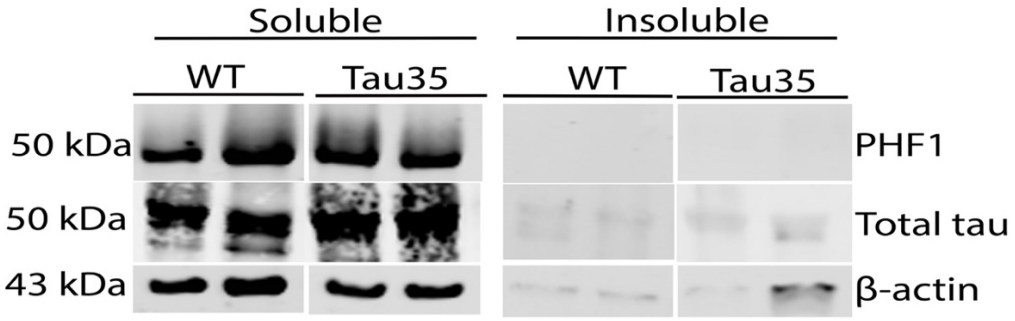

Figure 3.17: Sarkosyl-soluble and insoluble tau is comparable in Tau35 and WT mice. Western blot of sarkosyl-soluble and insoluble tau fractions from Tau35 and WT mice labelled with PHF1, total tau and β-actin antibodies. Molecular weight markers are shown on the left. n=3 for each genotype.

3.2.3.3 Glycogen synthase kinase 3β is activated in Tau35 mice

Several different proline-directed candidate kinases are responsible for increased tau phosphorylation in human tauopathy. GSK3 has the ability to phosphorylate tau in many of the serine and threonine residues in tau (Hanger et al., 1992, 2009; Mandelkow et al., 1992; Cho, 2003). The activity of GSK3 is regulated by opposing serine and tyrosine phosphorylation of the enzyme, in which phosphorylation of Ser9 in GSK3β or Ser21 in GSK3α inhibits GSK3 activity (Stambolic and Woodgett, 1994), whereas phosphorylation of Tyr216 in GSK-3β and Tyr279 in GSK3α activates GSK3 (Hughes et al., 1993). Tau35 mice showed a reduction in inhibitory Ser9 phosphorylation of GSK3β (Figure 3.18), indicating increased GSK3β activity in Tau35 hippocampus (Hanger et al., 1992; Mandelkow et al., 1992; Leclerc et al., 2001; Bhat et al., 2003). Interestingly, the elevated GSK3β activity paralleled the increase in tau phosphorylation in Tau35 mice. The phosphorylation sites Thr181, Thr231 and Ser396/Ser404 have all previously been shown to be phosphorylated by

GSK3β (Cho, 2003; Maldonado et al., 2011). No differences were observed in the amounts of either GSK3α phosphorylated at Ser21 (Figure 3.18b, left) or total GSK3α/β, relative to β-actin, between Tau35 and WT mice (Figure 3.18b and c, right). These results show a selective activation of GSK3β, but not GSK3α, in Tau35 mice.

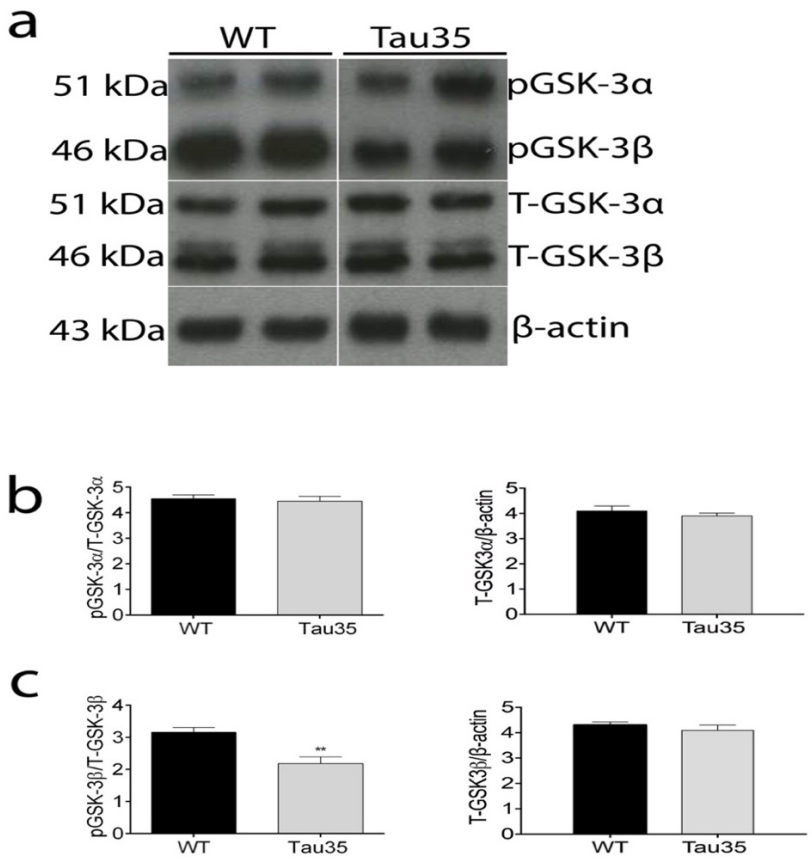

Figure 3.18: GSK3β activation in Tau35 mice (a) Western blots showing phosphorylated (inactive) glycogen synthase kinase-3α and β (pGSK3α/β) and total (T-) GSK3α and β **(b)** Phosphorylated pGSK3α and T-GSK3α are unchanged in Tau35 and WT mice. **(c)** pGSK3β relative to total T-GSK3β, is significantly decreased in Tau35 mice, indicating increased GSK3β activity. Values shown are mean ± SEM, n=6 for each genotype, **P < 0.01, ANOVA.

3.2.3.4 Lysosomal degradation markers are altered in Tau35

Alterations in lysosomal mediated degradation and/or autophagy are features of several human tauopathies (Piras et al., 2016). Therefore, lysosomal degradation in Tau35 mouse brain was determined by measuring the amount of microtubule-associated protein 1-light chain 3 (LC3) present. During autophagy, cytosolic LC3-I is conjugated to phosphatidylethanolamine to form LC3-II, which is targeted to the autophagosome and therefore LC3-II is a commonly studied marker of autophagy due to its importance in the elongation step of the autophagosomal membrane (Banduseela et al., 2013). Both LC3-I and LC3-II were found to be significantly increased, relative to β-actin, in the hippocampus of Tau35 mice aged 14 months, compared to age-matched WT animals (Figure 3.19a, $p<0.05$). However, the ratio of LC3-II to LC3-I did not change, indicating no alteration in the conversion of LC3-I to LC3-II. These results suggest altered autophagic/lysosomal processes in Tau35 mice through increased production of LC3-I, enhanced conversion of LC3-I to LC3-II, and/or reduced lysosomal degradation of LC3-II (Mizushima and Yoshimori, 2007).

A further marker of autophagy is the MT-associated protein 1A/1B-light chain 3 (LC3) and the ubiquitin-binding scaffold protein, p62/SQSTM1, which recognises ubiquitinated misfolded proteins such as highly phosphorylated tau and which is subsequently degraded by autophagy, accumulating under conditions when autophagy is inhibited (Kuusisto et al., 2002; Bjørkøy et al., 2006; Komatsu et al., 2007). Western blots of Tau35 mouse brain revealed a 4-fold increase in the amount of p62 (Figure 3.19b, $P<0.05$), supporting the view that autophagic/lysosomal function is impaired in Tau35 mice.

Cathepsins are important family of enzymes that are responsible for the degradation of proteins during lysosomal degradation and soluble tau has previously been identified as a substrate for these lysosomal proteases (Kenessey et al., 2002; Bendiske and Bahr, 2003). Measuring the amount of mature cathepsin D in Tau35 mice aged 14 months showed a significant decrease of 2.1- fold compared to WT mice, whereas the amount of pro-cathepsin D was unchanged (Figure 3.20a, $P<0.05$). These results indicate

lysosomal dysfunction in Tau35 mice which could be contributing further to defective autophagy.

Reduced tubulin acetylation has previously been identified in tangle-bearing neurons as an early event in tauopathies (Cook et al., 2014). Acetylated MTs are required for LC3-II degradation and for fusion of autophagosomes with lysosomes (Hempen and Brion, 1996; Xie et al., 2010; Cohen et al., 2011; Bánréti et al., 2013). Western blots of Tau35 mouse brain showed that acetylated α-tubulin was significantly reduced in Tau35 mice aged 14 months, whilst the total amount of α-tubulin was unchanged (Figure 3.20b). Taken together, these findings suggest that expression of Tau35 in mice results in a significant impairment of molecular mechanisms involved in autophagy and lysosomal-mediated degradation.

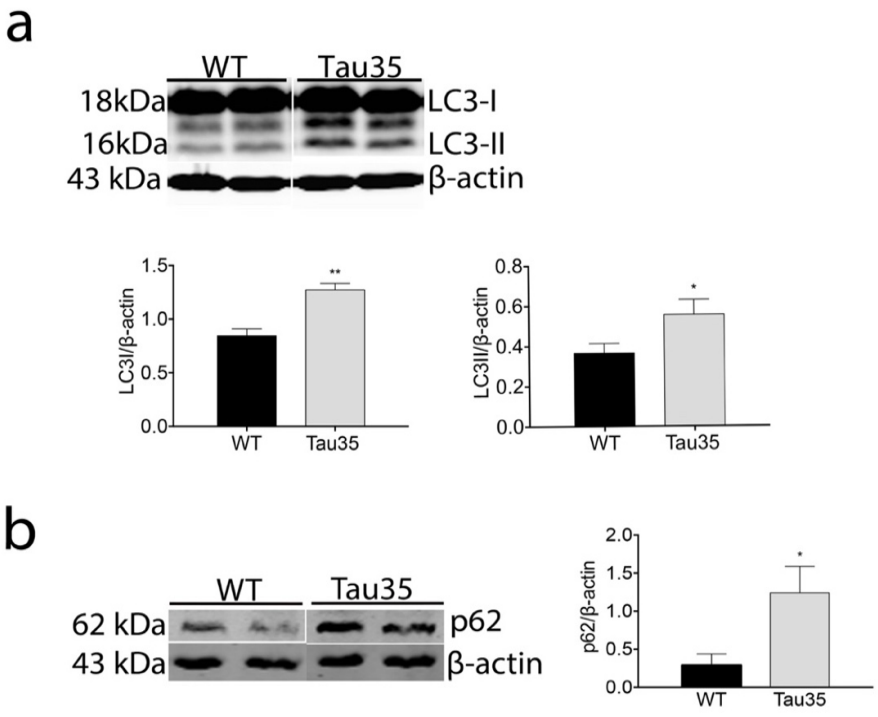

Figure 3.19: LC3 and p62 levels in Tau35 and WT mice. Western blots showing **(a)** the amounts of microtubule-associated protein 1-light chain 3 (LC3)-I and LC3-II, relative to β-actin, are increased in Tau35 mice **(b)** p62 is significantly increased, relative to β-actin, in Tau35 mice. Values shown are mean ± SEM, n=6 for each genotype, *P < 0.05, **P<0.01, ANOVA.

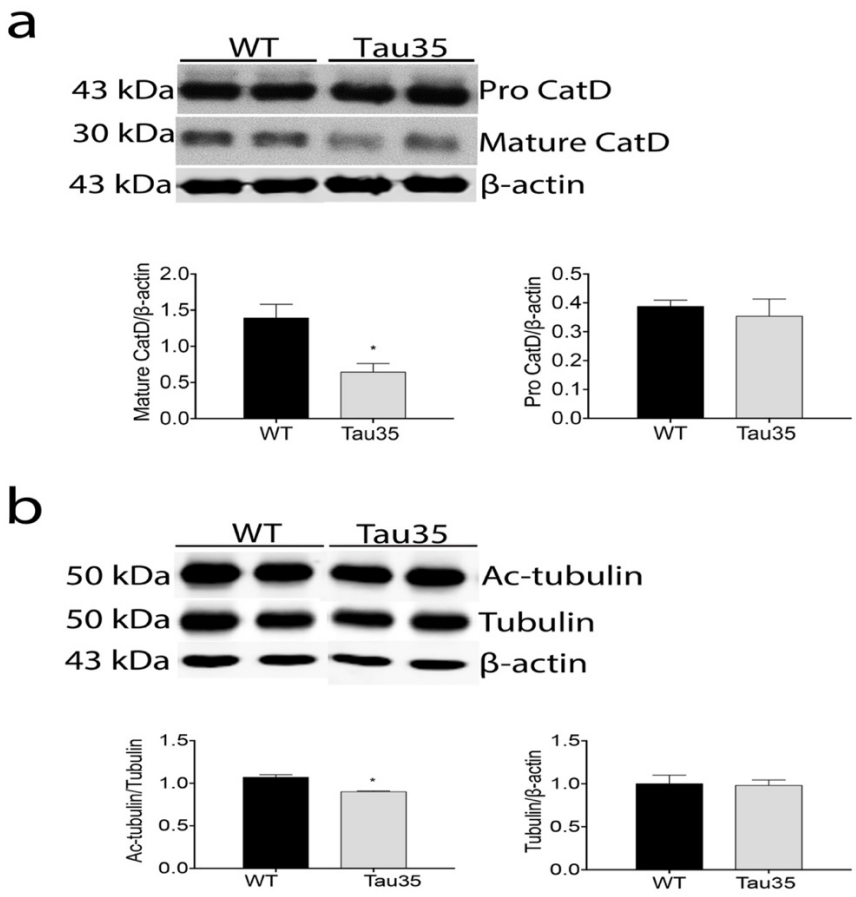

Figure 3.20: Cathepsin D and acetylated tubulin levels in Tau35 and WT mice. Western blot showing **(a)** Mature (active) cathepsin D (CatD) is reduced in Tau35 mice, whilst the amount of pro-cathepsin D (Pro CatD) is unchanged. **(b)** Western blots show a small but significant decrease in acetylated α-tubulin in Tau35 mice. The total amount of tubulin relative to β-actin is equivalent in both genotypes. Values shown are mean ± SEM., n=6 for each genotype. *P<0.05, **P<0.01, ANOVA.

3.2.3.5 Synaptic proteins in Tau35 mice

Synaptic loss and dysfunction are common features in tauopathies and in the case of AD, synaptic loss is correlated with disease progression. Hence it was important to determine whether Tau35 mice exhibit changes in synaptic proteins. To evaluate synaptic function, a range of pre- and post-synaptic markers were examined in the hippocampus of 14 months old Tau35 and WT mice. Synaptobrevin is a key element of the SNARE complex and is thought to play a major role in vesicular fusion with the plasma membrane (Parlati et al., 2000). A 2-fold reduction in the amount of synaptobrevin relative to α-tubulin was observed in Tau35 mice (Figure 3.22a, $P<0.001$), indicating a potential deficit in synaptic vesicle fusion and hence reduced neurotransmission. When measuring the pre-synaptic marker synapsin1, a 65% reduction in the amount of synapsin1 was observed (Figure 3.22b, $P<0.001$). No changes were found in the amounts of the scaffolding protein that is present in the post synaptic density, PSD95 (Figure 3.21a), the pre-synaptic marker synaptophysin (Figure 3.21b) or the calcium-dependent neurotransmitter release protein, synaptotagmin (Figure 3.21c) relative to tubulin. These results indicate a selective loss of releasable synaptic vesicles (Cesca et al., 2010) without affecting synaptophysin-regulated synaptic vesicle endocytosis (Kwon and Chapman, 2011).

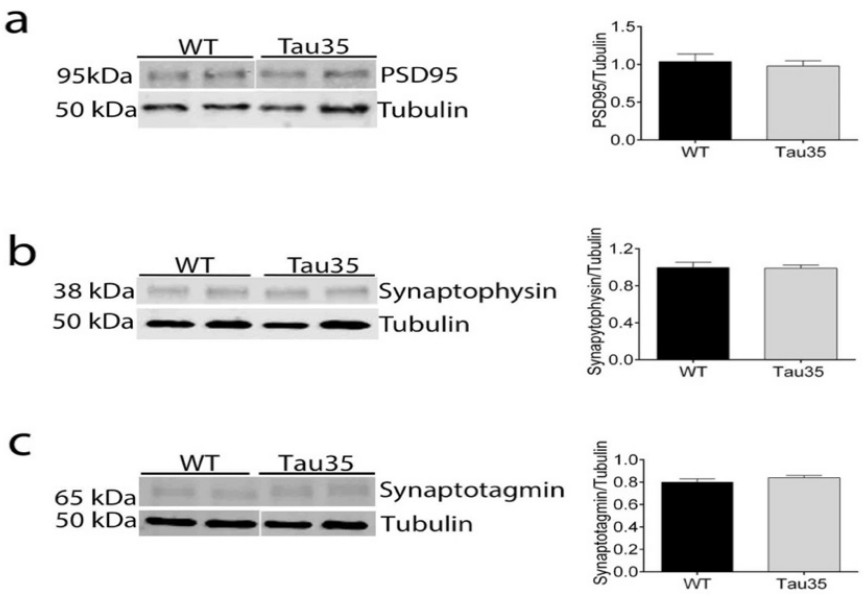

Figure 3.21: Synaptic markers in Tau35 mice. (a) Post synaptic marker PSD95 showed no changes when comparing Tau35 and WT mice normalised to a-tubulin. **(b)** Synaptophysin is unchanged in Tau35 mice. **(c)** Synaptotagmin levels are unchanged in Tau35 compared to WT mice. Values shown are mean ± SEM., n=6 for each genotype.

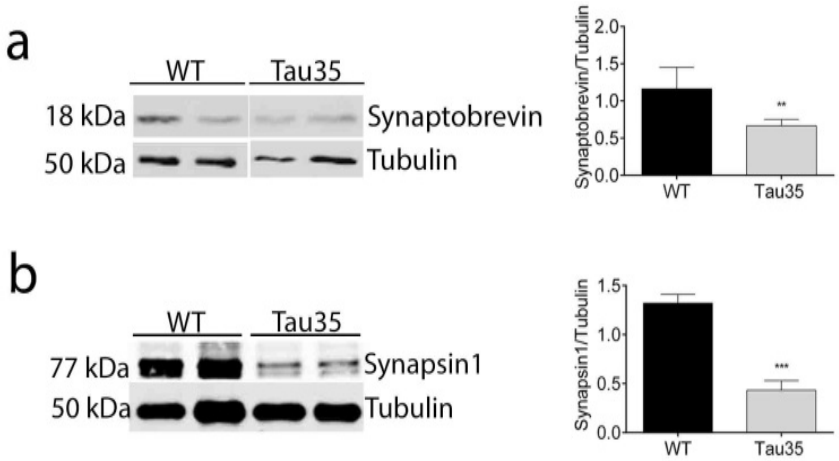

Figure 3.22: Synaptic markers in Tau35 mice. (a) The amount of synaptobrevin is reduced relative to tubulin in Tau35 mice. (b) The amount of synapsin1 is reduced relative to α-tubulin. Values shown are mean ± SEM., n=6 for each genotype, **P<0.01, ***P<0.001, ANOVA.

3.2.3.6 GFAP is not increased in Tau35 mice

A variety of tauopathies such as PSP exhibit astrocytic activation. However, Tau35 mice aged showed no changes in astrocyte morphology or the amount of glial fibrillary acidic protein (GFAP) at 14 months in the hippocampus and associated cortex (Figure 3.23a). Furthermore, no difference was observed via immunohistochemistry (Figure 3.23b). Indicating that Tau35 mice exhibit a progressive tauopathy characterised by conformationally-altered, aggregated and phosphorylated tau, in the absence of detectable astroglial activation.

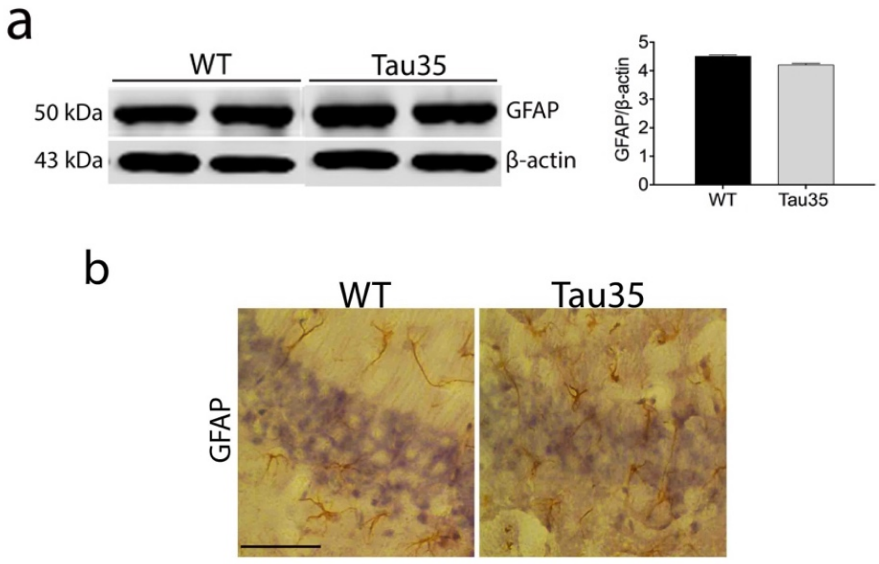

Figure 3.23: Tau 35 mice show no alteration in an astrocytic marker. **(a)** Western blots of GFAP in 14 months old mouse brains show no changes in Tau35 mice when normalised to β-actin. **(b)** Hippocampal sections from Tau35 and WT mice at 14 months of age probed with GFAP. Values shown are mean ± SEM., n=6 for each genotype, Scale bar=200μm.

3.2.4 Neuropathological analysis of Tau35 mouse brain

For immunohistochemical analysis, perfused brains from 2, 8, 14 and 16 months old Tau35 and WT mice were prepared as described in section 2.3.8 Tissue sectioning. The fixed brain tissue was labelled with antibodies directed towards key proteins of interest.

3.2.4.1 Tau35 mice exhibit increased phosphorylated tau immunoreactivity

Neurofibrillary tangle and pre-tangle formation is perhaps the most distinctive feature of tauopathies indicating extensive neuronal dysfunction and tau accumulation. When examining Tau35 and WT hippocampal and cortical brain sections for the presence of phosphorylated tau, pre-tangle pathology was evident. When labelling with the antibody for PHF1 (recognising tau phosphorylated at Ser396/Ser404), cytoplasmic neuronal labelling was apparent from 2 months of age in Tau35 mice, with dystrophic neurites labelling at 8 months and extensive pre-tangle pathology evident by 14 months of age (Figure 3.24, PHF1). When labelling with an antibody against tau phosphorylated at Ser202/Thr205 (AT8), cytoplasmic background cytoplasmic labelling was present in the hippocampus from 8 months of age. By 14-16 months, tangle-like structures labelled with AT8 were apparent in the hippocampus of Tau35 mice (Figure 3.24, AT8), similar to the pathology observed in tau over-expressing mutant tau mice (Hutton et al., 2000; Santacruz et al., 2005; Terwel et al., 2005; Schindowski et al., 2006; Yoshiyama et al., 2007). When labelling with phosphorylation-dependent antibodies AT100 (Thr212/Ser214) and pS422, appreciable amounts of background labelling were evident at 14 months of age in Tau35 mouse brain, which was absent from WT mice of the same age. There was an increase in labelling with pS422 antibody in the molecular layer of the hippocampus with only very few distinctive immunopositive structures for pS422 in Tau35 hippocampus (Figure 3.25, pS422). WT hippocampus up to 14-16 months of age did not show

any cytoplasmic or aggregated tau using the same tau antibodies (Figure 3.25, right lanes).

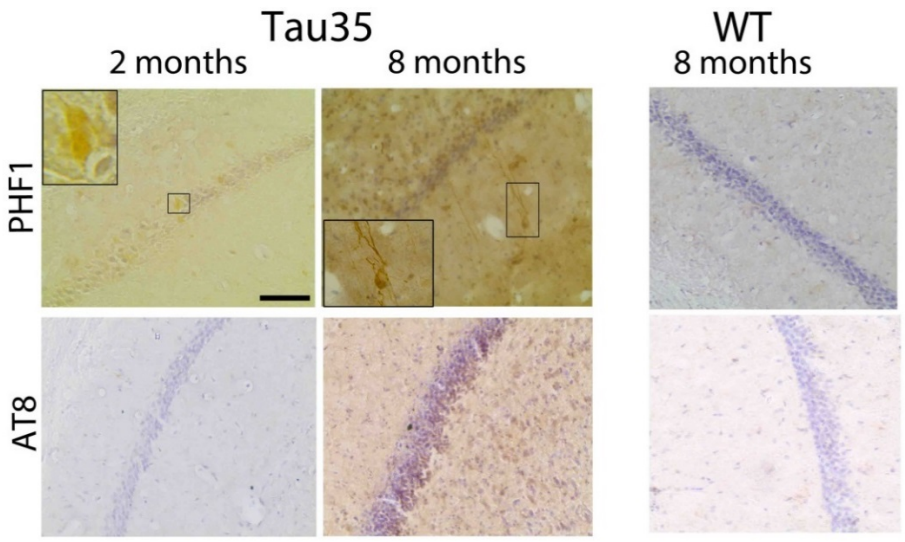

Figure 3.24: Tau immunoreactivity using a range of phosphorylation dependent tau antibodies in Tau35 mice at 2 and 8 months of age. CA1 hippocampal regions of Tau35 mouse brains at 2 and 8 months of age, and wild-type (WT) mice aged 8 months (right panels), labelled with tau antibodies, PHF1 and AT8 and counterstained with haematoxylin. PHF1 revealed tau-positive labelling at 2 and 8 months of age (right panels). n=5 mice for each genotype, scale bar=200μm.

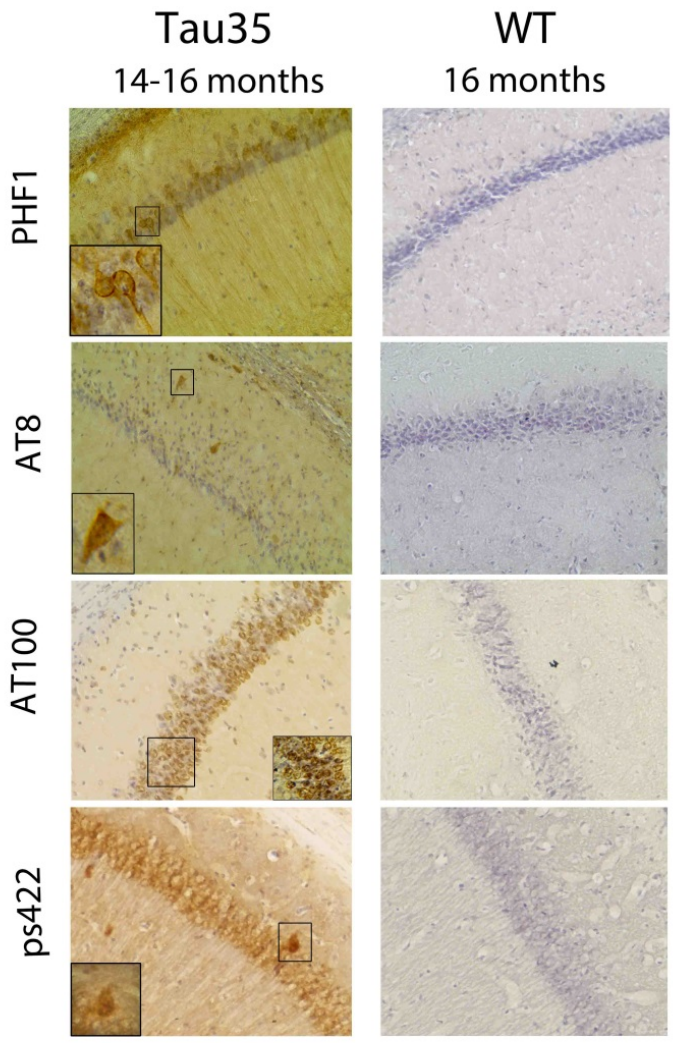

Figure 3.25: Tau immunoreactivity using a range of phosphorylation dependent tau antibodies in Tau35 at 14-16 months of age. CA1 hippocampal regions of Tau35 mouse brains at 14-16 months of age, and wild-type (WT) mice aged 16 months (right panels), labelled with tau antibodies, PHF1, AT8, AT100 and pS422, and counterstained with haematoxylin. n=5 mice for each genotype, scale bar=200μm.

3.2.4.2 Conformational tau antibodies show increased immunoreactivity in Tau35 mice

One of the neuropathological hallmarks of tauopathies is the accumulation of abnormally modified and oligomeric species of tau which are linked to cognitive decline seen in tauopathies (Brandt et al., 2005; Williams et al., 2006). When examining Tau35 for such species, mice showed increased cytoplasmic staining in the hippocampus at 8 months of age labelled with antibodies recognising oligomeric tau (TOC1) or abnormal tau conformations (MC1). At 14 months of age, tau-positive neurons became apparent in pre-tangle like structures (TOC1 and MC1). An antibody recognising nearly pathological tau conformation and phosphorylated tau (PG5) labelled tau phosphorylated at Ser409 in Tau35 hippocampus from 8 months of age (Figure 3.26, PG5). These three epitopes are unique to tauopathy and therefore they clearly distinguish abnormal tau from WT tau (Jicha et al., 1999). This indicates that marked tau immunoreactivity was present in Tau35 mice in the apical dendrites and in the cell bodies of CA1 neurons for conformational antibodies from 8 months of age, and oligomeric species from 14 months of age. There was also evidence of some pyramidal neurons containing somatodendritic tau immunoreactivity with all conformational antibodies tested.

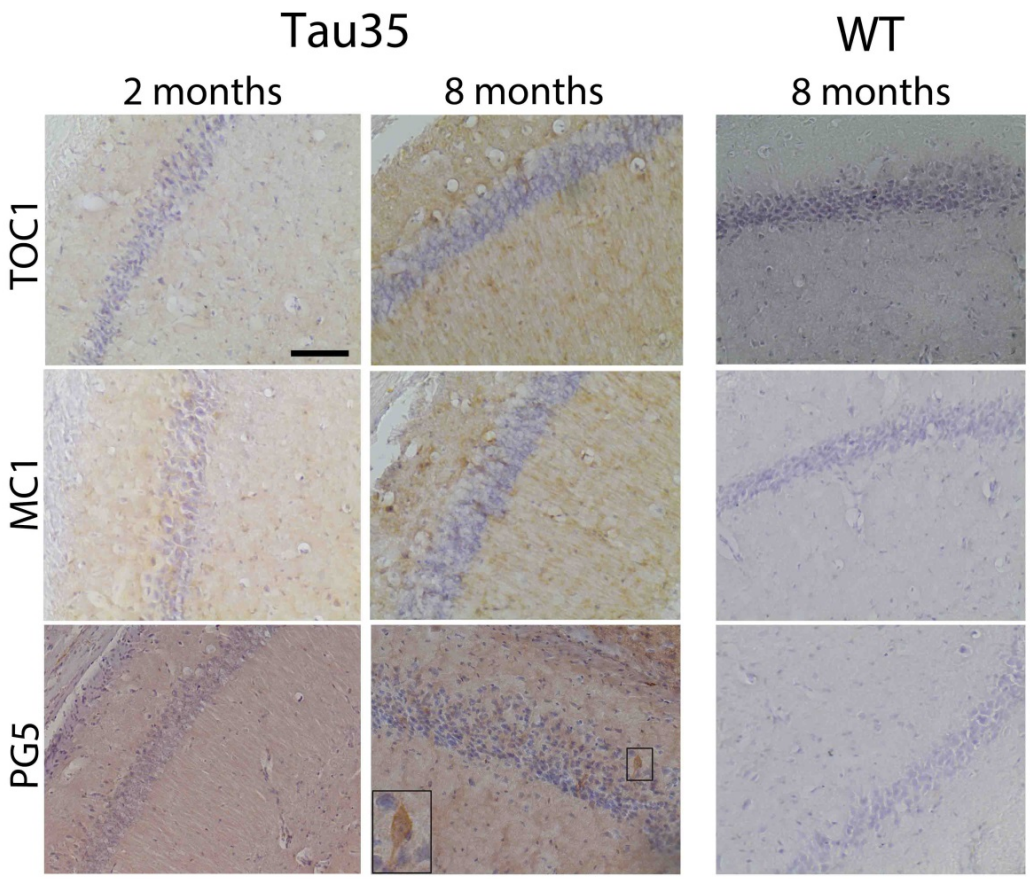

Figure 3.26: Altered tau Conformation in Tau35 mice. CA1 hippocampal sections of Tau35 mice at 2 and 8, months of age, and wild-type (WT) mice aged 8 months (right panels), labelled with oligomeric and conformational tau antibodies, TOC1, MC1, and PG5, and counterstained with haematoxylin. n=5 mice for each genotype, scale bar=200µm.

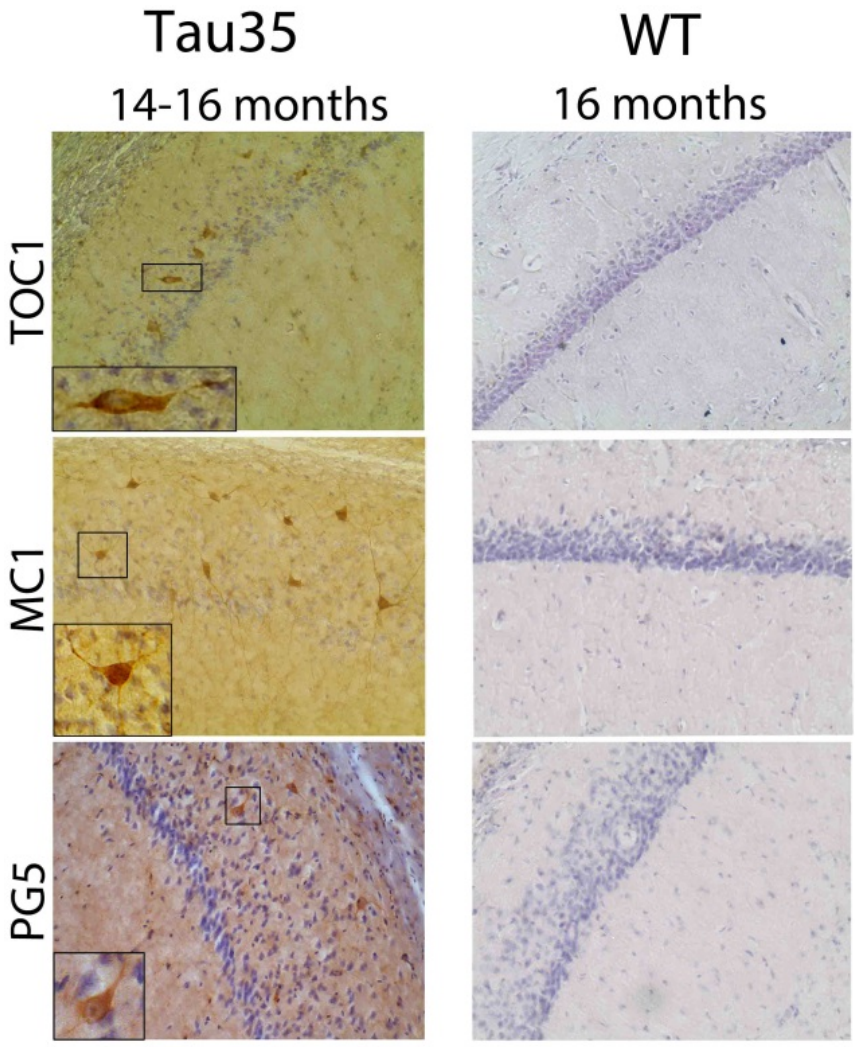

Figure 3.27: Altered tau Conformation in Tau35 mice at 14-16 months of age. CA1 hippocampal sections of Tau35 mice at 14-16 months of age, and wild-type (WT) mice aged 16 months (right panels), labelled with oligomeric and conformational tau antibodies, TOC1, MC1, and PG5, and counterstained with haematoxylin. n=5 mice for each genotype, scale bar=200µm.

3.2.4.3 Tau35 recruits endogenous mouse tau

The spreading of tau in a prion-like manner through the brain is an emerging concept that suggests that pathological tau can be seeded and transmitted to otherwise healthy cells to form inclusions which may underlie the stereotypical progression of neurodegenerative tauopathies (Goedert et al., 2010; Clavaguera et al., 2013). To assess the potential role of endogenous mouse tau in the formation of tau inclusions in Tau35 mice, hippocampal sections were probed using an antibody labelling the N-terminus of tau (TP007), which is absent from transgenically expressed Tau35. Tau35 mice showed increased cytoplasmic labelling with TP007 from 8 months of age, with tau inclusions becoming apparent at 14-16 months of age indicating misfolding of endogenous mouse tau (Figure 3.28).

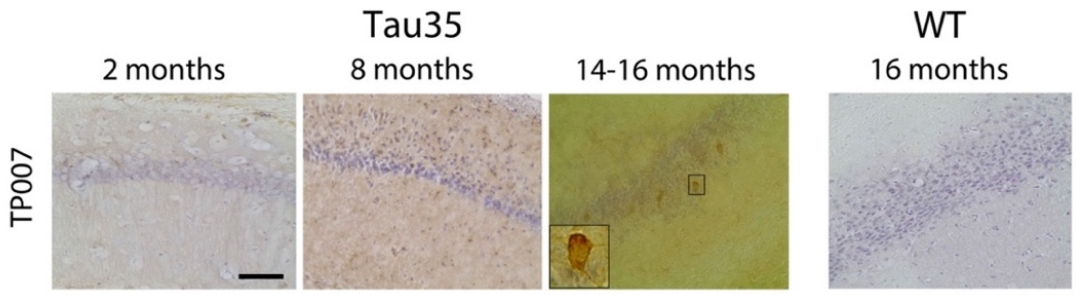

Figure 3.28: Labelling of tau inclusions with an antibody recognising the N-terminus of tau. CA1 hippocampal sections of Tau35 mice at 2, 8, and 14-16 months of age, and wild-type (WT) mice aged 16 months (right panels), labelled with tau antibody TP007, and counterstained with haematoxylin. Tau-positive labelling of inclusions in Tau35 brain, including dystrophic neurites and neuropil threads, was apparent at 14-16 months (inset). WT hippocampal sections showed no labelling of inclusions with these antibodies at 16 months of age. n=5 mice for each genotype, scale bar=200µm.

3.2.4.4 Analysis of pathology

A semi-quantitative analysis of tau antibodies used in this study was performed to profile tau immunoreactivity in Tau35 mice (Table 8). From the analysis it was clear that staining was most prominent in the CA1 of the hippocampus followed by CA3 and cortex.

Table 8: Immunolabelling with tau antibodies PHF1, TOC1, MC1, AT8, TP007, AT100 and pS422 in the hippocampus (CA1 and CA3 regions) and cortex (Cx) of Tau35 mice. The extent of tau pathology was assessed in mice 2-16 months of age (n=3) using a semi-quantitative scale of tau-positive inclusions: +++ moderate inclusions; ++ few inclusions; + no inclusions but increased background staining; - no tau immunoreactivity, N/A: not available.

Antibody	Age											
	2 months			8 months			14 months			16 months		
	CA1	CA3	Cx	CA1	CA3	Cx	CA1	CA3	Cx	CA1	CA3	Cx
PHF1	++	+	+	++	++	+	+++	++	++	+++	++	++
TOC1	-	-	-	+	+	+	+++	++	++	+++	++	++
MC1	-	-	-	+	+	+	+++	++	++	+++	++	++
AT8	-	-	-	+	+	+	++	++	++	+++	++	++
TP007	-	-	-	+	+	+	++	++	++	+++	++	++
AT100	N/A	N/A	N/A	N/A	N/A	N/A	++	++	++	++	++	++
pS422	N/A	N/A	N/A	N/A	N/A	N/A	++	++	++	++	++	++

3.2.4.5 Other pathologies in Tau35 mouse brain

The absence of distinct, mature neurofibrillary tangles in Tau35 mice, even towards the end stage of disease, suggests that other proteins may be involved in the mechanism underlying the development of the phenotypic, cognitive and motor deficits seen in these animals. Since impaired lysosomal degradation appeared to play a role in the abnormalities present in Tau35 mice, markers of autophagy and protein degradation were examined using immunohistochemistry.

Increased p62 immunolabelling was apparent in the hippocampus of Tau35 mice at 14-16 months of age, which was absent from WT mice (Figure 3.29a, insert). Ubiquitinated proteins bind to p62, targeting them for degradation, and p62 has previously been associated with tangle pathology in a variety of tauopathies (Kuusisto et al., 2001; Iqbal et al., 2005). Ubiquitin-positive inclusions were apparent in pyramidal cells of the hippocampus in Tau35 mice aged 14 months (Figure 3.29b, insert). These results suggest that highly phosphorylated tau aggregates are potentially ubiquitinated, marking them for degradation by the ubiquitin proteasome pathway. However, in Tau35 mice this clearance mechanism may be impaired, leading to the appearance of tau like aggregates.

Behavioural analysis of Tau35 mice identified significant motor dysfunction in these animals. Tauopathies can exhibit pathological features that overlap with other proteinopathies, such as Parkinson's disease, in which a primary clinical feature is severe motor dysfunction, (Xia and Mao, 2012). Motor dysfunction is also a prominent feature of mouse models of Parkinson's disease in which α-synuclein, the main component of the Lewy bodies present in Parkinson's disease, is over expressed (Spillantini et al., 1997; Goedert, 2001; Kim, 2013). Therefore, Tau35 mouse brain sections were examined for α-synuclein expression. Labelling with α-synuclein90 antibody, which recognises the central region of α-synuclein (Totterdell et al., 2004) revealed α-synuclein inclusions in Tau35 mice that were absent from WT mice (Figure 3.29c, insert). Although this was analysis was performed only at late stage of

the disease (14-16 months of age), these results suggest a potential role played by α-synuclein in the motor deficits exhibited by Tau35 mice.

Tau35 mice exhibit kyphosis and abnormal spinal curvature, a feature not normally observed in tauopathy, but rather a feature seen in ALS and prion models (Newman et al., 1995; Lenoir et al., 2010). One of the most distinctive pathological hallmarks of ALS is abnormal aggregation of TAR DNA-binding protein 43 (TDP-43) (Arai et al., 2006; Neumann et al., 2006). In order to explore the role TDP-43 may play in Tau35 mice, immunohistochemical labelling with an antibody recognising TDP-43 was performed. Labelling with TDP-43 showed staining both in Tau35 mice and in WT hippocampus, with Tau35 labelling appearing somewhat more intense in the nucleus of the molecular layer than in WT mice (Figure 3.30).

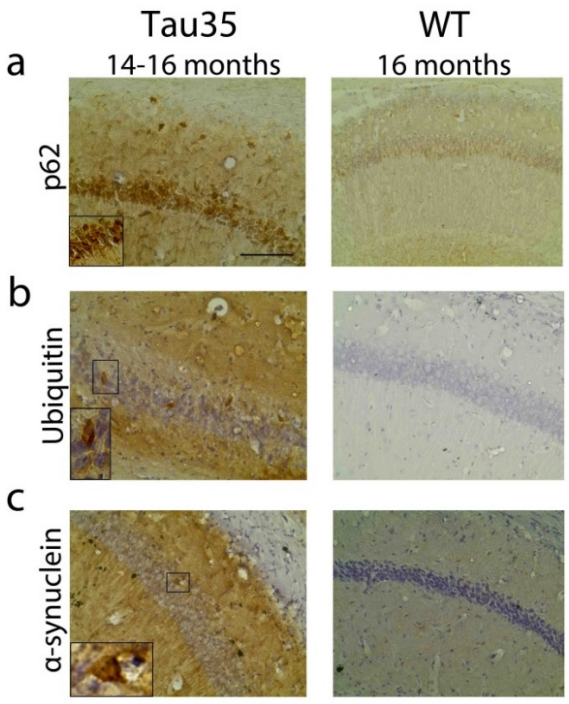

Figure 3.29: p62, ubiquitin and synuclein pathological changes in hippocampus from 14 months in Tau35 and WT mice. (a) Positive p62 labelling in inclusions was observed in CA1 and CA3 hippocampal regions **(b)** Ubiquitin positive inclusions were observed in Tau34 mice at 14 month of age in the hippocampus **(c)** α-synuclein labelling revealed n=5 mice for each genotype, scale bar=200μm.

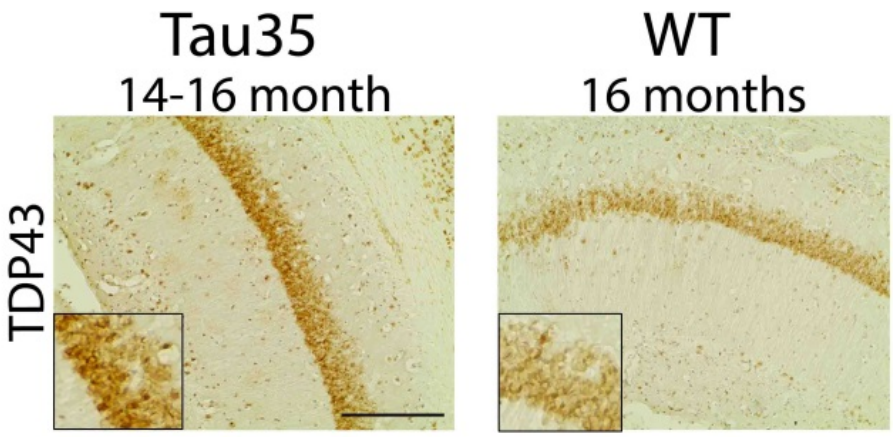

Figure 3.30: TDP43 immunohistochemistry in hippocampus of Tau35 and WT mice. Tau35 and WT mouse brain sections (14-16 months) were labelled with antibodies recognising TDP-43 and counterstained with hematoxylin and eosin. n=5 mice for each genotype, scale bar=200μm.

3.2.4.6 Tau35 mice show degenerative muscle pathology

Due to the significant motor and neuromuscular deficits seen in Tau35 mice, the muscle fibres in quadriceps (hind limb, main motor driving muscle) and latissimus (back muscle) muscles were examined in mice aged 8 and 16 months. The muscle fibres of Tau35 mice exhibited increased numbers of centrally located nuclei compared to WT animals at the same age (Figure 3.31a and b). The presence of centralised nuclei in muscle fibres is indicative of muscle degeneration/regeneration. Fibrous endomysial connective tissue and occasional split fibres were also present in Tau35 muscle in the absence of any inflammatory infiltration. Analysis of individual fibre sizes and distribution in mice aged 16 months showed an increased number of smaller muscle fibres in Tau35 mice, particularly fibres of 40-60μm diameter (Figure 3.31c), and a lack of large diameter muscle fibres. In contrast, WT muscle fibre numbers showed a peak diameter of 70-90μm. Labelling with a phosphorylation depended antibody PHF1, revealed extensive immunolabelling for PHF1 in Tau35 mouse quadriceps muscle fibres, indicating potential PHF1-positive inclusions (Figure

3.32). This data suggests that expression of Tau35 results in substantial changes in mouse muscle fibre morphology and induces pathology that parallels the motor and neuromuscular deficits previously observed in these animals.

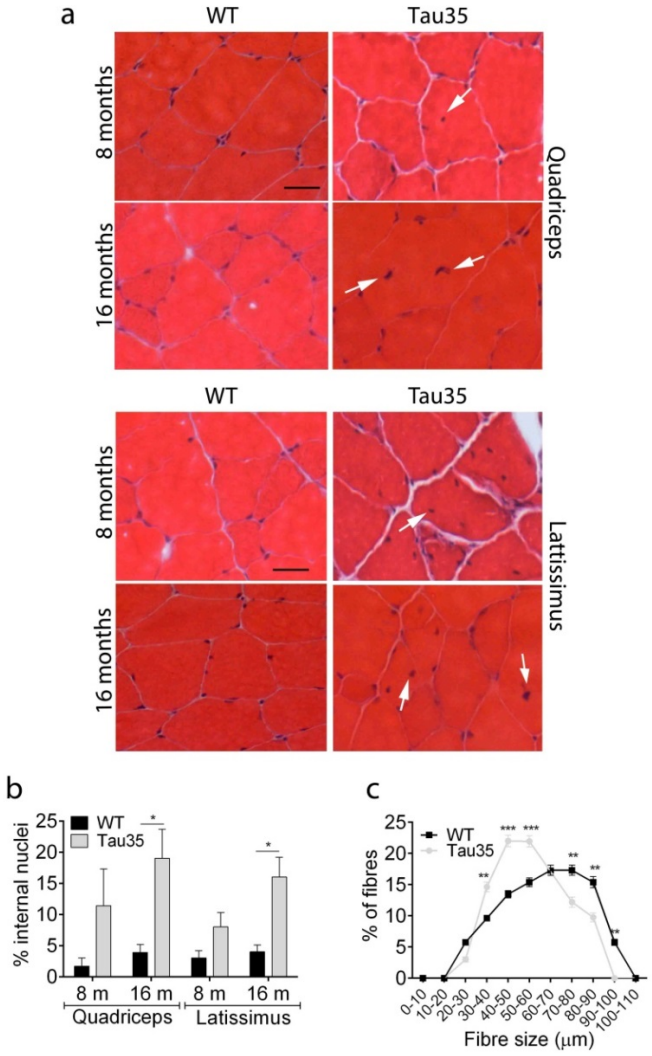

Figure 3.31: Muscle fibre morphology in Tau35 mice. (a) Haematoxylin and eosin staining of quadriceps and latissimus muscle from WT and Tau35 mice aged 8 and 16 months. Muscle fibres from Tau35 mice show centralised nuclei at 8 and 16 months (arrows). **(b)** Graphs show increased centralised nuclei (8 and 16 months) **(c)** Graph showing altered distribution of muscle fibre diameter (minimal Ferret's diameter, 16 months). Values shown are mean ± SEM., n=3, *P<0.05, **P<0.01, ***P<0.001. Scale bar = 60 μm

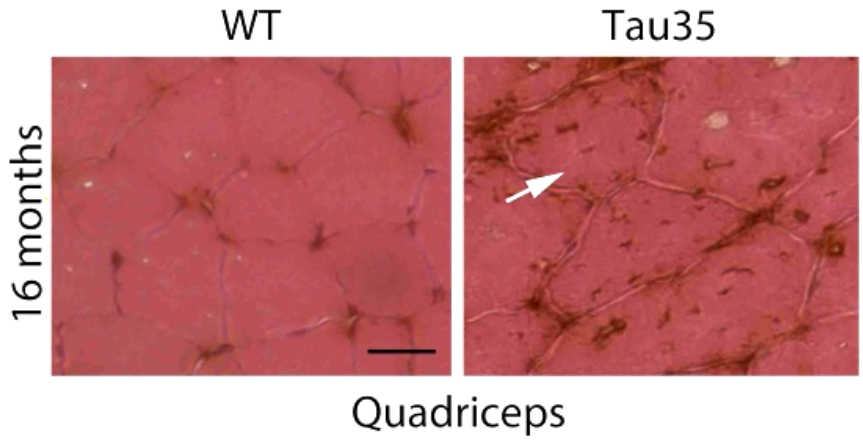

Figure 3.32: Tau phosphorylation in muscle of Tau35 and WT mice. (a) PHF1, haematoxylin and eosin- stained quadriceps muscle shows increased PHF1 immunolabelling in Tau35 muscle fibres. n=3 per genotype. Scale bar = 60μm.

3.3 Summary and Discussion

The main aim of the study was to characterise the behavioural, biochemical and pathological profile of Tau35 mice, to determine how well this new mouse line models the changes apparent in human tauopathies. Here it was demonstrated for the first time that low level expression of WT human tau comprising <10% of endogenous mouse tau leads to the development of behavioural, biochemical and pathological aspects of tauopathy which parallels that seen in human tauopathies.

The main findings of this work are that targeted insertion of N-terminally truncated WT human tau in mice leads to a number of significant changes related to human tauopathy:

1) Reduced survival lifespan, age-related clasping and kyphotic phenotype without any overt changes in animal weight.
2) Progressive motor and neuromuscular deterioration.
3) Progressive alterations in spatial learning and hippocampal-dependent memory cognition.
4) Progressive increases in phosphorylated, conformational and oligomeric tau, neuropathological changes consistent with human disease.
5) Seeding of endogenous mouse tau into filamentous tau inclusions.
6) Impaired lysosomal degradation/autophagy.
7) Evidence of some pathology involving other key proteins (α-synuclein, ubiquitin, TDP43 and p62) associated with neurodegenerative disease.

3.3.1 Tau35 mice exhibit progressive phenotypic, motor and cognitive deficits

In human tauopathies, motor deficits such as dysarthria, a loss of motor speech control in PSP (Morris et al., 1999; Lenoir et al., 2010), and extrapyramidal motor dysfunction in CBD (Rebeiz et al., 1968), often precede clinical signs of impaired cognition (Neary et al., 1988; Noble et al., 2010; Bruns and Josephs, 2013; Burrell et al., 2014; Litvan and Kong, 2014). The results presented in this chapter demonstrate that tau truncation can elicit a broad phenotypic profile, whereby mice display a commonly reported neurodegenerative clasping phenotype as well a reduced lifespan. As is the case for several 4R human tauopathies, Tau35 mice exhibit early deficits in motor learning ability and neuromuscular dysfunction, paralleled by the appearance of significant muscle pathology, followed by progressive cognitive decline and reduced survival. These phenotypic and behavioural deficits are potentially due to a variety of factors that may be initiated by the detrimental effects of N-terminal tau truncation on the propensity of tau to misfold and become highly phosphorylated. Tau truncation has previously been identified as a factor leading to potentially conformational, truncated or oligomeric toxic species (Flores-Rodríguez et al., 2015) and therefore, one potential mechanism for the muscle degeneration/denervation seen in Tau35 mice is a deterioration or malfunction of motor neurons in the spinal cord where tau is also abundantly expressed. Due to the presence of highly phosphorylated tau in muscle fibres, tau may also be transported into peripheral axons where it could accumulate and result in disruption of muscle fibres. Tau deposition has recently also been identified in diseases such as Huntington's disease and spinal muscular atrophy, suggesting additional roles for tau in muscle co-ordination and/or motor neuron degeneration in these disorders, and potentially also physiologically (Fernández-Nogales et al., 2014; Miller et al., 2015).

Cognitive decline is a common feature of tauopathy and spatial learning in the water maze is a very sensitive and widely accepted tool with which to assess hippocampal impairment and memory in rodents (Astur et al., 2002). The results obtained here with Tau35 mice indicate that expression of N-

terminally truncated tau leads to a progressive memory loss in these animals, which could be due to changes in synaptic plasticity and/or accumulation of neurofibrillary structures in the hippocampus, particularly the CA1 and CA3 regions, both of which have been implicated in the affects seen on memory formation in the tauopathies (Williams, 2006; Padurariu et al., 2012). Tau35 mice also required a longer path length to reach the target platform in the water maze, which is considered to be a specific measure of neurocognitive performance (Graziano et al., 2003).

3.3.2 Tau35 mice display increased phosphorylation, oligomerisation and abnormal conformations of tau

It is becoming increasingly evident that accumulation of phosphorylated and abnormally modified tau that forms as a result of tau truncation can lead to the neuropathology observed in human tauopathy (Delobel et al., 2008). Mounting evidence is now available linking proteases such as caspases, calpains and thrombins to tau truncation, which in turn can generate potentially toxic fragments and even initiate the aggregation of tau (Iqbal et al., 2005; Delobel et al., 2008; Lee and Shea, 2012; Zilka et al., 2012). The results described in this chapter verify the presence of phosphorylated, oligomeric and conformational tau species in Tau35 mice brains, particularly in the hippocampus.

Positive tau immunoreactivity consistent with neurofibrillary tangles, dystrophic neurites and neuropil threads was observed using several phosphorylation-dependent tau antibody PHF1 in Tau35 mice, and not observed in age-matched WT mice. Interestingly this antibody detects tau inside of the transgene. Additional antibodies TG3, AT100, AT8 and Tau1, also present inside the transgenically expressed construction showed high phosphorylation and dephosphorylation protein levels respectively in Tau35 compared to WT mice whereas AT270 and TP700 detects tau outside the transgene area indicating that endogenous mouse tau is included in the tau aggregates in Tau35 mice. Therefore, inclusions staining positive for these antibodies indicate phosphorylated tau aggregation generated from the fragment itself and potential recruitment of endogenous tau and hence the tau

fragment induces phosphorylation of native mouse tau and therefore seeds tau aggregation in Tau35 mice. Indeed, such a mechanism has previously been proposed by Clavaguera et al., who proposed that tau acts as a seed, similar to misfolded prion protein (Clavaguera et al., 2013). Her group and others have demonstrated that different human tauopathy aggregates have the ability to seed further aggregation of innate tau proteins, causing them to misfold in a prion-like manner (Sydow and Mandelkow, 2010; Clavaguera et al., 2013; Ren et al., 2014). The Tau35 mice exhibit neuropathological phosphorylated tau species from 2 months of age (PHF1 antibody) and misfolded tau is detectable from 8 months of age (PG5 antibody), indicating that phosphorylation is an early event in these mice. Furthermore, the temporal appearance of increased tau phosphorylation correlates well with the onset of progressive motor and cognitive decline witnessed in these mice, and this is followed by abnormal misfolding of tau.

The aggregation of tau in the hippocampus, a brain region responsible for spatial learning, could explain the deficits in memory seen in Tau35 mice. Previous studies have shown correlations between the presence of abnormal tau species and cognitive decline in mouse models and in human tauopathy (Arriagada et al., 1992; Ramsden, 2005; Armstrong et al., 2009). Multiple tau inclusions were observed in the CA1 and CA3 regions in Tau35 hippocampus. These tau deposits mainly took the form of pre-tangles located in the perinuclear region and cell body, and sometimes extending to the apical dendrites of neurons. In addition to these deposits, strong tau immunostaining was also seen in mossy fibres in the CA3 and dentate gyrus, from the age of 8 months onwards. Increased staining in the mossy fibre network could be due to a number of factors, including pre-tangle formation or increased sensitivity in these fibres to tau phosphorylation. A number of previously reported mouse models of tauopathy have presented with increased staining in the mossy fibre network and the mice have shown that CA3 fibres have impairments in synaptic transmission, leading to impaired memory formation (Gotz et al., 2001; Liu et al., 2004b; Decker et al., 2015). HA labelling was also intense in Tau35 mice indicating not only perfuse transgene expression but also that the

intense tau labelling could indicate that the human phospho-tau species are potentially transported into the axons

Tau has been shown to form dimers early in disease, and these dimers interact to form small oligomeric complexes, which later aggregate into filaments and neurofibrillary tangles (Lasagna-Reeves et al., 2012; Cowan and Mudher, 2013). The brains of Tau35 mice display age-dependent oligomeric and conformational tau inclusions from 8 months of age with antibodies (TOC1, MC1 and PG5), that bind tau oligomers in specific conformations and have been described as early stage markers of tau pathology (Ren and Sahara, 2013; Ward et al., 2013, 2014). Interestingly, Tau35 mice did not show any difference in total tau expression compared to WT mice at 14 months of age, which highlights the lack of tau overexpression in these mice. Importantly, this also shows that the pathological and behavioural defects observed in Tau35 mice are not due to potential artefacts caused by highly overexpressed tau.

Tau35 mice did not show any distinct sarkosyl-insoluble aggregated tau species relative to their WT littermates, and there was no apparent increase in insoluble tau, inferring that the dysfunction induced by low level expression of N-terminally truncated tau occurs in advance of significant accumulation of highly aggregated tau. Hence, the phenotypic changes reported here are more likely to result from oligomeric tau species in Tau35 mice, a phenomenon which has previously been reported in hTau-A152T and Tg4510 mice by other groups (de Calignon et al., 2010; Maeda et al., 2016). The PHF1 and total tau antibodies did detect weak bands corresponding to higher molecular weight species of tau on western blots (Figure 3.15a, arrow head), inferring that tau may be conformationally different in Tau35 mice. This finding suggests that the pathological tau species involved may take the form of oligomeric or seeded endogenous tau to form these species.

At the terminal stage of disease in Tau35 mice, a high density of tau inclusions was not observed, suggesting that the development of tangles may not be critical for the cognitive and motor deficits observed in these mice. A similar mechanism has previously been suggested, such as the P301L tau mutant overexpression model in which tangles carry on forming even after tau is no longer produced (Santacruz et al., 2005). It is therefore conceivable that

an early neuronal deficit, without an overt neuropathological signature, occurs before the appearance of widespread fibrillar tau in Tau35 mice and in human tauopathies, and this may be responsible for cognitive dysfunction.

3.3.3 Tau35 mice exhibit elevated GSK3β activity along with impaired autophagic lysosomal degradation

Expression of Tau35 has been shown to induce significant tau phosphorylation and tau pathology. This highlights the fact that N-terminal tau truncation can have deteriorating effects on tau proteostasis. The phosphorylation of tau is tightly regulated by several kinases that phosphorylate specific sites on tau (Ferrer et al., 2005; Hanger et al., 2009; Martin et al., 2013) A key tau candidate kinase is GSK3β, which is responsible for the phosphorylation of over 30 distinct phosphorylation sites (Hanger et al., 1992, 2007, 2009; Mandelkow et al., 1992). In this study, Tau35 mice exhibited a selective increase in GSK3β, but not GSK3α, activation suggesting an important role for this tau kinase in disease pathogenesis, possibly related to its association with autophagic pathways (Inoue et al., 2012). GSK3β activity has been shown to suppress lysosomal acidification and thereby to suppress autophagy in cells (Azoulay-Alfaguter et al., 2015). When GSK3 is inhibited, lysosomal numbers can be inherently increased due to activation of the autophagic network, perhaps due to the phosphorylation of transcription factors such as transcription factor EB (TFEB), the master regulator of lysosome biogenesis (Parr et al., 2012). This inhibition can in turn lead to increased nuclear localisation of TFEB and induction of the lysosomal-autophagy system (Marchand et al., 2015).

Synthesised misfolded proteins are primarily degraded via three main quality control mechanisms: the ubiquitin proteasome system (UPS), the unfolded protein response (UPR) and the autophagosome-lysosome pathway (ALP). The accumulation of misfolded, phosphorylated tau is considered a pathological hallmark of tauopathies and a number of studies have identified positive ubiquitin inclusions in tauopathies such as in PSP patient brains (Fergusson et al., 2000; Schubert et al., 2000; Nijholt et al., 2012; Takalo et al., 2013). Tau35 mice show ubiquitin labelled pre-tangles at 14 months of age,

suggesting a potential attempt to remove abnormal tau inclusions through ubiquitin tagging. However, as these inclusions are still present after 14 months, it suggests that this mechanism fails to efficiently remove the aggregated ubiquitinated proteins in Tau35 mouse brain. In support of this, a number of research groups have provided evidence that inactivation of the UPS leads to neurodegeneration coupled with the appearance of ubiquitin aggregates (Hara et al., 2006; Komatsu et al., 2006; Riley et al., 2010). Additionally, inhibition of the UPS stimulates tau accumulation in rats (Liu et al., 2009). Therefore, it is likely that when the level of tau aggregation exceeds the capacity of the UPS and ALP pathways, aggregated proteins are compartmentalised as inclusions, particularly as previous research has shown that inhibition of autophagy in neurons leads to the accumulation of phosphomimic tau (Rodríguez-Martín et al., 2013). Furthermore, it has also been suggested that excessive accumulation of aggregated tau can overload both systems, accelerating the disease process and leading to further protein aggregation and neurodegeneration (Bennett et al., 2005; Hol and Scheper, 2008; Cuervo et al., 2010).

Accumulation of autophagic and lysosomal markers have been reported in human tauopathy brains suggesting that disruption in these processes may be involved in disease pathogenesis (Piras et al., 2016). The autophagic marker p62 and its binding protein LC3-II (which is converted from LC3-I) are important regulatory components in quality control of the ALP, and both of these increase in Tau35 mice. Binding of p62 to LC3-II induces further binding of polyubiquitinated proteins, targeting them to the autophagosome for subsequent degradation, and these markers also accumulate if autophagy is defective (Komatsu et al., 2007; Ren and Sahara, 2013; Richter-Landsberg and Leyk, 2013). The increased amounts of p62, LC3-I and LC3-II in Tau35 mouse brain implies attenuation in the ALP as tau aggregates are tagged for degradation but ultimately are not cleared. This is supported by experiments showing that inactivation of p62, leads to accumulation of phosphorylated tau and neurodegeneration (Ramesh Babu et al., 2008). Furthermore, p62-deficient cells have a significantly reduced ability to form aggregates *in vitro* (Pankiv et al., 2007) and mice with impaired autophagosome formation

accumulate phosphorylated p62 (Kurosawa et al., 2016). The early accumulation of p62 in Tau35 mice suggests that this protein may play a role in tau aggregation. Evidence for this has been seen in AD brains in which p62 immunolabelling is tightly linked to the presence of tangles (Kuusisto et al., 2002). In Tau35 mice, ubiquitin-positive and p62-positive inclusions are present in neurons, suggesting that p62 accumulates in inclusions, as autophagy mechanisms are impaired. This implies that in tauopathies p62 accumulation reduces autophagic clearance of tau inclusions or that, p62 inclusions aggregate when autophagic clearance is impaired. It is possible that Tau35 protein is transported to the lysosome for degradation after binding to ubiquitin and p62 since increased LC3-1, LC3-II, p62 and ubiquitin were all observed in the hippocampus of these mice. Together with increased GSK3β activity, these findings suggest a potential blockage in endolysosomal trafficking and dysfunctional autophagy/lysosomal-mediated degradation as a potential neuropathological mechanism in Tau35 mice. Interestingly, GSK3 has previously been shown to phosphorylate p62, increase p62 and inhibit autophagic flux by reducing lysosomal acidification (Korolchuk et al., 2009; Azoulay-Alfaguter et al., 2015). As well as the reduced autophagic flux in aged neurons, the activity of autophagy can be adversely affected by the interaction with protein aggregates such as tau and α-synuclein (Cuervo et al., 2004; Wang et al., 2009; Orenstein et al., 2013), generated by impaired UPS. For instance, tau in FTD with ubiquitin positive inclusions and α-synuclein in PD bind LAMP-2A at several fold higher affinity leading to impaired cargo translocation across the lysosomal membrane (Cuervo et al., 2004).

Alpha- and beta-tubulin are the major component of MTs and acetylation of tubulin stabilises MTs. Decreased acetylated α-tubulin, a feature of tangle-bearing neurons (Hempen and Brion, 1996), plays a key role in the fusion of lysosomes with autophagosomes and the trafficking of these two organelles, as well as degradation of LC3-II (Xie et al., 2010; Mackeh et al., 2013). Therefore, the decrease of acetylated tubulin in Tau35 mice is a further indication of aberrant autophagy in these mice. The attenuation of the autophagy pathways could explain the further cognitive and motor decline seen in Tau35 mice. However, the precise mechanism underlying

neurodegeneration related to autophagy impairment remains elusive and needs to be investigated further.

Another key component of the lysosome is the hydrolase enzymatic activity catalysed by as the cathepsin family of proteases (Repnik et al., 2012). Tau35 mice show a marked reduction in mature cathepsin D, which is further indicative of lysosomal dysfunction in these mice. Taken together, these findings indicate that accumulation of protein targeted for degradation, reduced acetylated tubulin, increased ubiquitin, and impaired maturation of cathepsin D, can all lead to adverse neuronal effects which rely on autophagic degradation to clear accumulated misfolded/truncated proteins (Boland et al., 2008). These deficiencies in autophagy and lysosomal degradation support the idea that these mechanisms could be linked to the cognitive impairment seen in neurodegeneration (Nixon, 2007; Nixon and Yang, 2011; Schaeffer et al., 2012; Vilchez et al., 2014; Ciechanover and Kwon, 2015).

3.3.4 Tau35 exhibit impaired synaptic vesicle integrity

Selective loss of synaptic proteins and dysfunction of synapses occurs both early and in late-stage tauopathy, preceding the loss of neurons and correlating with the onset of cognitive decline (DeKosky et al., 1996). Synaptic damage is characterised by the deregulation of certain pre- and post-synaptic proteins (Coleman, 2003; Honer, 2003; Tao et al., 2003) and pattern of neurofibrillary structures occurs in the same brain regions (Serrano-Pozo et al., 2016).

Upon examination of pre-synaptic markers, it was evident that Tau35 mice aged 14 months showed a marked reduction in expression of both synapsin1 and synaptobrevin, but not of synaptophysin. Synaptophysin is the major synaptic vesicle-bound pre-synaptic protein, whereas synaptobrevin and synapsin1 are synaptic vesicle proteins involved in fusion and interaction with vesicle membranes and regulating the reserve pool of synaptic vesicles (Gitler, 2004). Mice that do not express synaptophysin exhibit functional neurotransmission, indicating that synaptophysin is not a necessary requirement for neurotransmitter release (Eshkind and Leube, 1995; McMahon et al., 1996). Therefore, selective reduction in these pre-synaptic

markers in Tau35 mice may suggest that the overall number of synaptic vesicles and integrity is reduced rather than the number of total synapses *per se*. A recent study in a transgenic rat model of tauopathy expressing truncated tau showed that, in the pre-synaptic compartment, truncated tau was associated with impaired dynamic stability of MTs, which could be responsible for the reduction of synaptic vesicles, without any decreasing synaptophysin in the pre- synaptic compartment (Jadhav et al., 2015).

Synaptophysin is the most common pre-synaptic marker used in models of tauopathy but, due to its wide expression pattern, including sites such as the nucleus, cell bodies and dendritic cytoplasm. Therefore, synaptophysin is perhaps not an optimum indicator of small changes in synaptic integrity, but rather a marker for gross synaptic loss. Similarly, synaptotagmin is expressed in neurons and also in non-neuronal cells, including astrocytes, which could also mask small changes in the complement of fully functional neurons at the synapse. Synapsin1 however, is expressed almost exclusively at synapses (De Camilli et al., 1983; Micheva et al., 2010) and indeed this pre-synaptic protein showed the most significant changes in Tau35 mice, suggesting it may be a preferred marker of small synaptic changes (Micheva et al., 2010). In fact, this highlights the importance of using multiple synaptic markers to fully understand synaptic complexity in novel transgenic models of neurological disease.

The reduction in these synaptic markers could indicate further evidence for the cognitive deficits seen in these mice. Synaptobrevin is essential for calcium-dependent neurotransmitter release and knockout of synaptobrevin has significant detrimental effects on synaptic transmission (Schoch et al., 2001). A near total abolition of evoked responses to electric field stimuli results from synaptobrevin knockout in cultured neurons and this could therefore have detrimental effects on synaptic communication and memory formation (Schoch et al., 2001).

Notably there was no significant difference in the amount of the postsynaptic marker PSD-95 in Tau35 mice. As PSD-95 is a major scaffolding protein, this could indicate that Tau35 protein does not target the post-synaptic proteasome, suggesting greater localisation in pre-synaptic terminals.

However, as this was the only post-synaptic marker tested in this study, these results may not be definitive and further studies need to be performed to fully understand this mechanism.

3.3.5 Tau35 mice show other proteinopathy pathology

Protein misfolding, accumulation and subsequent aggregation are common features of many neurodegenerative diseases. The existence of common mechanisms suggest that many neurodegenerative diseases might share the same triggers and that the nature of the neuropathology observed is primarily associated with the type of protein aggregation and post-translational modification. Therefore, the idea that there is an overlap in different proteinopathies is becoming increasingly popular.

This study for the first time demonstrates that Tau35 protein directly or indirectly leads to α-synuclein expression, a common feature seen in Parkinson's disease, which may be linked to the motor deficit seen in these mice. Although the accumulation of α-synuclein in the form of Lewy bodies is primarily a pathological hallmark of Parkinson's disease, Lewy pathology has also been described in human tauopathy brain (Hamilton, 2006). Positive α-synuclein immunoreactivity in Tau35 mice aged 14 months therefore implies its possible involvement in the observed motor defects. A number of other tau mouse models also develop Parkinsonian motor defects. For example, mice overexpressing P301L and P301S mutant tau exhibit motor deficits see Table 4 for a summary of mouse models exhibiting motor deficits (Hutton et al., 2000; Allen et al., 2002; Noble et al., 2010). However, although positive diffuse α-synuclein staining was observed, together with some tangle-like structures in Tau35 mice, no Lewy bodies were present. One possible reason is that the pathology here may be at an early stage at which α-synuclein is just starting to build up, similar to the tau pre-tangles before neurofibrillary tangles aggregates present. As significant motor defects are observed early in disease progression in Tau35 mice, it would be interesting to investigate α-synuclein staining in mice aged 8 months to determine if this correlates with the motor defects.

TDP-43 aggregations were also investigated in Tau35 mice and some differences were detected between Tau35 and WT mice, although this was not explored further due to time constraints. This result suggests a possible role for TDP-43 in the disease pathogenesis in Tau35 mice. To determine whether TDP-43 plays a role in this process, an antibody against phosphorylated TDP-43 would be useful to further investigate the potential role, if any, of TDP-43 in Tau35 mice.

Numerous tauopathies, particularly PSP, display extensive astrocytic pathology. Tau35 mice failed to show any astrocyte pathology. This finding was not entirely unexpected because appreciable amounts of tau are not normally found in astrocytes or microglia (microglia were not investigated in Tau35). A study of tauopathy in a transgenic mouse overexpressing mutant A152T tau, a tau mutation associated with increased risk of PSP, also lacked glial tau pathology (Sydow et al., 2016). In diseases such as PSP which exhibit glial pathology the presence of tau in glia may be related to pathological mechanisms involving glial uptake of neuronal expressed tau, however Tau35 mice lack glial pathology suggesting that altered tau expression/truncation alone may not be sufficient to cause the glial pathology seen in PSP.

3.3.6 Conclusions

In summary, the findings presented in this chapter suggest that Tau35 mice represent a pathophysiologically relevant mouse model that exhibits behavioural, biochemical and pathological features which parallel those in human tauopathy. Due to the normal physiological expression and the use of truncated WT tau, rather than overexpression under the control of the human tau promoter, this mouse model is unlike other previous in vivo models of tauopathy. In the following chapter, the use of this animal model is described in the evaluation of a potential therapeutic intervention using a clinical available compound.

CHAPTER 4

Phenylbutyrate rescues behavioural, biochemical and pathological deficits in Tau35 mice and rescues tau phosphorylation in a Tau35 cell-based model

4.1 Introduction

Sodium 4-phenylbutyrate (PBA), a short chain fatty acid compound (Figure 4.1), is a clinically approved, orally available pleiotropic drug with few side effects and is relatively safe for patients (Burlina et al., 2001). Importantly, PBA has the ability to cross the blood-brain barrier via the cerebrospinal fluid (Berg et al., 2001). PBA is primarily used to treat conditions such as urea acid cycle disorders (Brusilow and Maestri, 1996). Furthermore, PBA has been found to induce autophagy and eradicate tuberculosis (TB) in human macrophages (Rekha et al., 2015), and has also been used in clinical trials for the treatment of sickle cell anemia as it induces the formation of fetal haemoglobin (Dover et al., 1994). PBA has also been used in cancer treatment trials, however, its effectiveness is limited by toxicity caused by the high dosages needed (Carducci et al., 2001; Gore et al., 2002; Phuphanich, 2005). PBA inhibits most class I and class II HDACs and it has the ability to act as a molecular and chemical chaperone, protecting against endoplasmic reticulum (ER) stress and the unfolded protein response, as well as acting as a stabiliser for misfolded proteins (Wiley et al., 2010; Cohen et al., 2011; Mimori et al., 2012; Cho et al., 2014). Furthermore, PBA activates transcription of a variety of genes involved in the regulation of cell proliferation and development (Levenson et al., 2004). PBA has been extensively used as a therapeutic compound *in vitro* and *in vivo* and has shown an array of neuroprotective functions in several animal models of neurodegenerative disease. For example, in mice subjected to hypoxia-ischaemia, PBA protects against endoplasmic reticulum (ER) stress, as well as protecting against glutamate-induced, NMDA receptor-mediated excitotoxicity

in cerebellar granule cells. In a mouse model of Huntington's disease, hypoacetylation associated with gene downregulation, was alleviated by PBA (Qi, 2004; Gardian et al., 2005; Leng and Chuang, 2006; Ying et al., 2006; Sadri-Vakili et al., 2007; Chuang et al., 2009). Notably, PBA prevents dendritic spine loss, improves cognitive function and reduces tau phosphorylation in mice overexpressing a mutant form of amyloid precursor protein (APP), APPK670/671L (Tg2576 mice) (Ricobaraza et al., 2009, 2012), suggesting PBA as a potential candidate drug for the treatment of Tau35 mice.

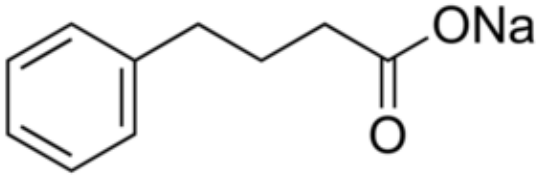

Figure 4.1: Chemical structure of sodium phenylbutyrate (Iannitti and Palmieri, 2011).

4.2 Results

The use of potentially therapeutic compounds in mouse models of tauopathy is crucial to evaluate safety and toxicity, and potentially to identify new therapeutics to cure the disease or to halt disease progression in human tauopathies. Tau35 mice were established as a model of human tauopathy, and hence it was important to evaluate whether these changes could be rescued by therapeutic intervention. Therefore, PBA or vehicle (sterile saline) was administered (400mg/kg, i.p., daily for 6 weeks), to two separate cohorts of Tau35 and WT mice (n=8 for each genotype in each group), as described previously in 2.3.12.10 Treatment of mice with (Ricobaraza et al., 2009). Two different groups of Tau35 and WT mice were treated with PBA or vehicle, the first younger group w (aged 7.5 months) and the second older group (8.5 months) for cognitive decline in the Morris water maze. At the end of the trial the younger cohort were 9 months and the older cohort 10 months of age.

Since PBA exhibits pleiotropy and has been shown to improve a number of behavioural and biochemical abnormalities in a variety of animal models of neurodegenerative disease, this study will determine whether PBA can exert a therapeutic effect in the Tau35 model of human tauopathy.

4.2.1 Phenylbutyrate treatment does not affect body mass of Tau35 mice

To assess whether PBA affects the body weight of Tau35 and WT mice, animals were weighed at weekly intervals from the start of the treatment with PBA and throughout the six week PBA or vehicle dosing period. The weight of each animal included in the study was measured 3 days prior to the first dosing and then at weekly intervals on the day of administration, 30 min prior to dosing. During the treatment period, there were no statistically significant differences ($P>0.05$) between the body weights of Tau35 and WT mice treated with PBA, compared to vehicle-treated controls (Figure 4.2). This finding indicates that daily administration of PBA at 400mg/kg for six weeks does not induce any harmful changes in the body mass of Tau35 or WT mice.

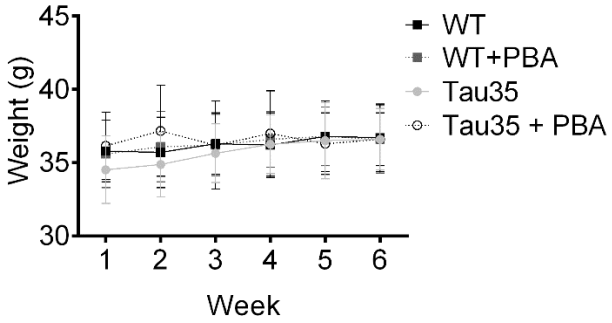

Figure 4.2: Lack of effect of Phenylbutyrate on the body mass of Tau35 and WT mice. Weights of Tau35 and WT mice were measured weekly during PBA or vehicle dosing for 6 weeks. Values shown are mean ± SEM., n=8 for each treatment group.

4.2.2 Phenylbutyrate rescues neuromuscular motor deficits in Tau35 mice

Tau35 mice experience significant neuromuscular motor deficits as described in section 3.2.2.5 Tau35 mice exhibit neuromuscular deficits. People with tauopathies such as PSP and CBD, also present clinically with motor deficits that are paralleled in Tau35 mice. Therefore, therapeutic interventions that target these motor deficits would be of significant clinical benefit in the tauopathies. Prior to dosing with PBA, the two groups of Tau35 mice, aged 7.5 and 8.5 months, exhibited reduced neuromuscular grip strength compared to their counterpart WT mice, as described previously in Chapter 3 (Figure 3.8). The 7.5 and 8.5 month old groups of Tau35 mice showed no statistically significant difference in grip strength ($P<0.05$) prior to treatment (Figure 4.3a,b, untreated), whereas Tau35 mice exhibited a significantly reduced grip strength compared to WT mice at the same ages (Figure 4.3a and b, untreated, $P<0.001$). Following 6 weeks of dosing with PBA, the grip strength of the younger cohort of Tau35 mice increased from a mean value of 61g (+/- 6.4) at 7.5 months to 73g (+/- 6.2) at 9 months, an increase of 17%, resulting in a statistically significant difference between PBA and vehicle-treated Tau35 mice ($P<0.001$). In contrast, the grip strengths of the younger group of WT mice, whether treated with vehicle or PBA, did not show significance but did increased slightly during the same period (PBA: from 76g to 79g, Vehicle: from 74g to 78g) (Figure 4.3a).

For the older cohort, PBA treatment resulted in an increase in grip strength of Tau35 mice from a mean value of 60g (+/-6.3) at 8.5 months to 77g (+/-6.1) at 10 months, an increase of 22%. In contrast, the grip strength of Tau35 mice treated with vehicle decreased from 62g (+/-4.1) to 57g (+/-3.9), resulting in a statistically significant difference ($P<0.001$) between PBA and vehicle-treated Tau35 mice. The grip strengths of WT mice, whether treated with vehicle or PBA, increased slightly during the same period (PBA: from 81g to 83g, Vehicle: from 78g to 80g) and did not show any significant differences under these two conditions (Figure 4.3b). These results indicate that PBA has

the ability to rescue motor deficits in Tau35 mice, without significantly affecting the grip strength of WT mice.

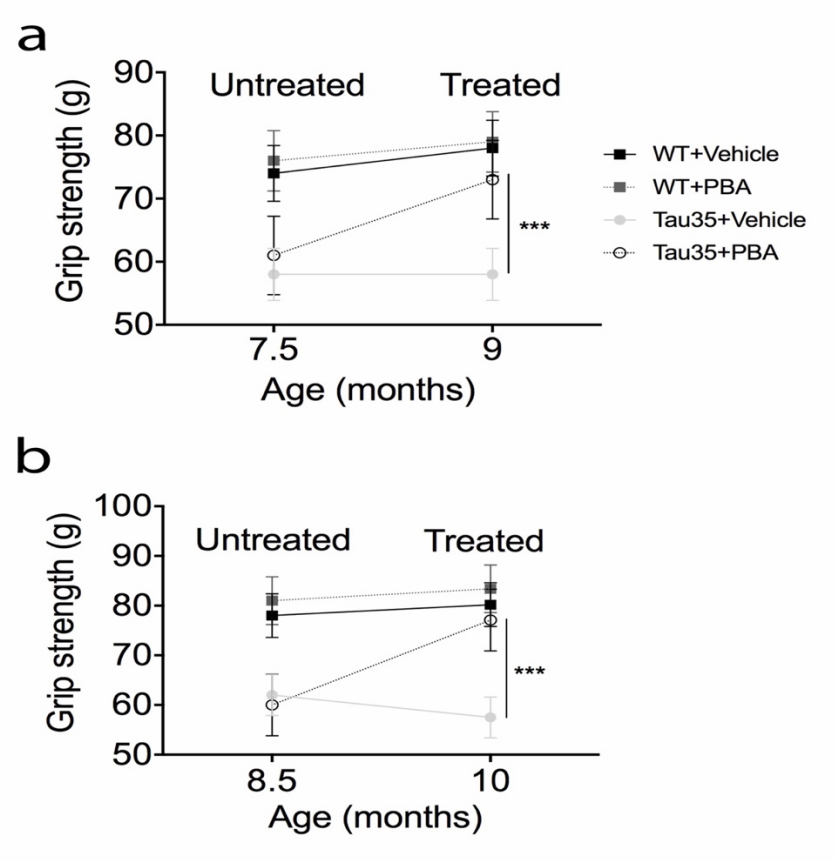

Figure 4.3: Phenylbutyrate restores grip strength in Tau35 mice. Grip strength of Tau35 and WT mice before and after 6 weeks' treatment with PBA or vehicle. Mice were aged 7.5 months **(a)** or 8.5 months **(b)** at the start of treatment. Grip strength of Tau35 was restored upon administration of PBA, but not vehicle. Values shown are mean ± SEM., n=8 for each genotype. ***P<0.001, ANOVA.

To assess whether the rescue in neuromuscular deficit correlates with improved muscle morphology, PBA and vehicle-treated quadriceps muscle sections, from Tau35 mice aged 10 months, were stained with haematoxylin and eosin (Figure 4.4a, b). PBA reduced the number of centralised nuclei by 3.5-fold in quadriceps muscle fibres of Tau35 mice compared with vehicle-treated Tau35 mice, indicative of muscle fibre degeneration/regeneration (Figure 4.4c, $P<0.05$). Interestingly, PBA-treated muscle morphology in Tau35 mice was similar to that seen in WT mice (Figure 3.31). These results indicate that PBA was able to reverse the muscle degenerative/regenerative phenotype observed in Tau35 mice.

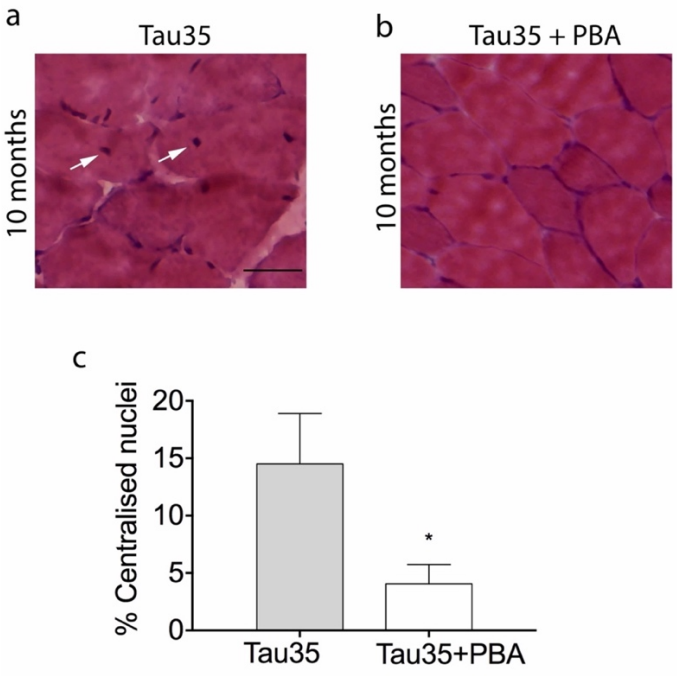

Figure 4.4: Phenylbutyrate rescues muscle fibre degeneration/regeneration in Tau35 mice. Haematoxylin and eosin staining of quadriceps muscle sections from vehicle-treated **(a)** and PBA-treated **(b)** Tau35 mice aged 10 months. Muscle fibres from vehicle-treated Tau35 mice show centralised nuclei (arrows), scale bar=200µm. **(c)** Graph shows the percentage of fibres in quadriceps muscle from Tau35 mice that exhibit centralised nuclei following 6 weeks of PBA (400mg/kg, i.p., daily) or vehicle treatment. Values shown are mean ± SEM., n=3 for each treatment group, *$P<0.05$, ANOVA.

4.2.3 Phenylbutyrate rescues spatial learning deficits in Tau35 mice in the Morris water maze when treated at 8.5 months of age

Reduced spatial learning was first observed in naïve Tau35 mice at 8 months of age, as described in section 3.2.2.8 Spatial learning and memory is impaired in Tau35 mice. To evaluate the effects of PBA on cognition, Tau35 mice were tested in the Morris water maze to identify whether PBA treatment could alleviate learning abnormalities. Groups of mice aged 7.5 months (younger cohort) and 8.5 months (older cohort) were tested before and after 6 weeks of treatment with PBA, as described in section 4.2 Results above. No statistically significant differences in cognitive ability were found between untreated and treated groups of Tau35 and WT mice during visible platform training prior or after dosing of either the younger or older mouse cohorts (Figure 4.5a, b, c and d). Following the 6-week dosing period, the latency of the younger cohort of Tau35 mice to find the platform on day 4 decreased by 36%, from a mean value of 15s at 7.5 months to 11s after PBA. In contrast, the latency to find the target for the younger group of vehicle-treated Tau35 mice decreased by only 12%, which did not reach statistical significance (Figure 4.5b). In contrast, the latency to find the platform of the younger WT mice, whether treated with vehicle or PBA, did not differ and did not show any significant differences under these two conditions. Although this data shows no significant differences, interestingly the biggest difference between day 1 and day 4 latencies was observed in Tau35 mice treated with PBA. The younger PBA-treated Tau35 mice exhibited a latency to find the platform of 31s on day 1, which reduced to 11s on day 4, a decrease of 65%. The younger vehicle-treated Tau35 mice, however, exhibited a 28% decrease in latency between days 1 and 4, which was 43% of the reduction in the PBA-treated animals. In contrast, both vehicle and PBA-treated WT mice showing a decreased latency of 50%, somewhat less than that observed in the PBA-treated Tau35 mice. This indicates that PBA may well have positively influenced spatial learning in Tau35 mice at this age, but did not reach significance perhaps due to the

amount of variation present between some groups of animals (Figure 4.5a, b). Interestingly, unlike the vehicle-treated Tau35 mice, by 9 months of age the performance of PBA-treated Tau35 mice in the water maze did appear to overlap somewhat with that of WT mice (Figure 4.5b). This indicates that although PBA did not significantly rescue the spatial learning impairment in Tau35 mice, it may have contributed towards a slight reduction in severity given that the expected memory impairment in Tau35 mice aged 8 months becomes evident only by day 4 of training and is not severe at this age (Figure 3.11d).

In the older cohort of mice aged 8.5 months, both the vehicle and PBA-treated Tau35 mice had a slightly longer escape latency than WT mice, although this was not significantly different, possibly due to amount of variation between the performance of the mice in each group (Figure 4.5c). All of the older groups of mice exhibited improved learning, with latencies between 8-12s shorter than on day 1. By day 4 of the learning trial, a comparison of Tau35 and WT mice showed an increase in escape latency of 6-8 s in Tau35 mice, compared to WT mice (Figure 4.5c). After 6 weeks of PBA treatment, Tau35 mice showed no significant differences in escape latency compared to vehicle-treated mice, on days 1-3. However, by day 4, the older cohort of PBA-treated Tau35 mice showed an improved spatial learning ability of more than 2-fold, compared to the vehicle-treated Tau35 mice (Figure 4.5d). These results showed that PBA effectively rescued the performance of the older group of Tau35 so that they became almost equivalent to the WT mice of the same age. These data indicate that PBA has the ability to rescue impaired learning in the older cohort of Tau35 mice and hence PBA can rescue of cognition when these mice were treated at 8.5 months of age.

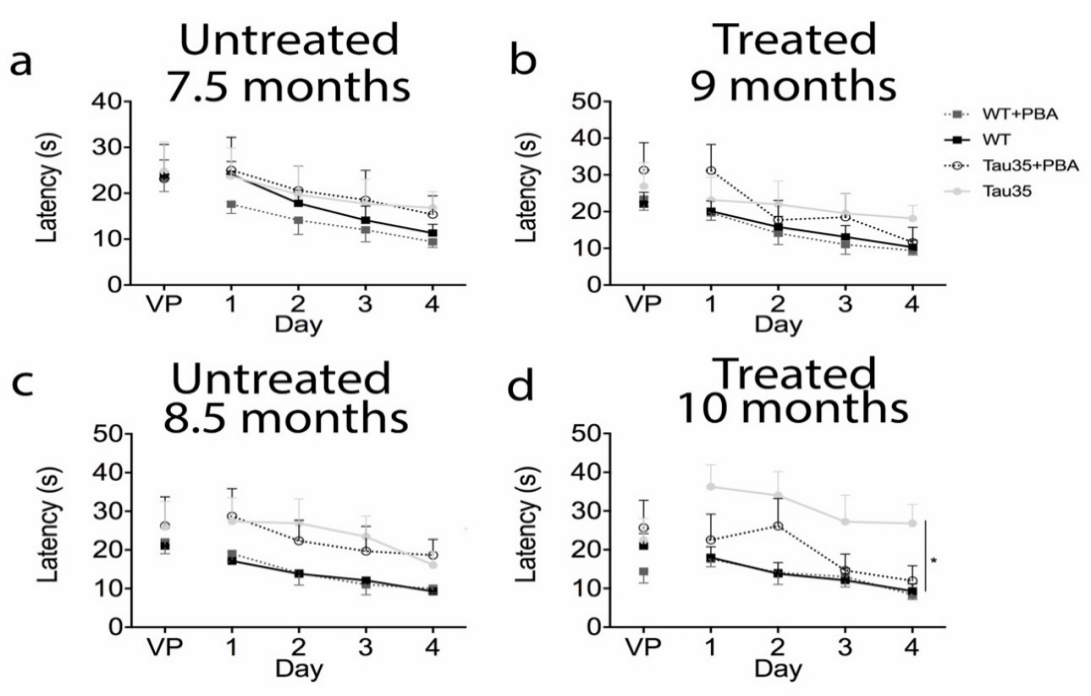

Figure 4.5: Phenylbutyrate rescues spatial learning in the Morris water maze in 8.5 months Tau35 mice. Morris water maze testing of Tau35 and WT mice treated with PBA or vehicle. 4-phenylbutyrate (PBA, dotted lines) and vehicle-treated (solid lines) mice aged 10 months Tau35 (circles) and wild-type (WT, squares) mice. **(a-b)** At 7.5 months before treatment (untreated) with PBA and 9 months after treatment with PBA (treated). **(c-d)** Water maze performance of mice before treatment with PBA at 8.5 months of age (untreated) and after treatment with PBA at 10 months of age (treated). Values shown are mean ± SEM., n=8 for each genotype, *P<0.05, ANOVA.

4.2.4 Phenylbutyrate rescues memory deficits in Tau35 mice in the Morris water maze when treated at 8.5 months of age

Previous studies have demonstrated the ability of HDAC inhibitors to accelerate memory formation in developing mice (Vecsey et al., 2007; Bredy and Barad, 2008) and to rescue memory formation and cognition in several neurodegenerative mouse models (Fischer et al., 2007; Fontán-Lozano et al., 2008). Tau35 mice show hippocampal-dependent memory deficits in the Morris water maze from 8 months of age, as described in section 3.2.2.9 Hippocampal dependent memory is impaired in Tau35 mice. After the learning trial, PBA and vehicle-treated mice were subjected to a probe trial, in which mice swim for 60s with no platform, and the time spent in the quadrant where the platform was previously located is recorded. The probe trial is used as an indication of the ability of the mice to retain hippocampal-dependent memory.

Prior to dosing with PBA, both groups of Tau35 mice aged 7.5 months did not show an increased latency in the target quadrant compared to WT mice (Figure 4.6a, untreated). Following PBA treatment for six weeks, Tau35 mice aged 9 months similarly failed to show increased latency in the target quadrant compared to vehicle-treated Tau35 (Figure 4.6a, treated). This highlights the fact that PBA was unable to prevent the onset of the memory deficit previously observed in Tau35 mice at this age. In the older cohorts of animals, untreated Tau35 mice aged 8.5 months showed a significant reduction of 10s in the time spent in the target quadrant compared to untreated WT mice (Figure 4.6b, untreated), indicating impaired memory in relation to the location of the hidden platform. After 6 weeks of dosing, the older Tau35 mice treated with PBA showed an improved latency of 23% in reaching the platform, compared to vehicle-treated Tau35 mice. At this stage, the PBA-treated Tau35 mice performed similarly to WT mice, the difference between these genotypes being only ~2 s (Figure 4.6b, treated, $P<0.05$).

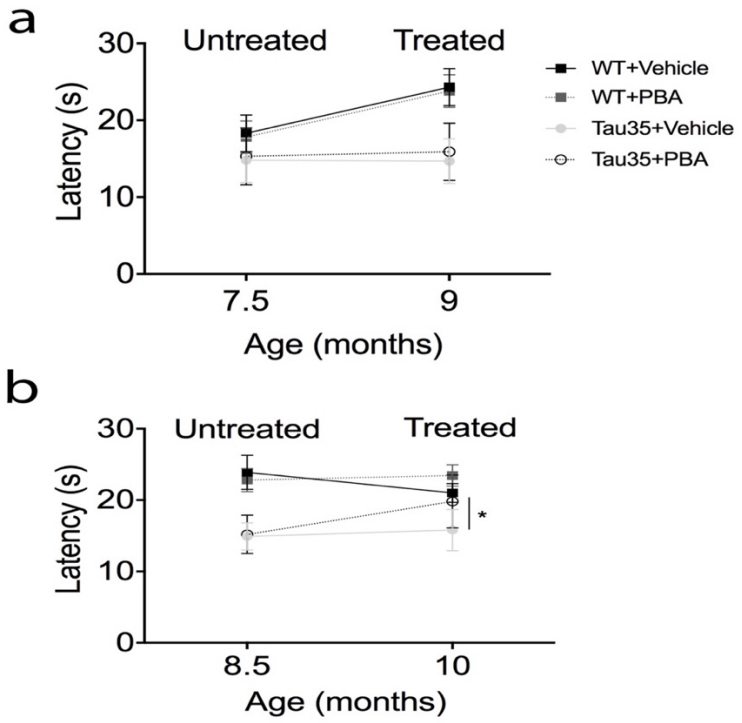

Figure 4.6: Probe trials of Tau35 and WT mice treated with phenylbutyrate (PBA). Morris water maze probe trial latencies in the target quadrant of PBA and vehicle-treated Tau35 and WT mice. **(a)** Probe trial before (7.5 months) and after (9 months) treatment **(b)** Probe trial before (8.5 months) and after (10 months) treatment. Values shown are mean ± SEM., n=8 for each genotype, *P<0.05, ANOVA.

When analysing the occupancy of the different quadrants in the Morris water maze in the younger cohorts of Tau35 and WT mice after PBA or vehicle treatment (i.e. mice aged 9 months), no statistically significant differences were observed between any of the groups (Figure 4.7a). However, for the older cohort, PBA treated Tau35 mice spend significantly longer in the target quadrant 36s (+/-3.1) compared to Tau35 mice treated with vehicle 26s (+/-2.05) at 10 months of age (Figure 4.7b, P<0.01). WT PBA or vehicle treated mice showed no difference in preference of target. This data indicates recued memory consolidation of Tau35 mice upon PBA treatment. Similarly, the total

distance travelled by the younger cohorts of mice at 7.5 (untreated) and 9 months (treated), also did not show any significant differences (Figure 4.8a).

When analysing the total distance swum the younger cohort showed no significant difference at 7.5 months (untreated) and 9 months (treated). Tau35 and WT groups did show a difference in total distance swum (Figure 4.8a) which has been previously shown in section 3.2.2.10 The distance swum in the Morris water maze, but not swim speed, is increased in Tau35 mice. At 8.5 months of age Tau35 and WT groups exhibited a difference in swim distance as Tau35 are impaired by this age as previously described in section 3.2.2.10 The distance swum in the Morris water maze, but not swim speed, is increased in Tau35 mice (Figure 4.8b, untreated). Following a 6 week dosing period with PBA, the total distance swum of the older cohort of Tau35 mice increased from a mean value of 459cm (+/-29) at 8.5 months to 388cm (+/-23) at 10 months, a decrease of 18%, whereas the swim distance of Tau35 mice treated with vehicle increased slightly, resulting in a statistically significant difference ($P<0.005$) between PBA and vehicle-treated Tau35 mice. In contrast, the swim distance of WT mice, whether treated with vehicle or PBA, decreased slightly during the same period and did not show any significant differences under these two conditions (Figure 4.3a, $P<0.001$). Swim speed was not influenced by PBA treatment in either cohort of mice (Figure 4.8c and d). This data suggests that PBA has the ability to rescue memory consolidation with no effect on overall swim speed.

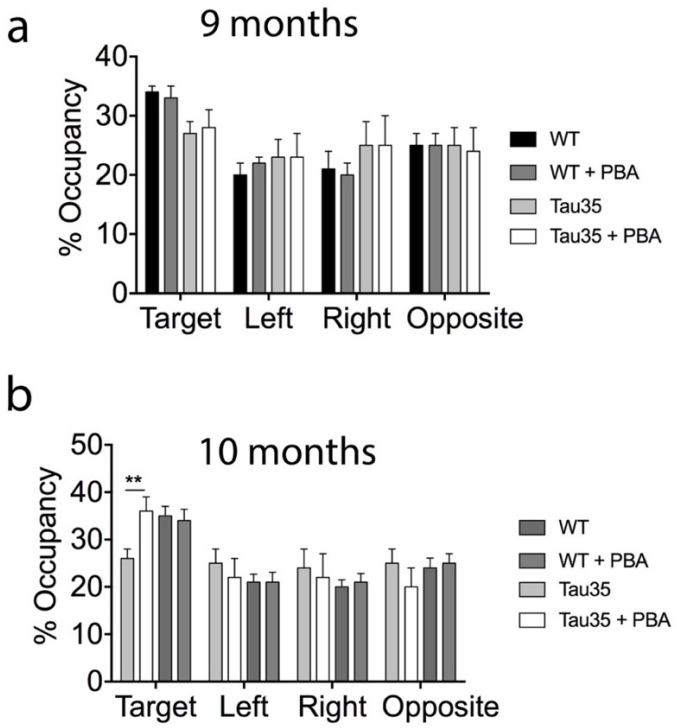

Figure 4.7: % Occupancy of Tau35 and WT after treatment with PBA and vehicle at 9 and 10 months of age. (a) Percentage occupancy of WT and Tau35 vehicle or PBA treated mice at 9 months **(b)** Percentage occupancy of WT and Tau35 vehicle or PBA treated mice at 10 months. Values shown are mean ± SEM., n=8 mice per genotype, **P<0.01, ANOVA.

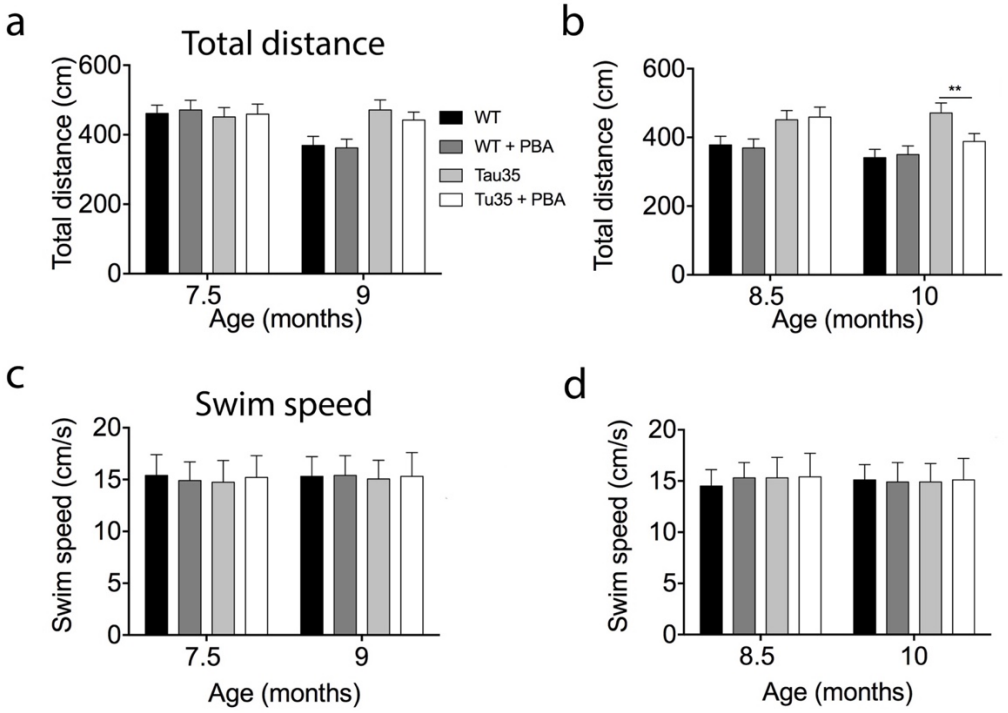

Figure 4.8: Total swim distance and swim speed and of Tau35 and WT before and after treatment with phenylbutyrate and vehicle. (a) Total distance travelled to escape platform at 7.5 and 9 months and at 8.5 and 10 months of age. Tau35 mice treated with PBA incurred a reduced swim distance to platform than vehicle-treated mice at 10 months of age **(b)** Total distance travelled to escape platform at 7.5 and 9 months and 8.5 and 10 months of age. Tau35 mice treated with PBA incurred a reduced swim distance to platform than vehicle-treated mice at 10 months of age **(c)** Total swim speed at 7.5 and 9 months of age. **(c)** Total swim speed at 8.5 and 10 months of age. Values shown are mean ± SEM, n=8 mice for each genotype, **P<0.01, ANOVA.

4.2.5 Phenylbutyrate rescues phosphorylated tau and decreases total tau

The brains of Tau35 mice harbour highly phosphorylated tau at several different epitopes (3.2.3.1 Tau is phosphorylated at several different epitopes in Tau35 mice whereas the total amount of tau is unchanged3.2.4.1 Tau35 mice exhibit increased phosphorylated tau immunoreactivity). Tau phosphorylation at the PHF1 epitope (pS396/pS404) is a well-studied phosphorylation site and this antibody can be used as a marker of AD pathology in human patients (Dickson et al., 1986). PBA has previously been shown to decrease phosphorylated tau at epitope Ser202/Thr205 (AT180) in the hippocampus of transgenic mice overexpressing mutant APP (Ricobaraza et al., 2009). Increased tau phosphorylation at the PHF1 epitope was identified in Tau35 mouse hippocampus between the ages of 2 and 14 months of age. As AT180 did not show very specific labelling in Tau35, PHF1 immunoreactivity in the older group of Tau35 mice was examined on WB and IHC after administration of PBA or vehicle. The WB results showed that PBA caused a decrease of 52% in the amount of phosphorylated tau, relative to total tau, in the hippocampal regions of Tau35 mice compared to vehicle-treated mice aged 10 months (Figure 4.9a, b, $P<0.001$). In addition, total tau, relative to β-actin, was also reduced by 18% in the older PBA-treated Tau35 mice (Figure 4.9a, c, $P<0.01$).

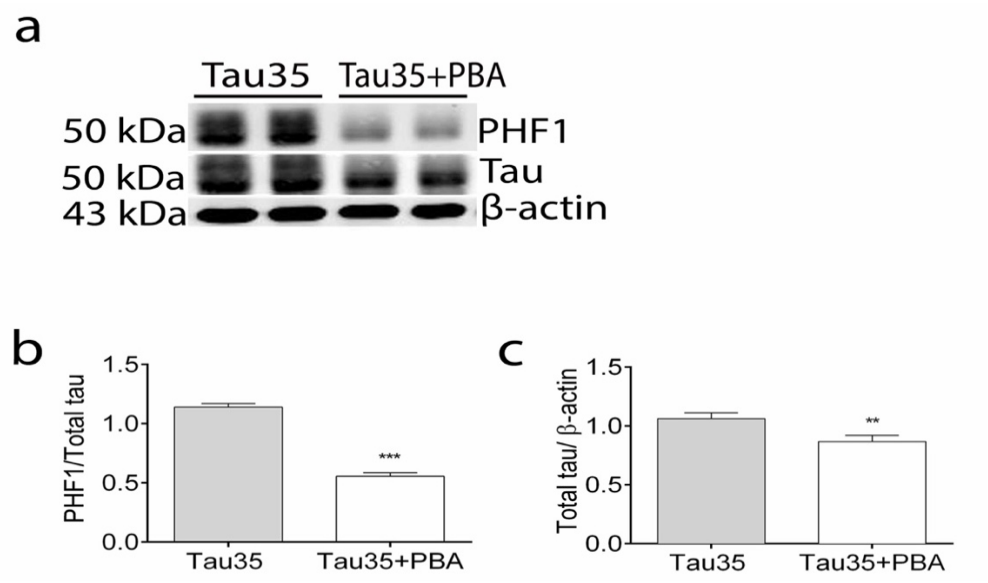

Figure 4.9: Phenylbutyrate reduces tau phosphorylation and total tau in Tau35 mice. (a) Western blots of hippocampal extracts of the older cohort of Tau35 mice following vehicle or PBA treatment for 6 weeks. Mice were aged 10 months when examined. Blots were probed with antibodies to phosphorylated tau (PHF1), total tau, and β-actin. Molecular weight markers are shown on the left. Graphs showing the amounts of **(b)** phosphorylated tau (PHF1), relative to total tau, and **(c)** total tau, relative to β-actin, in Tau35 hippocampus. Values shown are mean ± SEM., n=5 for each genotype, **P<0.01, ***P<0.001, ANOVA.

Tau phosphorylation at the PHF1 epitope was also examined by immunohistochemistry in the older Tau35 mice following PBA or vehicle administration (10 months). Although no tangles were detectable in this cohort of vehicle-treated Tau35 mice at this age, aggregated tau was apparent in the mossy fibres in the striatum lucid and the hilus, and this was not present in PBA-treated mice (Figure 4.10, arrows). These results suggest therefore that treatment with PBA removes the build-up of phosphorylated cytoplasmic tau in the hippocampal regions of Tau35 mice. However, further investigation and additional phosphorylation-dependent tau antibodies are necessary to fully elucidate the mechanism underlying the action of PBA in reducing tau phosphorylation.

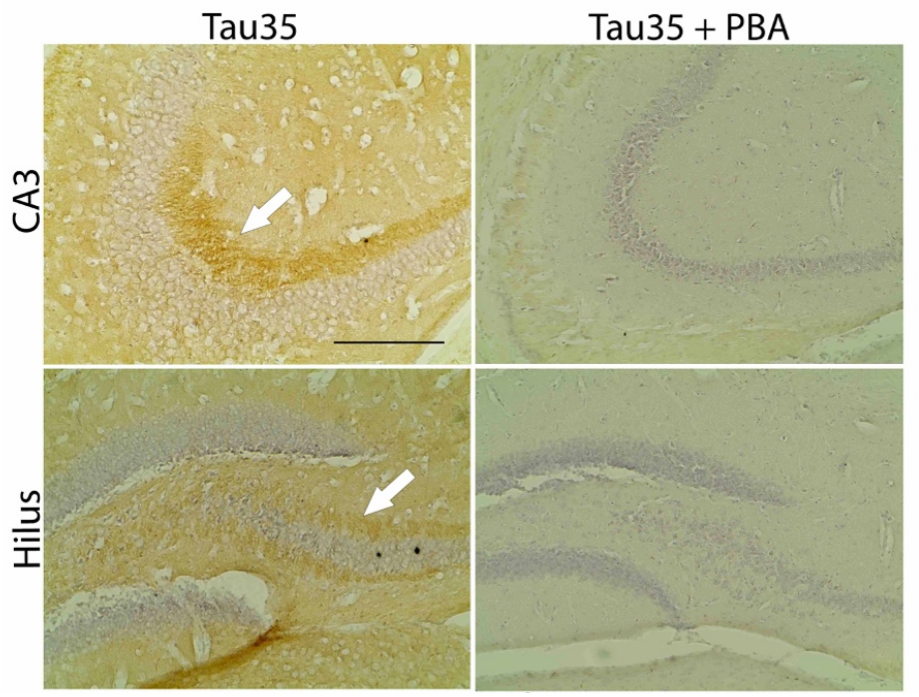

Figure 4.10: PHF1 immunoreactivity in Tau35 mice treated with vehicle or PBA. Hilus and CA3 hippocampal sections of Tau35 mice at 10 months of age following a 6week treatment with vehicle (left panels) or PBA (right panels). Sections were labelled with antibody to phosphorylated tau (PHF1) and counterstained with haematoxylin. White arrow indicating perfusily stained mossy fibre region in Tau35 vehicle treated mice. n=3 per treatment group. Scale bar=200μm.

4.2.6 Phenylbutyrate partially rescues lysosomal degradation

The results shown in Chapter 3 implicate autophagy, and the involvement of lysosomal degradation pathways, in the behavioural, biochemical and pathological changes observed in Tau35 mice. The formation of the autophagosome requires two key proteins, p62 and LC3, which are commonly used as autophagic markers. The LC3-II isoform is functionally important for elongation of autophagosome membrane (Banduseela et al., 2013), whereas the adaptor protein p62 recognises and attaches to ubiquitinated misfolded proteins, prior to binding to LC3-II to generate an autophagosome (Figure 1.11) (Banduseela et al., 2013). Tau35 mice show increases in both p62 and LC3 (Figure 3.19), implicating abnormal autophagosome function as a possible pathogenic mechanism. To determine whether this process can be rescued by PBA, LC3 and p62 were assessed in brain homogenates of PBA and vehicle-treated mice aged 10 months. Notably, PBA treatment had no effect on the elevated LC3-I and LC3-II observed in Tau35 mice (Figure 4.11)

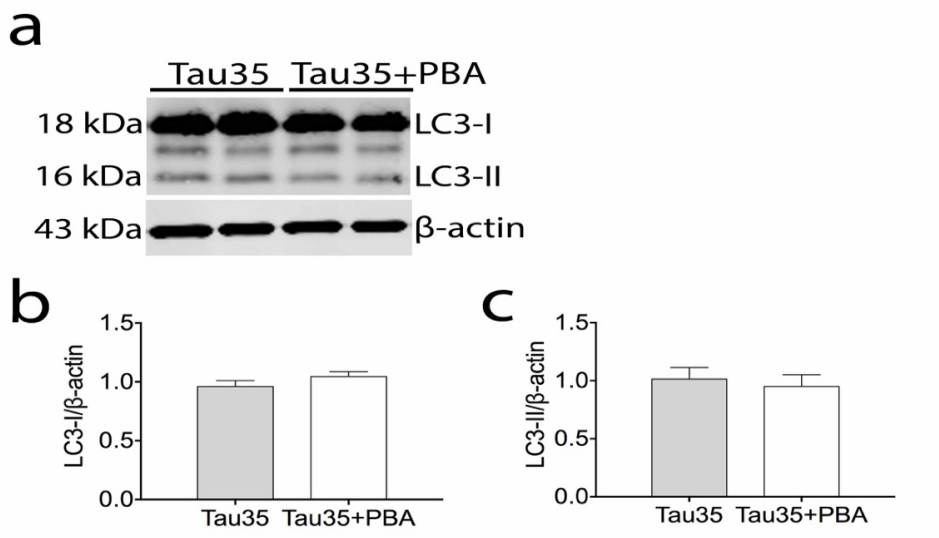

Figure 4.11: LC3-I and LC3-II in Tau35 mice treated with phenylbutyrate. **(a)** Western blots of microtubule-associated protein 1-light chain 3 (LC3)-I and LC3-II and β-actin, in PBA and vehicle-treated Tau35 mice aged 10 months. Graphs show quantitation of LC3-I (b) and LC3-II (c) in PBA and vehicle-treated mice. Values shown are mean ± SEM, n=5 per genotype.

Western blots of p62 in PBA and vehicle-treated Tau35 mouse brain showed a significant reduction of 57% induced by PBA (Figure 4.12, P<0.05). Furthermore, neither PBA nor vehicle affected the amount of p62 present in WT mice (Figure 4.12).

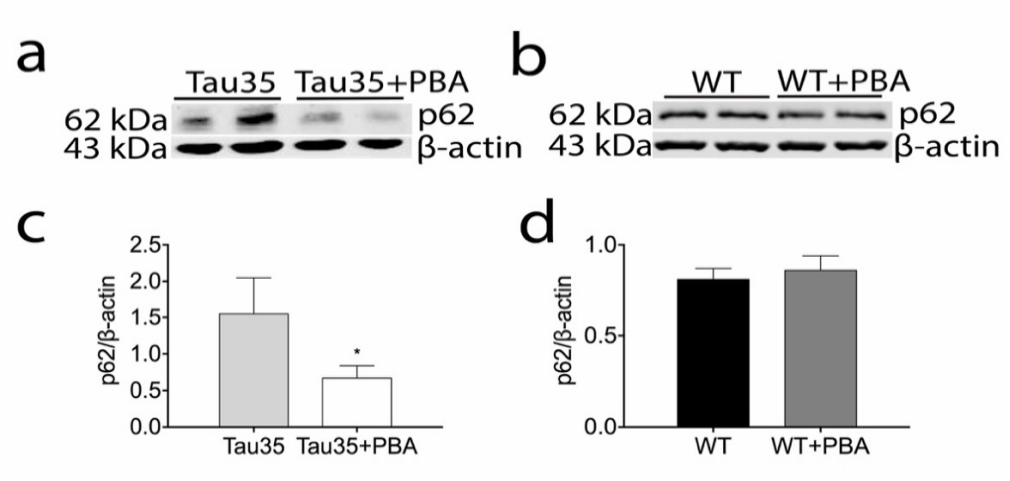

Figure 4.12: p62 in Tau35 and WT mice treated with phenylbutyrate or vehicle Western blot showing p62 in Tau35 mice **(a)** or WT mice **(b)** following administration of either PBA or vehicle for 6 weeks. Mice were aged 10 months when examined. **(c)** Graphs showing the amounts of p62, relative to β-actin, in Tau35 **(c)** or WT **(d)** mice. Values shown are mean ± SEM, n=5 for each genotype. *P<0.05, ANOVA.

Immunohistochemical analysis of Tau35 mice using an antibody recognising p62 showed that, whereas vehicle-treated mice showed increased p62 immunoreactivity in the pyramidal cell layer of the CA1 and CA3 of the hippocampus, in PBA-treated mice this labelling was absent (Figure 4.13).

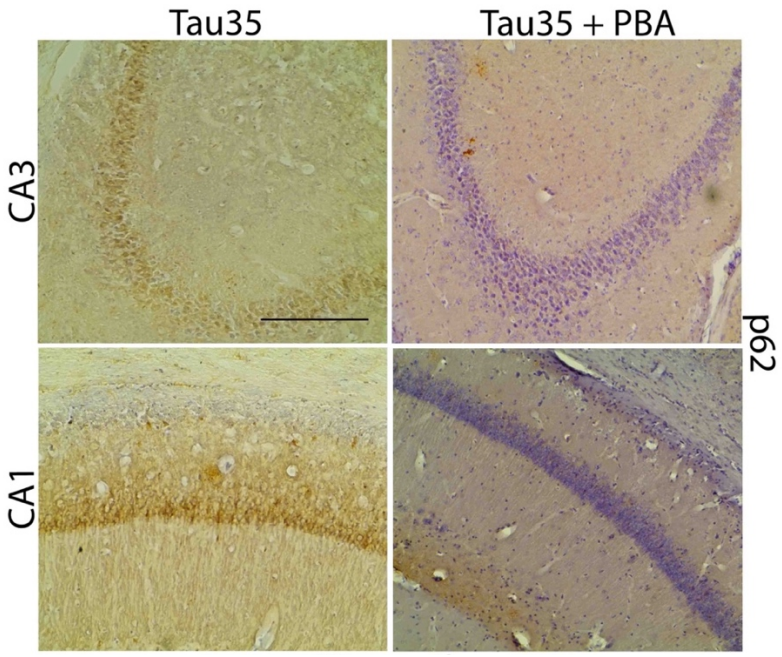

Figure 4.13: p62 labelling of Tau35 hippocampus following treatment with phenylbutyrate or vehicle. Hippocampal brains sections from PBA and vehicle-treated Tau35 mice. Positive p62 labelling was observed in CA1 and CA3 hippocampal regions in Tau35 mice treated with vehicle, which was absent from Tau35 mice treated with PBA. n=3 mice for each treatment group, Scale bar=200µm.

The autophagolysosome contains acidic proteases, including cathepsin family members that are responsible for the degradation of autophagic substrates. Cathepsin D is crucial for lysosomal degradation of proteins and reduced cathepsin D has previously been linked to impaired autophagic degradation (Tatti et al., 2012). The results shown in section 3.2.3.4 Lysosomal degradation markers are altered in Tau35 identified reduced mature cathepsin D in Tau35 mouse brain. Therefore, the effects of PBA administration on cathepsin D were examined on western blots of Tau35 mouse brain. PBA caused a 37% increase in the amount of mature (active) cathepsin D present in Tau35 mouse hippocampus, relative to β-actin (Figure 4.14a,c, $P<0.05$), without any significant effect on the amount of pro-cathepsin D (Figure 4.14a, b, $P>0.05$).

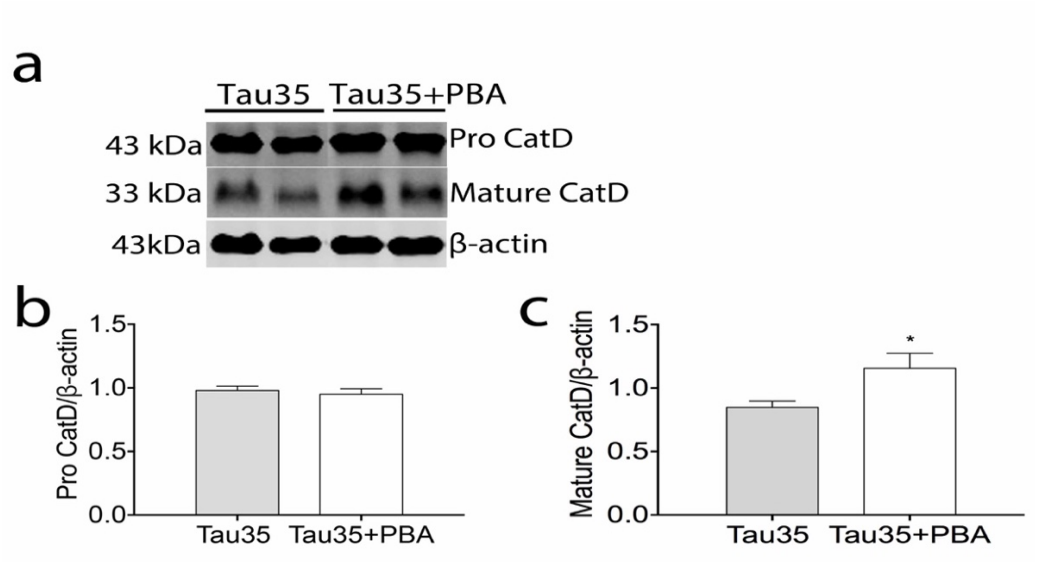

Figure 4.14: Cathepsin D in Tau35 mice treated with phenylbutyrate or vehicle (a) Western blot showing pro-cathepsin D (Pro CatD) and mature (active) cathepsin D in PBA and vehicle-treated Tau35 mice. Graphs showing the relative amounts of mature cathepsin D **(b)** and pro-cathepsin D **(c)** in Tau35 mice treated with PBA or vehicle. Values shown are mean ± SEM, n=5 per genotype, *$P<0.05$, ANOVA.

Tau35 mouse brain also exhibits a significantly reduced amount of acetylated tubulin, indicating that there may be a decreased ability to stabilise MTs in these animals (Figure 3.20). To determine whether PBA treatment can reverse this effect on tubulin acetylation, the amounts of acetylated and total α-tubulin were assessed in hippocampal homogenates from Tau35 mice aged 10 months (Figure 4.15). PBA induced a 2-fold increase in acetylated α-tubulin, relative to total α-tubulin in Tau35 mice (Figure 4.15a, b, $P<0.05$), without affecting the total amount of α-tubulin, relative to β-actin (Figure 4.15a, c).

Taken together, these results indicate that PBA has the ability to at least partially restore some of the abnormalities that lead to defective lysosomal degradation in Tau35 mice.

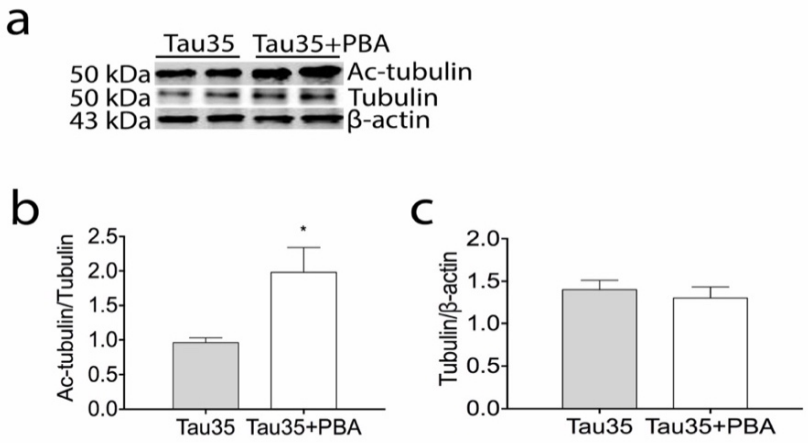

Figure 4.15: Acetylated tubulin and tubulin in phenylbutyrate treated Tau35 mice. (a) Western blot showing acetylated tubulin (Ac-tubulin) and tubulin levels in Tau35 mice treated with either phenylbutyrate (PBA) or vehicle. Graphs showing the amount of acetylated α-tubulin, relative to total α-tubulin **(b)** and total α-tubulin, relative to β-actin in Tau35 mice following PBA treatment. Values shown are mean ± SEM, n=5 per treatment group, *$P<0.05$, ANOVA.

4.2.7 Phenylbutyrate rescues synaptic integrity

Synapsin1, but not synaptophysin, was previously shown to be significantly reduced in Tau35 compared to WT mice (section 3.2.3.5 Synaptic proteins in Tau35 mice). To assess whether PBA could reverse this potential dysfunction in synaptic vesicle release, brain hippocampal homogenates from 10 months old Tau35 and WT mice treated with either PBA or vehicle were analysed on western blots to determine the amounts of synapsin1 and synaptophysin. Following PBA administration, the amount of synapsin1 increased two-fold in Tau35 mouse brain (Figure 4.16a, c, $P<0.01$), whereas synapsin1 was unchanged in the treated WT mice (Figure 4.16b, d). In contrast, synaptophysin was unaltered in Tau35 mice treated with PBA (Figure 4.16e). This finding was not surprising because the amount of synaptophysin was also not altered in untreated Tau35 mice at this age (Chapter 3, Figure 3.21b). These results indicate that PBA can potentially recover synaptic integrity in particular synaptic vesicular release deficits. However, the potential beneficial effect of PBA on synaptic health requires confirmation.

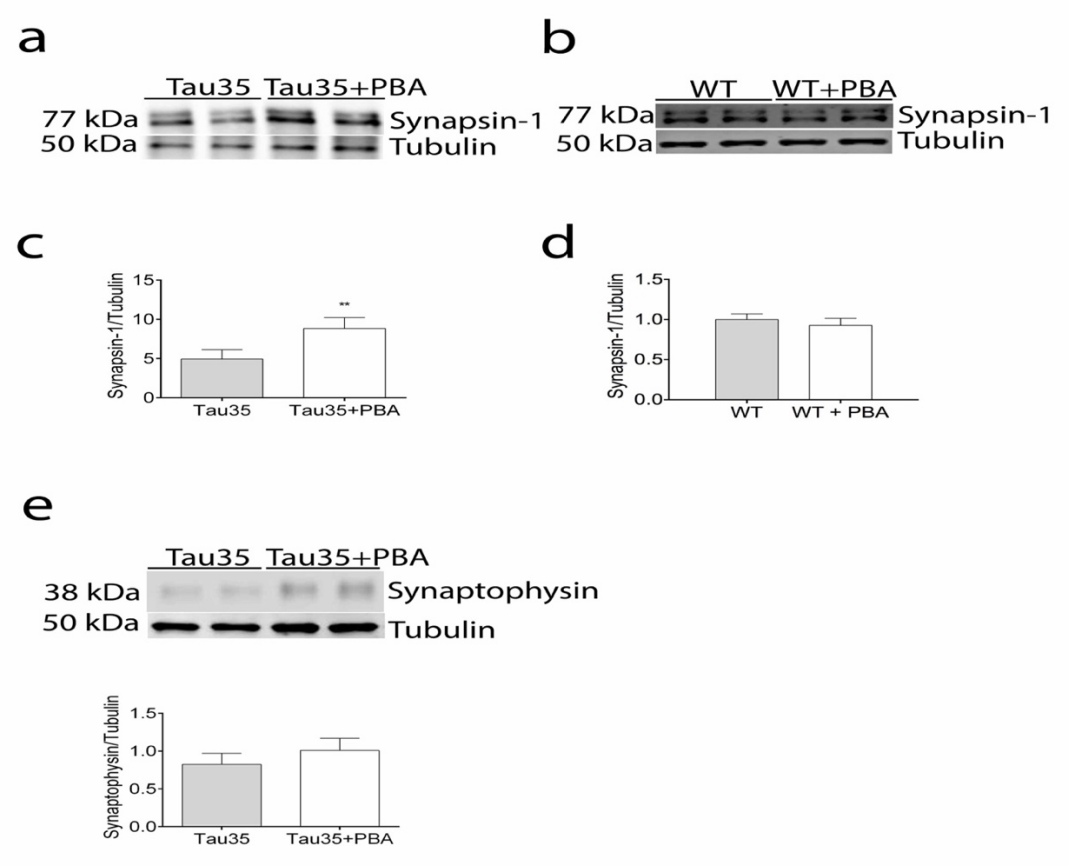

Figure 4.16: Synapsin1 and synaptophysin in Tau35 and WT mice treated with phenylbutyrate. Western blots of synapsin1 in Tau35 **(a)** and WT **(b)** mouse hippocampus treated with either vehicle or PBA at 10 months of age. **(c-d)** Graphs showing quantification of the amount of synapsin1, relative to α-tubulin. Synapsin1 was significantly increased in Tau35 mice following PBA treatment. **(e).** Western blot and graph showing the amount of synaptophysin in Tau35 vehicle and PBA-treated mice. Values shown are mean ± SEM, n=5 per treatment group and genotype, **P<0.01, ANOVA.

4.3 Summary and Discussion

The purpose of this study was to examine whether the tauopathy-like deficits seen in Tau35 mice could be reversed or rescued upon treatment with a therapeutic compound. HDAC inhibitors such as PBA have previously shown promising results in animal models for: ALS (Del Signore et al., 2009), AD (Ricobaraza et al., 2009), Huntington's disease (Ferrante et al., 2003), stroke (Qi, 2004), Parkinson's disease (Zhou et al., 2011) and dentatorubral-pallidoluysian atrophy (a rare autosomal dominant neurodegenerative progressive disorder of ataxia, myoclonus, epilepsy, and progressive intellectual deterioration in children and ataxia, choreoathetosis, and dementia) (Ying et al., 2006). Due to previous findings and the pleiotropic properties of PBA, this compound was selected to treat the Tau35 mice.

The main findings of this chapter are:

1) PBA did not alter the body mass of Tau35 or WT mice.
2) Progressive neuromuscular deterioration in Tau35 mice was rescued upon treatment with PBA.
3) Progressive spatial learning and hippocampal-dependent memory was rescued in 8.5 months treated Tau35 mice, but did not prevent the development of these impairments in Tau35 mice.
4) The increase in phosphorylated tau in Tau35 mice was reversed by PBA treatment.
5) Impaired lysosomal degradation/autophagy in Tau35 mice was partially restored following PBA treatment.
6) The observed reduction in synapsin1 in Tau35 mice was reversed upon treatment with PBA.

Taken together, these results show that treatment with the clinically approved drug PBA, is able to partially rescue the key phenotypical characteristics that emulate tauopathy in Tau35 mice at 10months of age.

4.3.1 Phenylbutyrate rescues motor deficits in Tau35

PBA has contributed to therapy for spinal muscular atrophy (SMA) (Andreassi et al., 2004) and has been tested in clinical trials for people with SMA during a 7 day pilot study. During this trial, patients showed improved motor function compared to baseline measurements (Mercuri et al., 2004). In the present study, motor impairment of Tau35 mice improved with increased grip strength evident in the mice at 9 and 10 months of age, indicating the ability of PBA to rescue muscular deficits in these mice. Muscle atrophy is associated with aging and neurodegenerative diseases such as amyotrophic lateral sclerosis (ALS) and it can occur when the rate of protein degradation exceeds that of protein synthesis (von Haehling et al., 2010). It is possible that PBA may act via rescuing SMA genes or via the two major protein degradation pathways that are activated during muscle atrophy known as the autophagic lysosomal pathway (also dysfunctional in Tau35) and the ubiquitin-proteasome systems which variably contributes to the loss of muscle mass (Sandri, 2013). The mechanistic roles PBA may have on the rescue of motor deficits and muscle pathology is further discussed in CHAPTER 7.

4.3.2 Phenylbutyrate rescues cognitive deficits in Tau35 mice

A common feature of memory formation, in particular long-term memory is the requirement for changes in gene expression essential for memory consolidation (Bailey et al., 2004). HDAC inhibitors, such as PBA, have the ability to alter chromatin structure and thereby enhance memory formation (Levenson et al., 2004). Previous studies have shown that PBA can successfully reduce, restore and recover learning and memory formation (Ricobaraza et al., 2009). The current study also identified that treatment of Tau35 mice aged 8.5 months with PBA, for a duration of 6 weeks, reversed and rescued spatial and learning memory deficits. Data from the present work further supports the view that PBA rescues memory deficits apparent in Tau35 mice in the Morris water maze, potentially through chromatin remodelling and/or upregulation of gene transcription, or even upregulation of synaptic plasticity.

PBA is known to act via HDAC inhibition which could improve protein remodelling and synaptic plasticity which could directly influence memory and learning. Histone acetylation is a highly controlled process by two types of enzymes, histone transferases (HATs) and HDACs, which in turn can drive gene expression (Guan et al., 2002; Soejima et al., 2004; Clayton et al., 2006). Previous research has implicated histone acetylation and its gene activation properties in memory and learning and increases histone acetylation can be observed after exposure to learning paradigms (Korzus et al., 2004; Levenson et al., 2004; Chwang, 2006; Chwang et al., 2007; Fischer et al., 2007; Mai et al., 2009; Peleg et al., 2010). PBA may therefore have an effect on epigenetic histone acetylation regulators which play a crucial role in neural gene expression involved in phenotypic and behavioural cognitive plasticity (Unterberger et al., 2006). In addition, PBA enhances the expression of several cell chaperons via HDAC inhibition and therefore contribute to possible reduction of ER stress (Ricobaraza et al., 2012). Interestingly PBA was not able to prevent memory deficits when mice were dosed at the age of 7.5 months, indicating that PBA preferentially acts on pre-existing deficits in Tau35 mice and rescues these rather than preventing the onset of disease. The possible mechanistic roles of PBA on memory are discussed in more detail in CHAPTER 7

4.3.3 Phenylbutyrate rescues phosphorylated tau and reduces total tau in Tau35 mice

Treatment of Tau35 mice with PBA for six weeks resulted in a significant decrease in phosphorylated tau in the hippocampus in biochemical immunoblots and immunohistochemically-labelled hippocampal brain sections (Figure 4.10) There was no detectable labelling of either inclusions or mossy fibres in PBA-treated Tau35 mice compared to those receiving vehicle, the latter of which exhibited extensive mossy fibre labelling in the CA3 and CA1 regions of the hippocampus. PBA exhibits a variety of metabolic effects, acting as a chaperone molecule, binding and masking surface exposed hydrophobic segments of unfolded proteins, stabilising proteins in their native

conformation, and reducing ER stress (Perlmutter, 2002; Papp, 2006; Yam et al., 2007). Results from western blots and immunohistochemistry studies reported here, indicate that PBA treatment ameliorates the increase in tau phosphorylation in Tau35 mouse hippocampus. It is therefore possible that the reduction of phosphorylated tau seen in PBA treated Tau35 mice is due to direct stabilisation of tau and therefore preventing the formation of oligomers, fibrils or other higher molecular tau species. Selenica and colleagues have proposed that spatial navigation was improved due to a reduction in total tau rather than aggregated tau (Selenica et al., 2014). Tau35 mice also showed a decrease in total tau upon treatment with PBA indicating that the reduction in tau may be linked to the spatial learning improvement seen in these animals.

Previous studies have identified that treating mouse models of AD (Tg2576 mice expressing mutant APP) or SMA (SMNΔ7 SMA mice lacking exon 7 which develop extensive motor deficits) with PBA, increases Ser9 phosphorylation of GSK3β, reducing GSK3 activity in the hippocampus, as well as decreasing Akt phosphorylation (Ricobaraza et al., 2009; Butchbach et al., 2016). As Tau35 mice exhibit increased GSK3β activity, the reduction in tau phosphorylation caused by PBA, may result in part from GSK3β inhibition. However, the present study described here did not investigate levels of GSK3 or Akt activity in PBA-treated Tau35 mice. Nevertheless, PBA modulation of the Akt/GSK3β pathway is one possible pathway that may contribute to the neuroprotective effects observed in PBA treated Tau35 mice.

4.3.4 Phenylbutyrate rescues lysosomal deficits in Tau35 mice

The present study demonstrates the ability of PBA, which has several different cellular actions, to partially diminish the impaired lysosomal degradation observed in Tau35 mice. PBA was able to increase the activity of cathepsin D, reduce the elevation in p62 and increase the amount of acetylated α-tubulin, without apparently affecting LC3-I or LC3-II. These findings indicate improved lysosomal autophagic function due to PBA administration in Tau35 mice. The molecular mechanisms underlying the protective effects of PBA on the

autophagic–lysosomal system are not known. However, it is well known that PBA has the ability to improve trafficking of the serotonin transporter (SERT) (Fujiwara et al., 2013) by decreasing the protein folding load in the ER and preventing protein misfolding, thereby providing protection against ER stress mechanisms.

Tau35 mice also show Parkinson-like motor abnormalities, and accumulation of α-synuclein, further implicating possible ER stress in disease pathogenesis, which could potentially be rescued by PBA. However, as ER stress was not directly measured in this study, this remains speculative and further investigation is necessary to fully evaluate the mechanisms affected by expression of Tau35.

4.3.5 Phenylbutyrate rescues synaptic deficits in Tau35 mice

Synaptic dysfunction is a pathological hallmark that features in several human tauopathies, it is also the major correlate of cognitive impairment in AD (Terry et al., 1991). Previous findings by Ricobaraza et al., (2009) showed that PBA increased histone acetylation, in turn elevating marker of synaptic plasticity (Ricobaraza et al., 2009). The present study revealed that PBA was able to rescue synapsin1 deficits in Tau35 mice aged 10 months. This finding indicates that inhibition of histone deacetylation can potentially lead to an upregulation of proteins involved in synaptic plasticity in Tau35 mice, which could be responsible for rescuing impairment of synaptic vesicle release.

Previous studies of gene expression have identified several genes in the formation of long-term memory, through the formation of new synaptic connections and interactions (Tully et al., 2003). It was previously determined that Tau35 mice have reduced synaptic vesicle release, leading to potential disruption of synaptic communication. Herein, the treatment with PBA alleviated this loss of synaptic disruption, which may be directly linked to memory formation. However, only two pre-synaptic markers were tested in the present study, and hence it is essential to examine other synaptic markers, as well as spine number and spine morphology, in order to fully elucidate the mechanism involved.

Another possibility is that the chaperone action of PBA leads to a reduction in tau truncation and or misfolding. Indeed, tau pathology in the mossy fibres, which is present in both naive and vehicle-treated Tau35 mice, is absent in Tau35 mice treated with PBA. This suggests that a potential action of PBA may be to reduce the accumulation of tau in the hippocampus in these animals. It is well established that phosphorylated tau is an integral component of human tauopathies, particularly in pre-tangles and NFTs, leading to neuronal disruption. Therefore, it is possible that dysregulation of tau phosphorylation in the hippocampus could translate into the cognitive deficits and synaptic dysfunction seen in these animals and this may be rescued upon treatment with PBA (Arendt et al., 2003).

4.3.6 Conclusions

Within this chapter it was clearly demonstrated that the disease course of Tau35 mice was modified upon treatment with PBA, a drug currently in clinical use for the treatment of a variety of conditions, including neurodegenerative proteinopathies (Iannitti and Palmieri, 2011). Interestingly PBA treatment showed rescue of symptoms when administered at 8.5 months of age and it may therefore provide efficacy if administered after diagnosis in people with sporadic tauopathies. Our results provide pre-clinical evidence for a beneficial role for PBA in Tau35 mice. Moreover, since there is emerging evidence that tau truncation plays a role in many neurodegenerative disorders, being able to rescue these effects will be important for future therapeutics.

CHAPTER 5

The effect of strain background on the phenotype of Tau35 mice

5.1 Introduction

Tau35 mice exhibit an array of behavioural, biochemical and pathological changes, several of which are rescued by PBA. However, previous disease modifying treatments for the human tauopathies have failed to alleviate symptoms or alter the disease course in clinical trials (Mangialasche et al., 2010). This is partially due to the fact that preclinical *in vivo* studies often use different strains of mice, which can impact on the disease phenotype at different stages and in different ways. For example, mouse strains exhibit variable anxiety, locomotor activity, visual and auditory ability, and differential inflammation, neurodegeneration and learning/memory patterns, all of which can impact on performance and measures of disease severity (Pugh et al., 2004). Well-established examples of these differences include, mouse strains 129/Sv and DBA/2, both of which perform less well in the Morris water maze than the C57BL/6 strain. Furthermore, backcrossing mice on a mixed C57BL/6:129 background onto a pure 129 mouse strain often masks cognitive deficits (Gerlai, 1996; Owen et al., 1997; Wolfer et al., 1997). These reports highlight a potential advantage of using mice on a hybrid background, which may be closer to the situation in humans where genetic variation might affect susceptibility to tauopathies and AD-related dysfunctions. However, these findings also show the importance of investigating phenotypic changes in pure inbred genetic backgrounds for comparison with mice on mixed backgrounds. Furthermore, the benefits of pure genetic inbred mouse models are that the potential manipulation and interference from other genetic factors can be minimised. The C57BL/6 ($WT^{Bl/6}$) mouse is the most commonly used mouse strain in neurodegeneration behavioural research and, although it is now

possible to generate gene-targeted mice using embryonic stem (ES) cells derived from C57BL/6 mice, most mouse models of neurodegenerative disease have been made using mouse ES cell lines derived from 129 mouse substrains (Simpson et al., 1997; Auerbach et al., 2000). As described in 2.1 Animals and tissue and 2.3.12.1 Animals. Tau35 mice were generated from embryonic stem cells derived from 129/Ola mice and clones were injected into C57BL/6 blastocysts. A further cross with C57BL/6 mice resulted in hybrid $Tau35^{Bl/6;129}$ and $WT^{Bl/6;129}$ mice with an average 75% BL/6; 25% 129/Ola. To investigate the effect of mouse background strain on the disease-relevant phenotype, and to attempt to reduce inter-animal variation, the $Tau35^{Bl/6;129}$ mice were backcrossed to pure C57BL/6 mice over 9 generations and behavioural analyses were performed to determine whether the previously observed changes were preserved in the new Tau35 mice on a pure inbred background ($Tau35^{Bl/6}$ mice).

5.2 Results

Male hemizygous $Tau35^{Bl/6}$ mice (n=10) were used in these experiments, as had been done previously with hybrid $Tau35^{Bl/6;129}$ mice (CHAPTER 3). This strategy (1) avoids the complications of the oestrous cycle during different stages and ages of mouse behaviour and (2) minimises potential inter-animal variation due to X-linked inactivation in female mice.

5.2.1 Breeding profile of $Tau35^{Bl/6}$ transgenic mice

The $Tau35^{Bl/6;129}$ original (N1) female heterozygous mice were crossed with C57BL/6 male mice obtained from Charles River over nine generations until N10 was reached (Figure 5.1, Table 9). These mice were then used throughout all the behavioural trials described here.

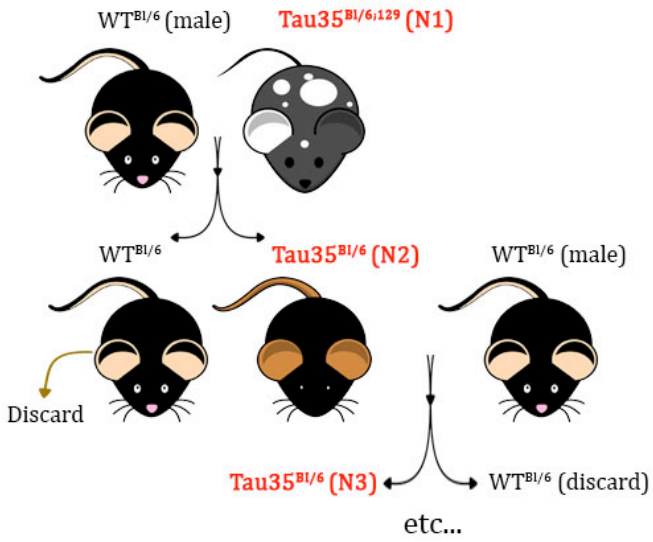

Figure 5.1: Backcross breeding procedure to generate Tau35$^{Bl/6}$ male mice. Heterozygous original N1 female Tau35$^{Bl/6;129}$ mice were crossed 9 times with male C57BL/6 mice until the N10 generation of 99.90% Tau35$^{Bl/6}$ mice was obtained.

Table 9: Table showing the increase in the percentage of C57BL/6 offspring DNA that constitutes the genome of the offspring (Charles River: http://www.criver.com/files/pdfs/gts/rm_gt_d_maxbax.aspx)

Generation	Recipient genome (C57BL/6)
N1 (original colony)	75%
N2	87.5%
N3	93.75%
N4	96.88%
N5	98.44%
N6	99.22%
N7	99.61%
N8	99.82%
N9	99.90%
N10	99.90%

5.2.2 Body mass is not altered in Tau35$^{Bl/6}$ mice

It was previously found that Tau35$^{Bl/6;129}$ mice did not display any difference in body mass compared to WT$^{Bl/6;129}$ animals between the ages of 2-18 months (Figure 3.5). When comparing WT$^{Bl/6}$ and Tau35$^{Bl/6}$ mice aged 2-18 months, there was also no significant difference between the groups at any age (Figure 5.2). Interestingly however, both the Tau35$^{Bl/6}$ and WT$^{Bl/6}$ mice appeared to be consistently of slightly lower body mass than Tau35$^{Bl/6;129}$ and WT$^{Bl/6;129}$ mice at comparable ages, although these differences were not statistically significant (Figure 5.2). This indicates that Tau35 expression did not influence body mass in these mice in either mixed or pure C57BL/6 backgrounds.

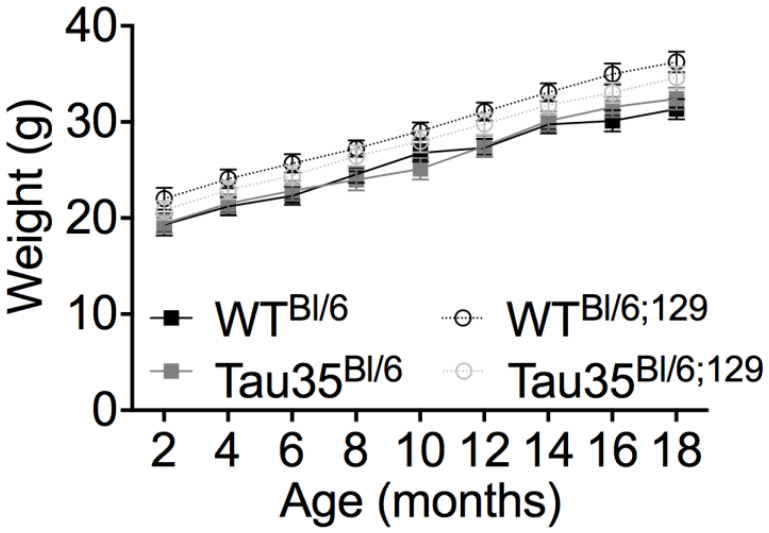

Figure 5.2: Body mass of Tau35 and WT mice on different backgrounds. Graph showing the body weights of age-matched WT$^{Bl/6}$, Tau35$^{Bl/6}$, WT$^{Bl/6;129}$, and Tau35$^{Bl/6;129}$ mice between 2-18 months of age. Values represent mean and ± SEM, n=8-10 per genotype.

5.2.3 Limb clasping in Tau35$^{Bl/6}$ mice

To assess whether Tau35$^{Bl/6}$ mice exhibited a similar limb clasping phenotype to the Tau35$^{Bl/6;129}$ mice, animals were suspended briefly by their tails and limb clasping was assessed as before (Figure 3.6). Tau35$^{Bl/6}$ mice showed distinct limb clasping, similar to the Tau35$^{Bl/6;129}$ hybrid mice (Figure 5.3). However, whereas clasping of Tau35$^{Bl/6;129}$ mice was apparent from 2 months of age, Tau35$^{Bl/6}$ mice exhibited clasping from 4 months of age. By 10 months, 60% of Tau35$^{Bl/6}$ mice were clasping and by 18 months of age, 100% of Tau35$^{Bl/6}$ mice showed the clasping phenotype, which was entirely consistent with the results previously obtained from the Tau35$^{Bl/6;129}$ mice (Figure 5.3b).

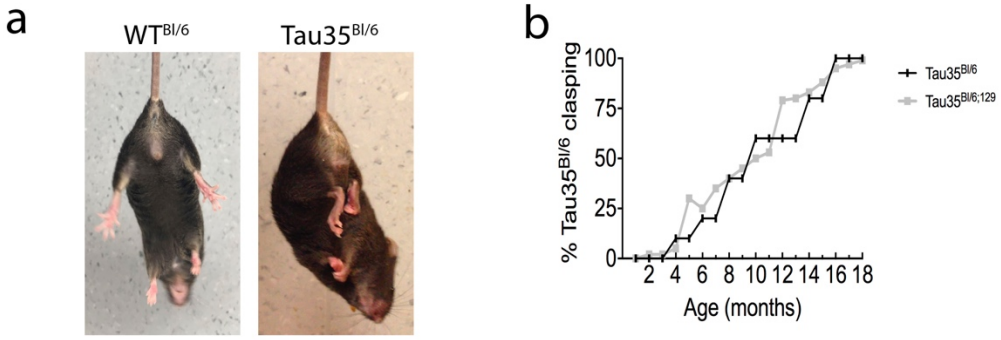

Figure 5.3: Limb clasping in Tau35$^{Bl/6}$ and Tau35$^{Bl/6;129}$ mice. (a) Tau35$^{Bl/6}$ mice clasp their hind limbs and forelimbs from an early age during brief tail suspension (left, WT$^{Bl/6}$; right, Tau35$^{Bl/6}$) both at 10 months of age. **(b)** The proportion of Tau35$^{Bl/6}$ mice exhibiting clasping was determined at intervals between 2 and 18 months of age. Clasping was not observed in WT$^{Bl/6}$ mice at any age examined. Tau35$^{Bl/6;129}$ data are shown for comparison (grey). Values show the percentage of total mice clasping their limbs, n=10-40 per genotype.

5.2.4 Locomotor activity is not altered in Tau35$^{Bl/6}$ mice

Locomotor activity was assessed in Tau35$^{Bl/6}$ mice aged 8 months to test for any patterns of anxiety or abnormal behaviour. Tau35$^{Bl/6}$ mice showed no significant differences in either the time spent in each zone (Figure 5.4a) or the total distance travelled during the monitoring period in the open field, compared to WT$^{Bl/6}$ mice (Figure 5.4b). These results show that similar to the Tau35$^{Bl/6;129}$ mice, Tau35$^{Bl/6}$ mice do not show increased anxiety.

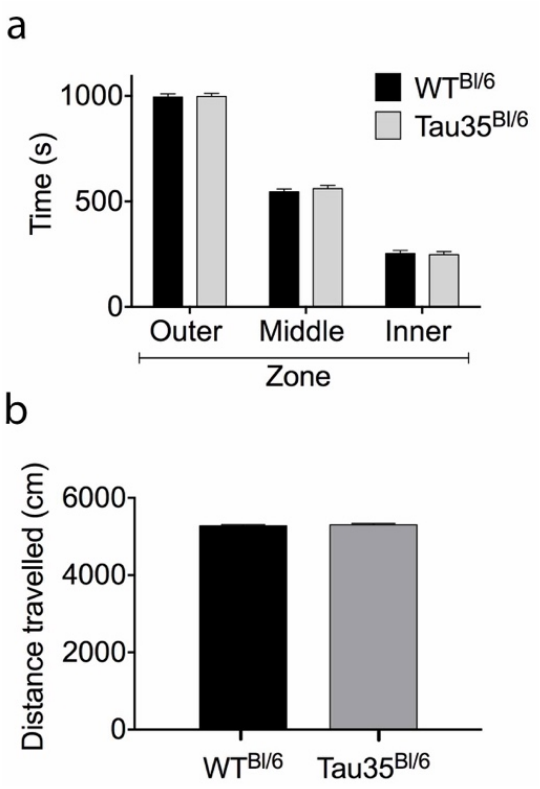

Figure 5.4 Locomotor activity in the open field test for WT$^{Bl/6}$ and Tau35$^{Bl/6}$ mice. (a) Results are expressed as the time spent in the outer, middle or inner zone of the open field during an observation period of 30 min. **(b)** Total distance travelled in the 30 min spent in the open field for Tau35$^{Bl/6}$ and WT$^{Bl/6}$ mice aged 8 months. Values shown are mean ± SEM., n=10 per genotype.

5.2.5 Assessment of motor deficits in Tau35$^{Bl/6}$ mice

Motor co-ordination was assessed on an accelerating Rotarod in Tau35$^{Bl/6}$ mice aged 1-16 months. Tau35$^{Bl/6}$ mice showed a significant reduction in the latency to fall from the Rotarod compared to WT$^{Bl/6}$ mice. Similar to the Tau35$^{Bl/6;129}$ mice, in which motor impairment was apparent from 1 month of age, Tau35$^{Bl/6}$ showed early impaired motor ability from 2 months of age, which progressively deteriorated (Figure 3.7). A comparison of the Rotarod performance of Tau35$^{Bl/6}$ and Tau35$^{Bl/6;129}$ mice showed that Tau35$^{Bl/6}$ mice performed marginally better than Tau35$^{Bl/6;129}$ mice (although this difference was not statistically significant) with an increased latency to fall from the Rotarod of approximately 20s, up to the age of 8 months (Figure 5.5a). By 14 months of age, there was no difference between the performance of Tau35$^{Bl/6}$ and Tau35$^{Bl/6;129}$ mice on the Rotarod (Figure 5.5b). The performance of the two background control strains of mice on the Rotarod was comparable at all ages tested and inter-animal variation was also similar for both background strains (Figure 5.5b).

Testing for motor co-ordination showed that, as found previously in the Tau35$^{Bl/6;129}$ mice, Tau35$^{Bl/6}$ mice have a reduced motor learning ability, which decreased with age, indicating a progressive age-related defect in motor co-ordination.

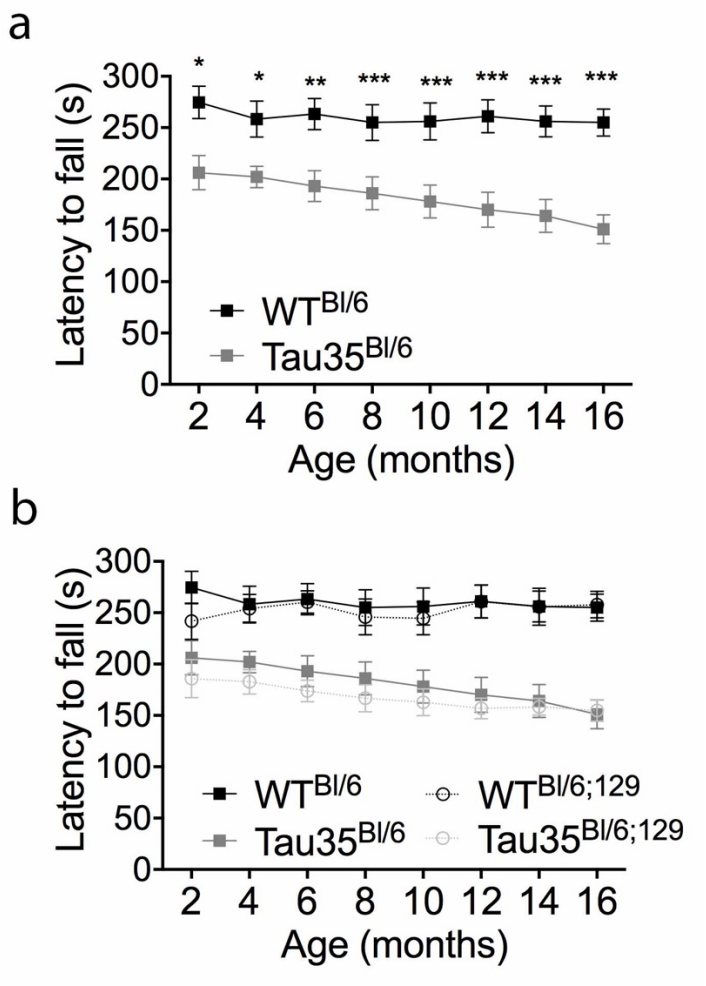

Figure 5.5: Motor learning performance of Tau35^{Bl6}, WT$^{Bl/6}$, Tau35$^{Bl/6;129}$ and WT$^{Bl/6;129}$ mice. (a) Mean latency to fall from an accelerating Rotarod for Tau35$^{Bl/6}$ and WT$^{Bl/6}$ mice at 2-16 months of age. Tau35$^{Bl/6}$ mice show a significant impairment compared to WT$^{Bl/6}$ mice at all ages tested. **(b)** Mean latency to fall from an accelerating Rotarod illustrating the comparison between the four genotypes of Tau35$^{Bl/6}$, WT$^{Bl/6}$, Tau35$^{Bl/6;129}$ and WT$^{Bl/6;129}$ mice. Values shown are mean ± SEM., n=8-10 per genotype *P<0.05, **P<0.01, ***P<0.001, ANOVA.

5.2.6 Neuromuscular deficits in Tau35$^{Bl/6}$ mice

Grip strength was assessed in Tau35$^{Bl/6}$ and WT$^{Bl/6}$ mice aged 4-16 months. Similar to the hybrid Tau35$^{Bl/6;129}$ mice, Tau35$^{Bl/6}$ mice exhibited reduced grip strength, compared to WT$^{Bl/6;129}$ mice from the age of 6 months, and this progressively decreased with age (Figure 5.6a). Notably, however, at 8 months of age Tau35$^{Bl/6}$ mice were scored approximately 10g lower than Tau35$^{Bl/6;129}$ mice and WT$^{Bl/6}$ scored 15g lower than WT$^{Bl/6;129}$ mice, indicating a possible difference in the grip strength in the WT background strains. This difference was less pronounced between Tau35$^{Bl/6}$ and Tau35$^{Bl/6;129}$ at the ages of 10, 12, 14 and 16 months of age with all mice being scored approximately 50g (Figure 5.6b). WT$^{Bl/6}$ mice however, did show a reduction of approximately 10g in grip strength at the ages of 10 and 12 months, compared to WT$^{Bl/6;129}$ mice, although this was not significantly different, and was less apparent in mice at 14 and 16 months of age (Figure 5.6b). Interestingly, the Tau35$^{Bl/6}$ and WT$^{Bl/6}$ grip strength data appeared to show less variance between animals than had been previously found for Tau35$^{Bl/6;129}$ and WT$^{Bl/6;129}$ mice (Figure 3.8). These results show a progressive deterioration in the muscle tone of Tau35$^{Bl/6}$ mice from an early age, similar to that determined previously for Tau35$^{Bl/6;129}$ mice. These results also show a slight strain difference particularly between the WT$^{Bl/6;129}$ and WT$^{Bl/6}$ mice, with WT$^{Bl/6}$ performing less well than WT$^{Bl/6;129}$ mice, which is not surprising given that there is often a difference in performance between different background strains.

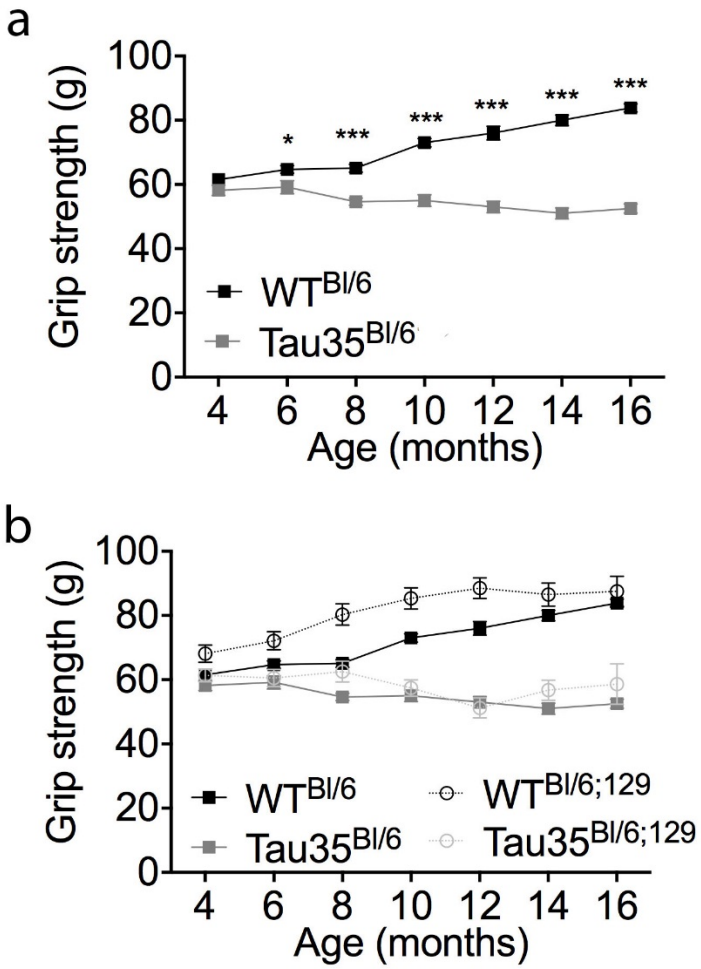

Figure 5.6: Grip strength of Tau35$^{Bl/6}$, WT$^{Bl/6}$, Tau35$^{Bl/6;129}$ and WT$^{Bl/6;129}$ mice (a) Grip strength (all limbs) of Tau35$^{Bl/6}$ and WT$^{Bl/6}$ mice at 4-16 months of age. Tau35$^{Bl/6}$ mice show a significant impairment compared to WT$^{Bl/6}$ mice from 6 months. **(b)** Grip strength of Tau35$^{Bl/6}$, WT$^{Bl/6}$, Tau35$^{Bl/6;129}$ and WT$^{Bl/6;129}$ mice to illustrate the differences between all four genotypes. Values shown are mean ± SEM., n=8-10 per genotype, *P<0.05, ***P<0.001, ANOVA.

5.2.7 Spatial learning is impaired in Tau35$^{Bl/6}$ mice

Previous results indicated that Tau35$^{Bl/6;129}$ mice show impaired spatial learning in the Morris water maze from 8 months of age (Figure 3.11). Tau35$^{Bl/6}$ mice did not show any deficit in spatial learning at 6 or 8 months of age in the water maze (Figure 5.7a, b) but they did show an impairment on day 4 at 10 and 12 months of age (Figure 5.7c, d, P<0.05). The ability of Tau35$^{Bl/6}$ mice to find the hidden platform deteriorated further at 14 and 16 months of age, when both days 3 and 4 were significantly different from WT$^{Bl/6}$ mice (Figure 5.7e, f).

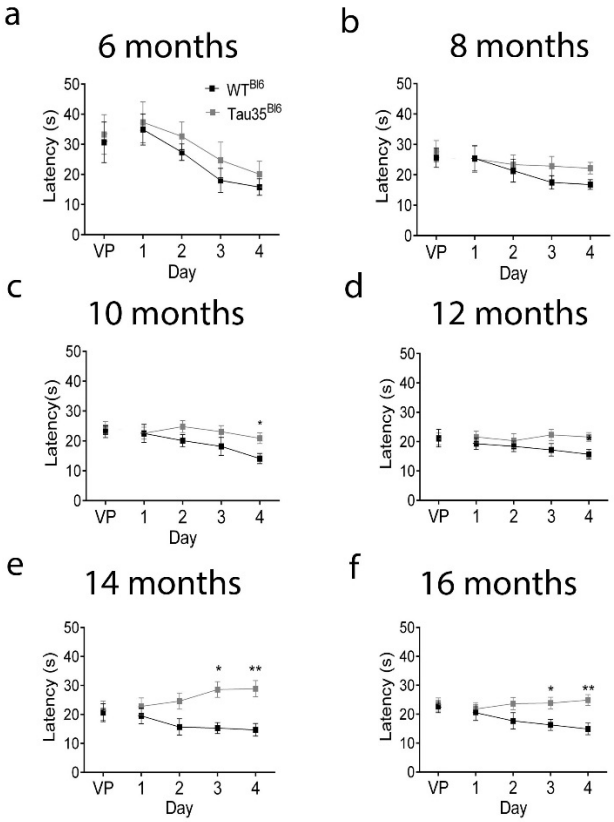

Figure 5.7 Spatial learning in the Morris water maze in Tau35$^{Bl/6}$ and WT$^{Bl/6}$ mice. (a-f) Graphs showing the latency to reach the platform in the Morris water maze for Tau35$^{Bl/6}$ and WT$^{Bl/6}$ mice at 6-16 months of age, during visible platform training (VP) on days 1-4. Values represent mean ± SEM, n=10 per genotype, *P<0.05, **P<0.01, ANOVA.

A comparison of spatial learning in Tau35$^{Bl/6}$ and Tau35$^{Bl/6;129}$ mice showed a difference in the onset of impairment in the two Tau35 mouse strains (Figure 5.8a) compared to their WT counterparts. The Tau35$^{Bl/6}$ mice showed a reduced ability to find the hidden platform from 10 months (Figure 5.7c), whereas this deficit was apparent two months earlier, at 8 months of age, in Tau35$^{Bl/6;129}$ mice (Figure 3.11d).

For visible platform training, only the 6 month time point showed a difference in performance between the background strains (Figure 5.8a). Whereas Tau35$^{Bl/6}$ and WT$^{Bl/6}$ mice showed an escape latency of approximately 30s at this age, both Tau35$^{Bl/6;129}$ and WT$^{Bl/6;129}$ mice performed much better with an escape latency of only 12s (Figure 5.8a). This apparent difference may have been due to the fact that Tau35$^{Bl/6;129}$ and WT$^{Bl/6;129}$ mice had previously been tested in the water maze at the age of 4 months, whereas the 6 months time point represented the first time that the Tau35$^{Bl/6}$ and WT$^{Bl/6}$ mice experienced the water maze. At the ages of 8, 10 and 12 months, visible platform training was similar for all background strains (Figure 5.8b, c and d).

During the hidden platform trials, the pattern of learning at 6 months of age was similar for both Tau35$^{Bl/6}$ and Tau35$^{Bl/6;129}$ mice between days 1 and 4 (Figure 5.8a). The only difference was that both Tau35$^{Bl/6;129}$ and WT$^{Bl/6;129}$ mice had a reduced latency compared Tau35$^{Bl/6}$ and WT$^{Bl/6}$ (Figure 5.8a). At 8 months of age, WT$^{Bl/6;129}$ and WT$^{Bl/6}$ mice performed similarly to each other (Figure 5.8b). Tau35$^{Bl/6;129}$ mice on the other hand performed slightly worse than Tau35$^{Bl/6}$mice (Figure 5.8b). By 10 months of age, WT$^{Bl/6}$ mice performed better in the hidden platform trial compared to WT$^{Bl/6;129}$ mice, with a difference of approximately 5-7s, whereas Tau35$^{Bl/6;129}$ and Tau35$^{Bl/6}$ mice performed at similar latencies at this age (Figure 5.8c). By 12 months of age, the difference between WT$^{Bl/6}$ and WT$^{Bl/6;129}$ mice were similar until days 3 and 4 when WT$^{Bl/6;129}$ mice performed better than WT$^{Bl/6}$ by approximately 5s. Tau35$^{Bl/6}$ mice performed better than Tau35$^{Bl/6;129}$ mice by approximately 7s, indicating that mice were still impaired, but somewhat less so than Tau35$^{Bl/6;129}$ mice tested at the same age (Figure 5.8d).

At the ages of 8, 10 and 12 months, it was apparent that WT$^{Bl/6;129}$ mice were learning faster than WT$^{Bl/6}$ mice during non-visible platform trials on

days 1-4, which was perhaps not surprising as $WT^{Bl/6}$ show to have a reduced escape latency compared to the hybrid mice (Figure 5.8b, c and d).

These results indicate that there is an age-dependent spatial learning impairment in $Tau35^{Bl/6}$ mice, which parallels the previous findings in the $Tau35^{Bl/6;129}$ mice (Chapter 3.2.2.8 Spatial learning and memory is impaired in Tau35 mice). One difference between the two transgenic Tau35 mouse strains is that this impairment commenced 2 months later in the $Tau35^{Bl/6}$ mice and it progressed slightly slower, possibly due to the different background strains of the animals.

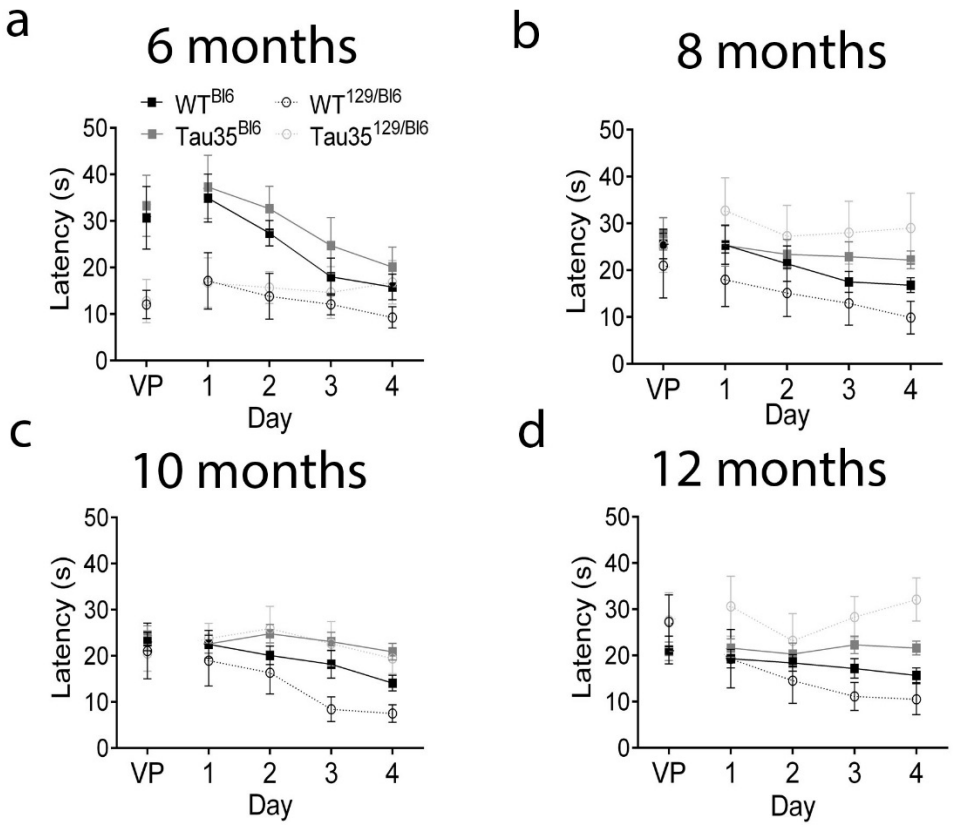

Figure 5.8: Spatial learning in the Morris water maze comparing $Tau35^{Bl/6}$, $WT^{Bl/6}$, $Tau35^{Bl/6;129}$ and $WT^{Bl/6;129}$ mice. (a-f) Graphs showing the time taken for $Tau35^{Bl/6}$, $WT^{Bl/6}$, $Tau35^{Bl/6;129}$ and $WT^{Bl/6;129}$ mice, at 6, 8, 10, and 12, months of age, during visible platform training (VP) and latency to reach the hidden platform in the Morris water maze on days 1-4. Values represent mean and ± SEM, n=8-10 per genotype.

5.2.8 Hippocampal-dependent memory is impaired in Tau35$^{Bl/6}$ mice

A probe trial was performed in the Morris water maze 24h after hidden platform training to assess whether hippocampal-dependent impairment in Tau35$^{Bl/6}$ mice paralleled that noted earlier in Tau35$^{Bl/6;129}$ mice (Chapter 3.2.2.9 Hippocampal dependent memory is impaired in Tau35 mice). Tau35$^{Bl/6}$ mice showed a progressive reduction in hippocampal-dependent memory that commenced at 10 months of age, which was the same time as the age of onset of impaired spatial learning in these animals (Figure 5.9a, $P<0.05$,).

When comparing the performance of the different background strains, at 6 months of age, all groups performed with a similar latency in the target quadrant (Figure 5.9b). At 8 months, Tau35$^{Bl/6}$ and Tau35$^{Bl/6;129}$ mice performed with a similar latency of 14s. On the other hand, the WT$^{Bl/6}$ mice performed on average 6s less well than the WT$^{Bl/6;129}$ mice, indicating that perhaps Tau35$^{Bl/6}$ and Tau35$^{Bl/6;129}$ mice are equally impaired, but because WT$^{Bl/6}$ mice performed less well than WT$^{Bl/6;129}$ mice, the difference appears less marked for the WT$^{Bl/6}$ mice. By 10 and 12 months of age, the latency in the target quadrant for WT$^{Bl/6}$ mice improved and was similar to that of WT$^{Bl/6;129}$ mice. At the 10 and 12 month time points, both Tau35$^{Bl/6}$ and Tau35$^{Bl/6;129}$ mice appeared to be equally impaired in the probe trial (Figure 5.9b).

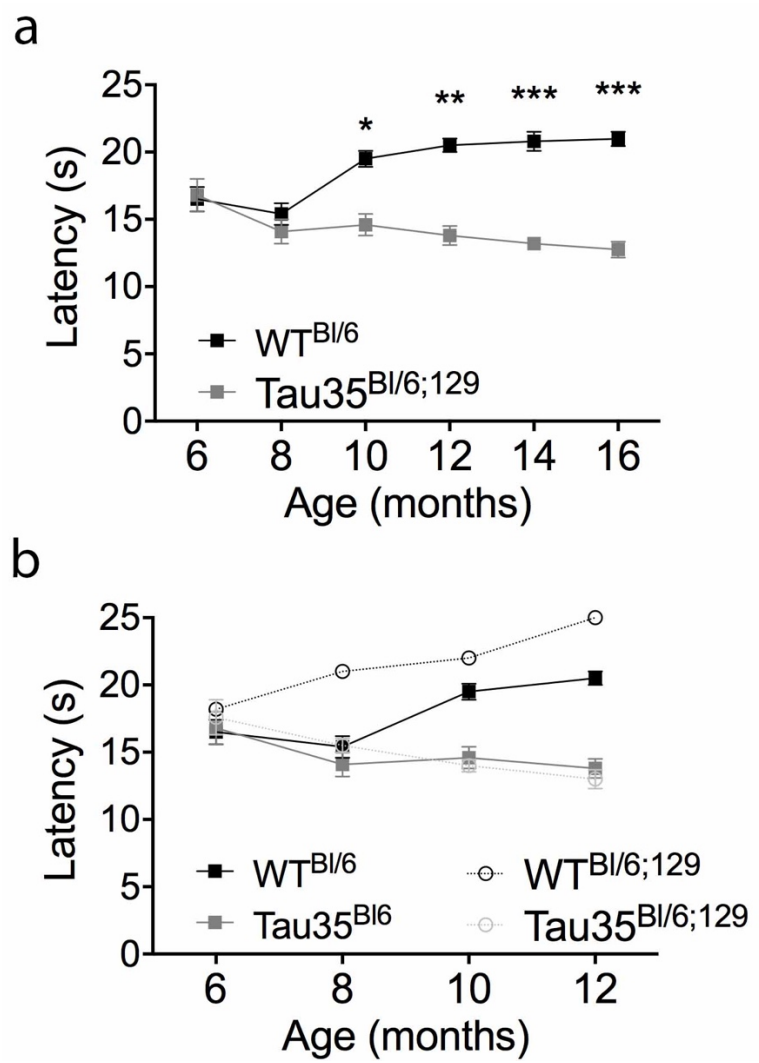

Figure 5.9: Morris water maze probe trial of Tau35$^{Bl/6}$, WT$^{Bl/6}$, Tau35$^{Bl/6;129}$ and WT$^{Bl/6;129}$ mice. (a) Mean latency in target quadrant for Tau35$^{Bl/6}$ and WT$^{Bl/6}$ mice at 6-16 months. **(b)** Comparison of mean latency in target quadrant of Tau35$^{Bl/6}$, WT$^{Bl/6}$, Tau35$^{Bl/6;129}$ and WT$^{Bl/6;129}$ mice aged 6-12 months to illustrate the differences between the genotypes. Values shown are mean ± SEM., n=8-10 for each genotype, *P<0.05, **P<0.01, ***P<0.001, ANOVA.

To validate whether the hippocampal-dependent memory deficit in $Tau35^{Bl/6}$ mice was related to a reduced ability to swim, the total swim distance to the hidden platform and the swim speed of the mice were determined. At the ages of 6 and 8 months, there were no significant differences in the total distances swum to reach the target platform by $Tau35^{Bl/6}$ and $WT^{Bl/6}$ mice (Figure 5.10a). At 10 months of age, $Tau35^{Bl/6}$ mice swum 181cm further than $WT^{Bl/6}$ mice to reach the platform, which correlated with the onset of impaired spatial learning and memory impairment in these animals (Figure 5.10; $P<0.05$). By 12-16 months of age, the distance swum in the probe trial by $Tau35^{Bl/6}$ mice increased by 180-205cm, compared to the $WT^{Bl/6}$ mice (Figure 5.10a). In comparison, the $Tau35^{Bl/6;129}$ mouse data showed a very similar pattern with the exception of 8 months of age, which may be due to the apparent later onset of memory impairment (Figure 5.10a). $Tau35^{Bl/6}$ mice showed no significant difference in their swim speed compared to $WT^{Bl/6}$ mice at any age tested, which is in agreement with the data previously obtained for the $Tau35^{Bl/6;129}$ and $WT^{Bl/6;129}$ mice (Figure 5.10b).

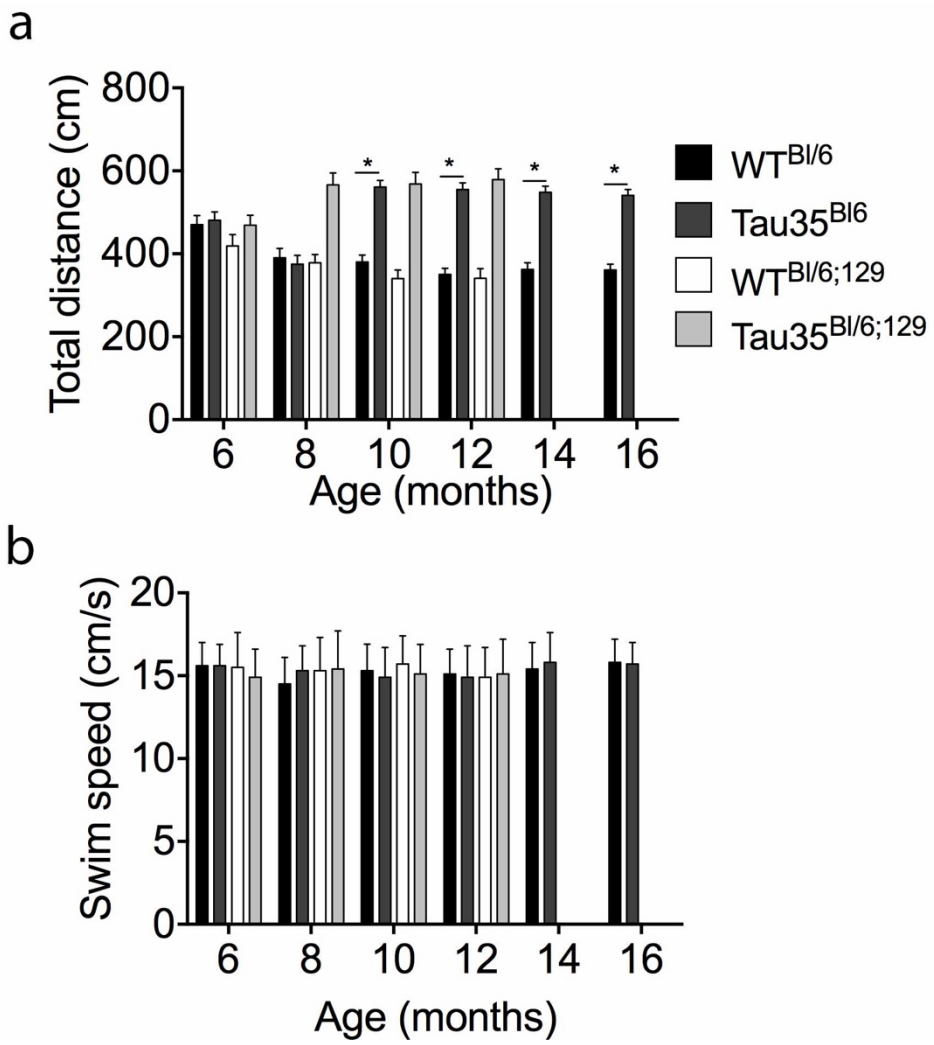

Figure 5.10: Total distance swum and swim speed in the Morris water maze of Tau35$^{Bl/6}$, WT$^{Bl/6}$, Tau35$^{Bl/6;129}$ and WT$^{Bl/6;129}$ mice. (a) Total distance swum at 6-12 or 16 months of age. **(b)** Swim speed at 6-12 or 16 months of age. Values shown are mean ± SEM., n=8-10 mice for each genotype, *P<0.05, ANOVA.

5.3 Summary and Discussion

The main aim of this study was to characterise the behavioural profile of Tau35$^{Bl/6}$ and WT$^{Bl/6}$ mice and to determine how well these changes parallel those previously observed in the hybrid Tau35$^{Bl/6;129}$ and WT$^{Bl/6;129}$ mice.

The main findings of this work are that Tau35$^{Bl/6}$ mice show:

1) Age-related limb clasping, which was apparent 2 months later than observed in Tau35$^{Bl/6;129}$ hybrid mice and in the absence of any overt changes in body weight.
2) Progressive motor and neuromuscular deterioration assessed on the Rotarod, paralleling the previous findings in Tau35$^{Bl/6;129}$ hybrid mice.
3) Progressive impairments in spatial learning and hippocampal-dependent memory cognition assessed in the Morris water maze, commencing 2 months later than in the Tau35$^{Bl/6;129}$ hybrid mice.

5.3.1 Tau35$^{Bl/6}$ mice exhibit similar phenotypic patterns to Tau35$^{Bl/6;129}$ mice.

Previous studies have determined that several mouse lines have variable phenotypic effects caused by differences in the backgrounds used to generate these mice. The result of this can be that animals which contain the same genetic background exhibit different phenotypic outcomes. This demonstrates that genes outside the target area may be involved in the phenotypic traits seen and may be partially responsible for some of the unsuccessful clinical reproducibility when translated to studies in humans (Sigmund, 2000). The most common strategy used to generate transgenic mice, which was also used to generate Tau35 $^{Bl/6;129}$ hybrid mice, is to create mice using 129-derived ES cells (ES cell lines derived from different 129 backgrounds) which are a very reliable and robust cell type for gene manipulation. However, mice generated from these lines often exhibit poor reproductively (Wahlsten, 1992). Therefore, genetically manipulated mice are commonly backcrossed to the well characterised BL/6 inbred mouse strain. Backcrossing in this way reduces the influence of the 129-derived genome whilst still endowing the knocking/knockout strain with the benefits of the C57BL/6 background. Nevertheless, previous studies have shown that however close to the target gene, the genetic background will always reflect the original ES strain rather than that of the recipient strain (Hospital, 2001). The most common procedure to obtain a pure genetic background is to backcross over several generations to C57BL/6 mice to generate a 99%+ C57BL/6 background and to facilitate phenotypic analysis and increase fertility. Therefore, Tau35$^{BL/6;129}$ mice were crossed over nine generations to generate Tau35$^{Bl/6}$ mice with an 99.90% identical genetic background. It was then investigated whether inbred Tau35$^{Bl/6}$ congenic mice exhibited difference in phenotypic patterns compared to Tau35$^{Bl/6;129}$ hybrid mice. Neither Tau35$^{Bl/6;129}$ hybrid or Tau35$^{Bl/6}$ congenic mice showed a significant difference in body mass compared to WT mice.

Several strains of 129 mice have shown differences in phenotypic traits, such as grooming, activity, habituation in the open field and anxiety, compared to C57BL/6 mice (Crawley et al., 1997; Bolivar, 2000, 2001; Bothe et al., 2004;

Kalueff and Tuohimaa, 2004; Ducottet and Belzung, 2005). Interestingly, however, the Tau35$^{BL/6}$ mice aged 8 months did not show any differences in habituation in the open field or activity, indicating no overt abnormalities, equivalent to the hybrid Tau35$^{Bl/6;129}$ mice.

Tau35$^{Bl/6}$ mice showed a similar clasping phenotype to Tau35$^{Bl/6;129}$ hybrid mice. However, in the Tau35$^{Bl/6}$ mice, clasping was apparent from 4 months of age which was 2 months after Tau35$^{Bl/6;129}$ first showed signs of clasping. This may be due to the fact that the number of animals included was lower for the Tau35$^{Bl/6}$ mice (n=10) as opposed to the Tau35$^{Bl/6;129}$ mice (n=40), which may have reduced the test sensitivity due to variable ages of onset of limb clasping in different mice. This difference could also be due to the change in mouse background causing a later onset of limb clasping. Questions have been raised previously regarding subtle behavioural and phenotypic deficits between different mouse lines, particularly in identifying whether changes are due to the target gene itself or due to the closely linked genes from the surrounding 129 background (Zhou et al., 2001). In future, to avoid such issues it may be more efficient to directly target genes in C57BL/6-derived ES cells and then to maintain these mice on the same genetic background (Seong et al., 2004).

5.3.2 Tau35$^{Bl/6}$ mice exhibit motor deficits that parallel those seen in Tau35$^{Bl/6;129}$ hybrid mice

As Tau35$^{Bl/6;129}$ hybrid mice showed an early motor deficit, it was essential to establish whether Tau35$^{BL/6}$ mice showed similar results. Tarantino (2000) and colleagues showed that C57BL/6 mice did not perform as well on the Rotarod compared to 129 lines (Tarantino et al., 2000), whereas McFadyen (2003) and colleagues showed that C57BL/6 mice perform significantly better on the Rotarod compared to 129 lines (McFadyen et al., 2003). In the present study, Tau35$^{BL/6}$ mice performed similarly to Tau35$^{BL/6;129}$ hybrid mice with

the hybrid mice performing only slightly worse at earlier ages, potentially indicating minimal differences between the two different backgrounds.

Previous findings have found that body size and weight of mice can influence Rotarod performance (Cook et al., 2002). Tau35$^{Bl/6;129}$ and WT$^{Bl/6;129}$ hybrid mice were slightly heavier than Tau35$^{Bl/6}$ and WT$^{Bl/6}$ mice, although these differences were not statistically significant. However, different mouse strains with similar body masses perform differently on the Rotarod and therefore this excludes the fact that this slightly difference in weight may have potentially influenced Rotarod performance of the Tau35$^{Bl/6;129}$ mice (McFadyen et al., 2003).

5.3.3 Learning and memory deficits are similar in Tau35$^{Bl/6}$ and Tau35$^{Bl/6;129}$ hybrid mice

As memory and learning difficulties are a major clinical component of tauopathies, it was important to establish whether the major behavioural deficits previously observed in Tau35$^{Bl/6;129}$ hybrid mice were also apparent in the backcrossed Tau35$^{Bl/6}$ mice, rather than being due to background strain differences. Several 129 mouse sub-strains exhibit behavioural deficits that differ from C57BL/6 mouse behaviour, including differences in learning, contextual fear conditioning and memory ability (Crawley et al., 1997; Bothe et al., 2004). Therefore, it was important to determine if the memory deficits seen in hybrid Tau35$^{Bl/6;129}$ were maintained after backcrossing, and to determine whether these were potentially due to the strain background or to expression of the Tau35 fragment. Interestingly, both Tau35$^{Bl/6;129}$ hybrid and Tau35$^{Bl/6}$ mice showed very similar learning and memory deficits. The only difference was that Tau35$^{Bl/6}$ had a slightly later onset of memory impairment, which was largely due to the poorer performance of WT$^{Bl/6}$ mice compared to WT$^{Bl/6;129}$ hybrid mice. Previous reports have indicated conflicting data regarding the memory abilities of 129 and C57BL/6 mice. Whereas some studies have shown that 129 mice exhibit cognitive impairment (Gerlai, 1996), others have shown that this performance is related to the particular mouse sub-strain being tested (Montkowski et al., 1997; Owen et al., 1997). However, previous findings

showed that C57BL/6 mice exhibited poorer performance compared to 129 mice in the Morris water maze (Rogers et al., 1999; Võikar et al., 2001). This was also the case in the present study in which $WT^{Bl/6}$ mice performed less well overall than hybrid $WT^{BL/6;129}$ mice in the Morris water maze. Moreover, learning and memory in the Morris water maze has previously been shown to be impaired by stress (Hölscher, 1999). Reports have shown that C57Bl/6 mice exhibit less anxiety behaviour than does the 129 mouse strain (Homanics et al., 1999; Rogers et al., 1999). Although none of the mice in this experiment showed signs of stress, this is a paradigm that could be investigated more comprehensively by testing potential hyperlocomotion in the open field setup.

5.3.4 Conclusion

In summary, the findings presented here suggest that $Tau35^{Bl/6}$ mice with some further studies could potentially be an improved mouse model of tauopathy due to reduced variation in genetic background, whilst still exhibiting behavioural deficits. However, for a full conclusion to be made, further investigations into the biochemistry and pathological deficits in these mice remain to be undertaken. Taken together, it has been fundamental and important to show that the experimental differences observed in the hybrid $Tau35^{Bl/6;129}$ mice were also apparent in the backcrossed $Tau35^{Bl/6}$ mice. With further investigation of these mice, this may lead to a more robust model with less inter-animal variation and may make it possible in future experiments to obtain reproducible data with reduced sample sizes. For instance, it would simplify breeding of the $Tau35^{Bl/6}$ mice to other relevant AD models such as APP or htau mice on BL/6 backgrounds in order to evaluate the effect of tau truncation in these models.

CHAPTER 6

Expression of Tau35 in a cell line to investigate the effects of potentially therapeutic compounds on tau phosphorylation

6.1 Introduction

Tau, in particular its state of phosphorylation is increasingly becoming of interest as a therapeutic target due to its pathological significance to disease status. Prevention or reduction of tau phosphorylation would make an ideal therapeutic target for neurodegenerative diseases. Therefore, it is important to develop new high throughput cell based assays to test novel and existing compounds, reducing cost and time associated with *in vivo* studies. A novel cell based assay was designed, using Tau35 stably expressed in Chinese hamster ovary (CHO) cells, in conjunction with phosphorylation dependent antibodies using the method described in 2.3.7 In-cell western. The basis of this assay was an in-cell western (ICW) technique (Li-Cor Biosciences), which has been reported previously for therapeutic screening and evaluation assays (Hoffman et al., 2010). The principle of this assay was to seed CHO cells stably expressing Tau35 (CHO-Tau35 cells) onto a 96-well plate, fix the cells followed by permeabilisation and then label them with appropriate antibodies. Finally, they were visualised *in situ* using near infra-red fluorescent secondary antibodies.

6.2 Results

6.2.1 In-cell western set up using a Chinese hamster ovary Tau35 cell line

This study used a CHO cell line, stably transfected with a plasmid expressing Tau35, but with a V5 tag fused to the C-terminus of tau in place of the HA tag expressed in Tau35 mice. The CHO cell line was previously generated in this laboratory (CHO-Tau35 cells, generated by Tong Guo, manuscript in preparation) and Tau35 expressed in these cells has been shown to be highly phosphorylated (Guo et al., manuscript in preparation). Initial experiments involved plating the cells at a density of either 10,000 (D1) or 20,000 (D2) cells per well of a 96-well plate to determine the optimum density for ICW assays. Cells were then exposed to either a monoclonal antibody recognising total tau (Tau5) and a polyclonal phosphorylation-dependent tau antibody (recognising either pSer396 or pSer422 in tau), or a polyclonal antibody to total tau (Dako) and a monoclonal phosphorylation-dependent tau antibody (Tau-1 or AT180), to establish the most sensitive pair of antibodies with which to assess tau phosphorylation changes in the CHO-Tau35 cells. Cells in parallel wells were labelled with an antibody to β-actin and total tau to establish relative levels of total tau expression under each condition tested. A density of 10,000 cells (D1) was used over 20,000 cells (D2) as this number was sufficient to generate a good readout without overt saturation (Figure 6.1). The results showed that cells probed with the phosphorylation-dependent tau antibody recognising Ser396 (Ser396), together with Tau5 (recognising total tau) exhibited the highest specificity. Blanks wells lacking primary antibodies were used to test for any abnormal signals subtracted from results in analysis. Therefore, 10,000 cell per well, and the combination of Ser396 and Tau5 antibodies were used for all future experiments (Figure 6.1d).

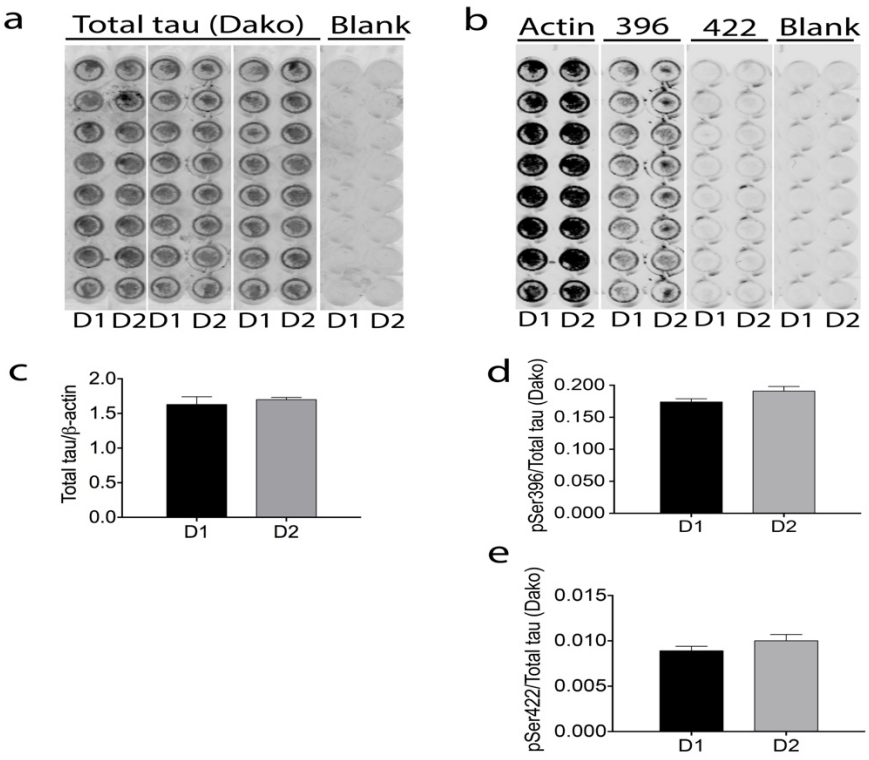

Figure 6.1: In Cell Western optimisation assay showing tau phosphorylation at serine pSer396 and pSer422 compared to total tau in transfected CHO-Tau35 cells at two different cell densities. (a-b) CHO-Tau35 cells at two different densities (D1: 10,000 cells per well or D2: 20,000 cells per well) probed with monoclonal antibodies against phosphorylated tau pSer396 and pSer422, polyclonal total tau (Dako), β-actin and blanks. **(c-e)** Graphs showing analysis of phosphorylation tau antibodies relative total tau, and total tau relative to β-actin. Values represent mean and ± SEM, n=8.

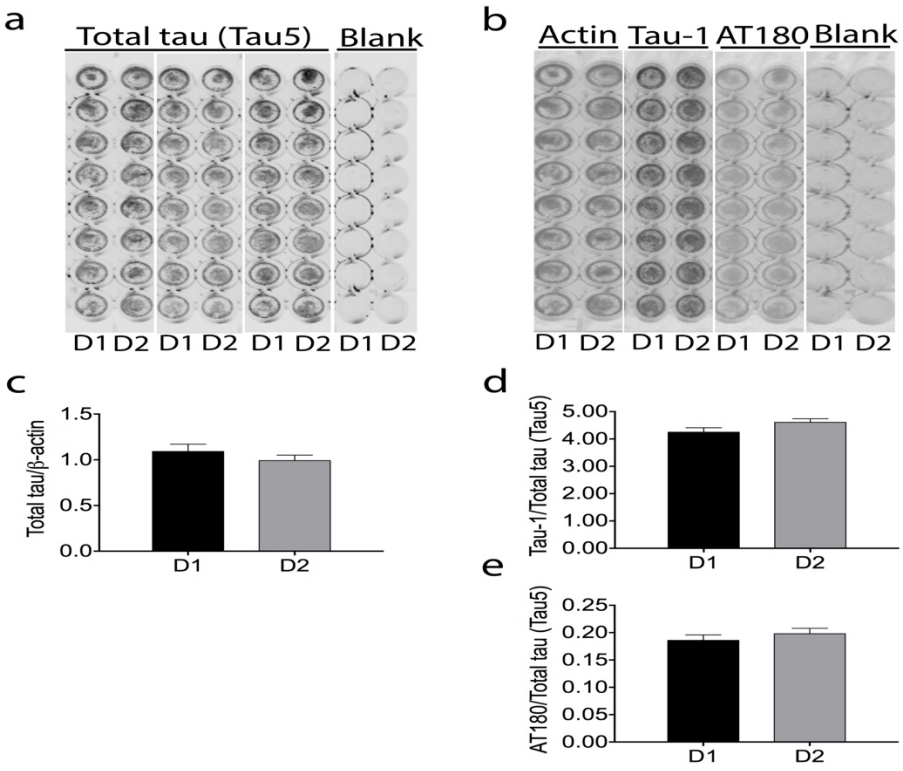

Figure 6.2: In Cell Western optimisation assay showing tau phosphorylation at serine pSer396 and pSer422 compared to total tau in transfected CHO-Tau35 cells at two different cell densities. (a-b) CHO-Tau35 cells at two different densities (D1: 10,000 cells per well or D2: 20,000 cells per well) probed with polyclonal antibodies against phosphorylated at Tau-1 and AT180, monoclonal total tau (Tau5), β-actin and blanks. **(c-e)** Graphs showing analysis of phosphorylation tau antibodies relative total tau, and total tau relative to β-actin. Values represent mean and ± SEM, n=8.

6.2.2 Lithium chloride and okadaic acid modulate tau phosphorylation in CHO-Tau35 cells

Once the most suitable combination of tau antibodies had been established, it was essential to determine the effects of LiCl and okadaic acid as positive and negative controls, respectively, for inhibition and induction of tau phosphorylation. LiCl (10μM, 4h) inhibits GSK3 activity and thereby reduces tau phosphorylation, whereas okadaic acid (100nM, 4h) inhibits protein phosphatase 2A and hence increases tau phosphorylation. CHO-Tau35 cells were incubated with these control compounds, and with the test compounds for 4h. The cells were then fixed and the ICW assay was used to determine the extent of tau phosphorylation in CHO-Tau35 cells. The results showed that, as expected, LiCl treatment reduced tau phosphorylation by 16% (Figure 6.3a, $P<0.01$) and okadaic acid increased tau phosphorylation by 16%, relative to total tau, in CHO-Tau35 cells (Figure 6.3a, $P<0.001$). Under these conditions, the total amount of tau was unchanged in both treatment groups (Figure 6.3b), indicating that LiCl and Ocadaic acid had no significant effect on overall total tau levels.

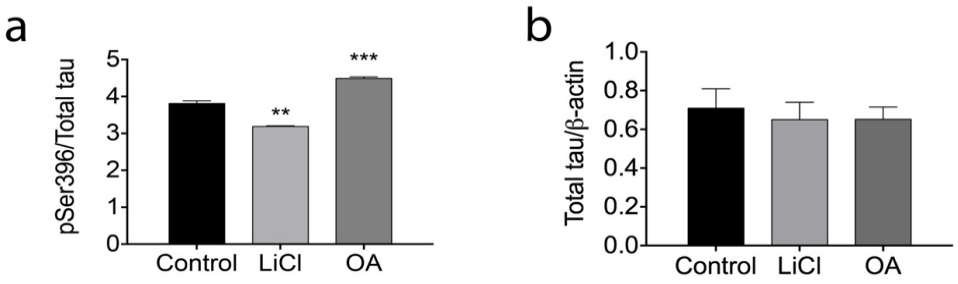

Figure 6.3: Tau phosphorylation in CHO-Tau35 cells is modulated by LiCl and okadaic acid without affecting total tau. CHO-Tau35 cells untreated, treated with LiCl (10mM) or okadaic acid (OA, 100mM) for 4h. **(a)** Graph show decrease phosphorylation at pSer396 with LiCl and increase with OA normalised to total tau (Tau5) **(b)**, Graph showing total tau levels normalised to β actin. Values are displayed as mean ± SEM; n = 8, **P<0.01, ***P<0.001.

6.2.3 CHO-Tau35 show reduced phosphorylation upon treatment with PBA

To evaluate the effect of PBA on tau phosphorylation, CHO-Tau35 cells were incubated with 10μM PBA or 10μM LiCl for 4 h and cells were analysed by ICW using ser396 and total tau (Tau5) antibodies. Two independent experiments were performed, with 8 replicate wells included in each experiment. The results indicated that, under these conditions, PBA reduced tau phosphorylation by approximately 36% and a reduction of 22% with LiCl (positive control) treatment (Figure 6.4a) without affecting the expression of total tau relative to β-actin (Figure 6.4b). These results show that PBA was able to rescue tau phosphorylation *in vitro*, paralleling the results previously obtained with PBA with respect to tau phosphorylation in Tau35 mice (CHAPTER 4).

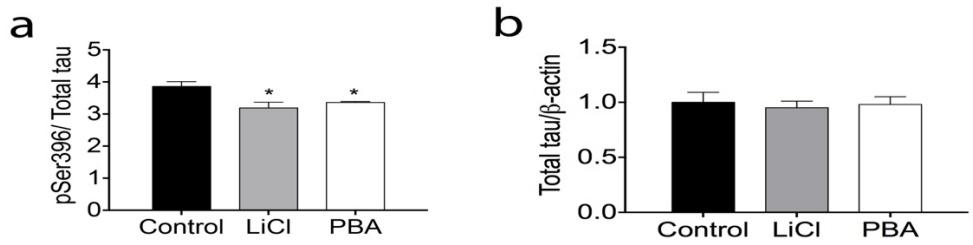

Figure 6.4: Tau phosphorylation in CHO-Tau35 cells is reduced by LiCl and phenylbutyrate without affecting total tau. CHO-Tau35 cells untreated, treated with LiCl (10mM) or phenylbutyrate (PBA, 10μM) for 4h. **(a)** Graph show decrease phosphorylation at pSer396 with LiCl and decrease with PBA normalised to total tau (Tau5) **(b)**, Graph showing total tau levels normalised to β actin. Values are displayed as mean ± SEM; n = 8, *P<0.05.

6.2.4 Tau phosphorylation in CHO-Tau35 cells is successfully reduced upon treatment with several pre-existing therapeutic compounds

To evaluate the effect of a range of different candidate compounds on tau phosphorylation, CHO-Tau35 cells were incubated for 4h with 10μM of compounds C1-C70, C72-C84, PBA (83 compounds in total) together with 10μM of LiCl (positive control). Each compound, was tested in a minimum of two independent experiments. Compounds that inhibited tau phosphorylation by 15% or more, compared to the control (0.1% DMSO) were tested in additional experiments (up to 4 times). The results indicated that 40 compounds (C39, C40, C42-C51, C53-C70, C72-C77, C81, C83 and PBA), were able to significantly reduce tau phosphorylation at Ser396 in CHO-Tau35 cells with above medium effect size (Table 10, red, P<0.001, d>0.8) and were deemed a successful 'hit'. Out of the 40 compounds that were deemed a successful 'hit' the majority did not significantly affect the total amount of tau, relative to β-actin. Most compounds increased total tau slightly (blue) and

several compounds reduced tau very slightly including C40, C60 and PBA (Table 11, green). Compound C73, C74, C62, C47 did significantly increase total tau (Table 11, $P<0.05$) indicating a potential detrimental effect to tau. Taken together these results show that several compounds including PBA were able to significantly rescue tau phosphorylation *in vitro* with a high effect size. These results also demonstrate the effective generation of a new cell based tau phosphorylation assay which can be used for future therapeutic targets.

Table 10: Table showing compound summary effect on tau phosphorylation after 4h treatment at 10μM concentration for all compounds tested in ICW. Compounds are ranked in order of increasing tau phosphorylation, relative to total tau (percentage of control). Red data: compounds which showed =or <85% of mean from control and therefore deemed a 'hit", NS: not significant, ND: no data.

Compound	Mean % control	SEM	n	P Value	Effect size (r)	Compound	Mean % control	SEM	n	Effect size (r)	P Value
Control	100	0.00	6	ND	ND	C38	87	5.64	3	3.82	0.000
LiCl	78	3.20	3	0.003	1.80	C80	87	4.18	2	ND	NS
C76	71	2.10	3	0.000	6.49	C35	88	8.71	2	2.87	0.002
C73	72	1.35	3	0.000	5.89	C12	89	ND	1	1.37	NS
C55	73	1.54	3	0.000	3.53	C13	90	ND	1	1.22	NS
C66	73	0.66	2	0.000	5.86	C29	90	ND	1	1.16	NS
C78	73	4.40	3	0.000	5.75	C31	91	ND	1	1.54	NS
C74	74	0.69	3	0.002	4.28	C34	91	ND	1	1.97	NS
C77	75	5.96	3	0.001	4.51	C84	91	ND	1	ND	NS
C64	76	3.23	2	0.000	5.95	C32	91	ND	1	ND	NS
C56	77	1.76	3	0.000	3.67	C9	91	ND	1	ND	NS
C75	77	1.28	2	0.000	6.72	C5	91	1.23	2	ND	NS
C59	77	5.22	2	0.000	4.73	C33	92	ND	1	1.42	NS
PBA	77	13.00	2	0.000	1.92	C10	92	ND	1	ND	NS
C48	77	0.61	2	0.000	3.73	C16	92	ND	1	ND	NS
C45	77	4.55	3	0.033	3.04	C36	92	4.14	2	1.85	0.013
C67	78	6.35	3	0.000	2.64	C6	92	1.40	2	ND	NS
C68	78	5.29	3	0.000	3.37	C30	93	ND	1	1.29	NS
C60	79	4.85	3	0.000	2.01	C14	94	ND	1	ND	NS
C61	79	7.32	3	0.000	2.65	C8	94	ND	1	D	NS
C62	79	6.56	3	0.000	2.51	C37	95	10.38	3	3.38	0.000
C49	80	1.24	2	0.000	2.67	C41	96	12.88	3	1.79	0.011
C72	80	2.44	2	0.001	2.66	C2	96	2.95	2	ND	NS
C44	80	2.01	3	0.000	3.68	C52	96	ND	1	ND	NS
C70	80	6.38	2	0.000	2.38	C3	98	8.59	2	1.26	0.021
C57	81	5.02	3	0.00	2.91	C4	98	10.98	2	ND	NS
C53	81	1.02	2	0.000	3.71	C20	99	ND	1	ND	NS
C63	81	6.18	3	0.000	2.74	C11	99	ND	1	ND	NS
C47	82	0.23	2	0.000	3.04	C7	101	4.83	2	ND	NS
C42	82	2.09	3	0.000	3.49	C17	101	ND	1	ND	NS
C81	82	5.29	4	0.000	5.36	C28	102	ND	1	ND	NS
C50	82	2.99	2	0.000	4.09	C1	102	3.37	2	ND	NS
C46	82	0.66	2	0.000	3.34	C21	102	ND	1	ND	NS
C51	83	3.68	2	0.000	4.15	C19	104	ND	1	ND	NS
C58	83	3.22	3	0.000	2.94	C22	105	ND	1	ND	NS
C43	83	4.85	3	0.000	3.27	C18	105	ND	1	ND	NS
C83	83	4.45	3	0.035	2.50	C15	106	ND	1	ND	NS
C54	84	9.50	3	0.001	1.18	C82	107	ND	1	ND	NS
C65	84	3.98	3	0.000	3.04	C23	110	ND	1	ND	NS
C69	85	4.43	3	0.001	0.67	C26	113	ND	1	-1.72	NS
C40	85	1.39	2	0.009	2.15	C24	114	ND	1	ND	NS
C39	85	1.76	3	0.000	3.11	C27	115	ND	1	-1.78	NS
C79	86	10.60	3	0.000	4.70	C25	116	ND	1	-1.70	NS

Table 11: Table showing compound summary effect on total tau relative to β-actin after 4h treatment at 10μM concentration for all compounds tested in ICW. Blue data: indicates "hit" compounds with increased total tau levels, Green data: indicates "hit" compounds with decreased total tau levels, NS: not significant, ND: no data.

Compound	Mean (% control)	SEM	N	P Value	Compound	Mean (% control)	SEM	n	P Value
Control	100	0	6	ND	C38	98	17	3	NS
LiCl	91	2	3	NS	C80	108	14	2	NS
C76	136	27	3	NS	C35	121	23	2	NS
C73	156	33	3	0.016	C12	51	ND	1	0.04
C55	107	7	3	NS	C13	112	ND	1	NS
C66	107	11	2	NS	C29	50	ND	1	0.039
C78	125	18	3	NS	C31	128	ND	1	NS
C74	144	24	3	0.032	C34	140	ND	1	0.016
C77	117	17	3	NS	C84	197	ND	1	0.012
C64	109	10	2	NS	C32	102	ND	1	NS
C56	117	32	3	NS	C9	45	ND	1	NS
C75	123	24	2	NS	C5	105	31	2	NS
C59	126	1	2	NS	C33	159	ND	1	NS
PBA	96	1	2	NS	C10	43	ND	1	0.001
C48	100	16	2	NS	C16	67	ND	1	0.037
C45	131	39	3	NS	C36	189	98	2	0.014
C67	113	16	3	NS	C6	102	21	2	NS
C68	129	17	3	NS	C30	60	ND	1	0.044
C60	87	13	3	NS	C14	67	ND	1	0.048
C61	121	18	3	NS	C8	53	ND	1	0.032
C62	142	13	3	0.034	C37	138	34	3	0.020
C49	127	43	2	NS	C41	135	31	3	NS
C72	113	7	2	NS	C2	96	35	2	NS
C44	133	36	3	NS	C52	75	ND	1	NS
C70	121	21	2	NS	C3	113	7	2	NS
C57	102	12	3	NS	C4	92	18	2	NS
C53	113	14	2	NS	C20	59	ND	1	0.024
C63	127	21	3	NS	C11	67	ND	1	0.01
C47	161	50	2	0.032	C7	105	28	2	NS
C42	108	20	3	NS	C17	62	ND	1	NS
C81	124	10	4	NS	C28	56	ND	1	0.026
C50	112	27	2	NS	C1	89	29	2	0.002
C46	107	19	2	NS	C21	63	ND	1	0.015
C51	107	24	2	NS	C19	58	ND	1	NS
C58	120	26	3	NS	C22	61	ND	1	0.018
C43	132	44	3	NS	C18	52	ND	1	0.014
C83	107	27	3	NS	C15	60	ND	1	0.015
C54	105	24	3	NS	C82	128	ND	1	NS
C65	134	25	3	NS	C23	51	ND	1	0.015
C69	105	7	3	NS	C26	67	ND	1	0.023
C40	93	15	2	NS	C24	59	ND	1	0.033
C39	118	25	3	NS	C27	56	ND	1	NS
C79	127	24	3	NS	C25	87	ND	1	NS

6.3 Summary and Discussion

The purpose of this study was to establish a novel cell based assay using a Tau35 CHO cell line.

The main findings of this chapter are:

1) Antibody for phosphorylated tau (pSer396) was an ideal candidate to establish increase and decrease of compounds upon tau phosphorylation.
2) Okadaic acid and lithium chloride increased and reduced tau phosphorylation, respectively, in CHO-Tau35 cells and these compounds were therefore ideal controls.
3) Phenylbutyrate reduced tau phosphorylation in the cell line which paralleled the changes observed in Tau35 mice.
4) Of the 83 candidate compounds tested, 39 compounds reduced tau phosphorylation in the CHO-Tau35 cell based assay.

6.3.1 Tau35 transfected CHO cells: A novel drug screening tool to test therapeutic compounds ability to reduce tau phosphorylation

Phosphorylation of tau at the Ser396 in the carboxy-terminal region of tau is an early event in AD, occurring prior to the appearance of fibrillary structures, and is therefore a potential early indicator of disease progression (Mondragón-Rodríguez et al., 2014). The ICW experiments showed that known modulators of tau phosphorylation, LiCl and okadaic acid, are capable of decreasing and increasing tau phosphorylation, respectively (Hong et al., 1997; Tanaka et al., 1998). This indicates that CHO-Tau35 cells together with antibodies recognising total and phosphorylated (pSer396) tau provide a suitable cell-based assay for testing the potential of compounds to modulate tau phosphorylation.

The results from ICW analysis of CHO-Tau35 cells, revealed that PBA was able to rescue Ser396 phosphorylation of tau. PBA has not previously been shown to reduce tau phosphorylation at Ser396 in cells, making this the first account of these findings. However, further studies of phosphorylated tau in hippocampal regions of Tau35 mice are required in order to determine whether phosphorylation at this site is also reduced in Tau35 mice treated with PBA. Furthermore 40 already commercially available compounds were able to successfully reduce tau phosphorylation at Ser396. However, some compounds did also have an effect on total tau and therefore further investigation into how these compounds interact with tau is necessary. Nevertheless, the data obtained in this study indicate that this is a robust and reproducible assay in which to test new therapeutic compounds and to determine the effects on tau phosphorylation.

6.3.2 Conclusions

Within this chapter it was clear that a new CHO-Tau35 cell based assay was established in which to test potential therapeutic targets and the effect these have on tau phosphorylation. PBA together with 39 other compounds were able to robustly and consistently reduce tau phosphorylation at Ser396. This novel cell-based assay together with other established tau and Aβ assays provides an excellent resource for early therapeutic screening. However, these findings are still very preliminary and further research is needed to validate and further establish this assay as well as establish other key phosphorylation antibodies which could be used as part of the assay.

CHAPTER 7

Discussion

The main aims of the studies reported in thesis were as follows:

1) To investigate the behavioural, biochemical and pathological changes in a novel mouse model of the human brain-derived, 35 kDa tau fragment (Tau35), which is expressed in the absence of any mutation and under the control of the human tau promoter.
2) To test a potential therapeutic intervention in Tau35 mice in order to alleviate the observed neuropathological and behavioural changes.
3) To investigate whether the phenotypic and behavioural changes are preserved when Tau35 hybrid mice are backcrossed onto a pure C57BL/6 background.
4) To establish a new cell based assay to test therapeutic targets for tauopathies using a CHO cell line stably expressing Tau35.

In summary, the primary findings of this thesis are:

N-terminal truncation of tau induces progressive phenotypic abnormalities and reduced lifespan, progressive motor and cognitive deficits in Tau35 mice. The results presented here support the hypothesis that the Tau35 truncated tau fragment can induce abnormal tau phosphorylation/aggregation and progressive motor and cognitive dysfunction, features which have previously been reported in tauopathies. Tau35 is associated with increased accumulation of tau pathology in the hippocampus and associated cortex as well as increased ubiquitin and synuclein pathology in the hippocampus. Moreover, these findings suggest the involvement of several pathways that result from tau truncation in 4R tauopathies. In particular, N-terminal tau truncation causes abnormally phosphorylated tau, progressive cognitive and motor deficits, kyphosis,

clasping, autophagic/lysosomal dysfunction, kinase dysfunction, loss of synaptic protein, and reduced life-span in Tau35 mice. Tau35 expression is also associated with reduced synapsin1 and synaptotagmin, increased GSK3β activity reduced cathepsin D, increased p62 and LC3 protein levels and reduced acetylated tubulin. This is the first report of low expression of WT human truncated tau expressed in mice to elicit such disease-relevant pathophysiological and behavioural changes.

Treatment of Tau35 mice with phenylbutyrate ameliorates neuromuscular and cognitive deficits, tau phosphorylation, autophagic deficits and synaptic deficits.

Importantly, several of the phenotypic changes in Tau35 mice were alleviated upon treatment with PBA (Buphenyl®), possibly through chromatin remodelling or HDAC inhibition. PBA is used to treat urea cycle disorders and is currently in clinical trials for a range of neurodegenerative diseases (Qi, 2004; Gardian et al., 2005; Leng and Chuang, 2006; Ying et al., 2006; Sadri-Vakili et al., 2007; Chuang et al., 2009). PBA rescued grip strength and spatial learning and hippocampal dependent memory deficits as tested in the Morris water maze. Treatment with PBA also reduced tau phosphorylation and p62, and restored acetylated tubulin, cathepsin D and synpasin-1 in Tau35 mice.

Backcrossing Tau35 mice onto a C57BL/6 background retained the phenotypic and behavioral abnormalities.

The phenotypic and behavioural differences observed in the hybrid Tau35 mice were conserved in mice backcrossed to generate a 99.9% C57BL/6 background. Tau35$^{Bl/6}$ mice maintained the abnormal patterns of clasping, motor deficits (grip strength and Rotarod) and cognitive deficits (Morris water maze). This finding eliminates the possibility of the phenotypic abnormalities in hybrid Tau35 mice being attributed to a specific genetic background.

CHO-Tau35 cells exhibit increased tau phosphorylation and can be used to test potential therapeutic compounds.

CHO-Tau35 cells showed increased tau phosphorylation at Ser396, which could be modulated by LiCl and OA. A CHO-Tau35 ICW cell-based assay was successfully established, which allowed potential therapeutic compounds to be tested and their ability to reduce tau phosphorylation at Ser396 evaluated in a high-throughput format.

Together, these findings suggest that N-terminal tau truncation is an important event in tauopathies that leads to extensive behavioural deficits and the accumulation of hyperphosphorylated, conformational and aggregated species of tau that can be targeted therapeutically.

7.0 $Tau35^{Bl/6;129}/Tau35^{Bl/6}$ mice: a new improved mouse model of human tauopathy

This thesis has evaluated a novel mouse model of human tauopathy, which expresses human WT tau at low physiological levels comprising only <10% of that of endogenously expressed total mouse tau. The major limitations with regard to existing tau transgenic mouse models have been (1) the generation of mice by random insertion of the transgene into the genome and therefore potential unwanted effects due to the insertion site, and (b) overexpression of tau in order to elicit a phenotype and acceleration of tauopathy within the relatively short lifetime of a mouse.

Several previous models have used various different promoters, examples including the prion promoter (PrP) which drives expression widely in the nervous system (Hsiao et al., 1996), the PDGF promoter which promotes high expression in the central nervous system and drives strong expression of exogenous transgenes in neurons (Games et al., 1995) and Thy promoters (Thy-1, Thy1.2) and inducible CaMKII promoters, which have been used for full-length tau expression (Götz et al., 1995). However, these promoters are typically not the promoters of the native gene but have been selected because

of their strong gene expression. Such heterologous promoters often lead to higher expression of the transgene with pathology in regions often unrelated to disease pathogenesis, than would be observed physiologically. Furthermore, the transgene is usually expressed on top of the endogenous mouse gene, leading to further overexpression (Elder et al., 2010). Tau35 mice employ the human tau promoter, the same as used previously in some other tau transgenic mice (Dawson et al., 2007). Using this promoter, Dawson and colleagues (Dawson et al., 2007) showed low expression of mutant forms of tau, including the T-279 mouse expressing the N279K and mice expressing the V337M mutation, which contributes to progressive neurodegeneration in FTLD-tau. In these mice multiple copies of the transgene result in <10% endogenous mouse tau protein (Tanemura et al., 2001; Dawson et al., 2007). In contrast, mice expressing wild-type human tau at 10% more than endogenous mouse tau (Tau264 mice) do not develop tau pathology (Umeda et al., 2013). However, in both these models, tau is expressed as a mutant protein and since such mutations occur only very infrequently in human tauopathy, these models do not represent the most common forms of tauopathies, which are indeed sporadic. Furthermore, the homologous natural rat tau promoter has also been used to express human tau cDNA with two FTLD-tau-associated mutations, K257T/P301S, in which expression was 5-10% of endogenous mouse tau and P301S (expressing the P301S mutant form of human MAPT). (Rosenmann et al., 2008). More recently, Sydow and colleagues showed that hTau40^{AT} mice, which express full-length human tau carrying the mutation A152T at low physiological levels, under the control of the murine GFAP promoter for glial expression, exhibit cognitive impairment and neuroinflammation (Sydow et al., 2016). These *in vivo* models highlight the importance of using relevant tau promoters to express pathophysiologically-relevant amounts of tau.

To date no other mice expressing low level WT human tau have been reported. As Tau35 mice express a truncated species of WT human tau they therefore represent a novel and highly relevant animal model of sporadic tauopathy. Furthermore, Tau 35 accurately represents the spectrum of sporadic human tauopathies in the absence of significantly increased tau expression or the presence of any tau mutation.

7.1 Human N-terminal truncated tau induces 4R tauopathy relevant phenotypic, behavioural, biochemical and pathological deficits in mice

7.1.1 Potential role of N-terminal tau truncation in reduced lifespan clasping, motor deficits and early phosphorylation dependent tau

An important finding here was the reduced lifespan and induction of early progressive phenotypic clasping and motor deficits in mice expressing N-terminally truncated tau (Tau35). The reduction of lifespan in Tau35 mice somewhat correlated with the early clasping and motor deficits measured on the Rotarod, and also with the onset of tau pathology (PHF1 epitope) by 2 months of age. PHF1 (pSer396/pSer404) is considered to be a robust marker of tau pathology (Santacruz et al., 2005; Spires et al., 2006). Interestingly, in line with human tauopathy studies in which phosphorylation of tau at Ser396/Ser404 is reported as an early event (Su et al., 1996; Uboga and Price, 2000), Tau35 mice also showed an early increase in phosphorylated tau, indicating their relevance to human tauopathy. In addition, because the motor deficits are seen as early as 1 month in Tau35 mice, it is plausible to assume that the progression of motor deficits may be causally related to abnormal tau phosphorylation. In AD, phosphorylation of PHF1 was detected at higher density in early AD than phosphorylation at AT8 (Mondragón-Rodríguez et al., 2014), similar to observations in Tau35 mice. Furthermore, 50% of the total PHF1-containing structures in AD brain were found as early phosphorylation tau aggregates with a well-preserved neuronal soma, which did not show fibrillary conformation (Mondragón-Rodríguez et al., 2014), which was also similar to Tau35 mice. Indeed, previous research has shown that inhibition of tau phosphorylation using a kinase inhibitor (K252a) was able to reverse motor phenotypes in JNPL3 mice (harbouring the P301L mutation) indicating

a link between motor deficits, motor deterioration and tau phosphorylation (Le Corre et al., 2006).

Reduced lifespan in Tau35 mice was significantly shortened by a median of 71 days compared to WT mice. Previous reports in rats expressing truncated tau have shown a direct link and strong dependency between human tau truncation, the onset of neurofibrillary pathology and reduced lifespan (Koson et al., 2008). Koson and colleagues also showed that rats expressing relatively higher levels of truncated tau (SHR72 rats, which express residues 151-391 at 7.5-fold endogenous rat tau) had a significant decrease in median survival of 223 days compared to rats expressing lower amounts of truncated tau (SHR318 rats, which express 44% less transgene than SHR72), which had a median survival of 295 days compared to non-transgenic rats. This group also used the AT8 antibody to establish neuronal loss and NFT load. Interestingly they found no difference in neuronal loss or NFT load between the two models at end stage proposing that these parameters were not necessarily dependent on human truncated tau (Koson et al., 2008). These results, together with the reduced lifespan of Tau35 mice, strongly suggests that human tau truncation can reduce lifespan in mammalian models and therefore contribute the tauopathy phenotypes and pathology observed. However just like in the rat models, Tau35 also did not show extensive NFTs or neuronal loss suggestive of the fact that there may be a 'tangle threshold' in the brain of these animal models regulated by the limited number of neurons that can develop NFTs (Koson et al., 2008). Interestingly tau truncation and modification is not only restricted to transgenic mice expressing tau. For example, mutant APP mice that exhibit cognitive and behavioural deficits exhibit ubiquitinated and physiologically acetylated tau species (Morris et al., 2015). Both WT and human APP (hAPP) mutant mice showed similar post translational modifications in tau, which further supports the hypothesis that dementia-related deficits can be generated from physiological forms of tau (Morris et al., 2015). Furthermore, evidence shows that post-translational modification of tau accelerates tau polymerisation and correlates with the severity of dementia seen in tauopathies (Gamblin et al., 2003; Amadoro et al., 2004; Morris et al., 2015).

Tau35 mice showed extensive muscle pathology and internalised nuclei induced by expression of truncated tau. Previous findings in mice expressing both full-length and truncated tau species (Δtau: 3R $tau_{151-421}$) show paralysis, severe muscle fibre atrophy and internalised nuclei, whereas mice expressing full-length 3R, full length 4R, or full length only tau did not experience these deficits (Ozcelik et al., 2016). This implies that muscle atrophy and motor deficits may require the interaction of both full-length and truncated tau to elicit these phenotypes. Interestingly, in Tau35 mice, it was evident from TP007 antibody labelling, that truncated tau recruited endogenous mouse tau into inclusions. Therefore, it is plausible that truncated tau in Tau35 mice sequesters full-length tau to elicit motor phenotypes and muscle atrophy. However, compared to the results obtained by Ozcelik and colleagues (Ozcelik et al., 2016) who used a 3R tau construct, Tau35 mice express a 4R truncated tau fragment and therefore, perhaps the muscle disorder in Tau35 mice was less severe due to 4R tau expression. Indeed, it is difficult to fully establish the extent the Tau35 fragment plays in muscle pathology as N-terminal cleavage sites on tau are poorly characterised, and only a few sites have been established, these being located primarily at the beginning of the acidic region (Rohn et al., 2002; Horowitz, 2004; Derisbourg et al., 2015).

7.1.2 Potential mechanism behind cognitive decline induced by truncated Tau35 in mice

$Tau35^{Bl/6;129}$ and $Tau35^{Bl/6}$ mice exhibited significant cognitive decline from 8 and 10 months of age, respectively. Di and colleagues (Di et al., 2016) generated an inducible pseudo-phosphorylated tau mouse model to study the effect of conformationally modified tau. Leakage of transgene expression resulted in lines of mice expressing either low or high levels pseudo-phosphorylated tau, compared to endogenous mouse tau (4% or 14%, respectively) (Di et al., 2016). Interestingly, in the higher expressing mice, cognitive impairment appeared to be a result of progressive neuronal loss, whereas in the low expressing mice, cognitive impairment was due to synaptic dysfunction (Di et al., 2016). Interestingly the cognitive impairment in Tau35 mice appears not to be as a

result of progressive neuronal loss as this was not detected in these mice. However, synaptic dysfunction was observed in Tau35 mice, suggesting a potential role of synaptic integrity, particularly with regard to synaptic vesicle regulation. Synaptic integrity and dysregulation has previously been reported in synaptic compartments of a rat model of tau truncation (expressing human N- and C-terminally truncated tau encompassing three repeats (aa 151–391; line SHR24 (Filipcik et al., 2012) using a synaptic fractionation protocol (Jadhav et al., 2015). Jadhav and colleagues (Jadhav et al., 2015) showed that tau protein is distributed differently in control and transgenic rats. Whereas in control rats the amount of endogenous tau in the post-synaptic fraction was significantly lower than in the pre-synaptic fractions, consistent with human brains, in transgenic rats, tau was predominantly in the post-synaptic density again consistent with human AD brains (Fein et al., 2008; Tai et al., 2012). Interestingly, this group also showed that the synaptic tau proteome exhibited different phosphorylation patterns in the pre-synaptic and post-synaptic fractions of transgenic rats. Truncated tau in the pre-synaptic compartment was heavily phosphorylated compared to the post-synaptic density (Jadhav et al., 2015). This indicates different phosphorylation patterns and potential attribution to NFTs in the different synaptic compartments. Furthermore, results show that the composition of truncated tau in different synaptic compartments can have a direct effect on the pattern of damage observed in transgenic rats (Jadhav et al., 2015). In Tau35 mice, the synaptic integrity of pre-synaptic proteins (synapsin1 and synaptobrevin) was altered compared to the post-synaptic marker PSD95, which was unchanged, indicating a potentially predominant dysregulation of pre-synaptic proteins in Tau35 mice. However, it would be interesting to examine different synaptic fractions in the Tau35 mice to evaluate the extent of endogenous and exogenous tau present in these in the synaptic fractions.

7.1.3 Potential mechanism underlying tau oligomeric pathology and phosphorylation at multiple epitopes induced by Tau35 expression

Several studies have implicated truncated species of tau in the pathogenesis of tauopathies (Canu et al., 1998; Gamblin et al., 2003; Rissman et al., 2004; Newman et al., 2005; Guillozet-Bongaarts et al., 2007; Wray et al., 2008). Biochemical and immunohistochemical analyses of neurofibrillary degeneration induced by human truncated tau was most prominently labelled by AT8, which effectively labelled all stages of tangle pathology (Zilka et al., 2006). As previously mentioned, Zilka and colleagues found that the higher the expression level of truncated tau the earlier the onset of tangle pathology (Zilka et al., 2006). Tau35 mice showed extensive tau pathology upon labelling with AT8, indicating that tau tangle-like development reflected the expression of truncated tau. Therefore, it is possible that Tau35 mice exhibit tangle-like pathology only at a late stage of the disease due to low expression of truncated tau

Interestingly, Gallyas silver and Thioflavine S staining were absent from the brains of Tau35 mice and similar findings have recently been reported in tau transgenic mice harbouring the mutation A152T (Maeda et al., 2016). This finding is consistent with the development of tauopathy being mediated, at least partially, by soluble and/or oligomeric tau species. It is often assumed that abnormal phosphorylation of tau is directly related to its aggregation state (Avila, 2006). However, observations in Tau35 mice indicate that the link between the formation of such biochemically defined abnormal tau species and histologically defined NFTs may not be direct. For instance, tau aggregation into NFTs and Sarkosyl-insoluble tau were not observed in Tau35 mice and, instead tangle-like structures were apparent. Tau aggregation, although considered a hallmark of tauopathies, has recently been proposed to not be the only toxic tau species, if indeed at all and accumulating evidence suggests early soluble tau oligomeric precursors to be the main driver (Marx, 2007; Brunden et al., 2008; Lasagna-Reeves et al., 2011). Although there were no detectable

changes in soluble tau in Tau35 mice, they did exhibit increased oligomeric tau pathology in the hippocampus, which was detectable with antibody specific to TOC1. These findings are in concordance with the idea that oligomeric, sarkosyl-soluble species may be essential for the pathogenesis of human tauopathies (Lasagna-Reeves et al., 2012; Blair et al., 2013; Gerson and Kayed, 2013), including AD and PSP brain (Maeda et al., 2006; Patterson et al., 2011; Gerson et al., 2014). Furthermore, accumulation of insoluble tau has previously been reported in *in vivo* models expressing aggregation-prone tau mutants such as V337M and ΔK280 tau (Kraemer et al., 2003; Fatouros et al., 2012). Furthermore, in htau transgenic mice, neuronal death also occurs independently of histologically observed NFTs (Andorfer, 2005). These reports support the view that tau species other than highly aggregated tau may be the primary toxic entity responsible for the behavioural manifestation of tauopathies.

Surprisingly, Tau35 showed no apparent glial pathology at late stage of the disease and previous human post-mortem studies have revealed that tau truncation does not appear to occur in PSP and CBD glia as part of the disease process. This may partially explain the absence of glial pathology in Tau35 mice as appreciable amounts of tau are not normally found in astrocytes or microglia and may therefore not be as directly linked as previously postulated (Guillozet-Bongaarts et al., 2007).

7.2 N-terminal truncation deficits in Tau35 mice can be rescued therapeutically

7.2.1 Potential mechanistic role of phenylbutyrate in the rescuing behavioural and biochemical deficits in Tau35 mice

PBA reduced some of the behavioural, biochemical and pathological deficits in Tau35 mice. *In vivo*, PBA is converted to phenylacetate, which conjugates to glutamine to form phenylacetylglutamine, which serves as an alternative to urea in ammonia excretion (James et al., 1972; Brusilow, 1991). The main mechanistic ways by which PBA may act in Tau35 are via chaperones stabilising the native structure of proteins, HDAC inhibition and potentially reduction of synuclein (Zhou et al., 2011). Any of these mechanisms, either in combination or individually, could act to alleviate tauopathy-like symptoms in Tau35 mice (Figure 7.1) (Cuadrado-Tejedor et al., 2011). Chemical chaperones prevent aggregation by promoting folding of mutant proteins, reducing misfolded aggregates of proteins and having an indirect effect on intracellular molecular chaperone capacity. Therefore, any therapeutics which have these functions are of increasing interest (Kahali et al., 2010; Ong and Kelly, 2011; Kolb et al., 2015). PBA is an example of these chemical chaperones having the ability to disrupt heat shock proteins (Hsps) and thereby increasing the exposure of hydrophobic surfaces which enhance Hsp chaperone activity (Hekmatimoghaddam et al., 2016). Chemical chaperons such as PBA are also responsible for preventing intermolecular interactions triggering chemical events that drive unfolded assembly of aggregates (Choi et al., 2008; Ono et al., 2009; Kahali et al., 2010; Ong and Kelly, 2011; Mimori et al., 2013). Interestingly, several chemical chaperones have previously been shown to reduce tau phosphorylation (Loy and Tariot, 2002; Hoshino et al., 2007; Venkataramani et al., 2010). PBA was able to reduce tau phosphorylation in Tau35 mice, suggesting that the mechanism through which PBA acts is at least partially mediated by its chaperone action.

7.2.2 Mechanistic role of PBA in rescuing motor deficits and muscle pathology in Tau35 mice

One mechanism proposed for the action of PBA in spinal muscular atrophy (SMA) is increasing gene expression by preserving the function of the survival motor neuron protein (SMN). Mutant SMN (harbouring the C>T point mutation in exon 7) mice show deficits in hindlimb grip strength but not in forelimb grip strength (Gladman et al., 2010), which is strikingly similar to the findings in Tau35 mice. Therefore, it is possible that Tau35 mice harbour dysfunctional SMN, which could contribute to the motor dysfunction seen in these animals, although this was not assessed in this study. Future experiments should identify if the SMN complex is impaired, and therefore might contribute to the motor impairment seen in Tau35 mice.

PBA alleviates the reduction in centralised nuclei in muscle fibres in Tau35 mice. There are no reports in the current literature describing the rescue of centralised nuclei and/or degenerative muscle pathology in any animal models or patients following PBA administration. However, the two major protein degradation pathways that are activated during muscle atrophy and pathological changes in muscles are the autophagic lysosomal pathway and the ubiquitin-proteasome systems, which variably contribute to the loss of muscle mass (Sandri, 2013). The autophagy pathway is involved a variety of atrophy-related genes, which are controlled by specific transcription factors, such as FoxO3, which is negatively regulated by Akt, and NF-κB. One study showed that PBA increases expression of NF-κB and hence could reverse or at least improve, neurodegenerative changes (Del Signore et al., 2009). NF-κB is an inducible transcription factor that plays a role in the anti-apoptotic response in mammals (Wang et al., 1996a) and after translocation to the nucleus, NF-κB activates gene transcription. PBA can enhance the ability of NF-κB to bind to DNA and thereby augment gene expression (Chen Lf et al., 2001). Furthermore, induction of NF-κB also suppresses apoptosis by inhibiting caspase expression (Beg and Baltimore, 1996; Wang et al., 1996a). Therefore, it is possible that in Tau35 mice treated with PBA, NF-κB may play a role in the rescue of muscle pathology and, due to the pleotropic effect of this compound,

and its extensive ability to activate transcriptional regulators, it is possible that PBA activates several other transcription factors associated with autophagy, which appears to be impaired in Tau35 mice. PBA would therefore lead to increased protein synthesis and rescue of muscle formation and regeneration. However, none of these factors have yet been examined in Tau35 mice, and therefore this remains a tentative plausible explanation for the effects of PBA in these animals.

Tau35 mice also exhibit α-synuclein accumulation in the hippocampus, which could be related to the Parkinsonian-like motor deficits in these mice. Previous studies have shown that PBA can reduce α-synuclein aggregation in mouse brain and *in vitro* and also to prevent age-related deterioration in motor and cognitive function (Ono et al., 2009; Saleh et al., 2015). Zhou and colleagues found that in a N27 dopamine cell line, PBA increased the expression of DJ-1 (associated with early-onset, autosomal recessive Parkinson's disease, PARK7) and rescued cells from oxidative stress and mutant α-synuclein toxicity. Furthermore, in another transgenic mouse expressing mutant Y39C α-synuclein, that develops Lewy body-like inclusions, long term administration of PBA was able to alleviate α-synuclein aggregation as well as improving motor and cognitive function (Zhou et al., 2011). Therefore, the rescue of motor behaviour deficits in Tau35 mice could be attributed to a potential reduction of α-synuclein aggregation.

7.2.3 Mechanistic role of PBA in rescuing cognitive deficits in Tau35

PBA reduced spatial learning and memory deficits, as well as synaptic function, in Tau35 mice, implicating the ability to restore histone acetylation and therefore restoring LTP memory. Histone acetylation is particularly important in terms of long-term memory (Peixoto and Abel, 2013), the primary memory malfunction also seen in Tau35 mice, which agrees with previous findings showing that HDAC inhibitors rescue age-dependent associative and spatial memory as well as improving consolidation deficits in mouse models of AD and neurodegeneration (Fischer et al., 2007; Fontán-Lozano et al., 2008;

Ricobaraza et al., 2009; Kilgore et al., 2010). In particularly HDAC2 has been suggested to play a putative role in synaptic plasticity and memory formation, since overexpression of HDAC2, but not HDAC1, decreases spine density and impairs memory formation in mice (Guan et al., 2009). HDAC3 is also linked to cognitive enhancement and is a negative regulator of long term memory, since administering selective HDAC3 inhibitors into the hippocampus, accelerates long-term memory formation (McQuown et al., 2011). Therefore, PBA may act through histone acetylation, through either HDAC2 or HDAC3, allowing the restoration of both long-term memory and spatial learning in Tau35 mice. However, HDACs were not analysed as part of this study and therefore this remains only a plausible mechanistic role which would be of interest to investigate further.

Previous studies have shown that PBA can successfully recover the pathological hallmarks of AD and enhance cognitive decline in Tg2576 mice overexpressing mutant APP (Ricobaraza et al., 2009; Cuadrado-Tejedor et al., 2011). This finding was similar in the Tau35 mice, in which both phosphorylated tau and cognitive decline were restored by PBA. Therefore, PBA is a multifunctional compound with the ability to effectively reduce cognitive impairments associated with neurodegeneration. One drawback with PBA use *in vivo* however, is the fact that in all previous studies, the doses required to alleviate these deficits have been relatively high (Cuadrado-Tejedor et al., 2011). Furthermore, it has been proposed that PBA can enhance proteostasis of proteins by binding to and stabilising them, through pharmacological chaperones or by enhancing the capacity of the proteaostasis network (Powers et al., 2009). Therefore, PBA may potentially act through enhancing tau proteostasis.

Notably, PBA was not able to prevent memory deficits in Tau35 mice dosed at the age of 7.5 months, indicating that PBA preferentially rescues pre-existing deficits in Tau35 mice, rather than preventing disease onset. This could be partially due to the slight variation seen between Tau35 mice and because at 8 months of age cognition is only mildly impaired and was perhaps not greatly distinguishable between the two treatment groups.

7.2.4 Mechanistic role of PBA in rescuing motor deficits and muscle pathology in Tau35

PBA was able to partially rescue lysosomal autophagic dysfunction in Tau35 mice. Although the molecular mechanisms underlying the protective effects of PBA on the autophagic–lysosomal is not well established, it is possible that PBA may act through an ER stress-related mechanism to elicit its beneficial actions. The ER is an organelle that is highly sensitive to metabolic disturbance, such as aggregated and truncated proteins that induce oxidative stress, and has been widely studied in relation to AD (Selkoe, 2001). ER stress, together with increased levels of phosphorylated tau have been reported in the hippocampus of patients with tauopathies, suggesting a relationship between these two parameters (Nijholt et al., 2012). Several studies have implicated PBA in reduction of ER stress by targeting ER stress markers such as CCAAT-enhancer-binding protein homologous protein (CHOP) and binding immunoglobulin protein (BiP) (Fonseca et al., 2012). PBA can also alleviate ER stress by acting via the Pael receptor, which is thought to accumulate in people harbouring mutations in the gene encoding parkin (*PARK2*), which results in Parkinson's disease (Kubota et al., 2006). PBA has the capability to reduce ER stress in animal models of type 2 diabetes (Ozcan, 2006), in *in vitro* models of type 2 diabetes and lipotoxicity including reducing palmitate-induced ER stress (Akerfeldt et al., 2008; Choi et al., 2008; Park et al., 2015), and in humans by ameliorating the insulin resistance and β-cell dysfunction induced by prolonged elevation of free fatty acids (Xiao et al., 2011). Therefore, it is possible that, in Tau35 mice, PBA might also act through the ER stress pathway, potentially mediated by decreasing insulin signalling as has previously been reported (Castro et al., 2013). Reduction of lysosomal markers following PBA treatment of Tau35 mice could indicate improvement in the ER stress response and increased clearance of misfolded and accumulated proteins.

The proposed mechanistic actions discussed herein and in Chapter 4 are summarised in Figure 7.1.

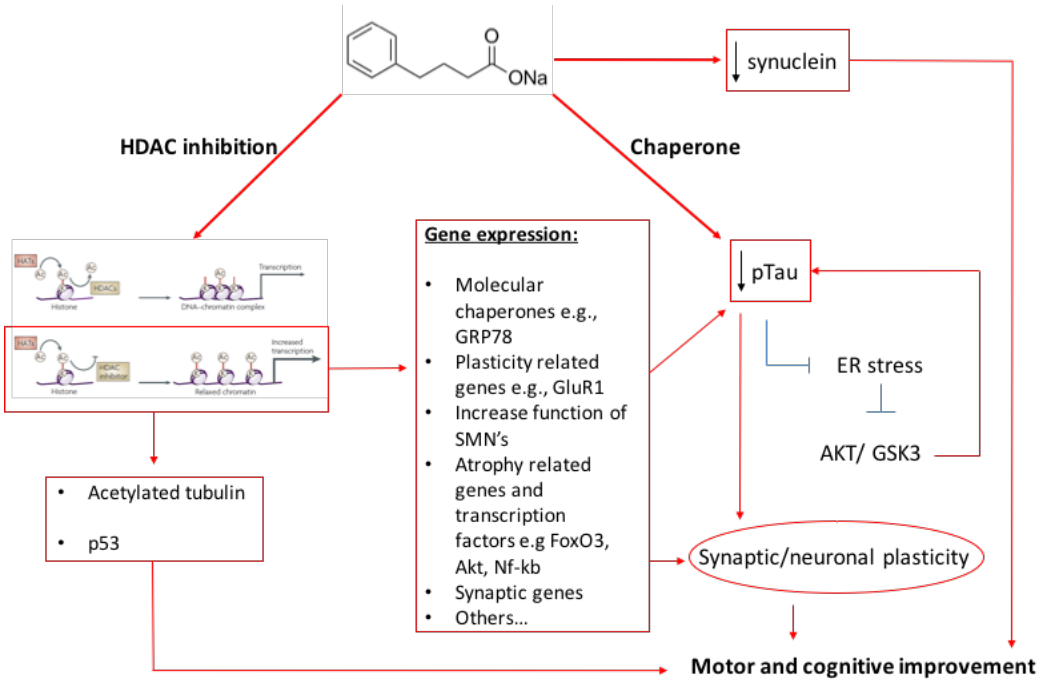

Figure 7.1: Proposed mechanism of phenylbutyrate-mediated cognitive and motor improvement in Tau35. Phenylbutyrate (PBA) can act either through HDAC inhibition, reduction in α-synuclein and/or a chaperone-mediated action to prevent tau phosphorylation, and conformational changes in tau. PBA may also enhance synaptic and neuronal plasticity and hence rescue and restore cognitive deficits (HDAC figure from Kazantsev and Thompson, 2008; image adapted from Cuadrado-Tejedor et al., 2011).

Taken together, although several proposed mechanistic of PBA are described, it is extremely difficult to establish exactly how PBA was acting in these mice without doing extensive further research both *in vivo* and *in vitro* to look at these different pathways. This is also partially to do with the fact that PBA is a pleiotropic compound affected several alternative routes and mechanisms chemically.

7.3. Targeting tau therapeutically

The World Health Organisation (WHO) has identified AD as a public health priority (Wimo et al., 2013, WHO 2015) and identifying new therapeutic targets is increasingly urgent. The diverse *in vitro* and *in vivo* models of tauopathy have allowed the identification of several tau targets for therapeutic intervention to alleviate either neurotoxic gain of function, or loss of function, based on tau pathology (Figure 7.2). It is essential to develop strategies to delay onset and/or prevent disease progression, since current treatments only focus on the symptoms rather than disease processes. One possible therapeutic strategy would be to reduce the amount of tau, because tau knockdown mice do not exhibit apparent pathological abnormalities and also reducing tau decreases Aβ-dependent neurotoxicity (Harada et al., 1994; Roberson et al., 2007). Potential therapeutic mechanisms would include reducing tau via small interfering RNAs (siRNAs), antisense oligonucleotides, or even transcription inhibitors (DeVos et al., 2013). Another potential strategy would be to inhibit tau phosphorylation as it is likely to be a primary contributor to tau aggregation and therefore, specific kinase inhibition would be a suitable target. The inhibition of kinases such as GSK3 and Cdk5 would be prime candidates as these have previously been shown to alleviate tau pathology in transgenic mice (Noble et al., 2005; Selenica et al., 2007; Hinners et al., 2008).

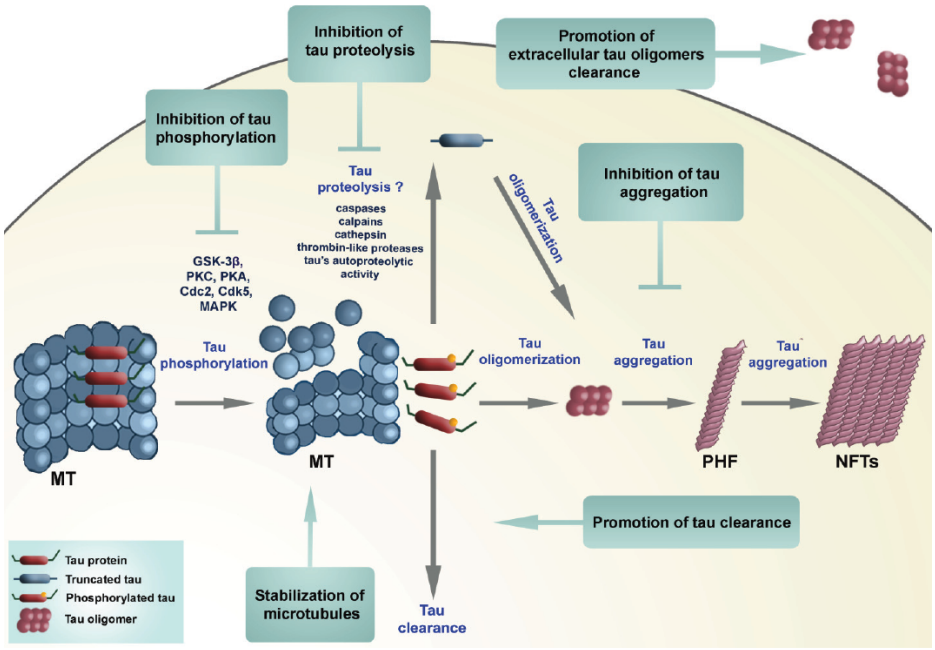

Figure 7.2: Diagram showing potential neuroprotective strategies to reduce tau aggregates. Proposed therapeutic interventions of tau based therapies including inhibition of tau phosphorylation/proteolysis, tau oligomer clearance, aggregation inhibitors, tau clearance and microtubule stabilisation (Šimić et al., 2016).

Furthermore, inhibition of GSK3 and Cdk5 have been shown to be neuroprotective in transgenic animals and in brain slice cultures (Noble et al., 2005; Selenica et al., 2007; Hinners et al., 2008), although clinical trials using kinase inhibitors have so far been unsuccessful. Given that evidence indicates reciprocal regulation between GSK3 and Cdk5, this adds a level of complexity to targeting specific tau kinase inhibitors to treat AD (Plattner et al., 2006; Engmann, 2009; Chow et al., 2014) and might explain, at least in part, the failure of efficacy in human trials of kinase inhibitors. Nevertheless, Tideglusib, a specific GSK3β inhibitor, has been shown to alleviate brain atrophy in patients with PSP, but not in AD (Wischik et al., 2015). The difference in therapeutic effect may be due to the presence of Aβ pathology in AD, but not in

PSP, and it is possible that Tideglusib may be a suitable compound for use only in disorders where Aβ is absent.

Targeting tau aggregation may be a more suitable target for the tauopathies and early prevention of tau aggregation may alleviate cognitive symptoms. Targeting tau aggregation, however, has been very difficult because most *in vitro* assays for tau aggregation are based on fibril formation, which require high concentrations of tau, and aggregation aids such as heparin (Ramachandran and Udgaonkar, 2011). Even if aggregated tau is disassociated, smaller oligomers may still be toxic and detrimental to neurons and hence targeting tau oligomers may be a better approach for pharmacological therapies (Šimić et al., 2016). A further proposed mechanism that may be suitable for therapeutic targeting is the control of proteasomal or autophagic protein degradation, which play a crucial role in preventing tau toxic species and aggregation (Blair et al., 2014; Karagöz et al., 2014). With age, protein degradation is compromised, leading to the accumulation of truncated, phosphorylated and aggregated forms of tau. Rapamycin, which induces autophagy, or inhibitors of certain Hsps, such as Hsp90, that bind to misfolded proteins, may make ideal candidates to target tau clearance (Berger, 2005; Ozcelik et al., 2013).

Finally, targeting tau proteolysis could be an important therapeutic target because normal conformations and functions of tau are inevitably lost once it becomes truncated. Not only do truncated and aggregated forms of tau make an ideal early diagnostic target for tauopathies (Wischik et al., 2014), but targeting enzymatic actions on tau may be simpler than targeting aggregated forms of tau. Cellular enzymes such as caspases, calpains, thrombin and cathepsins may also be of therapeutic interest, providing that their proteolytic activity can be shown to produce pathological and clinically critical manifestations. Furthermore, inhibiting tau truncation could potentially alleviate the transynaptic propagation of tau that results in disease progression.

7.4 Limitations of this work

Throughout this project, efforts were made to ensure that the experimental work carried out in this thesis was properly designed, planned and carefully controlled. However, it is important to highlight some of the limitations and shortfalls of this work in the studies presented herein.

The use of hippocampal tissue enabled valuable examination of the biochemical and neuropathological profile in Tau35 mice. However, there were some limitations associated with the progression of disease in these tissues. The sample size used was relatively low (n=6) but in order to comply with animal welfare the number of mice used was reduced to the lowest number required to detect any changes, without compromising the experiments.

In order to establish a comprehensive biochemical profile in Tau35 mouse brain, it would have been essential to examine more brain regions, as pathological features may vary substantially, depending on the brain area investigated.

Changes in Tau35 were observed in the synaptic markers. However, synaptosomal preparations would allow the separation of synaptic proteins into pre-synaptic and post-synaptic fractions, allowing further evaluation of the effects of Tau35 at synapses. For biochemical analyses, the brains of Tau35 mice aged 14 months were analysed. A wider age range would give more information and would determine whether changes occur early in the disease progress.

As pathology was only very mild and varied between animals only semi-quantitative evaluations were made from immunohistochemical analyses. It would be of interest to quantify NFT numbers stereologically, and in different brain areas, in Tau35 mice.

Several autophagy markers were investigated in Tau35 mice on western blots. For instance, Tau35 showed disruption of both p62 and LC3 and many previous studies measure autophagic activity on the interpretation of static protein levels or images of p62 and LC3 levels. However, this dynamic is difficult to assess as static scoring is an incomplete assessment of autophagy

without fully assessing autophagic flux. *In vitro* flux can be measured through direct lysosomal blockage, or indirect interference from p62/SQTM1 decline (Bjørkøy et al., 2006). One effective way to demonstrate the role of autophagy would be to knockdown ATG7 or inhibit ATG5 (Gottlieb et al., 2015).

It was essential to study behavioural deficits on a pure inbred C57BL/6 background of Tau35 mice. However, due to the time constraint and the time taken for eight generations it was only possible to do behavioural analysis on these mice and not biochemical and pathological profile of these mice. This is essential to do to further analyse and interpret how well the inbred strain parallels the hybrid strain and this would be essential to do in future experiments.

As previously described Tau35 mice exhibit reduced GSK3β activity and, although GSK3 activity was not measured in PBA-treated mice, it is possible that PBA can inhibit GSK3 by reducing phosphorylated tau, as shown previously in APP mice (Ricobaraza et al., 2009). The mechanistic actions remain unclear regarding the action of PBA inhibiting GSK3 via chaperone activity and/or HDAC inhibition, therefore it would be informative to measure GSK3 activity in PBA treated mice to further investigate the mechanistic role of PBA.

The CHO-Tau35 cell-based ICW high-throughput assay was established and used successfully to measure changes in tau phosphorylation with potentially therapeutic compounds. However, this assay did not examine the exact mechanism underlying the reduction in tau phosphorylation. Importantly, CHO cells do not constitutively express tau and are therefore this model may be subject to potential artefacts. It would be of considerable interest therefore to investigate these changes in neuronal cells derived from Tau35 mice to examine these potential therapeutic compounds.

7.6 Summary

In summary, the findings of this thesis yield some interesting and important insights into the role of a human tauopathy-derived N-terminal truncated species of WT tau in mice. The aim of this project was to investigate molecular and behavioural phenotype observed in a new transgenic mouse model of tauopathy that expresses a human tau fragment, Tau35, first identified in human post-mortem brain. Investigation of Tau35 mice revealed extensive phenotypic deficits including clasping, reduced lifespan and kyphosis as well as early motor deficits followed by cognitive decline. Interestingly, these behavioural deficits were preserved when breeding to a pure inbred C57BL/6 background. Extensive molecular impairments were observed including reduced tau phosphorylation, conformation and oligomeric tau species, impaired lysosomal degradation, impaired synaptic plasticity reduced acetylated tubulin and increased GSK3β activity, as summarised in Figure 7.3. Furthermore, a cell based CHO-Tau35 assay was successfully established in which to test new potential therapeutic compounds.

Taken together, the hypothesis that tau aggregation, mediated by the generation of Tau35, drives tau phosphorylation and aggregation, and associated behavioural changes that mirror those present in the tauopathies, was observed in this model. To our knowledge, this is the first report that a very low amount of a fragment of WT human truncated tau in mice leads to behavioural, neuropathological and biochemical changes that closely recapitulate human disease. The data further supports the hypothesis that tau truncation is an important potentially early event in tauopathies. As the deficits in these mice can be reversed by PBA, this cascade provides potential for the treatment of several tauopathies and related neurodegenerative diseases.

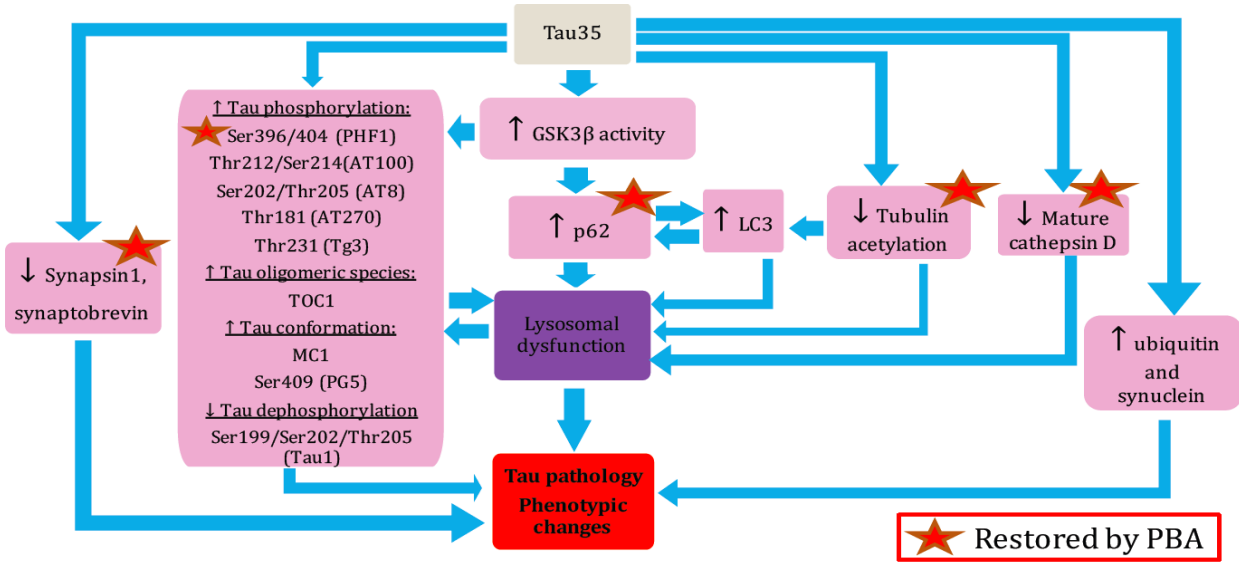

Figure 7.3: Proposed mechanism of Tau35 N-terminal fragment *in vivo*. Low expression of Tau35 induces increased tau phosphorylation at epitopes: Ser396/Ser404, Thr212/Ser412, Ser202/Thr205, Thr181, Thr231, decrease in both dephosphorylated tau at Ser199/Ser202/Thr205, and oligomeric tau species: TOC1 and conformational/phosphorylated tau species at Ser409 and MC1. Tau35 mice also exhibited increased GSK3β, p62 and LC3, decreased acetylated tubulin and cathepsin D activity, all leading to a potential decreased activity of lysosomal function and clearance of pathological tau species. Tau35 mice also exhibited reduced synaptic integrity: synapsin1 and synaptobrevin as well as increased ubiquitin and α-synuclein labelling. All which lead to proposed behavioural and pathological deficits seen in Tau35 mice. Phenylbutyrate (PBA) was able to rescue many of the deficits observed in Tau35 mice (red stars).

References

Adams SJ, Crook RJP, DeTure M, Randle SJ, Innes AE, Yu XZ, Lin W-L, Dugger BN, McBride M, Hutton M, Dickson DW, McGowan E (2009) Overexpression of Wild-Type Murine Tau Results in Progressive Tauopathy and Neurodegeneration. Am J Pathol 175:1598–1609.

Ahmed Z, Cooper J, Murray TK, Garn K, McNaughton E, Clarke H, Parhizkar S, Ward MA, Cavallini A, Jackson S, Bose S, Clavaguera F, Tolnay M, Lavenir I, Goedert M, Hutton ML, O'Neill MJ (2014) A novel in vivo model of tau propagation with rapid and progressive neurofibrillary tangle pathology: the pattern of spread is determined by connectivity, not proximity. Acta Neuropathol 127:667–683.

Aigner L, Arber S, Kapfhammer JP, Laux T, Schneider C, Botteri F, Brenner H-R, Caroni P (1995) Overexpression of the neural growth-associated protein GAP-43 induces nerve sprouting in the adult nervous system of transgenic mice. Cell 83:269–278.

Akerfeldt MC, Howes J, Chan JY, Stevens VA, Boubenna N, McGuire HM, King C, Biden TJ, Laybutt DR (2008) Cytokine-Induced -Cell Death Is Independent of Endoplasmic Reticulum Stress Signaling. Diabetes 57:3034–3044.

Allen B, Ingram E, Takao M, Smith MJ, Jakes R, Virdee K, Yoshida H, Holzer M, Craxton M, Emson PC, Atzori C, Migheli A, Crowther RA, Ghetti B, Spillantini MG, Goedert M (2002) Abundant tau filaments and nonapoptotic neurodegeneration in transgenic mice expressing human P301S tau protein. J Neurosci 22:9340–9351.

Alonso A del, Li B, Grundke-Iqbal I, Iqbal K (2008) Mechanism of Tau-Induced Neurodegeneration in Alzheimer Disease and Related Tauopathies. Curr Alzheimer Res 5:375–384.

Alonso A d. C, Zaidi T, Novak M, Grundke-Iqbal I, Iqbal K (2001) Hyperphosphorylation induces self-assembly of into tangles of paired helical filaments/straight filaments. Proc Natl Acad Sci 98:6923–6928.

Alonso A del C, Grundke-Iqbal I, Iqbal K (1996) Alzheimer's disease hyperphosphorylated tau sequesters normal tau into tangles of filaments and disassembles microtubules. Nat Med 2:783–787.

Alonso A del C, Li B, Grundke-Iqbal I, Iqbal K (2006) Polymerization of hyperphosphorylated tau into filaments eliminates its inhibitory activity. Proc Natl Acad Sci 103:8864–8869.

Alonso ADC, Mederlyova A, Novak M, Grundke-Iqbal I, Iqbal K (2004) Promotion of Hyperphosphorylation by Frontotemporal Dementia Tau Mutations. J Biol Chem 279:34873–34881.

Amadoro G, Corsetti V, Sancesario GM, Lubrano A, Melchiorri G, Bernardini S, Calissano P, Sancesario G (2014) Cerebrospinal fluid levels of a 20-22 kDa NH2 fragment of human tau provide a novel neuronal injury biomarker in Alzheimer's disease and other dementias. J Alzheimer's Dis 42:211–226.

Amadoro G, Corsetti V, Stringaro A, Colone M, D'Aguanno S, Meli G, Ciotti M, Sancesario G, Cattaneo A, Bussani R, Mercanti D, Calissano P (2010) A NH2 tau fragment targets neuronal mitochondria at AD synapses: possible implications for neurodegeneration. J Alzheimer's Dis 21:445–470.

Amadoro G, Serafino AL, Barbato C, Ciotti MT, Sacco A, Calissano P, Canu N (2004) Role of N-terminal tau domain integrity on the survival of cerebellar granule neurons. Cell Death Differ 11:217–230.

Anderton BH, Betts J, Blackstock WP, Brion JP, Chapman S, Connell J, Dayanandan R, Gallo JM, Gibb G, Hanger DP, Hutton M, Kardalinou E, Leroy K, Lovestone S, Mack T, Reynolds CH, Van Slegtenhorst M (2001) Sites of phosphorylation in tau and factors affecting their regulation. Biochem Soc Symp:73–80.

Andorfer C (2005) Cell-Cycle Reentry and Cell Death in Transgenic Mice Expressing Nonmutant Human Tau Isoforms. J Neurosci 25:5446–5454.

Andorfer C, Kress Y, Espinoza M, De Silva R, Tucker KL, Barde Y-A, Duff K, Davies P (2003) Hyperphosphorylation and aggregation of tau in mice expressing normal human tau isoforms. J Neurochem 86:582–590.

Andreadis A (2005) Tau gene alternative splicing: expression patterns, regulation and modulation of function in normal brain and neurodegenerative diseases. Biochim Biophys Acta - Mol Basis Dis 1739:91–103.

Andreadis A, Brown WM, Kosik KS (1992) Structure and novel exons of the human .tau. gene. Biochemistry 31:10626–10633.

Andreassi C, Angelozzi C, Tiziano FD, Vitali T, De Vincenzi E, Boninsegna A, Villanova M, Bertini E, Pini A, Neri G, Brahe C (2004) Phenylbutyrate increases SMN expression in vitro: relevance for treatment of spinal muscular atrophy. Eur J Hum Genet 12:59–65.

Aoyama K, Matsubara K, Kobayashi S (2006) Aging and oxidative stress in progressive supranuclear palsy. Eur J Neurol 13:89–92.

Arai T, Hasegawa M, Akiyama H, Ikeda K, Nonaka T, Mori H, Mann D, Tsuchiya K, Yoshida M, Hashizume Y, Oda T (2006) TDP-43 is a component of ubiquitin-positive tau-negative inclusions in frontotemporal lobar degeneration and amyotrophic lateral sclerosis. Biochem Biophys Res Commun 351:602–611.

Arai T, Ikeda K, Akiyama H, Nonaka T, Hasegawa M, Ishiguro K, Iritani S, Tsuchiya K, Iseki E, Yagishita S, Oda T, Mochizuki A (2004) Identification of amino-terminally cleaved tau fragments that distinguish progressive supranuclear palsy from corticobasal degeneration. Ann Neurol 55:72–79.

Arai T, Ikeda K, Akiyama H, Tsuchiya K, Iritani S, Ishiguro K, Yagishita S, Oda T, Odawara T, Iseki E (2003) Different immunoreactivities of the microtubule-binding region of tau and its molecular basis in brains from patients with Alzheimer's disease, Pick's disease, progressive supranuclear palsy and corticobasal degeneration. Acta Neuropathol 105:489–498.

Arendash GW, Lewis J, Leighty RE, McGowan E, Cracchiolo JR, Hutton M, Garcia MF (2004) Multi-metric behavioral comparison of APPsw and P301L models for Alzheimer's Disease: linkage of poorer cognitive performance to tau pathology in forebrain. Brain Res 1012:29–41.

Arendt T, Stieler J, Strijkstra AM, Hut R a, Rüdiger J, Van der Zee E a, Harkany T, Holzer M, Härtig W (2003) Reversible paired helical filament-like phosphorylation of tau is an adaptive process associated with neuronal plasticity in hibernating animals. J Neurosci 23:6972–6981.

Armstrong RA, Lantos PL, Cairns NJ (2009) Hippocampal pathology in progressive supranuclear palsy (PSP): a quantitative study of 8 cases. Clin Neuropathol 28:46–53.

Arnold SE, Hyman BT, Flory J, Damasio AR, Van Hoesen GW (1991) The Topographical and Neuroanatomical Distribution of Neurofibrillary Tangles and Neuritic Plaques in the Cerebral Cortex of Patients with Alzheimer's Disease. Cereb Cortex 1:103–116.

Arriagada P V, Growdon JH, Hedley-Whyte ET, Hyman BT (1992) Neurofibrillary tangles but not senile plaques parallel duration and severity of Alzheimer's disease. Neurology 42:631–639.

Astur RS, Taylor LB, Mamelak AN, Philpott L, Sutherland RJ (2002) Humans with hippocampus damage display severe spatial memory impairments in a virtual Morris water task. Behav Brain Res 132:77–84.

Auerbach W, Dunmore JH, Fairchild-Huntress V, Fang Q, Auerbach AB, Huszar D, Joyner AL (2000) Establishment and chimera analysis of 129/SvEv- and C57BL/6-derived mouse embryonic stem cell lines. Biotechniques 29:1024–1028, 1030, 1032.

Avila J (2006) Tau phosphorylation and aggregation in Alzheimer's disease pathology. FEBS Lett 580:2922–2927.

Ávila J, Lim F, Moreno F, Belmonte C, Cuello AC (2002) Tau Function and Dysfunction in Neurons. Mol Neurobiol 25:213–232.

Azoulay-Alfaguter I, Elya R, Avrahami L, Katz A, Eldar-Finkelman H (2015) Combined regulation of mTORC1 and lysosomal acidification by GSK-3 suppresses autophagy and contributes to cancer cell growth. Oncogene 34:4613–4623.

Bailey CH, Kandel ER, Si K (2004) The Persistence of Long-Term Memory. Neuron 44:49–57.

Ballatore C, Lee VM-Y, Trojanowski JQ (2007) Tau-mediated neurodegeneration in Alzheimer's disease and related disorders. Nat Rev Neurosci 8:663–672.

Banduseela VC, Chen Y-W, Kultima HG, Norman HS, Aare S, Radell P, Eriksson LI, Hoffman EP, Larsson L (2013) Impaired autophagy, chaperone expression, and protein synthesis in response to critical illness interventions in porcine skeletal muscle. Physiol Genomics 45:477–486.

Bánréti Á, Sass M, Graba Y (2013) The emerging role of acetylation in the regulation of autophagy. Autophagy 9:819–829.

Baumann K, Mandelkow E-M, Biernat J, Piwnica-Worms H, Mandelkow E (1993) Abnormal Alzheimer-like phosphorylation of tau-protein by cyclin-dependent kinases cdk2 and cdk5. FEBS Lett 336:417–424.

Bednarski E, Lynch G (2002) Cytosolic Proteolysis of tau by Cathepsin D in Hippocampus Following Suppression of Cathepsins B and L. J Neurochem 67:1846–1855.

Beg AA, Baltimore D (1996) An essential role for NF-kappaB in preventing TNF-alpha-induced cell death. Science (80-) 274:782–784.

Belarbi K, Schindowski K, Burnouf S, Caillierez R, Grosjean M-E, Demeyer D, Hamdane M, Sergeant N, Blum D, Buee L (2009) Early Tau Pathology Involving the Septo-Hippocampal Pathway in a Tau Transgenic Model: Relevance to Alzheimers Disease. Curr Alzheimer Res 6:152–157.

Bellucci A, Westwood AJ, Ingram E, Casamenti F, Goedert M, Spillantini MG (2004) Induction of Inflammatory Mediators and Microglial Activation in Mice Transgenic for Mutant Human P301S Tau Protein. Am J Pathol 165:1643–1652.

Bendiske J, Bahr B a (2003) Lysosomal Activation Is a Compensatory Response Against Protein Accumulation and Associated Synaptopathogenesis—An Approach for Slowing Alzheimer Disease? J Neuropathol Exp Neurol 62:451–463.

Bennett EJ, Bence NF, Jayakumar R, Kopito RR (2005) Global Impairment of the Ubiquitin-Proteasome System by Nuclear or Cytoplasmic Protein Aggregates Precedes Inclusion Body Formation. Mol Cell 17:351–365.

Berg S, Serabe B, Aleksic A, Bomgaars L, McGuffey L, Dauser R, Durfee J, Nuchtern J, Blaney S (2001) Pharmacokinetics and cerebrospinal fluid penetration of phenylacetate and phenylbutyrate in the nonhuman primate. Cancer Chemother Pharmacol 47:385–390.

Berger Z (2005) Rapamycin alleviates toxicity of different aggregate-prone proteins. Hum Mol Genet 15:433–442.

Berger Z, Roder H, Hanna A, Carlson A, Rangachari V, Yue M, Wszolek Z, Ashe K, Knight J, Dickson D, Andorfer C, Rosenberry TL, Lewis J, Hutton M, Janus C (2007) Accumulation of Pathological Tau Species and Memory Loss in a Conditional Model of Tauopathy. J Neurosci 27:3650–3662.

Bhaskar K, Yen S-H, Lee G (2005) Disease-related Modifications in Tau Affect the Interaction between Fyn and Tau. J Biol Chem 280:35119–35125.

Bhat R, Xue Y, Berg S, Hellberg S, Ormo M, Nilsson Y, Radesater A-C, Jerning E, Markgren P-O, Borgegard T, Nylof M, Gimenez-Cassina A, Hernandez F, Lucas JJ, Diaz-Nido J, Avila J (2003) Structural Insights and Biological Effects of Glycogen Synthase Kinase 3-specific Inhibitor AR-A014418. J Biol Chem 278:45937–45945.

Biernat J, Gustke N, Drewes G, Mandelkow E, Mandelkow E (1993) Phosphorylation of Ser262 strongly reduces binding of tau to microtubules: Distinction between PHF-like immunoreactivity and microtubule binding. Neuron 11:153–163.

Biernat J, Mandelkow E-M (1999) The Development of Cell Processes Induced by tau Protein Requires Phosphorylation of Serine 262 and 356 in the Repeat Domain and Is Inhibited by Phosphorylation in the Proline-rich Domains. Mol Biol Cell 10:727–740.

Billings LM, Oddo S, Green KN, McGaugh JL, LaFerla FM (2005) Intraneuronal Aβ Causes the Onset of Early Alzheimer's Disease-Related Cognitive Deficits in Transgenic Mice. Neuron 45:675–688.

Bjørkøy G, Lamark T, Johansen T (2006) p62/SQSTM1: A Missing Link between Protein Aggregates and the Autophagy Machinery. Autophagy 2:138–139.

Blair LJ et al. (2013) Accelerated neurodegeneration through chaperone-mediated oligomerization of tau. J Clin Invest 123:4158–4169.

Blair LJ, Sabbagh JJ, Dickey CA (2014) Targeting Hsp90 and its co-chaperones to treat Alzheimer's disease. Expert Opin Ther Targets 18:1219–1232.

Bloom O, Evergren E, Tomilin N, Kjaerulff O, Löw P, Brodin L, Pieribone VA, Greengard P, Shupliakov O (2003) Colocalization of synapsin and actin during synaptic vesicle recycling. J Cell Biol 161:737–747.

Boekhoorn K (2006) Improved Long-Term Potentiation and Memory in Young Tau-P301L Transgenic Mice before Onset of Hyperphosphorylation and Tauopathy. J Neurosci 26:3514–3523.

Boland B, Kumar A, Lee S, Platt FM, Wegiel J, Yu WH, Nixon RA (2008) Autophagy Induction and Autophagosome Clearance in Neurons: Relationship to Autophagic Pathology in Alzheimer's Disease. J Neurosci 28:6926–6937.

Bolivar VJ (2000) Habituation of Activity in an Open Field: A Survey of Inbred Strains and F1 Hybrids. Behav Genet 30:285–293.

Bolivar VJ (2001) Mapping of Quantitative Trait Loci with Knockout/Congenic Strains. Genome Res 11:1549–1552.

Bondulich MK, Guo T, Meehan C, Manion J, Rodriguez Martin T, Mitchell JC, Hortobagyi T, Yankova N, Stygelbout V, Brion J-P, Noble W, Hanger DP (2016) Tauopathy induced by low level expression of a human brain-derived tau fragment in mice is rescued by phenylbutyrate. Brain 139:2290–2306.

Bothe GWM, Bolivar VJ, Vedder MJ, Geistfeld JG (2004) Genetic and behavioral differences among five inbred mouse strains commonly used in the production of transgenic and knockout mice. Genes, Brain Behav 3:149–157.

Braak H, Braak E (1986) Chapter 12 Ratio of pyramidal cells versus non-pyramidal cells in the human frontal isocortex and changes in ratio with ageing and Alzheimer's disease. In: Progress in Brain Research, pp 185–212.

Braak H, Braak E (1991) Neuropathological stageing of Alzheimer-related changes. Acta Neuropathol 82:239–259.

Brandt R, Hundelt M, Shahani N (2005) Tau alteration and neuronal degeneration in tauopathies: mechanisms and models. Biochim Biophys Acta - Mol Basis Dis 1739:331–354.

Brandt R, Lee G (1993) Functional organization of microtubule-associated protein tau. Identification of regions which affect microtubule growth, nucleation, and bundle formation in vitro. J Biol Chem 268:3414–3419.

Bredy TW, Barad M (2008) The histone deacetylase inhibitor valproic acid enhances acquisition, extinction, and reconsolidation of conditioned fear. Learn Mem 15:39–45.

Brion J-P, Tremp G, Octave J-N (1999) Transgenic Expression of the Shortest Human Tau Affects Its Compartmentalization and Its Phosphorylation as in the Pretangle Stage of Alzheimer's Disease. Am J Pathol 154:255–270.

Brion JP, Anderton BH, Authelet M, Dayanandan R, Leroy K, Lovestone S, Octave JN, Pradier L, Touchet N, Tremp G (2001) Neurofibrillary tangles and tau phosphorylation. Biochem Soc Symp:81–88.

Bronson SK, Plaehn EG, Kluckman KD, Hagaman JR, Maeda N, Smithies O (1996) Single-copy transgenic mice with chosen-site integration. Proc Natl Acad Sci U S A 93:9067–9072.

Brookmeyer R, Johnson E, Ziegler-Graham K, Arrighi HM (2007) Forecasting the global burden of Alzheimer's disease. Alzheimer's Dement 3:186–191.

Brunden KR, Trojanowski JQ, Lee VM-Y (2008) Evidence that non-fibrillar tau causes pathology linked to neurodegeneration and behavioral impairments. J Alzheimer's Dis 14:393–399.

Bruns MB, Josephs K a (2013) Neuropsychiatry of corticobasal degeneration and progressive supranuclear palsy. Int Rev Psychiatry 25:197–209.

Brusilow SW (1991) Phenylacetylglutamine may replace urea as a vehicle for waste nitrogen excretion. Pediatr Res 29:147–150.

Brusilow SW, Maestri NE (1996) Urea cycle disorders: diagnosis, pathophysiology, and therapy. Adv Pediatr 43:127–170.

Buée L, Bussière T, Buée-Scherrer V, Delacourte A, Hof PR (2000) Tau protein isoforms, phosphorylation and role in neurodegenerative disorders11These authors contributed equally to this work. Brain Res Rev 33:95–130.

Bulinski JC (2007) Microtubule Modification: Acetylation Speeds Anterograde Traffic Flow. Curr Biol 17:R18–R20.

Burlina AB, Ogier H, Korall H, Trefz FK (2001) Long-Term Treatment with Sodium Phenylbutyrate in Ornithine Transcarbamylase-Deficient Patients. Mol Genet Metab 72:351–355.

Burrell JR, Hodges JR, Rowe JB (2014) Cognition in corticobasal syndrome and progressive supranuclear palsy: A review. Mov Disord 29:684–693.

Butchbach MER, Lumpkin CJ, Harris AW, Saieva L, Edwards JD, Workman E, Simard LR, Pellizzoni L, Burghes AHM (2016) Protective effects of butyrate-based compounds on a mouse model for spinal muscular atrophy. Exp Neurol 279:13–26.

Butner KA (1991) Tau protein binds to microtubules through a flexible array of distributed weak sites. J Cell Biol 115:717–730.

Callahan LM, Coleman PD (1995) Neurons bearing neurofibrillary tangles are responsible for selected synaptic deficits in Alzheimer's disease. Neurobiol Aging 16:311–314.

Callahan LM, Vaules WA, Coleman PD (1999) Quantitative Decrease in Synaptophysin Message Expression and Increase in Cathepsin D Message Expression in Alzheimer Disease Neurons Containing Neurofibrillary Tangles. J Neuropathol Exp Neurol 58:275–287.

Cantero JL, Hita-Yañez E, Moreno-Lopez B, Portillo F, Rubio A, Avila J (2010) Tau protein role in sleep-wake cycle. J Alzheimer's Dis 21:411–421.

Canu N, Dus L, Barbato C, Ciotti MT, Brancolini C, Rinaldi AM, Novak M, Cattaneo A, Bradbury A, Calissano P (1998) Tau cleavage and dephosphorylation in cerebellar granule neurons undergoing apoptosis. J Neurosci 18:7061–7074.

Carducci MA, Gilbert J, Bowling MK, Noe D, Eisenberger MA, Sinibaldi V, Zabelina Y, Chen TL, Grochow LB, Donehower RC (2001) A Phase I clinical and pharmacological evaluation of sodium phenylbutyrate on an 120-h infusion schedule. Clin Cancer Res 7:3047–3055.

Caroni P (1997) Overexpression of growth-associated proteins in the neurons of adult transgenic mice. J Neurosci Methods 71:3–9.

Castro-Alvarez JF, Uribe-Arias SA, MejÃ-a-Raigosa D, Cardona-GÃ³mez GP (2014) Cyclin-dependent kinase 5, a node protein in diminished tauopathy: a systems biology approach. Front Aging Neurosci 6:232.

Castro G, C. Areias MF, Weissmann L, Quaresma PGF, Katashima CK, Saad MJA, Prada PO (2013) Diet-induced obesity induces endoplasmic reticulum stress and insulin resistance in the amygdala of rats. FEBS Open Bio 3:443–449.

Cesca F, Baldelli P, Valtorta F, Benfenati F (2010) The synapsins: Key actors of synapse function and plasticity. Prog Neurobiol 91:313–348.

Chen Lf, Fischle W, Verdin E, Greene WC (2001) Duration of nuclear NF-kappaB action regulated by reversible acetylation. Science (80-) 293:1653–1657.

Chesser AS, Pritchard SM, Johnson GVW (2013) Tau Clearance Mechanisms and Their Possible Role in the Pathogenesis of Alzheimer Disease. Front Neurol 4:122.

Cho J-H (2003) Glycogen synthase kinase 3beta phosphorylates Tau at both primed and unprimed sites. Differential impact on microtuble binding. J Biol Chem 278:187–193.

Cho J-H, Johnson GVW (2004) Glycogen Synthase Kinase 3 Induces Caspase-cleaved Tau Aggregation in Situ. J Biol Chem 279:54716–54723.

Cho JA, Zhang X, Miller GM, Lencer WI, Nery FC (2014) 4-Phenylbutyrate Attenuates the ER Stress Response and Cyclic AMP Accumulation in DYT1 Dystonia Cell Models Witt SN, ed. PLoS One 9:e110086.

Choi S-E, Lee Y-J, Jang H-J, Lee K-W, Kim Y-S, Jun H-S, Kang SS, Chun J, Kang Y (2008) A chemical chaperone 4-PBA ameliorates palmitate-induced inhibition of glucose-stimulated insulin secretion (GSIS). Arch Biochem Biophys 475:109–114.

Chow H-M, Guo D, Zhou J-C, Zhang G-Y, Li H-F, Herrup K, Zhang J (2014) CDK5 activator protein p25 preferentially binds and activates GSK3β. Proc Natl Acad Sci 111:E4887–E4895.

Chuang D-M, Leng Y, Marinova Z, Kim H-J, Chiu C-T (2009) Multiple roles of HDAC inhibition in neurodegenerative conditions. Trends Neurosci 32:591–601.

Chung C-W, Song Y-H, Kim I-K, Yoon W-J, Ryu B-R, Jo D-G, Woo H-N, Kwon Y-K, Kim H-H, Gwag B-J, Mook-Jung I-H, Jung Y-K (2001) Proapoptotic Effects of Tau Cleavage Product Generated by Caspase-3. Neurobiol Dis 8:162–172.

Chwang WB (2006) ERK/MAPK regulates hippocampal histone phosphorylation following contextual fear conditioning. Learn Mem 13:322–328.

Chwang WB, Arthur JS, Schumacher A, Sweatt JD (2007) The Nuclear Kinase Mitogen- and Stress-Activated Protein Kinase 1 Regulates Hippocampal Chromatin Remodeling in Memory Formation. J Neurosci 27:12732–12742.

Ciechanover A, Kwon YT (2015) Degradation of misfolded proteins in neurodegenerative diseases: therapeutic targets and strategies. Exp Mol Med 47:e147.

Clavaguera F, Akatsu H, Fraser G, Crowther RA, Frank S, Hench J, Probst A, Winkler DT, Reichwald J, Staufenbiel M, Ghetti B, Goedert M, Tolnay M (2013) Brain homogenates from human tauopathies induce tau inclusions in mouse brain. Proc Natl Acad Sci 110:9535–9540.

Clavaguera F, Bolmont T, Crowther RA, Abramowski D, Frank S, Probst A, Fraser G, Stalder AK, Beibel M, Staufenbiel M, Jucker M, Goedert M, Tolnay M (2009) Transmission and spreading of tauopathy in transgenic mouse brain. Nat Cell Biol 11:909–913.

Clayton AL, Hazzalin CA, Mahadevan LC (2006) Enhanced Histone Acetylation and Transcription: A Dynamic Perspective. Mol Cell 23:289–296.

Cohen TJ, Guo JL, Hurtado DE, Kwong LK, Mills IP, Trojanowski JQ, Lee VMY (2011) The acetylation of tau inhibits its function and promotes pathological tau aggregation. Nat Commun 2:252.

Coleman P (2003) Synaptic slaughter in Alzheimer's disease. Neurobiol Aging 24:1023–1027.

Constantinidis J, Richard J, Tissot R (2008) Pick's Disease. Eur Neurol 11:208–217.

Cook C, Stankowski JN, Carlomagno Y, Stetler C, Petrucelli L (2014) Acetylation: a new key to unlock tau's role in neurodegeneration. Alzheimers Res Ther 6:29.

Cook MN, Bolivar VJ, McFadyen MP, Flaherty L (2002) Behavioral differences among 129 substrains: implications for knockout and transgenic mice. Behav Neurosci 116:600–611.

Couchie D, Mavilia C, Georgieff IS, Liem RK, Shelanski ML, Nunez J (1992) Primary structure of high molecular weight tau present in the peripheral nervous system. Proc Natl Acad Sci U S A 89:4378–4381.

Cowan CM, Mudher A (2013) Are Tau Aggregates Toxic or Protective in Tauopathies? Front Neurol 4:114.

Crawley JN, Belknap JK, Collins A, Crabbe JC, Frankel W, Henderson N, Hitzemann RJ, Maxson SC, Miner LL, Silva AJ, Wehner JM, Wynshaw-Boris A, Paylor R (1997) Behavioral phenotypes of inbred mouse strains: implications and recommendations for molecular studies. Psychopharmacology (Berl) 132:107–124.

Cruz JC, Tseng H-C, Goldman JA, Shih H, Tsai L-H (2003) Aberrant Cdk5 Activation by p25 Triggers Pathological Events Leading to Neurodegeneration and Neurofibrillary Tangles. Neuron 40:471–483.

Cuadrado-Tejedor M, García-Osta A, Ricobaraza A, Oyarzabal J, Franco R (2011) Defining the mechanism of action of 4-phenylbutyrate to develop a small-molecule-based therapy for Alzheimer's disease. Curr Med Chem 18:5545–5553.

Cuervo AM, Stefanis L, Fredenburg R, Lansbury PT, Sulzer D (2004) Impaired degradation of mutant alpha-synuclein by chaperone-mediated autophagy. Science (80-) 305:1292–1295.

Cuervo AM, Wong ESP, Martinez-Vicente M (2010) Protein degradation, aggregation, and misfolding. Mov Disord 25:S49–S54.

D'Souza I, Poorkaj P, Hong M, Nochlin D, Lee VM, Bird TD, Schellenberg GD (1999) Missense and silent tau gene mutations cause frontotemporal dementia with parkinsonism-chromosome 17 type, by affecting multiple alternative RNA splicing regulatory elements. Proc Natl Acad Sci U S A 96:5598–5603.

Dabir D V. (2006) Impaired Glutamate Transport in a Mouse Model of Tau Pathology in Astrocytes. J Neurosci 26:644–654.

DaRocha-Souto B, Coma M, Pérez-Nievas BG, Scotton TC, Siao M, Sánchez-Ferrer P, Hashimoto T, Fan Z, Hudry E, Barroeta I, Serenó L, Rodríguez M, Sánchez MB, Hyman BT, Gómez-Isla T (2012) Activation of glycogen synthase kinase-3 beta mediates β-amyloid induced neuritic damage in Alzheimer's disease. Neurobiol Dis 45:425–437.

David DC, Hauptmann S, Scherping I, Schuessel K, Keil U, Rizzu P, Ravid R, Dröse S, Brandt U, Müller WE, Eckert A, Götz J (2005) Proteomic and Functional Analyses Reveal a Mitochondrial Dysfunction in P301L Tau Transgenic Mice. J Biol Chem 280:23802–23814.

David DC, Layfield R, Serpell L, Narain Y, Goedert M, Spillantini MG (2002) Proteasomal degradation of tau protein. J Neurochem 83:176–185.

Dawson HN, Cantillana V, Chen L, Vitek MP (2007) The Tau N279K Exon 10 Splicing Mutation Recapitulates Frontotemporal Dementia and Parkinsonism Linked to Chromosome 17 Tauopathy in a Mouse Model. J Neurosci 27:9155–9168.

De Calignon A, Fox LM, Pitstick R, Carlson GA, Bacskai BJ, Spires-Jones TL, Hyman BT (2010) Caspase activation precedes and leads to tangles. Nature 464:1201–1204.

De Calignon A, Polydoro M, Suárez-Calvet M, William C, Adamowicz DH, Kopeikina KJ, Pitstick R, Sahara N, Ashe KH, Carlson GA, Spires-Jones TL, Hyman BT (2012) Propagation of Tau Pathology in a Model of Early Alzheimer's Disease. Neuron 73:685–697.

De Camilli P, Harris SM, Huttner WB, Greengard P (1983) Synapsin I (Protein I), a nerve terminal-specific phosphoprotein. II. Its specific association with synaptic vesicles demonstrated by immunocytochemistry in agarose-embedded synaptosomes. J Cell Biol 96:1355–1373.

De Silva R et al. (2006) An immunohistochemical study of cases of sporadic and inherited frontotemporal lobar degeneration using 3R- and 4R-specific tau monoclonal antibodies. Acta Neuropathol 111:329–340.

Decker JM, Krüger L, Sydow A, Zhao S, Frotscher M, Mandelkow E, Mandelkow E-M (2015) Pro-aggregant Tau impairs mossy fiber plasticity due to structural changes and Ca++ dysregulation. Acta Neuropathol Commun 3:23.

DeKosky ST, Scheff SW (1990) Synapse loss in frontal cortex biopsies in Alzheimer's disease: Correlation with cognitive severity. Ann Neurol 27:457–464.

DeKosky ST, Scheff SW, Styren SD (1996) Structural Correlates of Cognition in Dementia: Quantification and Assessment of Synapse Change. Neurodegeneration 5:417–421.

Del Signore SJ, Amante DJ, Kim J, Stack EC, Goodrich S, Cormier K, Smith K, Cudkowicz ME, Ferrante RJ (2009) Combined riluzole and sodium phenylbutyrate therapy in transgenic amyotrophic lateral sclerosis mice. Amyotroph Lateral Scler 10:85–94.

Delacourte A, Robitaille Y, Sergeant N, Buée L, Hof PR, Wattez A, Laroche-Cholette A, Mathieu J, Chagnon P, Gauvreau D (1996) Specific Pathological Tau Protein Variants Characterize Pick's Disease. J Neuropathol Exp Neurol 55:159–168.

Delobel P, Lavenir I, Fraser G, Ingram E, Holzer M, Ghetti B, Spillantini MG, Crowther RA, Goedert M (2008) Analysis of Tau Phosphorylation and Truncation in a Mouse Model of Human Tauopathy. Am J Pathol 172:123–131.

Denk F, Wade-Martins R (2009) Knock-out and transgenic mouse models of tauopathies. Neurobiol Aging 30:1–13.

Derisbourg M, Leghay C, Chiappetta G, Fernandez-Gomez F-J, Laurent C, Demeyer D, Carrier S, Buée-Scherrer V, Blum D, Vinh J, Sergeant N, Verdier Y, Buée L, Hamdane M (2015) Role of the Tau N-terminal region in microtubule stabilization revealed by new endogenous truncated forms. Sci Rep 5:9659.

Desai A, Mitchison TJ (1997) Microtubule polymerization dynamics. Annu Rev Cell Dev Biol 13:83–117.

DeVos SL, Goncharoff DK, Chen G, Kebodeaux CS, Yamada K, Stewart FR, Schuler DR, Maloney SE, Wozniak DF, Rigo F, Bennett CF, Cirrito JR, Holtzman DM, Miller TM (2013) Antisense Reduction of Tau in Adult Mice Protects against Seizures. J Neurosci 33:12887–12897.

Di J, Cohen LS, Corbo CP, Phillips GR, El Idrissi A, Alonso AD (2016) Abnormal tau induces cognitive impairment through two different mechanisms: synaptic dysfunction and neuronal loss. Sci Rep 6:20833.

Dickson DW (2006) Pick's Disease: A Modern Approach. Brain Pathol 8:339–354.

Dickson DW, Kouri N, Murray ME, Josephs KA (2011) Neuropathology of Frontotemporal Lobar Degeneration-Tau (FTLD-Tau). J Mol Neurosci 45:384–389.

Dickson DW, Yen SH, Horoupian DS (1986) Pick body-like inclusions in the dentate fascia of the hippocampus in Alzheimer's disease. Acta Neuropathol 71:38–45.

Dompierre JP, Godin JD, Charrin BC, Cordelieres FP, King SJ, Humbert S, Saudou F (2007) Histone Deacetylase 6 Inhibition Compensates for the Transport Deficit in Huntington's Disease by Increasing Tubulin Acetylation. J Neurosci 27:3571–3583.

Dover GJ, Brusilow S, Charache S (1994) Induction of fetal hemoglobin production in subjects with sickle cell anemia by oral sodium phenylbutyrate. Blood 84:339–343.

Downing KH (2000) Structural Basis for the Interaction of Tubulin with Proteins and Drugs that Affect Microtubule Dynamics 1. Annu Rev Cell Dev Biol 16:89–111.

Drewes G, Ebneth A, Preuss U, Mandelkow E-M, Mandelkow E (1997) MARK, a Novel Family of Protein Kinases That Phosphorylate Microtubule-Associated Proteins and Trigger Microtubule Disruption. Cell 89:297–308.

Driver JA, Zhou XZ, Lu KP (2014) Regulation of protein conformation by Pin1 offers novel disease mechanisms and therapeutic approaches in Alzheimer's disease. Discov Med 17:93–99.

Ducottet C, Belzung C (2005) Correlations between behaviours in the elevated plus-maze and sensitivity to unpredictable subchronic mild stress: evidence from inbred strains of mice. Behav Brain Res 156:153–162.

Duff K, Knight H, Refolo LM, Sanders S, Yu X, Picciano M, Malester B, Hutton M, Adamson J, Goedert M, Burki K, Davies P (2000) Characterization of Pathology in Transgenic Mice Over-Expressing Human Genomic and cDNA Tau Transgenes. Neurobiol Dis 7:87–98.

Ebneth A, Godemann R, Stamer K, Illenberger S, Trinczek B, Mandelkow E-M, Mandelkow E (1998) Overexpression of Tau Protein Inhibits Kinesin-dependent Trafficking of Vesicles, Mitochondria, and Endoplasmic Reticulum: Implications for Alzheimer's Disease. J Cell Biol 143:777–794.

Eckermann K, Mocanu M-M, Khlistunova I, Biernat J, Nissen A, Hofmann A, Schonig K, Bujard H, Haemisch A, Mandelkow E, Zhou L, Rune G, Mandelkow E-M (2007) The beta-Propensity of Tau Determines Aggregation and Synaptic Loss in Inducible Mouse Models of Tauopathy. J Biol Chem 282:31755–31765.

El-Husseini AE, Schnell E, Chetkovich DM, Nicoll RA, Bredt DS (2000) PSD-95 involvement in maturation of excitatory synapses. Science (80-) 290:1364–1368.

Elder GA, Gama Sosa MA, De Gasperi R (2010) Transgenic Mouse Models of Alzheimer's Disease. Mt Sinai J Med A J Transl Pers Med 77:69–81.

Engmann O (2009) Crosstalk between Cdk5 and GSK3β: Implications for Alzheimer's Disease. Front Mol Neurosci 2:2.

Eshkind LG, Leube RE (1995) Mice lacking synaptophysin reproduce and form typical synaptic vesicles. Cell Tissue Res 282:423–433.

Fasulo L, Ugolini G, Visintin M, Bradbury A, Brancolini C, Verzillo V, Novak M, Cattaneo A (2002) The Neuronal Microtubule-Associated Protein Tau Is a Substrate for Caspase-3 and an Effector of Apoptosis. J Neurochem 75:624–633.

Fatouros C, Pir GJ, Biernat J, Koushika SP, Mandelkow E, Mandelkow E-M, Schmidt E, Baumeister R (2012) Inhibition of tau aggregation in a novel Caenorhabditis elegans model of tauopathy mitigates proteotoxicity. Hum Mol Genet 21:3587–3603.

Feany MB, Dickson DW (1996) Neurodegenerative disorders with extensive tau pathology: A comparative study and review. Ann Neurol 40:139–148.

Feng G, Mellor RH, Bernstein M, Keller-Peck C, Nguyen QT, Wallace M, Nerbonne JM, Lichtman JW, Sanes JR (2000) Imaging Neuronal Subsets in Transgenic Mice Expressing Multiple Spectral Variants of GFP. Neuron 28:41–51.

Fergusson J, Landon M, Lowe J, Ward L, van Leeuwen FW, Mayer RJ (2000) Neurofibrillary tangles in progressive supranuclear palsy brains exhibit immunoreactivity to frameshift mutant ubiquitin-B protein. Neurosci Lett 279:69–72.

Fernández-Nogales M, Cabrera JR, Santos-Galindo M, Hoozemans JJM, Ferrer I, Rozemuller AJM, Hernández F, Avila J, Lucas JJ (2014) Huntington's disease is a four-repeat tauopathy with tau nuclear rods. Nat Med 20:881–885.

Ferrante RJ, Kubilus JK, Lee J, Ryu H, Beesen A, Zucker B, Smith K, Kowall NW, Ratan RR, Luthi-Carter R, Hersch SM (2003) Histone deacetylase inhibition by sodium butyrate chemotherapy ameliorates the neurodegenerative phenotype in Huntington's disease mice. J Neurosci 23:9418–9427.

Ferreira A, Bigio E (2011) Calpain-mediated tau cleavage: a mechanism leading to neurodegeneration shared by multiple tauopathies. Mol Med 17:1.

Ferrer I, Gomez-Isla T, Puig B, Freixes M, Ribe E, Dalfo E, Avila J (2005) Current Advances on Different Kinases Involved in Tau Phosphorylation, and Implications in Alzheimers Disease and Tauopathies. Curr Alzheimer Res 2:3–18.

Feuillette S, Blard O, Lecourtois M, Frébourg T, Campion D, Dumanchin C (2005) Tau is not normally degraded by the proteasome. J Neurosci Res 80:400–405.

Filali M, Lalonde R, Theriault P, Julien C, Calon F, Planel E (2012) Cognitive and non-cognitive behaviors in the triple transgenic mouse model of Alzheimer's disease expressing mutated APP, PS1, and Mapt (3xTg-AD). Behav Brain Res 234:334–342.

Filipcik P, Zilka N, Bugos O, Kucerak J, Koson P, Novak P, Novak M (2012) First transgenic rat model developing progressive cortical neurofibrillary tangles. Neurobiol Aging 33:1448–1456.

Fischer A, Sananbenesi F, Wang X, Dobbin M, Tsai L-H (2007) Recovery of learning and memory is associated with chromatin remodelling. Nature 447:178–182.

Flament S, Delacourte A, Verny M, Hauw JJ, Javoy-Agid F (1991) Abnormal Tau proteins in progressive supranuclear palsy. Similarities and differences with the neurofibrillary degeneration of the Alzheimer type. Acta Neuropathol 81:591–596.

Flores-Rodríguez P, Ontiveros-Torres MA, CÃ¡rdenas-Aguayo MC, Luna-Arias JP, Meraz-RÃ-os MA, Viramontes-Pintos A, Harrington CR, Wischik CM, Mena R, FlorÃ¡n-GarduÃ±o B, Luna-MuÃ±oz J (2015) The relationship between truncation and phosphorylation at the C-terminus of tau protein in the paired helical filaments of Alzheimer's disease. Front Neurosci 9:33.

Fonseca SG, Urano F, Weir GC, Gromada J, Burcin M (2012) Wolfram syndrome 1 and adenylyl cyclase 8 interact at the plasma membrane to regulate insulin production and secretion. Nat Cell Biol 14:1105–1112.

Fontán-Lozano Á, Romero-Granados R, Troncoso J, Múnera A, Delgado-García JM, Carrión ÁM (2008) Histone deacetylase inhibitors improve learning consolidation in young and in KA-induced-neurodegeneration and SAMP-8-mutant mice. Mol Cell Neurosci 39:193–201.

Forman MS (2005) Transgenic Mouse Model of Tau Pathology in Astrocytes Leading to Nervous System Degeneration. J Neurosci 25:3539–3550.

Foster NL, Wilhelmsen K, Sima AAF, Jones MZ, D'Amato CJ, Gilman S (1997) Frontotemporal dementia and parkinsonism linked to chromosome 17: A consensus conference. Ann Neurol 41:706–715.

Freedman KG, Radhakrishna S, Escanilla O, Linster C (2013) Duration and Specificity of Olfactory Nonassociative Memory. Chem Senses 38:369–375.

Frost B, Jacks RL, Diamond MI (2009) Propagation of Tau Misfolding from the Outside to the Inside of a Cell. J Biol Chem 284:12845–12852.

Fujiwara M, Yamamoto H, Miyagi T, Seki T, Tanaka S, Hide I, Sakai N (2013) Effects of the Chemical Chaperone 4-Phenylbutylate on the Function of the Serotonin Transporter (SERT) Expressed in COS-7 Cells. J Pharmacol Sci 122:71–83.

Fulga T a, Elson-Schwab I, Khurana V, Steinhilb ML, Spires TL, Hyman BT, Feany MB (2007) Abnormal bundling and accumulation of F-actin mediates tau-induced neuronal degeneration in vivo. Nat Cell Biol 9:139–148.

Gamblin TC, Chen F, Zambrano A, Abraha A, Lagalwar S, Guillozet AL, Lu M, Fu Y, Garcia-Sierra F, LaPointe N, Miller R, Berry RW, Binder LI, Cryns VL (2003) Caspase cleavage of tau: Linking amyloid and neurofibrillary tangles in Alzheimer's disease. Proc Natl Acad Sci 100:10032–10037.

Games D et al. (1995) Alzheimer-type neuropathology in transgenic mice overexpressing V717F β-amyloid precursor protein. Nature 373:523–527.

García-Sierra F, Mondragón-Rodríguez S, Basurto-Islas G (2008) Truncation of tau protein and its pathological significance in Alzheimer's disease. J Alzheimer's Dis 14:401–409.

Gardian G, Browne SE, Choi D-K, Klivenyi P, Gregorio J, Kubilus JK, Ryu H, Langley B, Ratan RR, Ferrante RJ, Beal MF (2005) Neuroprotective Effects of Phenylbutyrate in the N171-82Q Transgenic Mouse Model of Huntington's Disease. J Biol Chem 280:556–563.

Gendron TF, Petrucelli L (2009) The role of tau in neurodegeneration. Mol Neurodegener 4:13.

Geng J, Xia L, Li W, Dou F (2015) The C-Terminus of Tau Protein Plays an Important Role in Its Stability and Toxicity. J Mol Neurosci 55:251–259.

Gerlai R (1996) Gene-targeting studies of mammalian behavior: is it the mutation or the background genotype? Trends Neurosci 19:177–181.

Gerson JE, Kayed R (2013) Formation and Propagation of Tau Oligomeric Seeds. Front Neurol 4:93.

Gerson JE, Sengupta U, Lasagna-Reeves CA, Guerrero-Muñoz MJ, Troncoso J, Kayed R (2014) Characterization of tau oligomeric seeds in progressive supranuclear palsy. Acta Neuropathol Commun 2:73.

Gerst JL, Siedlak SL, Nunomura A, Castellani R, Perry G, Smith M a (1999) Role of Oxidative Stress in Frontotemporal Dementia. Dement Geriatr Cogn Disord 10:85–87.

Ghetti B, Oblak AL, Boeve BF, Johnson KA, Dickerson BC, Goedert M (2015) Invited review: Frontotemporal dementia caused by microtubule-associated protein tau gene (MAPT) mutations: a chameleon for neuropathology and neuroimaging. Neuropathol Appl Neurobiol 41:24–46.

Gitler D (2004) Different Presynaptic Roles of Synapsins at Excitatory and Inhibitory Synapses. J Neurosci 24:11368–11380.

Gladman JT, Bebee TW, Edwards C, Wang X, Sahenk Z, Rich MM, Chandler DS (2010) A humanized Smn gene containing the SMN2 nucleotide alteration in exon 7 mimics SMN2 splicing and the SMA disease phenotype. Hum Mol Genet 19:4239–4252.

Goedert M (2001) Alpha-synuclein and neurodegenerative diseases. Nat Rev Neurosci 2:492–501.

Goedert M, Clavaguera F, Tolnay M (2010) The propagation of prion-like protein inclusions in neurodegenerative diseases. Trends Neurosci 33:317–325.

Goedert M, Jakes R (1990) Expression of separate isoforms of human tau protein: correlation with the tau pattern in brain and effects on tubulin polymerization. EMBO J 9:4225–4230.

Goedert M, Spillantini MG (2011) Pathogenesis of the Tauopathies. J Mol Neurosci 45:425–431.

Goedert M, Spillantini MG, Cairns NJ, Crowther RA (1992a) Tau proteins of alzheimer paired helical filaments: Abnormal phosphorylation of all six brain isoforms. Neuron 8:159–168.

Goedert M, Spillantini MG, Crowther RA (1992b) Cloning of a big tau microtubule-associated protein characteristic of the peripheral nervous system. Proc Natl Acad Sci U S A 89:1983–1987.

Goedert M, Spillantini MG, Jakes R, Rutherford D, Crowther RA (1989a) Multiple isoforms of human microtubule-associated protein tau: sequences and localization in neurofibrillary tangles of Alzheimer's disease. Neuron 3:519–526.

Goedert M, Spillantini MG, Potier MC, Ulrich J, Crowther RA (1989b) Cloning and sequencing of the cDNA encoding an isoform of microtubule-associated protein tau containing four tandem repeats: differential expression of tau protein mRNAs in human brain. EMBO J 8:393–399.

Gómez de Barreda E, Dawson HN, Vitek MP, Avila J (2010) Tau deficiency leads to the upregulation of BAF-57, a protein involved in neuron-specific gene repression. FEBS Lett 584:2265–2270.

Gómez-Isla T, Hollister R, West H, Mui S, Growdon JH, Petersen RC, Parisi JE, Hyman BT (1997) Neuronal loss correlates with but exceeds neurofibrillary tangles in Alzheimer's disease. Ann Neurol 41:17–24.

Gómez-Ramos A, Díaz-Hernández M, Rubio A, Díaz-Hernández JI, Miras-Portugal MT, Avila J (2009) Characteristics and consequences of muscarinic receptor activation by tau protein. Eur Neuropsychopharmacol 19:708–717.

Gong CX, Singh TJ, Grundke-Iqbal I, Iqbal K (1993) Phosphoprotein phosphatase activities in Alzheimer disease brain. J Neurochem 61:921–927.

Good CD (2003) Dementia and ageing. Br Med Bull 65:159–168.

Gorath M, Stahnke T, Mronga T, Goldbaum O, Richter-Landsberg C (2001) Developmental changes of tau protein and mRNA in cultured rat brain oligodendrocytes. Glia 36:89–101.

Gore SD, Weng L-J, Figg WD, Zhai S, Donehower RC, Dover G, Grever MR, Griffin C, Grochow LB, Hawkins A, Burks K, Zabelena Y, Miller CB (2002) Impact of prolonged infusions of the putative differentiating agent sodium phenylbutyrate on myelodysplastic syndromes and acute myeloid leukemia. Clin Cancer Res 8:963–970.

Gottlieb RA, Andres AM, Sin J, Taylor DPJ (2015) Untangling Autophagy Measurements: All Fluxed Up. Circ Res 116:504–514.

Gotz J, Chen F, Barmettler R, Nitsch RM (2001) Tau Filament Formation in Transgenic Mice Expressing P301L Tau. J Biol Chem 276:529–534.

Götz J, Deters N, Doldissen A, Bokhari L, Ke Y, Wiesner A, Schonrock N, Ittner LM (2007) A Decade of Tau Transgenic Animal Models and Beyond. Brain Pathol 17:91–103.

Götz J, Probst A, Spillantini MG, Schäfer T, Jakes R, Bürki K, Goedert M (1995) Somatodendritic localization and hyperphosphorylation of tau protein in transgenic mice expressing the longest human brain tau isoform. EMBO J 14:1304–1313.

Götz J, Tolnay M, Barmettler R, Chen F, Probst A, Nitsch RM (2001) Oligodendroglial tau filament formation in transgenic mice expressing G272V tau. Eur J Neurosci 13:2131–2140.

Graziano A, Petrosini L, Bartoletti A (2003) Automatic recognition of explorative strategies in the Morris water maze. J Neurosci Methods 130:33–44.

Grueninger F, Bohrmann B, Czech C, Ballard TM, Frey JR, Weidensteiner C, von Kienlin M, Ozmen L (2010) Phosphorylation of Tau at S422 is enhanced by Aβ in TauPS2APP triple transgenic mice. Neurobiol Dis 37:294–306.

Gu Y, Oyama F, Ihara Y (2002) τ Is Widely Expressed in Rat Tissues. J Neurochem 67:1235–1244.

Guan J-S, Haggarty SJ, Giacometti E, Dannenberg J-H, Joseph N, Gao J, Nieland TJF, Zhou Y, Wang X, Mazitschek R, Bradner JE, DePinho RA, Jaenisch R, Tsai L-H (2009) HDAC2 negatively regulates memory formation and synaptic plasticity. Nature 459:55–60.

Guan Z, Giustetto M, Lomvardas S, Kim J-H, Miniaci MC, Schwartz JH, Thanos D, Kandel ER (2002) Integration of long-term-memory-related synaptic plasticity involves bidirectional regulation of gene expression and chromatin structure. Cell 111:483–493.

Guillozet-Bongaarts AL, Cahill ME, Cryns VL, Reynolds MR, Berry RW, Binder LI (2006) Pseudophosphorylation of tau at serine 422 inhibits caspase cleavage: in vitro evidence and implications for tangle formation in vivo. J Neurochem 97:1005–1014.

Guillozet-Bongaarts AL, Garcia-Sierra F, Reynolds MR, Horowitz PM, Fu Y, Wang T, Cahill ME, Bigio EH, Berry RW, Binder LI (2005) Tau truncation during neurofibrillary tangle evolution in Alzheimer's disease. Neurobiol Aging 26:1015–1022.

Guillozet-Bongaarts AL, Glajch KE, Libson EG, Cahill ME, Bigio E, Berry RW, Binder LI (2007) Phosphorylation and cleavage of tau in non-AD tauopathies. Acta Neuropathol 113:513–520.

Guo JL, Lee VMY (2013) Neurofibrillary tangle-like tau pathology induced by synthetic tau fibrils in primary neurons over-expressing mutant tau. FEBS Lett 587:717–723.

Gustke N, Trinczek B, Biernat J, Mandelkow EM, Mandelkow E (1994) Domains of tau protein and interactions with microtubules. Biochemistry 33:9511–9522.

Halverson R a (2005) Tau Protein Is Cross-Linked by Transglutaminase in P301L Tau Transgenic Mice. J Neurosci 25:1226–1233.

Hamilton RL (2006) Lewy Bodies in Alzheimer's Disease: A Neuropathological Review of 145 Cases Using α-Synuclein Immunohistochemistry. Brain Pathol 10:378–384.

Hanger DP, Anderton BH, Noble W (2009) Tau phosphorylation: the therapeutic challenge for neurodegenerative disease. Trends Mol Med 15:112–119.

Hanger DP, Betts JC, Loviny TLF, Blackstock WP, Anderton BH (2002) New Phosphorylation Sites Identified in Hyperphosphorylated Tau (Paired Helical Filament-Tau) from Alzheimer's Disease Brain Using Nanoelectrospray Mass Spectrometry. J Neurochem 71:2465–2476.

Hanger DP, Byers HL, Wray S, Leung K-Y, Saxton MJ, Seereeram A, Reynolds CH, Ward MA, Anderton BH (2007) Novel Phosphorylation Sites in Tau from Alzheimer Brain Support a Role for Casein Kinase 1 in Disease Pathogenesis. J Biol Chem 282:23645–23654.

Hanger DP, Hughes K, Woodgett JR, Brion J-P, Anderton BH (1992) Glycogen synthase kinase-3 induces Alzheimer's disease-like phosphorylation of tau: Generation of paired helical filament epitopes and neuronal localisation of the kinase. Neurosci Lett 147:58–62.

Hanger DP, Wray S (2010) Tau cleavage and tau aggregation in neurodegenerative disease: Figure 1. Biochem Soc Trans 38:1016–1020.

Hara T, Nakamura K, Matsui M, Yamamoto A, Nakahara Y, Suzuki-Migishima R, Yokoyama M, Mishima K, Saito I, Okano H, Mizushima N (2006) Suppression of basal autophagy in neural cells causes neurodegenerative disease in mice. Nature 441:885–889.

Harada A, Oguchi K, Okabe S, Kuno J, Terada S, Ohshima T, Sato-Yoshitake R, Takei Y, Noda T, Hirokawa N (1994) Altered microtubule organization in small-calibre axons of mice lacking tau protein. Nature 369:488–491.

Hardy J, Selkoe DJ (2002) The amyloid hypothesis of Alzheimer's disease: progress and problems on the road to therapeutics. Science (80-) 297:353–356.

Harris JA, Koyama A, Maeda S, Ho K, Devidze N, Dubal DB, Yu G-Q, Masliah E, Mucke L (2012) Human P301L-Mutant Tau Expression in Mouse Entorhinal-Hippocampal Network Causes Tau Aggregation and Presynaptic Pathology but No Cognitive Deficits. PLoS One 7:e45881.

Hauw JJ, Daniel SE, Dickson D, Horoupian DS, Jellinger K, Lantos PL, McKee A, Tabaton M, Litvan I (1994) Preliminary NINDS neuropathologic criteria for Steele-Richardson-Olszewski syndrome (progressive supranuclear palsy). Neurology 44:2015–2019.

He C, Klionsky DJ (2009) Regulation Mechanisms and Signaling Pathways of Autophagy. Annu Rev Genet 43:67–93.

Heald R, Nogales E (2002) Microtubule dynamics. J Cell Sci 115:3–4.

Hekmatimoghaddam S, Zare-Khormizi MR, Pourrajab F (2016) Underlying mechanisms and chemical/biochemical therapeutic approaches to ameliorate protein misfolding neurodegenerative diseases. BioFactors Epub ahead.

Hempen B, Brion J-P (1996) Reduction of Acetylated α-Tubulin Immunoreactivity in Neurofibrillary Tangle-bearing Neurons in Alzheimer's Disease. J Neuropathol Exp Neurol 55:964–972.

Henderson JM, Carpenter K, Cartwright H, Halliday GM (2000) Loss of thalamic intralaminar nuclei in progressive supranuclear palsy and Parkinson's disease: clinical and therapeutic implications. Brain 123:1410–1421.

Hernández F, Avila J (2007) Tauopathies. Cell Mol Life Sci 64:2219–2233.

Higuchi M, Ishihara T, Zhang B, Hong M, Andreadis A, Trojanowski JQ, Lee VM-Y (2002) Transgenic Mouse Model of Tauopathies with Glial Pathology and Nervous System Degeneration. Neuron 35:433–446.

Himmler A, Drechsel D, Kirschner MW, Martin DW (1989) Tau consists of a set of proteins with repeated C-terminal microtubule-binding domains and variable N-terminal domains. Mol Cell Biol 9:1381–1388.

Hinners I, Hill A, Otto U, Michalsky A, Mack TGA, Striggow F (2008) Tau kinase inhibitors protect hippocampal synapses despite of insoluble tau accumulation. Mol Cell Neurosci 37:559–567.

Hof PR, Bouras C, Perl DP, Morrison JH (1994) Quantitative neuropathologic analysis of Pick's disease cases: cortical distribution of Pick bodies and coexistence with Alzheimer's disease. Acta Neuropathol 87:115–124.

Hoffman GR, Moerke NJ, Hsia M, Shamu CE, Blenis J (2010) A High-Throughput, Cell-Based Screening Method for siRNA and Small Molecule Inhibitors of mTORC1 Signaling Using the In Cell Western Technique. Assay Drug Dev Technol 8:186–199.

Hol EM, Scheper W (2008) Protein Quality Control in Neurodegeneration: Walking the Tight Rope Between Health and Disease. J Mol Neurosci 34:23–33.

Holmes BB, Diamond MI (2014) Prion-like Properties of Tau Protein: The Importance of Extracellular Tau as a Therapeutic Target. J Biol Chem 289:19855–19861.

Hölscher C (1999) Stress impairs performance in spatial water maze learning tasks. Behav Brain Res 100:225–235.

Homanics GE, Quinlan JJ, Firestone LL (1999) Pharmacologic and Behavioral Responses of Inbred C57BL/6J and Strain 129/SvJ Mouse Lines. Pharmacol Biochem Behav 63:21–26.

Honer W (2003) Pathology of presynaptic proteins in Alzheimer's disease: more than simple loss of terminals. Neurobiol Aging 24:1047–1062.

Hong M, Chen DCR, Klein PS, Lee VM-Y (1997) Lithium Reduces Tau Phosphorylation by Inhibition of Glycogen Synthase Kinase-3. J Biol Chem 272:25326–25332.

Hong M, Zhukareva V, Vogelsberg-Ragaglia V, Wszolek Z, Reed L, Miller BI, Geschwind DH, Bird TD, McKeel D, Goate A, Morris JC, Wilhelmsen KC, Schellenberg GD, Trojanowski JQ, Lee VM (1998) Mutation-specific functional impairments in distinct tau isoforms of hereditary FTDP-17. Science (80-) 282:1914–1917.

Hooper C, Killick R, Lovestone S (2008) The GSK3 hypothesis of Alzheimer's disease. J Neurochem 104:1433–1439.

Horowitz PM (2004) Early N-Terminal Changes and Caspase-6 Cleavage of Tau in Alzheimer's Disease. J Neurosci 24:7895–7902.

Hoshino T, Nakaya T, Araki W, Suzuki K, Suzuki T, Mizushima T (2007) Endoplasmic reticulum chaperones inhibit the production of amyloid-β peptides. Biochem J 402:581–589.

Hospital F (2001) Size of donor chromosome segments around introgressed loci and reduction of linkage drag in marker-assisted backcross programs. Genetics 158:1363–1379.

Hrnkova M, Zilka N, Minichova Z, Koson P, Novak M (2007) Neurodegeneration caused by expression of human truncated tau leads to progressive neurobehavioural impairment in transgenic rats. Brain Res 1130:206–213.

Hsiao K, Chapman P, Nilsen S, Eckman C, Harigaya Y, Younkin S, Yang F, Cole G (1996) Correlative Memory Deficits, A Elevation, and Amyloid Plaques in Transgenic Mice. Science (80-) 274:99–103.

Hughes K, Nikolakaki E, Plyte SE, Totty NF, Woodgett JR (1993) Modulation of the glycogen synthase kinase-3 family by tyrosine phosphorylation. EMBO J 12:803–808.

Hutton M et al. (1998) Association of missense and 5'-splice-site mutations in *tau* with the inherited dementia FTDP-17. Nature 393:702–705.

Hutton M, Lewis J, McGowan E, Rockwood J, Melrose H, Nacharaju P, Van Slegtenhorst M, Gwinn-Hardy K, Paul Murphy M, Baker M, Yu X, Duff K, Hardy J, Corral A, Lin W-L, Yen S-H, Dickson DW, Davies P (2000) No Title. Nat Genet 25:402–405.

Hyman B, Van Hoesen G, Damasio A, Barnes C (1984) Alzheimer's disease: cell-specific pathology isolates the hippocampal formation. Science (80-) 225:1168–1170.

Iannitti T, Palmieri B (2011) Clinical and Experimental Applications of Sodium Phenylbutyrate. Drugs R D 11:227–249.

Iba M, Guo JL, McBride JD, Zhang B, Trojanowski JQ, Lee VM-Y (2013) Synthetic Tau Fibrils Mediate Transmission of Neurofibrillary Tangles in a Transgenic Mouse Model of Alzheimer's-Like Tauopathy. J Neurosci 33:1024–1037.

Ichimura Y, Kumanomidou T, Sou Y -s., Mizushima T, Ezaki J, Ueno T, Kominami E, Yamane T, Tanaka K, Komatsu M (2008) Structural Basis for Sorting Mechanism of p62 in Selective Autophagy. J Biol Chem 283:22847–22857.

Igaz LM, Kwong LK, Xu Y, Truax AC, Uryu K, Neumann M, Clark CM, Elman LB, Miller BL, Grossman M, McCluskey LF, Trojanowski JQ, Lee VM-Y (2008) Enrichment of C-Terminal Fragments in TAR DNA-Binding Protein-43 Cytoplasmic Inclusions in Brain but not in Spinal Cord of Frontotemporal Lobar Degeneration and Amyotrophic Lateral Sclerosis. Am J Pathol 173:182–194.

Ikeda K, Akiyama H, Haga C, Haga S (1992) Evidence that neurofibrillary tangles undergo glial modification. Acta Neuropathol 85:101–104.

Ikeda M, Kawarai T, Kawarabayashi T, Matsubara E, Murakami T, Sasaki A, Tomidokoro Y, Ikarashi Y, Kuribara H, Ishiguro K, Hasegawa M, Yen S-H, Chishti MA, Harigaya Y, Abe K, Okamoto K, St. George-Hyslop P, Westaway D, Shoji† M (2005) Accumulation of Filamentous Tau in the Cerebral Cortex of Human Tau R406W Transgenic Mice. Am J Pathol 166:521–531.

Ingelson M, Vanmechelen E, Lannfelt L (1996) Microtubule-associated protein tau in human fibroblasts with the Swedish Alzheimer mutation. Neurosci Lett 220:9–12.

Inoue K, Rispoli J, Kaphzan H, Klann E, Chen EI, Kim J, Komatsu M, Abeliovich A (2012) Macroautophagy deficiency mediates age-dependent neurodegeneration through a phospho-tau pathway. Mol Neurodegener 7:48.

Iqbal K, del C. Alonso A, Chen S, Chohan MO, El-Akkad E, Gong C-X, Khatoon S, Li B, Liu F, Rahman A, Tanimukai H, Grundke-Iqbal I (2005) Tau pathology in Alzheimer disease and other tauopathies. Biochim Biophys Acta - Mol Basis Dis 1739:198–210.

Iqbal K, Liu F, Gong C-X (2015) Tau and neurodegenerative disease: the story so far. Nat Rev Neurol 12:15–27.

Iqbal K, Liu F, Gong C-X, Grundke-Iqbal I (2010) Tau in Alzheimer Disease and Related Tauopathies. Curr Alzheimer Res 7:656–664.

Iqbal K, Wisniewski HM, Grundke-Iqbal I, Korthals JK, Terry RD (1975) Chemical pathology of neurofibrils. Neurofibrillary tangles of Alzheimer's presenile-senile dementia. J Histochem Cytochem 23:563–569.

Irvine G, El-Agnaf O (2008) Protein Aggregation in the Brain: The Molecular Basis for Alzheimer's and Parkinson's Diseases. Mol Med 14:1.

Ishihara T, Hong M, Zhang B, Nakagawa Y, Lee MK, Trojanowski JQ, Lee VM-Y (1999) Age-Dependent Emergence and Progression of a Tauopathy in Transgenic Mice Overexpressing the Shortest Human Tau Isoform. Neuron 24:751–762.

Ishihara T, Zhang B, Higuchi M, Yoshiyama Y, Trojanowski JQ, Lee VM-Y (2001) Age-Dependent Induction of Congophilic Neurofibrillary Tau Inclusions in Tau Transgenic Mice. Am J Pathol 158:555–562.

Ishizawa K, Ksiezak-Reding H, Davies P, Delacourte A, Tiseo P, Yen SH, Dickson DW (2000) A double-labeling immunohistochemical study of tau exon 10 in Alzheimer's disease, progressive supranuclear palsy and Pick's disease. Acta Neuropathol 100:235–244.

Ittner A, Ke YD, Eersel J van, Gladbach A, Götz J, Ittner LM (2011) Brief update on different roles of tau in neurodegeneration. IUBMB Life 63:495–502.

Ittner LM, Fath T, Ke YD, Bi M, van Eersel J, Li KM, Gunning P, Gotz J (2008) Parkinsonism and impaired axonal transport in a mouse model of frontotemporal dementia. Proc Natl Acad Sci 105:15997–16002.

Ittner LM, Ke YD, Delerue F, Bi M, Gladbach A, van Eersel J, Wölfing H, Chieng BC, Christie MJ, Napier IA, Eckert A, Staufenbiel M, Hardeman E, Götz J (2010) Dendritic Function of Tau Mediates Amyloid-β Toxicity in Alzheimer's Disease Mouse Models. Cell 142:387–397.

Ittner LM, Ke YD, Gotz J (2009) Phosphorylated Tau Interacts with c-Jun N-terminal Kinase-interacting Protein 1 (JIP1) in Alzheimer Disease. J Biol Chem 284:20909–20916.

Ivanov S, Roy CR (2009) NDP52: the missing link between ubiquitinated bacteria and autophagy. Nat Immunol 10:1137–1139.

Jadhav S, Katina S, Kovac A, Kazmerova Z, Novak M, Zilka N (2015) Truncated tau deregulates synaptic markers in rat model for human tauopathy. Front Cell Neurosci 9:24.

James MO, Smith RL, Williams RT, Reidenberg M (1972) The Conjugation of Phenylacetic Acid in Man, Sub-Human Primates and Some Non-Primate Species. Proc R Soc B Biol Sci 182:25–35.

Janelsins MC, Mastrangelo M a, Oddo S, LaFerla FM, Federoff HJ, Bowers WJ (2005) No Title. J Neuroinflammation 2:23.

Jicha GA, Berenfeld B, Davies P (1999) Sequence requirements for formation of conformational variants of tau similar to those found in Alzheimer's disease. J Neurosci Res 55:713–723.

Johansen T, Lamark T (2011) Selective autophagy mediated by autophagic adapter proteins. Autophagy 7:279–296.

Johnson GVW, Litersky JM, Whitaker JN (1991) Proteolysis of Microtubule-Associated Protein 2 and Tubulin by Cathepsin D. J Neurochem 57:1577–1583.

Johnson GVW, Stoothoff WH (2004) Tau phosphorylation in neuronal cell function and dysfunction. J Cell Sci 117:5721–5729.

Jucker M, Walker LC (2011) Pathogenic protein seeding in alzheimer disease and other neurodegenerative disorders. Ann Neurol 70:532–540.

Kabeya Y (2000) LC3, a mammalian homologue of yeast Apg8p, is localized in autophagosome membranes after processing. EMBO J 19:5720–5728.

Kahali S, Sarcar B, Fang B, Williams ES, Koomen JM, Tofilon PJ, Chinnaiyan P (2010) Activation of the Unfolded Protein Response Contributes toward the Antitumor Activity of Vorinostat. Neoplasia 12:80–86.

Kalueff A V., Tuohimaa P (2004) Contrasting grooming phenotypes in C57Bl/6 and 129S1/SvImJ mice. Brain Res 1028:75–82.

Kang MJ, Kim C, Jeong H, Cho B-K, Ryou AL, Hwang D, Mook-Jung I, Yi EC (2013) Synapsin-1 and tau reciprocal O-GlcNAcylation and phosphorylation sites in mouse brain synaptosomes. Exp Mol Med 45:e29.

Karagöz GE, Duarte AMS, Akoury E, Ippel H, Biernat J, Morán Luengo T, Radli M, Didenko T, Nordhues BA, Veprintsev DB, Dickey CA, Mandelkow E, Zweckstetter M, Boelens R, Madl T, Rüdiger SGD (2014) Hsp90-Tau Complex Reveals Molecular Basis for Specificity in Chaperone Action. Cell 156:963–974.

Karsten SL, Sang T-K, Gehman LT, Chatterjee S, Liu J, Lawless GM, Sengupta S, Berry RW, Pomakian J, Oh HS, Schulz C, Hui K-S, Wiedau-Pazos M, Vinters H V., Binder LI, Geschwind DH, Jackson GR (2006) A Genomic Screen for Modifiers of Tauopathy Identifies Puromycin-Sensitive Aminopeptidase as an Inhibitor of Tau-Induced Neurodegeneration. Neuron 51:549–560.

Kato S, Nakamura H (1990) Presence of two different fibril subtypes in the Pick body: an immunoelectron microscopic study. Acta Neuropathol 81:125–129.

Katsuse O, Lin W-L, Lewis J, Hutton ML, Dickson DW (2006) Neurofibrillary tangle-related synaptic alterations of spinal motor neurons of P301L tau transgenic mice. Neurosci Lett 409:95–99.

Kazantsev AG, Thompson LM (2008) Therapeutic application of histone deacetylase inhibitors for central nervous system disorders. Nat Rev Drug Discov 7:854–868.

Kenessey A, Nacharaju P, Ko L, Yen S-H (2002) Degradation of Tau by Lysosomal Enzyme Cathepsin D: Implication for Alzheimer Neurofibrillary Degeneration. J Neurochem 69:2026–2038.

Khatoon S, Grundke-Iqbal I, Iqbal K (2002) Guanosine Triphosphate Binding to β-Subunit of Tubulin in Alzheimer's Disease Brain: Role of Microtubule-Associated Protein τ. J Neurochem 64:777–787.

Khlistunova I, Biernat J, Wang Y, Pickhardt M, von Bergen M, Gazova Z, Mandelkow E, Mandelkow E-M (2006) Inducible expression of Tau repeat domain in cell models of tauopathy: aggregation is toxic to cells but can be reversed by inhibitor drugs. J Biol Chem 281:1205–1214.

Khlistunova I, Pickhardt M, Biernat J, Wang Y, Mandelkow E-M, Mandelkow E (2007) Inhibition of Tau Aggregation in Cell Models of Tauopathy. Curr Alzheimer Res 4:544–546.

Kilgore M, Miller CA, Fass DM, Hennig KM, Haggarty SJ, Sweatt JD, Rumbaugh G (2010) Inhibitors of Class 1 Histone Deacetylases Reverse Contextual Memory Deficits in a Mouse Model of Alzheimer's Disease. Neuropsychopharmacology 35:870–880.

Kim H-J (2013) Alpha-Synuclein Expression in Patients with Parkinson's Disease: A Clinician's Perspective. Exp Neurobiol 22:77.

Kimura T, Yamashita S, Fukuda T, Park J-M, Murayama M, Mizoroki T, Yoshiike Y, Sahara N, Takashima A (2007) Hyperphosphorylated tau in parahippocampal cortex impairs place learning in aged mice expressing wild-type human tau. EMBO J 26:5143–5152.

Kolarova M, García-Sierra F, Bartos A, Ricny J, Ripova D (2012) Structure and Pathology of Tau Protein in Alzheimer Disease. Int J Alzheimers Dis 2012:1–13.

Kolb PS, Ayaub EA, Zhou W, Yum V, Dickhout JG, Ask K (2015) The therapeutic effects of 4-phenylbutyric acid in maintaining proteostasis. Int J Biochem Cell Biol 61:45–52.

Komatsu M et al. (2007) Homeostatic Levels of p62 Control Cytoplasmic Inclusion Body Formation in Autophagy-Deficient Mice. Cell 131:1149–1163.

Komatsu M, Waguri S, Chiba T, Murata S, Iwata J, Tanida I, Ueno T, Koike M, Uchiyama Y, Kominami E, Tanaka K (2006) Loss of autophagy in the central nervous system causes neurodegeneration in mice. Nature 441:880–884.

Köpke E, Tung YC, Shaikh S, Alonso AC, Iqbal K, Grundke-Iqbal I (1993) Microtubule-associated protein tau. Abnormal phosphorylation of a non-paired helical filament pool in Alzheimer disease. J Biol Chem 268:24374–24384.

Kornau H-C, Schenker L, Kennedy M, Seeburg P (1995) Domain interaction between NMDA receptor subunits and the postsynaptic density protein PSD-95. Science (80-) 269:1737–1740.

Korolchuk VI, Mansilla A, Menzies FM, Rubinsztein DC (2009) Autophagy Inhibition Compromises Degradation of Ubiquitin-Proteasome Pathway Substrates. Mol Cell 33:517–527.

Korzus E, Rosenfeld MG, Mayford M (2004) CBP Histone Acetyltransferase Activity Is a Critical Component of Memory Consolidation. Neuron 42:961–972.

Koson P, Zilka N, Kovac A, Kovacech B, Korenova M, Filipcik P, Novak M (2008) Truncated tau expression levels determine life span of a rat model of tauopathy without causing neuronal loss or correlating with terminal neurofibrillary tangle load. Eur J Neurosci 28:239–246.

Kovacech B, Novak M (2010) Tau Truncation is a Productive Posttranslational Modification of Neurofibrillary Degeneration in Alzheimers Disease. Curr Alzheimer Res 7:708–716.

Kraemer BC, Zhang B, Leverenz JB, Thomas JH, Trojanowski JQ, Schellenberg GD (2003) Neurodegeneration and defective neurotransmission in a Caenorhabditis elegans model of tauopathy. Proc Natl Acad Sci 100:9980–9985.

Kubota K, Niinuma Y, Kaneko M, Okuma Y, Sugai M, Omura T, Uesugi M, Uehara T, Hosoi T, Nomura Y (2006) Suppressive effects of 4-phenylbutyrate on the aggregation of Pael receptors and endoplasmic reticulum stress. J Neurochem 97:1259–1268.

Kurosawa M, Matsumoto G, Sumikura H, Hatsuta H, Murayama S, Sakurai T, Shimogori T, Hattori N, Nukina N (2016) Serine 403-phosphorylated p62/SQSTM1 immunoreactivity in inclusions of neurodegenerative diseases. Neurosci Res 103:64–70.

Kuusisto E, Salminen A, Alafuzoff I (2001) Ubiquitin-binding protein p62 is present in neuronal and glial inclusions in human tauopathies and synucleinopathies. Neuroreport 12:2085–2090.

Kuusisto E, Salminen A, Alafuzoff I (2002) Early accumulation of p62 in neurofibrillary tangles in Alzheimer's disease: possible role in tangle formation. Neuropathol Appl Neurobiol 28:228–237.

Kwon SE, Chapman ER (2011) Synaptophysin Regulates the Kinetics of Synaptic Vesicle Endocytosis in Central Neurons. Neuron 70:847–854.

Lander ES et al. (2001) Initial sequencing and analysis of the human genome. Nature 409:860–921.

Lasagna-Reeves C a, Castillo-Carranza DL, Sengupta U, Clos AL, Jackson GR, Kayed R (2011) Tau oligomers impair memory and induce synaptic and mitochondrial dysfunction in wild-type mice. Mol Neurodegener 6:39.

Lasagna-Reeves C a., Castillo-Carranza DL, Sengupta U, Sarmiento J, Troncoso J, Jackson GR, Kayed R (2012) Identification of oligomers at early stages of tau aggregation in Alzheimer's disease. FASEB J 26:1946–1959.

Lau DHW, Hogseth M, Phillips EC, O'Neill MJ, Pooler AM, Noble W, Hanger DP (2016) Critical residues involved in tau binding to fyn: implications for tau phosphorylation in Alzheimer's disease. Acta Neuropathol Commun 4:49.

Laws N (2004) Progression of kyphosis in mdx mice. J Appl Physiol 97:1970–1977.

Le Corre S, Klafki HW, Plesnila N, Hubinger G, Obermeier A, Sahagun H, Monse B, Seneci P, Lewis J, Eriksen J, Zehr C, Yue M, McGowan E, Dickson DW, Hutton M, Roder HM (2006) An inhibitor of tau hyperphosphorylation prevents severe motor impairments in tau transgenic mice. Proc Natl Acad Sci 103:9673–9678.

Leclerc S, Garnier M, Hoessel R, Marko D, Bibb JA, Snyder GL, Greengard P, Biernat J, Wu YZ, Mandelkow EM, Eisenbrand G, Meijer L (2001) Indirubins inhibit glycogen synthase kinase-3 beta and CDK5/p25, two protein kinases involved in abnormal tau phosphorylation in Alzheimer's disease. A property common to most cyclin-dependent kinase inhibitors? J Biol Chem 276:251–260.

Lee G, Cowan N, Kirschner M (1988) The primary structure and heterogeneity of tau protein from mouse brain. Science (80-) 239:285–288.

Lee G, Neve RL, Kosik KS (1989) The microtubule binding domain of tau protein. Neuron 2:1615–1624.

Lee G, Newman ST, Gard DL, Band H, Panchamoorthy G (1998) Tau interacts with src-family non-receptor tyrosine kinases. J Cell Sci 111:3167–3177.

Lee MJ, Lee JH, Rubinsztein DC (2013) Tau degradation: The ubiquitin–proteasome system versus the autophagy-lysosome system. Prog Neurobiol 105:49–59.

Lee S, Shea TB (2012) Caspase-Mediated Truncation of Tau Potentiates Aggregation. Int J Alzheimers Dis 2012:1–7.

Lee VM-Y, Goedert M, Trojanowski JQ (2001) Neurodegenerative tauopathies. Annu Rev Neurosci 24:1121–1159.

Lei P, Ayton S, Finkelstein DI, Spoerri L, Ciccotosto GD, Wright DK, Wong BXW, Adlard P a, Cherny R a, Lam LQ, Roberts BR, Volitakis I, Egan GF, McLean C a, Cappai R, Duce J a, Bush AI (2012) Tau deficiency induces parkinsonism with dementia by impairing APP-mediated iron export. Nat Med 18:291–295.

Lein ES et al. (2007) Genome-wide atlas of gene expression in the adult mouse brain. Nature 445:168–176.

Leng Y, Chuang D-M (2006) Endogenous -Synuclein Is Induced by Valproic Acid through Histone Deacetylase Inhibition and Participates in Neuroprotection against Glutamate-Induced Excitotoxicity. J Neurosci 26:7502–7512.

Lenoir T, Guedj N, Boulu P, Guigui P, Benoist M (2010) Camptocormia: the bent spine syndrome, an update. Eur Spine J 19:1229–1237.

Leroy K, Bretteville A, Schindowski K, Gilissen E, Authelet M, De Decker R, Yilmaz Z, Buée L, Brion J-P (2007) Early Axonopathy Preceding Neurofibrillary Tangles in Mutant Tau Transgenic Mice. Am J Pathol 171:976–992.

Levenson JM, O'Riordan KJ, Brown KD, Trinh MA, Molfese DL, Sweatt JD (2004) Regulation of Histone Acetylation during Memory Formation in the Hippocampus. J Biol Chem 279:40545–40559.

Lew J, Huang Q-Q, Qi Z, Winkfein RJ, Aebersold R, Hunt T, Wang JH (1994) A brain-specific activator of cyclin-dependent kinase 5. Nature 371:423–426.

Li B-S, Ma W, Jaffe H, Zheng Y, Takahashi S, Zhang L, Kulkarni AB, Pant HC (2003) Cyclin-dependent kinase-5 is involved in neuregulin-dependent activation of phosphatidylinositol 3-kinase and Akt activity mediating neuronal survival. J Biol Chem 278:35702–35709.

Li T, Hawkes C, Qureshi HY, Kar S, Paudel HK (2006) Cyclin-Dependent Protein Kinase 5 Primes Microtubule-Associated Protein Tau Site-Specifically for Glycogen Synthase Kinase 3β †. Biochemistry 45:3134–3145.

Liazoghli D, Perreault S, Micheva KD, Desjardins M, Leclerc N (2005) Fragmentation of the Golgi Apparatus Induced by the Overexpression of Wild-Type and Mutant Human Tau Forms in Neurons. Am J Pathol 166:1499–1514.

Lim F, Hernández F, Lucas JJ, Gómez-Ramos P, Morán MA, Ávila J (2001) FTDP-17 Mutations in tau Transgenic Mice Provoke Lysosomal Abnormalities and Tau Filaments in Forebrain. Mol Cell Neurosci 18:702–714.

Lin C-H (2001) Neurological abnormalities in a knock-in mouse model of Huntington's disease. Hum Mol Genet 10:137–144.

Lin W-L, Lewis J, Yen S-H, Hutton M, Dickson DW (2003) Ultrastructural neuronal pathology in transgenic mice expressing mutant (P301L) human tau. J Neurocytol 32:1091–1105.

Lippens G, Sillen A, Landrieu I, Amniai L, Sibille N, Barbier P, Leroy A, Hanoulle X, Wieruszeski J-M (2007) Tau aggregation in Alzheimer's disease: what role for phosphorylation? Prion 1:21–25.

Litersky JM, Johnson G V, Jakes R, Goedert M, Lee M, Seubert P (1996) Tau protein is phosphorylated by cyclic AMP-dependent protein kinase and calcium/calmodulin-dependent protein kinase II within its microtubule-binding domains at Ser-262 and Ser-356. Biochem J 316:655–660.

Litvan I, Kong M (2014) Rate of decline in progressive supranuclear palsy. Mov Disord 29:463–468.

Liu C, Song X, Nisbet R, Götz J (2016) Co-immunoprecipitation with Tau Isoform-specific Antibodies Reveals Distinct Protein Interactions and Highlights a Putative Role for 2N Tau in Disease. J Biol Chem 291:8173–8188.

Liu F, Grundke-Iqbal I, Iqbal K, Gong C-X (2005) Contributions of protein phosphatases PP1, PP2A, PP2B and PP5 to the regulation of tau phosphorylation. Eur J Neurosci 22:1942–1950.

Liu F, Iqbal K, Grundke-Iqbal I, Hart GW, Gong C-X (2004a) O-GlcNAcylation regulates phosphorylation of tau: A mechanism involved in Alzheimer's disease. Proc Natl Acad Sci 101:10804–10809.

Liu F, Zaidi T, Iqbal K, Grundke-Iqbal I, Merkle RK, Gong C-X (2002) Role of glycosylation in hyperphosphorylation of tau in Alzheimer's disease. FEBS Lett 512:101–106.

Liu SJ, Zhang JY, Li HL, Fang ZY, Wang Q, Deng HM, Gong CX, Grundke-Iqbal I, Iqbal K, Wang JZ (2004b) Tau Becomes a More Favorable Substrate for GSK-3 When It Is Prephosphorylated by PKA in Rat Brain. J Biol Chem 279:50078–50088.

Liu Y-H, Wei W, Yin J, Liu G-P, Wang Q, Cao F-Y, Wang J-Z (2009) Proteasome inhibition increases tau accumulation independent of phosphorylation. Neurobiol Aging 30:1949–1961.

Loy R, Tariot PN (2002) Neuroprotective properties of valproate: potential benefit for AD and tauopathies. J Mol Neurosci 19:303–307.

Lu M, Kosik KS (2001) Competition for Microtubule-binding with Dual Expression of Tau Missense and Splice Isoforms. Mol Biol Cell 12:171–184.

Mackeh R, Perdiz D, Lorin S, Codogno P, Pous C (2013) Autophagy and microtubules - new story, old players. J Cell Sci 126:1071–1080.

Maeda S, Djukic B, Taneja P, Yu G-Q, Lo I, Davis A, Craft R, Guo W, Wang X, Kim D, Ponnusamy R, Gill TM, Masliah E, Mucke L (2016) Expression of A152T human tau causes age-dependent neuronal dysfunction and loss in transgenic mice. EMBO Rep 17:530–551.

Maeda S, Sahara N, Saito Y, Murayama S, Ikai A, Takashima A (2006) Increased levels of granular tau oligomers: An early sign of brain aging and Alzheimer's disease. Neurosci Res 54:197–201.

Mahapatra RK, Edwards MJ, Schott JM, Bhatia KP (2004) Corticobasal degeneration. Lancet Neurol 3:736–743.

Mai A, Rotili D, Valente S, Kazantsev A (2009) Histone Deacetylase Inhibitors and Neurodegenerative Disorders: Holding the Promise. Curr Pharm Des 15:3940–3957.

Maldonado H, Ramírez E, Utreras E, Pando ME, Kettlun AM, Chiong M, Kulkarni AB, Collados L, Puente J, Cartier L, Valenzuela MA (2011) Inhibition of cyclin-dependent kinase 5 but not of glycogen synthase kinase 3-β prevents neurite retraction and tau hyperphosphorylation caused by secretable products of human T-cell leukemia virus type I-infected lymphocytes. J Neurosci Res 89:1489–1498.

Mandelkow E-M, Drewes G, Biernat J, Gustke N, Van Lint J, Vandenheede JR, Mandelkow E (1992) Glycogen synthase kinase-3 and the Alzheimer-like state of microtubule-associated protein tau. FEBS Lett 314:315–321.

Mangialasche F, Solomon A, Winblad B, Mecocci P, Kivipelto M (2010) Alzheimer's disease: clinical trials and drug development. Lancet Neurol 9:702–716.

Mann SS, Hammarback JA (1994) Molecular characterization of light chain 3. A microtubule binding subunit of MAP1A and MAP1B. J Biol Chem 269:11492–11497.

Marchand B, Arsenault D, Raymond-Fleury A, Boisvert F-M, Boucher M-J (2015) Glycogen Synthase Kinase-3 (GSK3) Inhibition Induces Prosurvival Autophagic Signals in Human Pancreatic Cancer Cells. J Biol Chem 290:5592–5605.

Martin L, Latypova X, Wilson CM, Magnaudeix A, Perrin M-L, Yardin C, Terro F (2013) Tau protein kinases: Involvement in Alzheimer's disease. Ageing Res Rev 12:289–309.

Marttinen M, Kurkinen KM, Soininen H, Haapasalo A, Hiltunen M (2015) Synaptic dysfunction and septin protein family members in neurodegenerative diseases. Mol Neurodegener 10:16.

Marx J (2007) Alzheimer's disease. A new take on tau. Science (80-) 316:1416–1417.

Masliah E, Terry RD, DeTeresa RM, Hansen LA (1989) Immunohistochemical quantification of the synapse-related protein synaptophysin in Alzheimer disease. Neurosci Lett 103:234–239.

Masters CL, Simms G, Weinman NA, Multhaup G, McDonald BL, Beyreuther K (1985) Amyloid plaque core protein in Alzheimer disease and Down syndrome. Proc Natl Acad Sci 82:4245–4249.

Mathew R, Bak TH, Hodges JR (2012) Diagnostic criteria for corticobasal syndrome: a comparative study. J Neurol Neurosurg Psychiatry 83:405–410.

Maurage C-A, Bussiere T, Sergeant N, Ghesteem A, Figarella-Branger D, Ruchoux M-M, Pellissier J-F, Delacourte A (2004) Tau aggregates are abnormally phosphorylated in inclusion body myositis and have an immunoelectrophoretic profile distinct from other tauopathies. Neuropathol Appl Neurobiol 30:624–634.

Mawal-Dewan M, Henley J, Van de Voorde A, Trojanowski JQ, Lee VM (1994) The phosphorylation state of tau in the developing rat brain is regulated by phosphoprotein phosphatases. J Biol Chem 269:30981–30987.

McFadyen MP, Kusek G, Bolivar VJ, Flaherty L (2003) Differences among eight inbred strains of mice in motor ability and motor learning on a rotorod. Genes, Brain Behav 2:214–219.

McKhann GM (2001) Clinical and Pathological Diagnosis of Frontotemporal Dementia. Arch Neurol 58:1803.

McMahon HT, Bolshakov VY, Janz R, Hammer RE, Siegelbaum S a, Südhof TC (1996) Synaptophysin, a major synaptic vesicle protein, is not essential for neurotransmitter release. Proc Natl Acad Sci U S A 93:4760–4764.

McMillan PJ, Kraemer BC, Robinson L, Leverenz JB, Raskind M, Schellenberg G (2011) Truncation of tau at E391 Promotes Early Pathologic Changes in Transgenic Mice. J Neuropathol Exp Neurol 70:1006–1019.

McQuown SC, Barrett RM, Matheos DP, Post RJ, Rogge GA, Alenghat T, Mullican SE, Jones S, Rusche JR, Lazar MA, Wood MA (2011) HDAC3 Is a Critical Negative Regulator of Long-Term Memory Formation. J Neurosci 31:764–774.

Medina M, Avila J (2014) The role of extracellular Tau in the spreading of neurofibrillary pathology. Front Cell Neurosci 8:113.

Melis V et al. (2015) Different pathways of molecular pathophysiology underlie cognitive and motor tauopathy phenotypes in transgenic models for Alzheimer's disease and frontotemporal lobar degeneration. Cell Mol Life Sci 72:2199–2222.

Mercuri E, Bertini E, Messina S, Pelliccioni M, D'Amico A, Colitto F, Mirabella M, Tiziano FD, Vitali T, Angelozzi C, Kinali M, Main M, Brahe C (2004) Pilot trial of phenylbutyrate in spinal muscular atrophy. Neuromuscul Disord 14:130–135.

Micheva KD, Busse B, Weiler NC, O'Rourke N, Smith SJ (2010) Single-Synapse Analysis of a Diverse Synapse Population: Proteomic Imaging Methods and Markers. Neuron 68:639–653.

Miller N, Feng Z, Edens BM, Yang B, Shi H, Sze CC, Hong BT, Su SC, Cantu JA, Topczewski J, Crawford TO, Ko C-P, Sumner CJ, Ma L, Ma Y-C (2015) Non-Aggregating Tau Phosphorylation by Cyclin-Dependent Kinase 5 Contributes to Motor Neuron Degeneration in Spinal Muscular Atrophy. J Neurosci 35:6038–6050.

Mimori S, Ohtaka H, Koshikawa Y, Kawada K, Kaneko M, Okuma Y, Nomura Y, Murakami Y, Hamana H (2013) 4-Phenylbutyric acid protects against neuronal cell death by primarily acting as a chemical chaperone rather than histone deacetylase inhibitor. Bioorg Med Chem Lett 23:6015–6018.

Mimori S, Okuma Y, Kaneko M, Kawada K, Hosoi T, Ozawa K, Nomura Y, Hamana H (2012) Protective Effects of 4-Phenylbutyrate Derivatives on the Neuronal Cell Death and Endoplasmic Reticulum Stress. Biol Pharm Bull 35:84–90.

Min S-W, Cho S-H, Zhou Y, Schroeder S, Haroutunian V, Seeley WW, Huang EJ, Shen Y, Masliah E, Mukherjee C, Meyers D, Cole PA, Ott M, Gan L (2010) Acetylation of Tau Inhibits Its Degradation and Contributes to Tauopathy. Neuron 67:953–966.

Mizushima N, Yoshimori T (2007) How to Interpret LC3 Immunoblotting. Autophagy 3:542–545.

Mocanu M-M, Nissen A, Eckermann K, Khlistunova I, Biernat J, Drexler D, Petrova O, Schonig K, Bujard H, Mandelkow E, Zhou L, Rune G, Mandelkow E-M (2008) The Potential for -Structure in the Repeat Domain of Tau Protein Determines Aggregation, Synaptic Decay, Neuronal Loss, and Coassembly with Endogenous Tau in Inducible Mouse Models of Tauopathy. J Neurosci 28:737–748.

Mondragón-Rodríguez S, Basurto-Islas G, Santa-Maria I, Mena R, Binder LI, Avila J, Smith MA, Perry G, García-Sierra F (2008) Cleavage and conformational changes of tau protein follow phosphorylation during Alzheimer's disease. Int J Exp Pathol 89:81–90.

Mondragón-Rodríguez S, Perry G, Luna-Muñoz J, Acevedo-Aquino MC, Williams S (2014) Phosphorylation of tau protein at sites Ser 396-404 is one of the earliest events in Alzheimer's disease and Down syndrome. Neuropathol Appl Neurobiol 40:121–135.

Mondragon-Rodriguez S, Trillaud-Doppia E, Dudilot A, Bourgeois C, Lauzon M, Leclerc N, Boehm J (2012) Interaction of Endogenous Tau Protein with Synaptic Proteins Is Regulated by N-Methyl-D-aspartate Receptor-dependent Tau Phosphorylation. J Biol Chem 287:32040–32053.

Montkowski A, Poettig M, Mederer A, Holsboer F (1997) Behavioural performance in three substrains of mouse strain 129. Brain Res 762:12–18.

Morris HR, Wood NW, Lees a J (1999) Progressive supranuclear palsy (Steele-Richardson-Olszewski disease). Postgrad Med J 75:579–584.

Morris M, Knudsen GM, Maeda S, Trinidad JC, Ioanoviciu A, Burlingame AL, Mucke L (2015) Tau post-translational modifications in wild-type and human amyloid precursor protein transgenic mice. Nat Neurosci 18:1183–1189.

Morris R (1984) Developments of a water-maze procedure for studying spatial learning in the rat. J Neurosci Methods 11:47–60.

Murakami T et al. (2006) Cortical Neuronal and Glial Pathology in TgTauP301L Transgenic Mice. Am J Pathol 169:1365–1375.

Murayama S, Mori H, Ihara Y, Tomonaga M (1990) Immunocytochemical and ultrastructural studies of Pick's disease. Ann Neurol 27:394–405.

Nath U, Ben-Shlomo Y, Thomson RG, Morris HR, Wood NW, Lees AJ, Burn DJ (2001) The prevalence of progressive supranuclear palsy (Steele–Richardson–Olszewski syndrome) in the UK. Brain 124:1438–1449.

Navarro P, Guerrero R, Gallego E, Avila J, Luquin R, Ruiz PJG, Sanchez MP (2008) Memory and exploratory impairment in mice that lack the Park-2 gene and that over-express the human FTDP-17 mutant Tau. Behav Brain Res 189:350–356.

Nave K-A, Werner HB (2014) Myelination of the Nervous System: Mechanisms and Functions. Annu Rev Cell Dev Biol 30:503–533.

Neary D, Snowden JS, Northen B, Goulding P (1988) Dementia of frontal lobe type. J Neurol Neurosurg Psychiatry 51:353–361.

Neumann M, Sampathu DM, Kwong LK, Truax AC, Micsenyi MC, Chou TT, Bruce J, Schuck T, Grossman M, Clark CM, McCluskey LF, Miller BL, Masliah E, Mackenzie IR, Feldman H, Feiden W, Kretzschmar HA, Trojanowski JQ, Lee VM-Y (2006) Ubiquitinated TDP-43 in Frontotemporal Lobar Degeneration and Amyotrophic Lateral Sclerosis. Science (80-) 314:130–133.

Newman DS, Aggarwal SK, Silbergleit R (1995) Thoracic radicular symptoms in amyotrophic lateral sclerosis. J Neurol Sci 129:38–41.

Newman J, Rissman RA, Sarsoza F, Kim RC, Dick M, Bennett DA, Cotman CW, Rohn TT, Head E (2005) Caspase-cleaved tau accumulation in neurodegenerative diseases associated with tau and α-synuclein pathology. Acta Neuropathol 110:135–144.

NIA-Reagan Working Group (1997) Consensus recommendations for the postmortem diagnosis of Alzheimer disease from the National Institute on Aging and the Reagan Institute Working Group on diagnostic criteria for the neuropathological assessment of Alzheimer disease. J Neuropathol Exp Neurol 56:1095–1097.

Nijholt DA, van Haastert ES, Rozemuller AJ, Scheper W, Hoozemans JJ (2012) The unfolded protein response is associated with early tau pathology in the hippocampus of tauopathies. J Pathol 226:693–702.

Nishimura I, Yang Y, Lu B (2004) PAR-1 Kinase Plays an Initiator Role in a Temporally Ordered Phosphorylation Process that Confers Tau Toxicity in Drosophila. Cell 116:671–682.

Nixon RA (2007) Autophagy, amyloidogenesis and Alzheimer disease. J Cell Sci 120:4081–4091.

Nixon RA, Wegiel J, Kumar A, Yu WH, Peterhoff C, Cataldo A, Cuervo AM (2005) Extensive Involvement of Autophagy in Alzheimer Disease: An Immuno-Electron Microscopy Study. J Neuropathol Exp Neurol 64:113–122.

Nixon RA, Yang D-S (2011) Autophagy failure in Alzheimer's disease—locating the primary defect. Neurobiol Dis 43:38–45.

Noble W, Hanger DP, Gallo J-M (2010) Transgenic Mouse Models of Tauopathy in Drug Discovery. CNS Neurol Disord - Drug Targets 9:403–428.

Noble W, Olm V, Takata K, Casey E, Mary O, Meyerson J, Gaynor K, LaFrancois J, Wang L, Kondo T, Davies P, Burns M, Veeranna, Nixon R, Dickson D, Matsuoka Y, Ahlijanian M, Lau L-F, Duff K (2003) Cdk5 Is a Key Factor in Tau Aggregation and Tangle Formation In Vivo. Neuron 38:555–565.

Noble W, Planel E, Zehr C, Olm V, Meyerson J, Suleman F, Gaynor K, Wang L, LaFrancois J, Feinstein B, Burns M, Krishnamurthy P, Wen Y, Bhat R, Lewis J, Dickson D, Duff K (2005) Inhibition of glycogen synthase kinase-3 by lithium correlates with reduced tauopathy and degeneration in vivo. Proc Natl Acad Sci 102:6990–6995.

Nogales E (2001) Structural Insights into Microtubule Function. Annu Rev Biophys Biomol Struct 30:397–420.

Nonaka T, Watanabe ST, Iwatsubo T, Hasegawa M (2010) Seeded Aggregation and Toxicity of -Synuclein and Tau: Cellular Models of Neurodegenerative Diseases. J Biol Chem 285:34885–34898.

Norton S, Matthews FE, Barnes DE, Yaffe K, Brayne C (2014) Potential for primary prevention of Alzheimer's disease: an analysis of population-based data. Lancet Neurol 13:788–794.

Novák M (1994) Truncated tau protein as a new marker for Alzheimer's disease. Acta Virol 38:173–189.

Novak M, Kabat J, Wischik CM (1993) Molecular characterization of the minimal protease resistant tau unit of the Alzheimer's disease paired helical filament. EMBO J 12:365–370.

Nunez J (1988) Immature and mature variants of MAP2 and tau proteins and neuronal plasticity. Trends Neurosci 11:477–479.

Oddo S (2003) Amyloid deposition precedes tangle formation in a triple transgenic model of Alzheimer's disease. Neurobiol Aging 24:1063–1070.

Oddo S, Caccamo A, Shepherd JD, Murphy MP, Golde TE, Kayed R, Metherate R, Mattson MP, Akbari Y, LaFerla FM (2003) Triple-Transgenic Model of Alzheimer's Disease with Plaques and Tangles. Neuron 39:409–421.

Ohshima T, Nagle JW, Pant HC, Joshi JB, Kozak CA, Brady RO, Kulkarni AB (1995) Molecular Cloning and Chromosomal Mapping of the Mouse Cyclin-Dependent Kinase 5 Gene. Genomics 28:585–588.

Olesen OF (1994) Proteolytic Degradation of Microtubule-Associated Protein τ by Thrombin. Biochem Biophys Res Commun 201:716–721.

Ong DST, Kelly JW (2011) Chemical and/or biological therapeutic strategies to ameliorate protein misfolding diseases. Curr Opin Cell Biol 23:231–238.

Ono K, Ikemoto M, Kawarabayashi T, Ikeda M, Nishinakagawa T, Hosokawa M, Shoji M, Takahashi M, Nakashima M (2009) A chemical chaperone, sodium 4-phenylbutyric acid, attenuates the pathogenic potency in human α-synuclein A30P+A53T transgenic mice. Parkinsonism Relat Disord 15:649–654.

Orenstein SJ, Kuo S-H, Tasset I, Arias E, Koga H, Fernandez-Carasa I, Cortes E, Honig LS, Dauer W, Consiglio A, Raya A, Sulzer D, Cuervo AM (2013) Interplay of LRRK2 with chaperone-mediated autophagy. Nat Neurosci 16:394–406.

Owen E., Logue S., Rasmussen D., J. M. Wehner (1997) Assessment of learning by the Morris water task and fear conditioning in inbred mouse strains and F1 hybrids: implications of genetic background for single gene mutations and quantitative trait loci analyses. Neuroscience 80:1087–1099.

Ozcan U (2006) Chemical Chaperones Reduce ER Stress and Restore Glucose Homeostasis in a Mouse Model of Type 2 Diabetes. Science (80-) 313:1137–1140.

Ozcelik S, Fraser G, Castets P, Schaeffer V, Skachokova Z, Breu K, Clavaguera F, Sinnreich M, Kappos L, Goedert M, Tolnay M, Winkler DT (2013) Rapamycin Attenuates the Progression of Tau Pathology in P301S Tau Transgenic Mice. PLoS One 8:e62459.

Ozcelik S, Sprenger F, Skachokova Z, Fraser G, Abramowski D, Clavaguera F, Probst A, Frank S, Müller M, Staufenbiel M, Goedert M, Tolnay M, Winkler DT (2016) Co-expression of truncated and full-length tau induces severe neurotoxicity. Mol Psychiatry Epub ahead.

Pacheco CD, Elrick MJ, Lieberman AP (2008) Tau deletion exacerbates the phenotype of Niemann-Pick type C mice and implicates autophagy in pathogenesis. Hum Mol Genet 18:956–965.

Padurariu M, Ciobica A, Mavroudis I, Fotiou D, Baloyannis S (2012) Hippocampal neuronal loss in the CA1 and CA3 areas of Alzheimer's disease patients. Psychiatr Danub 24:152–158.

Pankiv S, Clausen TH, Lamark T, Brech A, Bruun J-A, Outzen H, Øvervatn A, Bjørkøy G, Johansen T (2007) p62/SQSTM1 Binds Directly to Atg8/LC3 to Facilitate Degradation of Ubiquitinated Protein Aggregates by Autophagy. J Biol Chem 282:24131–24145.

Papp E (2006) Changes of endoplasmic reticulum chaperone complexes, redox state, and impaired protein disulfide reductase activity in misfolding 1-antitrypsin transgenic mice. FASEB J 20:1018–1020.

Park M, Sabetski A, Kwan Chan Y, Turdi S, Sweeney G (2015) Palmitate Induces ER Stress and Autophagy in H9c2 Cells: Implications for Apoptosis and Adiponectin Resistance. J Cell Physiol 230:630–639.

Parlati F, McNew JA, Fukuda R, Miller R, Söllner TH, Rothman JE (2000) Topological restriction of SNARE-dependent membrane fusion. Nature 407:194–198.

Parr C, Carzaniga R, Gentleman SM, Van Leuven F, Walter J, Sastre M (2012) Glycogen Synthase Kinase 3 Inhibition Promotes Lysosomal Biogenesis and Autophagic Degradation of the Amyloid- Precursor Protein. Mol Cell Biol 32:4410–4418.

Patrick GN, Zhou P, Kwon YT, Howley PM, Tsai L-H (1998) p35, the Neuronal-specific Activator of Cyclin-dependent Kinase 5 (Cdk5) Is Degraded by the Ubiquitin-Proteasome Pathway. J Biol Chem 273:24057–24064.

Patrick GN, Zukerberg L, Nikolic M, de la Monte S, Dikkes P, Tsai LH (1999) Conversion of p35 to p25 deregulates Cdk5 activity and promotes neurodegeneration. Nature 402:615–622.

Patterson KR, Remmers C, Fu Y, Brooker S, Kanaan NM, Vana L, Ward S, Reyes JF, Philibert K, Glucksman MJ, Binder LI (2011) Characterization of Prefibrillar Tau Oligomers in Vitro and in Alzheimer Disease. J Biol Chem 286:23063–23076.

Paudel HK, Lew J, Ali Z, Wang JH (1993) Brain proline-directed protein kinase phosphorylates tau on sites that are abnormally phosphorylated in tau associated with Alzheimer's paired helical filaments. J Biol Chem 268:23512–23518.

Pei J-J, Braak E, Braak H, Grundke-Iqbal I, Iqbal K, Winblad B, Cowburn RF (1999) Distribution of Active Glycogen Synthase Kinase 3β (GSK-3β) in Brains Staged for Alzheimer Disease Neurofibrillary Changes. J Neuropathol Exp Neurol 58:1010–1019.

Pei J-J, Gong C-X, An W-L, Winblad B, Cowburn RF, Grundke-Iqbal I, Iqbal K (2003) Okadaic-Acid-Induced Inhibition of Protein Phosphatase 2A Produces Activation of Mitogen-Activated Protein Kinases ERK1/2, MEK1/2, and p70 S6, Similar to That in Alzheimer's Disease. Am J Pathol 163:845–858.

Peixoto L, Abel T (2013) The Role of Histone Acetylation in Memory Formation and Cognitive Impairments. Neuropsychopharmacology 38:62–76.

Peleg S, Sananbenesi F, Zovoilis A, Burkhardt S, Bahari-Javan S, Agis-Balboa RC, Cota P, Wittnam JL, Gogol-Doering A, Opitz L, Salinas-Riester G, Dettenhofer M, Kang H, Farinelli L, Chen W, Fischer A (2010) Altered Histone Acetylation Is Associated with Age-Dependent Memory Impairment in Mice. Science (80-) 328:753–756.

Pennanen L, Wolfer DP, Nitsch RM, Gotz J (2006) Impaired spatial reference memory and increased exploratory behavior in P301L tau transgenic mice. Genes, Brain Behav 5:369–379.

Pérez M, Hernández F, Lim F, Díaz-Nido J, Avila J (2003) Chronic lithium treatment decreases mutant tau protein aggregation in a transgenic mouse model. J Alzheimer's Dis 5:301–308.

Perlmutter DH (2002) Series Introduction: The cellular response to aggregated proteins associated with human disease. J Clin Invest 110:1219–1220.

Phuphanich S (2005) Oral sodium phenylbutyrate in patients with recurrent malignant gliomas: A dose escalation and pharmacologic study. Neuro Oncol 7:177–182.

Piperno G, Fuller MT (1985) Monoclonal antibodies specific for an acetylated form of alpha-tubulin recognize the antigen in cilia and flagella from a variety of organisms. J Cell Biol 101:2085–2094.

Piras A, Collin L, Grüninger F, Graff C, Rönnbäck A (2016) Autophagic and lysosomal defects in human tauopathies: analysis of post-mortem brain from patients with familial Alzheimer disease, corticobasal degeneration and progressive supranuclear palsy. Acta Neuropathol Commun 4:22.

Plattner F, Angelo M, Giese KP (2006) The Roles of Cyclin-dependent Kinase 5 and Glycogen Synthase Kinase 3 in Tau Hyperphosphorylation. J Biol Chem 281:25457–25465.

Polydoro M, Acker CM, Duff K, Castillo PE, Davies P (2009) Age-Dependent Impairment of Cognitive and Synaptic Function in the htau Mouse Model of Tau Pathology. J Neurosci 29:10741–10749.

Pooler AM, Noble W, Hanger DP (2014) A role for tau at the synapse in Alzheimer's disease pathogenesis. Neuropharmacology 76:1–8.

Poorkaj P, Bird TD, Wijsman E, Nemens E, Garruto RM, Anderson L, Andreadis A, Wiederholt WC, Raskind M, Schellenberg GD (1998) Tau is a candidate gene for chromosome 17 frontotemporal dementia. Ann Neurol 43:815–825.

Powers ET, Morimoto RI, Dillin A, Kelly JW, Balch WE (2009) Biological and Chemical Approaches to Diseases of Proteostasis Deficiency. Annu Rev Biochem 78:959–991.

Probst A, Götz J, Wiederhold KH, Tolnay M, Mistl C, Jaton AL, Hong M, Ishihara T, Lee VM-Y, Trojanowski JQ, Jakes R, Crowther RA, Spillantini MG, Bürki K, Goedert M (2000) Axonopathy and amyotrophy in mice transgenic for human four-repeat tau protein. Acta Neuropathol 99:469–481.

Probst A, Tolnay M, Langui D, Goedert M, Spillantini MG (1996) Pick's disease: hyperphosphorylated tau protein segregates to the somatoaxonal compartment. Acta Neuropathol 92:588–596.

Prusiner SB (1982) Novel proteinaceous infectious particles cause scrapie. Science (80-) 216:136–144.

Pugh PL, Ahmed SF, Smith MI, Upton N, Hunter AJ (2004) A behavioural characterisation of the FVB/N mouse strain. Behav Brain Res 155:283–289.

Qi X (2004) Sodium 4-Phenylbutyrate Protects against Cerebral Ischemic Injury. Mol Pharmacol 66:899–908.

Quadros A, Weeks OI, Ait-Ghezala G (2007) Role of tau in Alzheimer's dementia and other neurodegenerative diseases. J Appl Biomed 5:1–12.

Quintanilla R a, Matthews-Roberson T a, Dolan PJ, Johnson GVW (2009) Caspase-cleaved tau expression induces mitochondrial dysfunction in immortalized cortical neurons: implications for the pathogenesis of Alzheimer disease. J Biol Chem 284:18754–18766.

Rahman A, Grundke-Iqbal I, Iqbal K (2005) Phosphothreonine-212 of Alzheimer Abnormally Hyperphosphorylated Tau is a Preferred Substrate of Protein Phosphatase-1. Neurochem Res 30:277–287.

Ramachandran G, Udgaonkar JB (2011) Understanding the Kinetic Roles of the Inducer Heparin and of Rod-like Protofibrils during Amyloid Fibril Formation by Tau Protein. J Biol Chem 286:38948–38959.

Ramalho RM, Viana RJS, Castro RE, Steer CJ, Low WC, Rodrigues CMP (2008) Apoptosis in transgenic mice expressing the P301L mutated form of human tau. Mol Med 14:309–317.

Ramesh Babu J, Lamar Seibenhener M, Peng J, Strom A-L, Kemppainen R, Cox N, Zhu H, Wooten MC, Diaz-Meco MT, Moscat J, Wooten MW (2008) Genetic inactivation of p62 leads to accumulation of hyperphosphorylated tau and neurodegeneration. J Neurochem 106:107–120.

Rametti A, Esclaire F, Yardin C, Terro F (2004) Linking Alterations in Tau Phosphorylation and Cleavage during Neuronal Apoptosis. J Biol Chem 279:54518–54528.

Ramsden M (2005) Age-Dependent Neurofibrillary Tangle Formation, Neuron Loss, and Memory Impairment in a Mouse Model of Human Tauopathy (P301L). J Neurosci 25:10637–10647.

Rebeiz JJ, Kolodny EH, Richardson EP (1968) Corticodentatonigral degeneration with neuronal achromasia. Arch Neurol 18:20–33.

Reddy PH, Mani G, Park BS, Jacques J, Murdoch G, Whetsell W, Kaye J, Manczak M (2005) Differential loss of synaptic proteins in Alzheimer's disease: implications for synaptic dysfunction. J Alzheimer's Dis 7:103–117; discussion 173–180.

Rekha RS, Rao Muvva SSVJ, Wan M, Raqib R, Bergman P, Brighenti S, Gudmundsson GH, Agerberth B (2015) Phenylbutyrate induces LL-37-dependent autophagy and intracellular killing of Mycobacterium tuberculosis in human macrophages. Autophagy 11:1688–1699.

Ren Y, Lin W-L, Sanchez L, Ceballos C, Polydoro M, Spires-Jones TL, Hyman BT, Dickson DW, Sahara N (2014) Endogenous tau aggregates in oligodendrocytes of rTg4510 mice induced by human P301L tau. J Alzheimer's Dis 38:589–600.

Ren Y, Sahara N (2013) Characteristics of Tau Oligomers. Front Neurol 4.

Repnik U, Stoka V, Turk V, Turk B (2012) Lysosomes and lysosomal cathepsins in cell death. Biochim Biophys Acta - Proteins Proteomics 1824:22–33.

Reynolds CH, Garwood CJ, Wray S, Price C, Kellie S, Perera T, Zvelebil M, Yang A, Sheppard PW, Varndell IM, Hanger DP, Anderton BH (2008) Phosphorylation Regulates Tau Interactions with Src Homology 3 Domains of Phosphatidylinositol 3-Kinase, Phospholipase C 1, Grb2, and Src Family Kinases. J Biol Chem 283:18177–18186.

Reynolds MR, Berry RW, Binder LI (2007) Nitration in neurodegeneration: deciphering the "Hows" "nYs". Biochemistry 46:7325–7336.

Ribé EM, Pérez M, Puig B, Gich I, Lim F, Cuadrado M, Sesma T, Catena S, Sánchez B, Nieto M, Gómez-Ramos P, Morán MA, Cabodevilla F, Samaranch L, Ortiz L, Pérez A, Ferrer I, Avila J, Gómez-Isla T (2005) Accelerated amyloid deposition, neurofibrillary degeneration and neuronal loss in double mutant APP/tau transgenic mice. Neurobiol Dis 20:814–822.

Richter-Landsberg C, Leyk J (2013) Inclusion body formation, macroautophagy, and the role of HDAC6 in neurodegeneration. Acta Neuropathol 126:793–807.

Ricobaraza A, Cuadrado-Tejedor M, Marco S, Pérez-Otaño I, García-Osta A (2012) Phenylbutyrate rescues dendritic spine loss associated with memory deficits in a mouse model of Alzheimer disease. Hippocampus 22:1040–1050.

Ricobaraza A, Cuadrado-Tejedor M, Pérez-Mediavilla A, Frechilla D, Del Río J, García-Osta A (2009) Phenylbutyrate Ameliorates Cognitive Deficit and Reduces Tau Pathology in an Alzheimer's Disease Mouse Model. Neuropsychopharmacology 34:1721–1732.

Riley BE, Kaiser SE, Shaler TA, Ng ACY, Hara T, Hipp MS, Lage K, Xavier RJ, Ryu K-Y, Taguchi K, Yamamoto M, Tanaka K, Mizushima N, Komatsu M, Kopito RR (2010) Ubiquitin accumulation in autophagy-deficient mice is dependent on the Nrf2-mediated stress response pathway: a potential role for protein aggregation in autophagic substrate selection. J Cell Biol 191:537–552.

Rissman RA, Poon WW, Blurton-Jones M, Oddo S, Torp R, Vitek MP, LaFerla FM, Rohn TT, Cotman CW (2004) Caspase-cleavage of tau is an early event in Alzheimer disease tangle pathology. J Clin Invest 114:121–130.

Roberson ED, Scearce-Levie K, Palop JJ, Yan F, Cheng IH, Wu T, Gerstein H, Yu G-Q, Mucke L (2007) Reducing Endogenous Tau Ameliorates Amyloid -Induced Deficits in an Alzheimer's Disease Mouse Model. Science (80-) 316:750–754.

Robertson LA, Moya KL, Breen KC (2004) The potential role of tau protein O-glycosylation in Alzheimer's disease. J Alzheimer's Dis 6:489–495.

Rocher AB, Crimins JL, Amatrudo JM, Kinson MS, Todd-Brown MA, Lewis J, Luebke JI (2010) Structural and functional changes in tau mutant mice neurons are not linked to the presence of NFTs. Exp Neurol 223:385–393.

Rodríguez-Martín T, Cuchillo-Ibáñez I, Noble W, Nyenya F, Anderton BH, Hanger DP (2013) Tau phosphorylation affects its axonal transport and degradation. Neurobiol Aging 34:2146–2157.

Rodríguez-Martín T, Pooler AM, Lau DHWW, Mórotz GM, De Vos KJ, Gilley J, Coleman MP, Hanger DP (2016) Reduced number of axonal mitochondria and tau hypophosphorylation in mouse P301L tau knockin neurons. Neurobiol Dis 85:1–10.

Rodríguez-Navarro JA, Gómez A, Rodal I, Perucho J, Martinez A, Furió V, Ampuero I, Casarejos MJ, Solano RM, de Yébenes JG, Mena MA (2008) Parkin deletion causes cerebral and systemic amyloidosis in human mutated tau over-expressing mice. Hum Mol Genet 17:3128–3143.

Rogers DC, Jones DN, Nelson PR, Jones CM, Quilter CA, Robinson TL, Hagan JJ (1999) Use of SHIRPA and discriminant analysis to characterise marked differences in the behavioural phenotype of six inbred mouse strains. Behav Brain Res 105:207–217.

Rogers J, Morrison JH (1985) Quantitative morphology and regional and laminar distributions of senile plaques in Alzheimer's disease. J Neurosci 5:2801–2808.

Rohn TT, Rissman RA, Davis MC, Kim YE, Cotman CW, Head E (2002) Caspase-9 Activation and Caspase Cleavage of tau in the Alzheimer's Disease Brain. Neurobiol Dis 11:341–354.

Rosenmann H, Grigoriadis N, Eldar-Levy H, Avital A, Rozenstein L, Touloumi O, Behar L, Ben-Hur T, Avraham Y, Berry E, Segal M, Ginzburg I, Abramsky O (2008) A novel transgenic mouse expressing double mutant tau driven by its natural promoter exhibits tauopathy characteristics. Exp Neurol 212:71–84.

Rösner H, Rebhan M, Vacun G, Vanmechelen E (1995) Developmental expression of tau proteins in the chicken and rat brain: Rapid down-regulation of a paired helical filament epitope in the rat cerebral cortex coincides with the transition from immature to adult tau isoforms. Int J Dev Neurosci 13:607–617.

Rouzier R, Rajan R, Wagner P, Hess KR, Gold DL, Stec J, Ayers M, Ross JS, Zhang P, Buchholz TA, Kuerer H, Green M, Arun B, Hortobagyi GN, Symmans WF, Pusztai L (2005) Microtubule-associated protein tau: A marker of paclitaxel sensitivity in breast cancer. Proc Natl Acad Sci 102:8315–8320.

Roy S, Zhang B, Lee VM-Y, Trojanowski JQ (2005) Axonal transport defects: a common theme in neurodegenerative diseases. Acta Neuropathol 109:5–13.

Sadri-Vakili G, Bouzou B, Benn CL, Kim M-O, Chawla P, Overland RP, Glajch KE, Xia E, Qiu Z, Hersch SM, Clark TW, Yohrling GJ, Cha J-HJ (2007) Histones associated with downregulated genes are hypo-acetylated in Huntington's disease models. Hum Mol Genet 16:1293–1306.

Saleh H, Saleh A, Yao H, Cui J, Shen Y, Li R (2015) Mini review: linkage between α-Synuclein protein and cognition. Transl Neurodegener 4:5.

Sandri M (2013) Protein breakdown in muscle wasting: Role of autophagy-lysosome and ubiquitin-proteasome. Int J Biochem Cell Biol 45:2121–2129.

Santacruz K, Lewis J, Spires T, Paulson J, Kotilinek L, Ingelsson M, Guimaraes A, DeTure M, Ramsden M, McGowan E, Forster C, Yue M, Orne J, Janus C, Mariash A, Kuskowski M, Hyman B, Hutton M, Ashe KH (2005) Tau suppression in a neurodegenerative mouse model improves memory function. Science (80-) 309:476–481.

Sasaki A, Kawarabayashi T, Murakami T, Matsubara E, Ikeda M, Hagiwara H, Westaway D, George-Hyslop PS, Shoji M, Nakazato Y (2008) Microglial activation in brain lesions with tau deposits: comparison of human tauopathies and tau transgenic mice TgTauP301L. Brain Res 1214:159–168.

Sawa A, Oyama F, Matsushita M, Ihara Y (1994) Molecular diversity at the carboxyl terminus of human and rat tau. Brain Res Mol Brain Res 27:111–117.

Scaravilli T, Tolosa E, Ferrer I (2005) Progressive supranuclear palsy and corticobasal degeneration: Lumping versus splitting. Mov Disord 20:S21–S28.

Schaeffer V, Lavenir I, Ozcelik S, Tolnay M, Winkler DT, Goedert M (2012) Stimulation of autophagy reduces neurodegeneration in a mouse model of human tauopathy. Brain 135:2169–2177.

Schindowski K, Belarbi K, Bretteville A, Ando K, Buée L (2008) Neurogenesis and cell cycle-reactivated neuronal death during pathogenic tau aggregation. Genes, Brain Behav 7:92–100.

Schindowski K, Bretteville A, Leroy K, Bégard S, Brion J-P, Hamdane M, Buée L (2006) Alzheimer's disease-like tau neuropathology leads to memory deficits and loss of functional synapses in a novel mutated tau transgenic mouse without any motor deficits. Am J Pathol 169:599–616.

Schoch S, Deák F, Königstorfer A, Mozhayeva M, Sara Y, Südhof TC, Kavalali ET (2001) SNARE function analyzed in synaptobrevin/VAMP knockout mice. Science (80-) 294:1117–1122.

Schrag A, Ben-Shlomo Y, Quinn NP (1999) Prevalence of progressive supranuclear palsy and multiple system atrophy: a cross-sectional study. Lancet 354:1771–1775.

Schubert U, Antón LC, Gibbs J, Norbury CC, Yewdell JW, Bennink JR (2000) Rapid degradation of a large fraction of newly synthesized proteins by proteasomes. Nature 404:770–774.

Scott CW, Spreen RC, Herman JL, Chow FP, Davison MD, Young J, Caputo CB (1993) Phosphorylation of recombinant tau by cAMP-dependent protein kinase. Identification of phosphorylation sites and effect on microtubule assembly. J Biol Chem 268:1166–1173.

Selenica M-L, Jensen HS, Larsen a K, Pedersen ML, Helboe L, Leist M, Lotharius J (2007) Efficacy of small-molecule glycogen synthase kinase-3 inhibitors in the postnatal rat model of tau hyperphosphorylation. Br J Pharmacol 152:959–979.

Selenica M-LB, Davtyan H, Housley SB, Blair LJ, Gillies A, Nordhues BA, Zhang B, Liu J, Gestwicki JE, Lee DC, Gordon MN, Morgan D, Dickey CA (2014) Epitope analysis following active immunization with tau proteins reveals immunogens implicated in tau pathogenesis. J Neuroinflammation 11:152.

Selkoe DJ (2001) Alzheimer's disease: genes, proteins, and therapy. Physiol Rev 81:741–766.

Sengupta S, Horowitz PM, Karsten SL, Jackson GR, Geschwind DH, Fu Y, Berry RW, Binder LI (2006) Degradation of tau protein by puromycin-sensitive aminopeptidase in vitro. Biochemistry 45:15111–15119.

Seong E, Saunders TL, Stewart CL, Burmeister M (2004) To knockout in 129 or in C57BL/6: that is the question. Trends Genet 20:59–62.

Sergeant N, Delacourte A, Buée L (2005) Tau protein as a differential biomarker of tauopathies. Biochim Biophys Acta - Mol Basis Dis 1739:179–197.

Serrano-Pozo A, Betensky RA, Frosch MP, Hyman BT (2016) Plaque-Associated Local Toxicity Increases over the Clinical Course of Alzheimer Disease. Am J Pathol 186:375–384.

Serrano-Pozo A, Frosch MP, Masliah E, Hyman BT (2011) Neuropathological alterations in Alzheimer disease. Cold Spring Harb Perspect Med 1:a006189.

Sigmund CD (2000) Viewpoint: are studies in genetically altered mice out of control? Arterioscler Thromb Vasc Biol 20:1425–1429.

Silverman JL, Yang M, Lord C, Crawley JN (2010) Behavioural phenotyping assays for mouse models of autism. Nat Rev Neurosci 11:490–502.

Šimić G, Babić Leko M, Wray S, Harrington C, Delalle I, Jovanov-Milošević N, Bažadona D, Buée L, de Silva R, Di Giovanni G, Wischik C, Hof P (2016) Tau Protein Hyperphosphorylation and Aggregation in Alzheimer's Disease and Other Tauopathies, and Possible Neuroprotective Strategies. Biomolecules 6:6.

Simpson EM, Linder CC, Sargent EE, Davisson MT, Mobraaten LE, Sharp JJ (1997) Genetic variation among 129 substrains and its importance for targeted mutagenesis in mice. Nat Genet 16:19–27.

Singh TJ, Grundke-Iqbal I, Iqbal K (1995a) Phosphorylation of tau protein by casein kinase-1 converts it to an abnormal Alzheimer-like state. J Neurochem 64:1420–1423.

Singh TJ, Grundke-Iqbal I, McDonald B, Iqbal K (1994) Comparison of the phosphorylation of microtubule-associated protein tau by non-proline dependent protein kinases. Mol Cell Biochem 131:181–189.

Singh TJ, Wang J-Z, Novak M, Kontzekova E, Grundke-Iqbal I, Iqbal K (1996) Calcium/calmodulin-dependent protein kinase II phosphorylates tau at Ser-262 but only partially inhibits its binding to microtubules. FEBS Lett 387:145–148.

Singh TJ, Zaidi T, Grundke-Iqbal I, Iqbal K (1995b) Modulation of GSK-3-catalyzed phosphorylation of microtubule-associated protein tau by non-proline-dependent protein kinases. FEBS Lett 358:4–8.

Sironi JJ, Yen SH, Gondal JA, Wu Q, Grundke-Iqbal I, Iqbal K (1998) Ser-262 in human recombinant tau protein is a markedly more favorable site for phosphorylation by CaMKII than PKA or PhK. FEBS Lett 436:471–475.

Sjöberg MK, Shestakova E, Mansuroglu Z, Maccioni RB, Bonnefoy E (2006) Tau protein binds to pericentromeric DNA: a putative role for nuclear tau in nucleolar organization. J Cell Sci 119:2025–2034.

Soejima H, Joh K, Mukai T (2004) DNA damage repair and transcription. Cell Mol Life Sci 61:2168.

Soltys K, Rolkova G, Vechterova L, Filipcik P, Zilka N, Kontsekova E, Novak M (2005) First insert of tau protein is present in all stages of tau pathology in Alzheimer's disease. Neuroreport 16:1677–1681.

Souter S, Lee G (2009) Microtubule-associated protein tau in human prostate cancer cells: Isoforms, phosphorylation, and interactions. J Cell Biochem 108:555–564.

Spillantini MG, Goedert M (2013) Tau pathology and neurodegeneration. Lancet Neurol 12:609–622.

Spillantini MG, Murrell JR, Goedert M, Farlow MR, Klug A, Ghetti B (1998) Mutation in the tau gene in familial multiple system tauopathy with presenile dementia. Proc Natl Acad Sci U S A 95:7737–7741.

Spillantini MG, Schmidt ML, Lee VM-Y, Trojanowski JQ, Jakes R, Goedert M (1997) No Title. Nature 388:839–840.

Spires-Jones TL, de Calignon A, Matsui T, Zehr C, Pitstick R, Wu H-Y, Osetek JD, Jones PB, Bacskai BJ, Feany MB, Carlson GA, Ashe KH, Lewis J, Hyman BT (2008) In vivo imaging reveals dissociation between caspase activation and acute neuronal death in tangle-bearing neurons. J Neurosci 28:862–867.

Spires-Jones TL, Hyman BT (2014) The Intersection of Amyloid Beta and Tau at Synapses in Alzheimer's Disease. Neuron 82:756–771.

Spires TL, Orne JD, SantaCruz K, Pitstick R, Carlson GA, Ashe KH, Hyman BT (2006) Region-specific Dissociation of Neuronal Loss and Neurofibrillary Pathology in a Mouse Model of Tauopathy. Am J Pathol 168:1598–1607.

Spittaels K, Van den Haute C, Van Dorpe J, Bruynseels K, Vandezande K, Laenen I, Geerts H, Mercken M, Sciot R, Van Lommel A, Loos R, Van Leuven F (1999) Prominent Axonopathy in the Brain and Spinal Cord of Transgenic Mice Overexpressing Four-Repeat Human tau Protein. Am J Pathol 155:2153–2165.

Spittaels K, Van den Haute C, Van Dorpe J, Geerts H, Mercken M, Bruynseels K, Lasrado R, Vandezande K, Laenen I, Boon T, Van Lint J, Vandenheede J, Moechars D, Loos R, Van Leuven F (2000) Glycogen synthase kinase-3beta phosphorylates protein tau and rescues the axonopathy in the central nervous system of human four-repeat tau transgenic mice. J Biol Chem 275:41340–41349.

Stambolic V, Woodgett JR (1994) Mitogen inactivation of glycogen synthase kinase-3 beta in intact cells via serine 9 phosphorylation. Biochem J 303 (Pt 3:701–704.

Steele J, Richardson J, Olszewski J (1964) Progressive Supranuclear Palsy: A Heterogeneous Degeneration Involving the Brain Stem, Basal Ganglia and Cerebellum With Vertical Gaze and Pseudobulbar Palsy, Nuchal Dystonia and Dementia. Arch Neurol 10:333–359.

Steele J, Richardson J, Olszewski J (2014) Progressive Supranuclear Palsy: A Heterogeneous Degeneration Involving the Brain Stem, Basal Ganglia and Cerebellum With Vertical Gaze and Pseudobulbar Palsy, Nuchal Dystonia and Dementia. Semin Neurol 34:129–150.

Steiner B, Mandelkow EM, Biernat J, Gustke N, Meyer HE, Schmidt B, Mieskes G, Söling HD, Drechsel D, Kirschner MW (1990) Phosphorylation of microtubule-associated protein tau: identification of the site for Ca2(+)-calmodulin dependent kinase and relationship with tau phosphorylation in Alzheimer tangles. EMBO J 9:3539–3544.

Su JH, Cummings BJ, Cotman CW (1996) Plaque biogenesis in brain aging and Alzheimer's disease. Brain Res 739:79–87.

Sultan A, Nesslany F, Violet M, Begard S, Loyens A, Talahari S, Mansuroglu Z, Marzin D, Sergeant N, Humez S, Colin M, Bonnefoy E, Buee L, Galas M-C (2011) Nuclear Tau, a Key Player in Neuronal DNA Protection. J Biol Chem 286:4566–4575.

Sydow A, Hochgräfe K, Könen S, Cadinu D, Matenia D, Petrova O, Joseph M, Dennissen FJ, Mandelkow E-M (2016) Age-dependent neuroinflammation and cognitive decline in a novel Ala152Thr-Tau transgenic mouse model of PSP and AD. Acta Neuropathol Commun 4:17.

Sydow A, Mandelkow E-M (2010) "Prion-Like" Propagation of Mouse and Human Tau Aggregates in an Inducible Mouse Model of Tauopathy. Neurodegener Dis 7:28–31.

Tai H-C, Serrano-Pozo A, Hashimoto T, Frosch MP, Spires-Jones TL, Hyman BT (2012) The Synaptic Accumulation of Hyperphosphorylated Tau Oligomers in Alzheimer Disease Is Associated With Dysfunction of the Ubiquitin-Proteasome System. Am J Pathol 181:1426–1435.

Takalo M, Salminen A, Soininen H, Hiltunen M, Haapasalo A (2013) Protein aggregation and degradation mechanisms in neurodegenerative diseases. Am J Neurodegener Dis 2:1–14.

Takanashi M, Mori H, Arima K, Mizuno Y, Hattori N (2002) Expression patterns of tau mRNA isoforms correlate with susceptible lesions in progressive supranuclear palsy and corticobasal degeneration. Brain Res Mol Brain Res 104:210–219.

Takauchi S, Hosomi M, Marasigan S, Sato M, Hayashi S, Miyoshi K (1984) An ultrastructural study of Pick bodies. Acta Neuropathol 64:344–348.

Takeda N, Kishimoto Y, Yokota O (2012) Pick's disease. Adv Exp Med Biol 724:300–316.

Takei Y, Teng J, Harada A, Hirokawa N (2000) Defects in Axonal Elongation and Neuronal Migration in Mice with Disrupted tau and map1b Genes. J Cell Biol 150:989–1000.

Tanaka T, Zhong J, Iqbal K, Trenkner E, Grundke-Iqbal I (1998) The regulation of phosphorylation of tau in SY5Y neuroblastoma cells: the role of protein phosphatases. FEBS Lett 426:248–254.

Tanemura K, Akagi T, Murayama M, Kikuchi N, Murayama O, Hashikawa T, Yoshiike Y, Park J-M, Matsuda K, Nakao S, Sun X, Sato S, Yamaguchi H, Takashima A (2001) Formation of Filamentous Tau Aggregations in Transgenic Mice Expressing V337M Human Tau. Neurobiol Dis 8:1036–1045.

Tanemura K, Murayama M, Akagi T, Hashikawa T, Tominaga T, Ichikawa M, Yamaguchi H, Takashima A (2002) Neurodegeneration with tau accumulation in a transgenic mouse expressing V337M human tau. J Neurosci 22:133–141.

Tanida I, Minematsu-Ikeguchi N, Ueno T, Kominami E (2005) Lysosomal turnover, but not a cellular level, of endogenous LC3 is a marker for autophagy. Autophagy 1:84–91.

Taniguchi T, Doe N, Matsuyama S, Kitamura Y, Mori H, Saito N, Tanaka C (2005) Transgenic mice expressing mutant (N279K) human tau show mutation dependent cognitive deficits without neurofibrillary tangle formation. FEBS Lett 579:5704–5712.

Tao F, Tao Y-X, Mao P, Johns RA (2003) Role of postsynaptic density protein-95 in the maintenance of peripheral nerve injury-induced neuropathic pain in rats. Neuroscience 117:731–739.

Tarantino LM, Gould TJ, Druhan JP, Bucan M (2000) Behavior and mutagenesis screens: the importance of baseline analysis of inbred strains. Mamm Genome 11:555–564.

Tatebayashi Y, Miyasaka T, Chui D-H, Akagi T, Mishima K, Iwasaki K, Fujiwara M, Tanemura K, Murayama M, Ishiguro K, Planel E, Sato S, Hashikawa T, Takashima A (2002) Tau filament formation and associative memory deficit in aged mice expressing mutant (R406W) human tau. Proc Natl Acad Sci U S A 99:13896–13901.

Tatti M, Motta M, Di Bartolomeo S, Scarpa S, Cianfanelli V, Cecconi F, Salvioli R (2012) Reduced cathepsins B and D cause impaired autophagic degradation that can be almost completely restored by overexpression of these two proteases in Sap C-deficient fibroblasts. Hum Mol Genet 21:5159–5173.

Tavares IA, Touma D, Lynham S, Troakes C, Schober M, Causevic M, Garg R, Noble W, Killick R, Bodi I, Hanger DP, Morris JDH (2013) Prostate-derived sterile 20-like kinases (PSKs/TAOKs) phosphorylate tau protein and are activated in tangle-bearing neurons in Alzheimer disease. J Biol Chem 288:15418–15429.

Tennstaedt A, Pöpsel S, Truebestein L, Hauske P, Brockmann A, Schmidt N, Irle I, Sacca B, Niemeyer CM, Brandt R, Ksiezak-Reding H, Tirniceriu AL, Egensperger R, Baldi A, Dehmelt L, Kaiser M, Huber R, Clausen T, Ehrmann M (2012) Human high temperature requirement serine protease A1 (HTRA1) degrades tau protein aggregates. J Biol Chem 287:20931–20941.

Tenreiro S, Eckermann K, Outeiro TF (2014) Protein phosphorylation in neurodegeneration: friend or foe? Front Mol Neurosci 7:42.

Terry RD, Masliah E, Salmon DP, Butters N, DeTeresa R, Hill R, Hansen LA, Katzman R (1991) Physical basis of cognitive alterations in alzheimer's disease: Synapse loss is the major correlate of cognitive impairment. Ann Neurol 30:572–580.

Terwel D, Lasrado R, Snauwaert J, Vandeweert E, Van Haesendonck C, Borghgraef P, Van Leuven F (2005) Changed Conformation of Mutant Tau-P301L Underlies the Moribund Tauopathy, Absent in Progressive, Nonlethal Axonopathy of Tau-4R/2N Transgenic Mice. J Biol Chem 280:3963–3973.

Tint I, Slaughter T, Fischer I, Black MM (1998) Acute inactivation of tau has no effect on dynamics of microtubules in growing axons of cultured sympathetic neurons. J Neurosci 18:8660–8673.

Tortosa E, Montenegro-Venegas C, Benoist M, Hartel S, Gonzalez-Billault C, Esteban JA, Avila J (2011) Microtubule-associated Protein 1B (MAP1B) Is Required for Dendritic Spine Development and Synaptic Maturation. J Biol Chem 286:40638–40648.

Totterdell S, Hanger D, Meredith GE (2004) The ultrastructural distribution of alpha-synuclein-like protein in normal mouse brain. Brain Res 1004:61–72.

Trinczek B, Ebneth A, Mandelkow EM, Mandelkow E (1999) Tau regulates the attachment/detachment but not the speed of motors in microtubule-dependent transport of single vesicles and organelles. J Cell Sci 112:2355–2367.

Trojanowski JQ, Schuck T, Schmidt ML, Lee VM (1989) Distribution of tau proteins in the normal human central and peripheral nervous system. J Histochem Cytochem 37:209–215.

Troussard A a, Tan C, Yoganathan TN, Dedhar S (1999) Cell-Extracellular Matrix Interactions Stimulate the AP-1 Transcription Factor in an Integrin-Linked Kinase- and Glycogen Synthase Kinase 3-Dependent Manner. Mol Cell Biol 19:7420–7427.

Tsai LH, Takahashi T, Caviness VS, Harlow E (1993) Activity and expression pattern of cyclin-dependent kinase 5 in the embryonic mouse nervous system. Development 119:1029–1040.

Tully T, Bourtchouladze R, Scott R, Tallman J (2003) Targeting the CREB pathway for memory enhancers. Nat Rev Drug Discov 2:267–277.

Turenne GA, Price BD (2001) Glycogen synthase kinase3 beta phosphorylates serine 33 of p53 and activates p53's transcriptional activity. BMC Cell Biol 2:12.

Uboga N., Price J. (2000) Formation of diffuse and fibrillar tangles in aging and early Alzheimer's disease☆. Neurobiol Aging 21:1–10.

Umeda T, Yamashita T, Kimura T, Ohnishi K, Takuma H, Ozeki T, Takashima A, Tomiyama T, Mori H (2013) Neurodegenerative Disorder FTDP-17–Related Tau Intron 10 +16C→T Mutation Increases Tau Exon 10 Splicing and Causes Tauopathy in Transgenic Mice. Am J Pathol 183:211–225.

Unterberger U, Höftberger R, Gelpi E, Flicker H, Budka H, Voigtländer T (2006) Endoplasmic Reticulum Stress Features Are Prominent in Alzheimer Disease but Not in Prion Diseases In Vivo. J Neuropathol Exp Neurol 65:348–357.

Usardi A, Pooler AM, Seereeram A, Reynolds CH, Derkinderen P, Anderton B, Hanger DP, Noble W, Williamson R (2011) Tyrosine phosphorylation of tau regulates its interactions with Fyn SH2 domains, but not SH3 domains, altering the cellular localization of tau. FEBS J 278:2927–2937.

Van der Jeugd A, Hochgräfe K, Ahmed T, Decker JM, Sydow A, Hofmann A, Wu D, Messing L, Balschun D, D'Hooge R, Mandelkow E-M (2012) Cognitive defects are reversible in inducible mice expressing pro-aggregant full-length human Tau. Acta Neuropathol 123:787–805.

Vanier MT, Neuville P, Michalik L, Launay JF (1998) Expression of specific tau exons in normal and tumoral pancreatic acinar cells. J Cell Sci 111 (Pt 1:1419–1432.

Vecsey CG, Hawk JD, Lattal KM, Stein JM, Fabian SA, Attner MA, Cabrera SM, McDonough CB, Brindle PK, Abel T, Wood MA (2007) Histone deacetylase inhibitors enhance memory and synaptic plasticity via CREB:CBP-dependent transcriptional activation. J Neurosci 27:6128–6140.

Venkataramani V, Rossner C, Iffland L, Schweyer S, Tamboli IY, Walter J, Wirths O, Bayer TA (2010) Histone Deacetylase Inhibitor Valproic Acid Inhibits Cancer Cell Proliferation via Down-regulation of the Alzheimer Amyloid Precursor Protein. J Biol Chem 285:10678–10689.

Vianello S, Bouyon S, Benoit E, Sebrié C, Boerio D, Herbin M, Roulot M, Fromes Y, de la Porte S (2014) Arginine butyrate per os protects mdx mice against cardiomyopathy, kyphosis and changes in axonal excitability. Neurobiol Dis 71:325–333.

Vilchez D, Saez I, Dillin A (2014) The role of protein clearance mechanisms in organismal ageing and age-related diseases. Nat Commun 5:5659.

Võikar V, Kõks S, Vasar E, Rauvala H (2001) Strain and gender differences in the behavior of mouse lines commonly used in transgenic studies. Physiol Behav 72:271–281.

von Haehling S, Morley JE, Anker SD (2010) An overview of sarcopenia: facts and numbers on prevalence and clinical impact. J Cachexia Sarcopenia Muscle 1:129–133.

von Muhlinen N, Akutsu M, Ravenhill BJ, Foeglein Á, Bloor S, Rutherford TJ, Freund SMV, Komander D, Randow F (2012) LC3C, Bound Selectively by a Noncanonical LIR Motif in NDP52, Is Required for Antibacterial Autophagy. Mol Cell 48:329–342.

Vrljic M, Strop P, Ernst JA, Sutton RB, Chu S, Brunger AT (2010) Molecular mechanism of the synaptotagmin–SNARE interaction in Ca2+-triggered vesicle fusion. Nat Struct Mol Biol 17:325–331.

Wadia PM, Lang AE (2007) The many faces of corticobasal degeneration. Parkinsonism Relat Disord 13:S336–S340.

Wahlsten D (1992) The problem of test reliability in genetic studies of brain-behavior correlation. In: Techniques For The Genetic Analysis Of Brain And Behavior: Focus on The Mouse (Goldowitz D, Wahlsten D, Wimer RE, eds), pp 407–422. Amsterdam: Elsevier.

Wang CY, Mayo MW, Baldwin a S (1996a) TNF- and cancer therapy-induced apoptosis: potentiation by inhibition of NF-kappaB. Science (80-) 274:784–787.

Wang JZ, Wu Q, Smith A, Grundke-Iqbal I, Iqbal K (1998) Tau is phosphorylated by GSK-3 at several sites found in Alzheimer disease and its biological activity markedly inhibited only after it is prephosphorylated by A-kinase. FEBS Lett 436:28–34.

Wang QJ, Ding Y, Kohtz DS, Kohtz S, Mizushima N, Cristea IM, Rout MP, Chait BT, Zhong Y, Heintz N, Yue Z (2006) Induction of autophagy in axonal dystrophy and degeneration. J Neurosci 26:8057–8068.

Wang X, An S, Wu JM (1996b) Specific processing of native and phosphorylated tau protein by proteases. Biochem Biophys Res Commun 219:591–597.

Wang Y, Garg S, Mandelkow E-M, Mandelkow E (2010) Proteolytic processing of tau. Biochem Soc Trans 38:955–961.

Wang Y, Mandelkow E (2015) Tau in physiology and pathology. Nat Rev Neurosci 17:22–35.

Wang Y, Martinez-Vicente M, Krüger U, Kaushik S, Wong E, Mandelkow E-M, Cuervo AM, Mandelkow E (2009) Tau fragmentation, aggregation and clearance: the dual role of lysosomal processing. Hum Mol Genet 18:4153–4170.

Ward SM, Himmelstein DS, Lancia JK, Fu Y, Patterson KR, Binder LI (2013) TOC1: characterization of a selective oligomeric tau antibody. J Alzheimer's Dis 37:593–602.

Ward SM, Himmelstein DS, Ren Y, Fu Y, Yu X-W, Roberts K, Binder LI, Sahara N (2014) TOC1: a valuable tool in assessing disease progression in the rTg4510 mouse model of tauopathy. Neurobiol Dis 67:37–48.

Warren NM, Burn DJ (2007) Progressive supranuclear palsy. Pract Neurol 7:16–23.

Welsh GI, Proud CG (1993) Glycogen synthase kinase-3 is rapidly inactivated in response to insulin and phosphorylates eukaryotic initiation factor eIF-2B. Biochem J 294:625–629.

Wiley JC, Meabon JS, Frankowski H, Smith EA, Schecterson LC, Bothwell M, Ladiges WC (2010) Phenylbutyric acid rescues endoplasmic reticulum stress-induced suppression of APP proteolysis and prevents apoptosis in neuronal cells. PLoS One 5:e9135.

Williams A, Jahreiss L, Sarkar S, Saiki S, Menzies FM, Ravikumar B, Rubinsztein DC (2006) Aggregate-prone proteins are cleared from the cytosol by autophagy: therapeutic implications. Curr Top Dev Biol 76:89–101.

Williams DR (2006) Tauopathies: classification and clinical update on neurodegenerative diseases associated with microtubule-associated protein tau. Intern Med J 36:652–660.

Williams DR, Lees AJ (2009) Progressive supranuclear palsy: clinicopathological concepts and diagnostic challenges. Lancet Neurol 8:270–279.

Wilquet V, De Strooper B (2004) Amyloid-beta precursor protein processing in neurodegeneration. Curr Opin Neurobiol 14:582–588.

Wimo A, Jönsson L, Bond J, Prince M, Winblad B (2013) The worldwide economic impact of dementia 2010. Alzheimer's Dement 9:1–11.e3.

Wischik CM, Harrington CR, Storey JMD (2014) Tau-aggregation inhibitor therapy for Alzheimer's disease. Biochem Pharmacol 88:529–539.

Wischik CM, Novak M, Edwards PC, Klug A, Tichelaar W, Crowther RA (1988a) Structural characterization of the core of the paired helical filament of Alzheimer disease. Proc Natl Acad Sci 85:4884–4888.

Wischik CM, Novak M, Thøgersen HC, Edwards PC, Runswick MJ, Jakes R, Walker JE, Milstein C, Roth M, Klug A (1988b) Isolation of a fragment of tau derived from the core of the paired helical filament of Alzheimer disease. Proc Natl Acad Sci U S A 85:4506–4510.

Wischik CM, Staff RT, Wischik DJ, Bentham P, Murray AD, Storey JMD, Kook KA, Harrington CR (2015) Tau aggregation inhibitor therapy: an exploratory phase 2 study in mild or moderate Alzheimer's disease. J Alzheimer's Dis 44:705–720.

Witman GB, Cleveland DW, Weingarten MD, Kirschner MW (1976) Tubulin requires tau for growth onto microtubule initiating sites. Proc Natl Acad Sci U S A 73:4070–4074.

Wolfer DP, Müller U, Stagliar M, Lipp HP (1997) Assessing the effects of the 129/Sv genetic background on swimming navigation learning in transgenic mutants: a study using mice with a modified beta-amyloid precursor protein gene. Brain Res 771:1–13.

Wong CW, Quaranta V, Glenner GG (1985) Neuritic plaques and cerebrovascular amyloid in Alzheimer disease are antigenically related. Proc Natl Acad Sci U S A 82:8729–8732.

Wood JG, Mirra SS, Pollock NJ, Binder LI (1986) Neurofibrillary tangles of Alzheimer disease share antigenic determinants with the axonal microtubule-associated protein tau (tau). Proc Natl Acad Sci U S A 83:4040–4043.

Woodgett JR (1990) Molecular cloning and expression of glycogen synthase kinase-3/factor A. EMBO J 9:2431–2438.

Wray S, Saxton M, Anderton BH, Hanger DP (2008) Direct analysis of tau from PSP brain identifies new phosphorylation sites and a major fragment of N-terminally cleaved tau containing four microtubule-binding repeats. J Neurochem 105:2343–2352.

Xia R, Mao Z-H (2012) Progression of motor symptoms in Parkinson's disease. Neurosci Bull 28:39–48.

Xiao C, Giacca A, Lewis GF (2011) Sodium phenylbutyrate, a drug with known capacity to reduce endoplasmic reticulum stress, partially alleviates lipid-induced insulin resistance and beta-cell dysfunction in humans. Diabetes 60:918–924.

Xie HQ, Johnson G V (1998) Calcineurin inhibition prevents calpain-mediated proteolysis of tau in differentiated PC12 cells. J Neurosci Res 53:153–164.

Xie R, Nguyen S, McKeehan WL, Liu L (2010) Acetylated microtubules are required for fusion of autophagosomes with lysosomes. BMC Cell Biol 11:89.

Yagishita S, Itoh Y, Nan W, Amano N (1981) Reappraisal of the fine structure of Alzheimer's neurofibrillary tangles. Acta Neuropathol 54:239–246.

Yam GH-F, Gaplovska-Kysela K, Zuber C, Roth J (2007) Sodium 4-Phenylbutyrate Acts as a Chemical Chaperone on Misfolded Myocilin to Rescue Cells from Endoplasmic Reticulum Stress and Apoptosis. Investig Opthalmology Vis Sci 48:1683.

Yan MH, Wang X, Zhu X (2013) Mitochondrial defects and oxidative stress in Alzheimer disease and Parkinson disease. Free Radic Biol Med 62:90–101.

Yen SS (2011) Proteasome degradation of brain cytosolic tau in Alzheimer's disease. Int J Clin Exp Pathol 4:385–402.

Ying M, Xu R, Wu X, Zhu H, Zhuang Y, Han M, Xu T (2006) Sodium Butyrate Ameliorates Histone Hypoacetylation and Neurodegenerative Phenotypes in a Mouse Model for DRPLA. J Biol Chem 281:12580–12586.

Yoshimura N (1989) Topography of Pick body distribution in Pick's disease: a contribution to understanding the relationship between Pick's and Alzheimer's diseases. Clin Neuropathol 8:1–6.

Yoshiyama Y, Higuchi M, Zhang B, Huang S-M, Iwata N, Saido TC, Maeda J, Suhara T, Trojanowski JQ, Lee VM-Y (2007) Synapse Loss and Microglial Activation Precede Tangles in a P301S Tauopathy Mouse Model. Neuron 53:337–351.

Yu WH, Kumar A, Peterhoff C, Shapiro Kulnane L, Uchiyama Y, Lamb BT, Cuervo AM, Nixon RA (2004) Autophagic vacuoles are enriched in amyloid precursor protein-secretase activities: implications for beta-amyloid peptide over-production and localization in Alzheimer's disease. Int J Biochem Cell Biol 36:2531–2540.

Zampieri C, Di Fabio RP (2006) Progressive supranuclear palsy: disease profile and rehabilitation strategies. Phys Ther 86:870–880.

Zehr C, Lewis J, McGowan E, Crook J, Lin W-L, Godwin K, Knight J, Dickson DW, Hutton M (2004) Apoptosis in oligodendrocytes is associated with axonal degeneration in P301L tau mice. Neurobiol Dis 15:553–562.

Zhang B, Higuchi M, Yoshiyama Y, Ishihara T, Forman MS, Martinez D, Joyce S, Trojanowski JQ, Lee VM-Y (2004) Retarded axonal transport of R406W mutant tau in transgenic mice with a neurodegenerative tauopathy. J Neurosci 24:4657–4667.

Zhang M, Haapasalo A, Kim DY, Ingano LAM, Pettingell WH, Kovacs DM (2006) Presenilin/gamma-secretase activity regulates protein clearance from the endocytic recycling compartment. FASEB J 20:1176–1178.

Zhang Q, Zhang X, Sun A (2009) Truncated tau at D421 is associated with neurodegeneration and tangle formation in the brain of Alzheimer transgenic models. Acta Neuropathol 117:687–697.

Zhang Z, Song M, Liu X, Kang SS, Kwon I-S, Duong DM, Seyfried NT, Hu WT, Liu Z, Wang J-Z, Cheng L, Sun YE, Yu SP, Levey AI, Ye K (2014) Cleavage of tau by asparagine endopeptidase mediates the neurofibrillary pathology in Alzheimer's disease. Nat Med 20:1254–1262.

Zhou L, Rowley DL, Mi QS, Sefcovic N, Matthes HW, Kieffer BL, Donovan DM (2001) Murine inter-strain polymorphisms alter gene targeting frequencies at the mu opioid receptor locus in embryonic stem cells. Mamm Genome 12:772–778.

Zhou W, Bercury K, Cummiskey J, Luong N, Lebin J, Freed CR (2011) Phenylbutyrate up-regulates the DJ-1 protein and protects neurons in cell culture and in animal models of Parkinson disease. J Biol Chem 286:14941–14951.

Zilka N, Filipcik P, Koson P, Fialova L, Skrabana R, Zilkova M, Rolkova G, Kontsekova E, Novak M (2006) Truncated tau from sporadic Alzheimer's disease suffices to drive neurofibrillary degeneration in vivo. FEBS Lett 580:3582–3588.

Zilka N, Korenova M, Novak M (2009) Misfolded tau protein and disease modifying pathways in transgenic rodent models of human tauopathies. Acta Neuropathol 118:71–86.

Zilka N, Kovacech B, Barath P, Kontsekova E, Novák M (2012) The self-perpetuating tau truncation circle. Biochem Soc Trans 40:681–686.